

University of Warwick institutional repository: <http://go.warwick.ac.uk/wrap>

A Thesis Submitted for the Degree of PhD at the University of Warwick

<http://go.warwick.ac.uk/wrap/61919>

This thesis is made available online and is protected by original copyright.

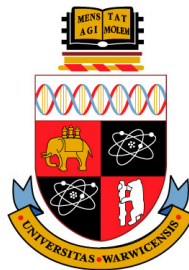
Please scroll down to view the document itself.

Please refer to the repository record for this item for information to help you to cite it. Our policy information is available from the repository home page.

THE INVESTIGATION AND APPLICATION OF ICE RECRYSTALLIZATION INHIBITORS AS CRYOPROTECTANTS

Robert Christopher Deller

A thesis submitted in fulfillment of the
requirements for the degree of
Doctor of Philosophy



Molecular Organization and Assembly of Cells
Doctoral Training Centre, University of Warwick.

December 2013

TABLE OF CONTENTS

ACKNOWLEDGEMENTS	V
DECLARATIONS	VI
ABSTRACT	VII
ABBREVIATIONS	VIII
LIST OF FIGURES, TABLES AND EQUATIONS	X
1. INTRODUCTION	1
1.1. IMPACT OF ICE IN THE MODERN WORLD.....	1
1.2. NATURAL MOLECULAR ADAPTATIONS.....	3
1.2.1. <i>Antifreeze (glyco)proteins (AF(G)Ps)</i>	3
1.2.2. <i>Antifreeze Proteins (AFPs)</i>	7
1.2.3. <i>Non-protein based strategies of cold acclimatization</i>	9
1.3. MOLECULAR INTERACTIONS OF AFPs AND AF(G)Ps WITH ICE.....	12
1.3.1. <i>Ice Recrystallization Inhibition (IRI)</i>	12
1.3.2. <i>Thermal Hysteresis (TH)</i>	14
1.3.3. <i>Dynamic Ice Shaping (DIS)</i>	15
1.4. SYNTHETIC MIMICS OF AFPs AND AF(G)Ps.....	17
1.5. CURRENT STORAGE STRATEGIES OF BIOLOGICAL MATERIALS.....	27
1.5.1. <i>Haematology</i>	27
1.5.2. <i>Reproductive medicine</i>	37
1.5.3. <i>Transplantation medicine</i>	41
1.5.4. <i>Pharmaceuticals and biotechnology</i>	45
1.6. REFERENCES.....	48
2. ICE RECRYSTALLIZATION INHIBITION ACTIVITIES OF CARBOHYRATES, SMALL MOLECULES AND POLYMERS	68
2.1. CHAPTER SUMMARY.....	68
2.2. INTRODUCTION.....	70
2.3. RESULTS AND DISCUSSION.....	77
2.3.1. <i>IRI activity of monosaccharides, disaccharides and oligosaccharides</i>	77
2.3.2. <i>IRI activity of low MW polyols</i>	90
2.3.3. <i>IRI activity of synthetic and natural polymeric macromolecules</i>	94
2.3.4. <i>IRI activity of PVA over an extended time frame</i>	100
2.3.5. <i>Investigation of the hydrophobic and surfactant characteristics of PVA underlying its anomalously high IRI activity</i>	102
2.3.6. <i>The effect of freezing rates and DMSO content on ice crystal formation and growth</i>	106
2.3.7. <i>Investigation of freezing and thawing by Differential Scanning Calorimetry</i>	109

2.4. CONCLUSION.....	117
2.5. MATERIALS AND METHODS.	118
2.5.1. <i>Preparation of Phosphate Buffered Saline.</i>	118
2.5.2. <i>IRI compounds and the purification of HES, PVA, PEG and Dextran.</i>	118
2.5.3. <i>Assessment of ice recrystallization inhibition (IRI) activity.</i>	119
2.5.4. <i>Assessment of ice formation in PBS solutions at various cooling rates.</i>	120
2.5.5. <i>Assessment of Critical Micelle Concentration (CMC).</i>	121
2.5.6. <i>Assessment of vitrification by cryomicroscopy.</i>	121
2.5.7. <i>Preparation of samples for differential scanning calorimetry (DSC).</i>	122
2.5.8. <i>Freezing and thawing of DSC samples and evaluation of DSC spectra.</i>	122
2.6. APPENDIX.	123
2.7. REFERENCES.	125
3. ICE RECRYSTALLIZATION INHIBITORS IMPROVE THE CRYOPRESERVATION OF RED BLOOD CELLS.	133
3.1. CHAPTER SUMMARY.	133
3.2. INTRODUCTION.	134
3.3. RESULTS AND DISCUSSION.	137
3.3.1. <i>Degradation of Ovine RBCs stored at 4 °C and 23 °C.</i>	137
3.3.2. <i>Cytotoxicity of current cryopreservatives to Ovine and Human RBCs.</i>	138
3.3.3. <i>Cryopreservation of Ovine RBCs with HES.</i>	144
3.3.4. <i>Cryopreservation of Ovine RBCs with HES supplemented with PVA.</i>	149
3.3.5. <i>Cryopreservation of Human RBCs with HES supplemented with PVA.</i>	155
3.4. CONCLUSIONS.....	158
3.5. MATERIALS AND METHODS.	159
3.5.1. <i>Purification of HES, PVA and PEG.</i>	159
3.5.2. <i>Preparation of Ovine RBCs.</i>	159
3.5.3. <i>Preparation of Human RBCs.</i>	159
3.5.4. <i>Haemolysis measurement of Ovine RBCs stored at 4 °C and 23 °C.</i>	160
3.5.5. <i>Measurement of Glycerol, DMSO, HES and PVA cytotoxicity in Ovine and Human RBCs.</i>	161
3.5.6. <i>Cryopreservation of Ovine and Human RBCs with HES.</i>	161
3.5.7. <i>Cryopreservation of Ovine and Human RBCs with HES and/or 9 kDa PVA.</i>	162
3.5.8. <i>Cryopreservation of Ovine RBCs with 9 kDa PVA or 8 kDa PEG.</i>	162
3.6. REFERENCES.	163
4. ICE RECRYSTALLIZATION INHIBITORS IMPROVE THE CRYOPRESERVATION OF IMMORTALIZED CELL LINES.	168
4.1. CHAPTER SUMMARY.	168
4.2. INTRODUCTION.	170

4.3. RESULTS AND DISCUSSION.....	173
4.3.1. Cytotoxicity of DMSO to lung adenocarcinoma (A549) cells.....	173
4.3.2. Cryopreservation of lung adenocarcinoma (A549) cells.....	176
4.3.3. Uptake of FITC conjugated 9 kDa PVA in lung adenocarcinoma (A549) cells.	182
4.3.4. Cryopreservation of human choriocarcinoma (BeWo) cells.....	184
4.3.5. Cryopreservation of rat hepatoma (FAO) cells.....	192
4.4. CONCLUSIONS.....	199
4.5. MATERIALS AND METHODS.....	201
4.5.1. Cell culture reagents and conditions.....	201
4.5.2. Rejuvenation of cells from cryopreserved stocks.....	201
4.5.3. Passaging of cultured cells.....	202
4.5.4. Cytotoxicity of DMSO, 9 kDa PVA and 31 kDa PVA.....	202
4.5.5. Cryopreservation of cells using a rapid freezing rate in the absence of complete medium.....	203
4.5.6. Cryopreservation of cells using a slow freezing rate in the presence of complete medium.....	204
4.5.7. MTT reduction assay.....	204
4.5.8. Neutral red uptake assay.....	205
4.5.9. Resazurin reduction assay.....	207
4.5.10. Conjugation and purification of FITC-labeled PVA.....	208
4.5.11. Determination of FITC conjugation.....	208
4.5.12. Assessment of conjugated FITC-9 kDa PVA uptake in A549 cells.....	209
4.5.13. Forskolin treatment of BeWo cells to incite syncytialization and β -HCG expression.....	210
4.5.14. β -HCG detection via immunochromatographic and (ELISA) enzyme-linked immunosorbent assays.....	210
4.5.15. Tyrosine amino transferase (TAT) enzymatic assay.....	211
4.6. REFERENCES.....	213

5. ICE RECRYSTALLIZATION INHIBITORS IMPROVE THE CRYOPRESERVATION OF PRIMARY CELLS.....	220
5.1. CHAPTER SUMMARY.....	220
5.2. INTRODUCTION.....	222
5.3. RESULTS AND DISCUSSION.....	225
5.3.1. Cryopreservation of Primary Rat Hepatocytes.....	225
5.3.2. Cryopreservation of Mouse Mesenchymal Stem Cells.....	229
5.4. CONCLUSIONS.....	236
5.5. MATERIALS AND METHODS.....	237
5.5.1. Isolation and preparation of Rat Hepatocytes.....	237
5.5.2. Cytotoxicity assessment of 9 kDa PVA with Rat Hepatocytes.....	237

5.5.3. Cryopreservation assessment of 9 kDa PVA with Rat Hepatocytes.	238
5.5.4. Preparation and cryopreservation of Mouse Mesenchymal Stem Cells.....	239
5.5.5. Adipogenesis of Mouse Mesenchymal Stem Cells.	241
5.6. REFERENCES.	242
CONCLUSIONS.....	247
AWARDS AND CONFERENCE PROCEEDINGS.....	248
CURRICULUM VITAE	250
CONTRIBUTIONS TO PUBLISHED WORK.	252

ACKNOWLEDGEMENTS

I would like to first recognize and thank the contribution of each of my Ph.D supervisors Dr. Dan Mitchell, Dr. Manu Vatish and especially Dr. Matthew Gibson for their superb enthusiasm and insights that made this achievable and for making the process as painless as possible. Furthermore the Molecular Organization and Assembly of Cell Doctoral Training Centre (MOAC DTC) for taking me on and the EPSRC for funding my studies through out alongside the rest of my cohort who has made tackling the last few years far easier than it would have been alone. In addition to this I wish to acknowledge and appreciate the support that other members of the Gibson Group have provided plus colleagues at the Clinical Sciences Research Institute. I wish to thank all of the above with regards to their support and in arranging and providing advice on the fortunate 3-month secondment that I was able to undertake at The Albert Einstein College Of Medicine, NY, USA under the guidance of Prof. Jeffrey Pessin supported by Warwick Transatlantic Fellowship program. Outside of work I want to thank all the times spent with Warwick Mountains and Warwick Canoe Polo who have provided much needed and loved serenity and exhilaration in equal measure. My immediate family Johanna Deller, Tim Deller and Alex Deller for helping shape who I am and finally to Heather Churchill who continues to brighten my day everyday and make all the hard work worthwhile.

DECLARATIONS

The work presented in this thesis is entirely my own work, except where acknowledged accordingly in the text. I confirm that this thesis has not been submitted for a degree at another University.

Parts of the work derived from this thesis have been published by the author.

Deller, R. et al. Ice recrystallisation inhibition by polyols: comparison of molecular and macromolecular inhibitors and role of hydrophobic units. *Biomater. Sci.* 1, 478–485 (2013).

Deller, R. et al. Synthetic polymers enable non-vitreous cellular cryopreservation by reducing ice crystal growth during thawing. *Nat. Commun.* 5, 3244, doi:10.1038/ncomms4244 (2014).

ABSTRACT

There is a continuing need for improvements in the cryopreservation of clinically relevant cells, tissues and organs as advances in transplantation science and regenerative medicine rise alongside an aging populace that intensifies demand. Antifreeze (glyco)proteins (AF(G)Ps) and antifreeze proteins (AFPs) are classes of proteins found in cold acclimatized species. Ice recrystallization is a highly damaging process that occurs upon the thawing of frozen specimens with AF(G)Ps and AFPs limiting this effect in a process termed ice recrystallization inhibition (IRI). However AF(G)Ps and AFPs largely fail to improve *in vitro* and *ex vivo* cryopreservation due to their secondary property of dynamic ice shaping. The biocompatible and synthetically accessible polymer poly(vinyl alcohol) (PVA) has been shown to possess a strong IRI activity. The IRI property of PVA along with numerous other polymers and polyols is investigated to highlight the uniqueness of PVA (Chapter 2). PVA is then explored as a cryoprotectant with red blood cells (Chapter 3), immortalized mammalian cell lines (Chapter 4) and primary cells (Chapter 5) with a significant advantageous effect observed with each cell type in terms of the number of cells recovered post thaw. However, this is despite the use of proportionately low concentrations of PVA compared to traditional membrane permeable cryoprotectants. The application of PVA as a cryoadjuvant could therefore improve the cryopreservation of cells, tissues and organs resulting in widespread clinical benefits.

ABBREVIATIONS

- β -hCG	=	Human chorionic gonadotropin
- A549	=	Lung adenocarcinoma cell line
- AF(G)P	=	Antifreeze (glyco)protein
- AFP	=	Antifreeze protein
- ATP	=	Adenosine triphosphate
- BeWo	=	Human choriocarcinoma cell line
- Caco-2	=	Human epithelial colorectal adenocarcinoma cell line
- CD	=	Circular dichroism
- CPA	=	Cryoprotective agent
- DIS	=	Dynamic ice shaping
- DMEM	=	Dulbecco's modified eagle medium
- DMSO	=	Dimethyl sulphoxide
- DNA	=	Deoxyribonucleic acid
- DPG	=	2,3-Diphosphoglycerate
- DPH	=	1,6-Diphenyl-1,3,5-hexatriene
- DSC	=	Differential scanning calorimetry
- EDTA	=	Ethylenediaminetetraacetic acid
- ELISA	=	Enzyme linked immunosorbent assays
- EU	=	European Union
- F12K	=	Kaighn's modification of Ham's F12
- FAO	=	Rat H4IIE hepatoma cell line
- FBS	=	Fetal bovine serum
- FDA	=	Food and Drug Administration
- FITC	=	Fluorescein 5-isothiocyanate
- FTIR	=	Fourier transform infra red
- HEK 293	=	Human embryonic kidney cell line
- HepG2	=	Human hepatocellular carcinoma cell line
- HES	=	Hydroxyethyl Starch
- IR	=	Ice recrystallization
- IRI	=	Ice recrystallization inhibition
- ISP	=	Ice shaping protein
- kDa	=	Kilodalton
- MCF7	=	Michigan cancer foundation 7 breast cancer cell line
- MD	=	Molecular dynamics
- MLGS	=	Mean largest grain size
- MSC	=	Mesenchymal stem cell
- MTT	=	3-(4,5-Dimethylthiazol-2-yl)-2,5-diphenyltetrazolium bromide
- MW	=	Molecular weight

- MWCO	=	Molecular weight cut off
- NMR	=	Nuclear magnetic resonance
- PAA	=	Poly(acrylic acid)
- PBS	=	Phosphate buffered saline
- PEG	=	Poly(ethylene) glycol
- pHBA	=	<i>p</i> -hydroxybenzaldehyde
- pHPP	=	<i>p</i> -hydroxyphenylpyruvic acid
- PMAMGlc	=	Poly(methyl-6-O-methacryloyl- α -D-glucopyranoside)
- PVA	=	Poly(vinyl alcohol)
- PVP	=	Poly(vinyl pyrrolidone)
- QLL	=	Quasi liquid layer
- RBC	=	Red blood cell
- Rh	=	Rhesus
- RPMI	=	Roswell park memorial institute medium
- SDS	=	Sodium dodecyl sulphate
- SPPS	=	Solid phase peptide synthesis
- TGA	=	Thermogravimetric analysis
- TH	=	Thermal hysteresis
- UCB	=	Umbilical cord blood
- UK	=	United Kingdom
- USA	=	United States of America
- UW	=	University of Wisconsin

LIST OF FIGURES, TABLES AND EQUATIONS.

Figure 1.1. Structural representation of a typical AF(G)P.	4
Figure 1.2. Structural representations of various AFPs highlighting secondary structure motifs and structural diversity.	8
Figure 1.3. Representative non-protein based low MW weight cryoprotectants (non-exhaustive list).	10
Figure 1.4. Example micrographs taken from “splat” IRI measurements.	14
Figure 1.5. Mechanisms and consequences of DIS.	16
Figure 1.6. AF(G)P analogues developed by Ben and co-workers.	19
Figure 1.7. Other AF(G)P mimics.	23
Figure 1.8. Select polymeric compounds assessed for antifreeze activities.	25
Figure 1.9. Antifreeze active Zirconium compounds.	26
Table 1.1. Breakdown of the clinical use of donated blood units in the UK	28
Figure 1.10. UK blood stocks over a 14-week period.	28
Table 1.2. Detailed breakdown of UK blood stocks over a 14 week period.	29
Figure 2.1. Strategies for the rationale design of AF(G)P mimics.	73
Figure 2.2. Structures of various monosaccharides investigated for IRI activity.	78
Figure 2.3. IRI activity of (11) monosaccharides.	80
Figure 2.4. Structures of various disaccharides investigated for IRI activity.	81
Figure 2.5. IRI activity of (7) disaccharides.	82
Figure 2.6. IRI activity of (7) disaccharides against hydration number.	84
Figure 2.7. IRI activity of (7) disaccharides against hydration index.	85
Figure 2.8. Structures of various oligosaccharides investigated for IRI activity.	86
Figure 2.9. IRI activity of (4) oligosaccharides.	88
Figure 2.10. Comparative IRI activity of monosaccharides, disaccharides and oligosaccharides.	89

Figure 2.11. Structures of various small non-carbohydrate derived polyols investigated for IRI activity.	91
Figure 2.12. IRI activity of (16) small molecule polyols.	92
Figure 2.13. Structures of various high molecular weight polymers assessed for IRI activity.	96
Figure 2.14. IRI activity of different polymers of various molecular weights and polydispersities	97
Figure 2.15. Micrographs of polynucleated ice crystal wafers.	97
Figure 2.16. Selection of low MW compounds tested for IRI activity compared to 31 kDa PVA, 40 kDa Dextran and 140 kDa HES.	99
Figure 2.17. IRI activity of a range of concentrations of 9 kDa and 31 kDa PVA.	99
Figure 2.18. IRI activity of 9 kDa PVA and 31 kDa PVA at various concentrations over a 120-minute period.	101
Figure 2.19. Micrographs of polynucleated ice crystal wafers after 120 minutes.	102
Figure 2.20. Assessment of critical micelle concentration (mg/mL) using fluorescence spectroscopy.	104
Figure 2.21. Micrographs illustrating ice crystal growth during freezing at various cooling rates.	108
Figure 2.22. Micrographs of DMSO solutions cooled to -80 °C at 40 °C/min.	108
Figure 2.23. DSC traces upon cooling various concentrations (% (v/v)) of DMSO.	111
Figure 2.24. DSC traces upon thawing various concentrations (% (v/v)) of DMSO.	112
Figure 2.25. DSC traces upon cooling various concentrations (mg/mL) of 9 kDa PVA.	114
Figure 2.26. DSC traces upon thawing various concentrations (mg/mL) of 9 kDa PVA.	116
Equation 2.1: Calculation of MLGS (%) from MLGS (μm) of compound and MLGS (μm) of PBS.	120
Figure 2.27. Comprehensive overview of the IRI activities of all investigated monosaccharides and disaccharides.	123
Figure 2.28. Comprehensive overview of the IRI activities of all investigated	124

oligosaccharides and low MW polyols.	
Figure 3.1. Hypothermic storage of ovine RBCs.	138
Figure 3.2. Cytotoxicity of the cryoprotectant glycerol to RBCs.	141
Figure 3.3. Cytotoxicity of the cryoprotectant DMSO to human and ovine RBCs.	143
Figure 3.4. Ice recrystallization inhibition activity and composition of HES.	144
Figure 3.5. Cryopreservation of RBCs using HES.	147
Figure 3.6. Impact of thawing temperature (°C) on ovine RBC cryopreservation.	149
Figure 3.7. Cytotoxicity of 15 mg/mL 9 kDa PVA to ovine RBCs.	151
Figure 3.8. Cryopreservation of ovine RBCs supplemented with 130 mg/mL HES and/or 10 mg/mL 9 kDa PVA.	152
Figure 3.9. Cryopreservation of ovine RBCs with either 9 kDa PVA or 8 kDa PEG.	154
Figure 3.10. Impact of thawing temperature (°C) on human RBC cryopreservation.	156
Figure 3.11. Cryopreservation of human RBCs supplemented with 215 mg/mL HES and/or 1 mg/mL 9 kDa PVA.	157
Equation 3.1. Equations used to calculate (A) (%) Haemolysis and (B) (%) Cell Recovery of ovine and human RBCs.	160
Equation 4.1. Calculation of (%) relative metabolic activity using the MTT assay.	175
Figure 4.2. Cryopreservation of A549 cells with various concentrations of DMSO.	177
Figure 4.3. Cytotoxicity and cryopreservation impact of 9 kDa PVA on A549 cells.	179
Figure 4.4. Cryopreservation of A549 cells with 9 kDa PVA, 31 kDa PVA, 8 kDa PEG and lower DMSO (% (v/v)) concentrations.	180
Figure 4.5. Relative uptake of 5 mg/mL 9 kDa PVA conjugated with FITC in A549 cells.	183
Figure 4.6. Cytotoxicity and cryopreservation impact of 9 kDa PVA on BeWo cells.	186
Figure 4.7. Cryopreservation of BeWo cells with 6 % (v/v) DMSO and 9 kDa PVA.	187
Figure 4.8. Qualitative assessment of BeWo cell syncytialization subsequent to forskolin treatment (50 µM).	189
Figure 4.9. Quantitative assessment of BeWo cell syncytialization subsequent to	190

forskolin treatment (50 μ M).

Figure 4.10. Cytotoxicity of 9 kDa PVA, 31 kDa PVA and DMSO on Confluent FAO cells.	193
Figure 4.11. Cryopreservation of FAO cells with various concentrations of DMSO.	194
Figure 4.12. Cryopreservation of FAO cells with 6 % (v/v) DMSO and 9 kDa PVA.	195
Figure 4.13. TAT assay standards and measurements with FAO cells.	197
Figure 4.14. Cryopreservation of FAO cells with 6 % (v/v) DMSO and 9 kDa PVA at smaller concentration intervals.	198
Figure 4.15. Phase contrasted micrograph of A549 cells after MTT assay.	205
Equation 4.1. Calculation of (%) Cell recovery using the MTT assay.	205
Figure 4.16. Phase contrasted micrograph of A549 cells after NR assay.	206
Equation 4.2. Calculation of (%) relative dye uptake using the NR assay.	206
Figure 4.17. Assessment of resorufin and hydroresorufin production in FAO cells.	207
Equation 4.3. Calculation of (%) relative fluorescence using the resazurin assay.	208
Equation 4.4. Beer-Lambert law	209
Equation 4.5. Calculation of 9 kDa PVA – FITC uptake.	210
Figure 5.1. Phase contrast light micrographs of primary rat hepatocytes.	225
Figure 5.2. Cytotoxicity of 9 kDa PVA to rat hepatocytes.	227
Figure 5.3. Impact of 9 kDa PVA on the cryopreservation of rat hepatocytes.	228
Figure 5.4. Phase contrast light micrographs of mouse mesenchymal stem cells.	229
Figure 5.5. Impact of 9 kDa PVA on the cryopreservation of Mouse MSCs.	231
Figure 5.6. Visual assessment of mouse MSC adipogenesis.	232
Figure 5.7. Fluorescence intensities of Hoechst 33258 and LipidTOX ^{IM} Red as indicators of adipogenesis.	233
Equation 5.1. Calculation of (%) Cell viability at specific time points using the resazurin assay.	238

CHAPTER 1.

1. INTRODUCTION.

1.1. IMPACT OF ICE IN THE MODERN WORLD.

Ice has and continues to play a pivotal role in the natural world. Historically ice has influenced the course of evolution as organisms attempt to occupy and inhabit every conceivable niche on earth with profound genetic consequences on divergence and speciation.¹ Paleoclimatology has in particular emphasized the impact of ice ages and the consequential genetic legacies that have been left behind as these climatic oscillations incite extinction events and apply a strong natural selection criterion.² Recent ice ages have also been attributed to influencing human migration patterns by analysis of mitochondrial DNA chronology.³ The reason for these dramatic shifts is that simply the formation of ice in biological systems tends to be highly destructive. Though many physical and behavioral adaptations have been abundantly recorded for centuries, these alone are not sufficient to explain how numerous species prosper in environments that even in the present day mankind struggles to subsist in.⁴ However this not only applies to extremes of cold but also extremes of heat⁵, pressure⁶, pH⁷ and altitude⁸ whereby oxygen and nitrogen availability is limited. The majority of extremophiles are microorganisms and thus have minimal capacity for physical or behavior adaptations and therefore unable to regulate

their temperature despite an excellent capacity to develop antimicrobial resistance mechanisms and utilize a wide variety of metabolites. Much interest has therefore been shown in identifying, isolating and manipulating the molecular mechanisms that permit their survival⁹, with advances in genomic sequencing enhancing the rate and reducing the cost at which an organism can be sequenced.^{10,11} Genomic sequencing has enabled prolific improvements in the molecular biology toolkit by providing thermostable enzymes including DNA polymerases and DNA ligases. Improvements have and continue to be exploited in related disciplines such as catalysis and biotechnology.

In contrast to other extremophiles there has been a comparatively limited amount of success in utilizing the molecular mechanisms of cold acclimatized species. However the scope for manipulating such adaptations is enormous especially in cryobiology and by association transplantation science and regenerative medicine. These fields currently have an over-reliance on organic solvents that are decidedly cytotoxic.¹²⁻¹⁴ There is also a demand from many engineering and materials science disciplines particularly in the area of transportation such as aviation^{15,16} but also in energy generation¹⁷⁻²⁰ and communications²¹. Therefore there is great potential for improvement and interest is intensifying due to the discovery of antifreeze (glyco)proteins (AF(G)Ps)²² and antifreeze proteins (AFPs)²³ from multicellular organisms. Understanding the mechanisms and the properties of these molecules in particular their interactions with ice is an ongoing pursuit with studies targeting the molecules directly but also in utilizing synthetically more accessible derivatives and polymeric mimics.²⁴

1.2. NATURAL MOLECULAR ADAPTATIONS.

1.2.1. Antifreeze (glyco)proteins (AF(G)Ps).

The discovery of Antifreeze (glyco)proteins (AF(G)Ps) occurred a little over 40 years ago shortly after the unusually high freeze tolerance of several antarctic²⁵ and arctic²⁶ fish species was identified and attributed to select abnormal body fluid characteristics.²⁷ The landmark paper of DeVries and Wohlschlag in 1969 was the first to describe the presence and influence of a mixture of glycoproteins (later termed AF(G)Ps) isolated from the serum of three antarctic fish species including the two very different species *Trematomus borchgrevinki* and *Dissostichus mawsoni* of the nototheniidae family.²⁸ Plus how these proteins accounted for approximately 30 % of the observable freezing point depression and postulated how AF(G)Ps enabled their survival in seawater at subzero (-2 °C) temperatures.²⁹ It was also noted that the contribution of AF(G)Ps to the freezing point depression was greater than expected for the given number of particles in solution (colligative effect). Colligative freezing point depression is defined by Blagden's law that states that in an ideal solution the freezing point depression of that solution is defined by the product of the molality, cryoscopic constant (H₂O = 1.853 °C.kg/mol) and van't hoff factors of any additional solutes.^{30,31} As a consequence and to account for the abnormally high freezing point depression there must be the existence of an active (non-colligative) property. Further work quickly acknowledged the presence of several AF(G)Ps of different molecular weights (MW) in the blood sera and an elemental analysis further clarified their composition.³² The composition of AF(G)Ps was proposed to be a tripeptide repeat consisting of one threonine and two alanine residues with an O-linked disaccharide moiety conjugated to each threonine residue. The disaccharide moiety of which was later confirmed as the complex disaccharide β-

D-galactosyl(1→3)- α -N-acetyl-D-galactosamine giving rise to a complete primary AF(G)P structure (Figure 1.1.).³³ The substitution of a minority of alanine residues for proline was also apparent in some low molecular weight (MW) AF(G)Ps from these early observations.³⁴ No known naturally occurring β -D-galactosyl(1→3)- α -N-acetyl-D-galactosamine substitutions were identified and this remains the case up to the present day emphasizing the importance of this specific disaccharide moiety, that is not frequent elsewhere in nature. However this disaccharide is present on a T-antigen associated with >85 % of human carcinomas.³⁵ The isolation and identification of AF(G)Ps from an arctic fish species occurred soon after.^{36,37} A significant freezing point depression had been previously noted though in the blood sera of another arctic fish species (*Eleginus gracilis*) prior to this.³⁸ AF(G)Ps have since also been discovered in several insect species.^{39,40}

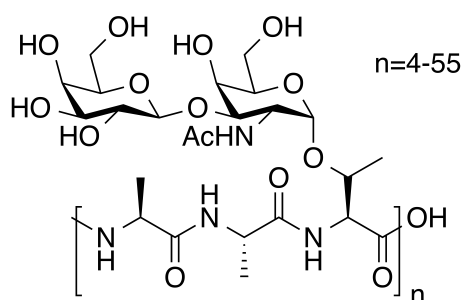


Figure 1.1. Structural representation of a typical AF(G)P. AF(G)P comprising of an AAT tripeptide backbone with an O-linked β -D-galactosyl(1→3)- α -N-acetyl-D-galactosamine disaccharide moiety, with AF(G)Ps isolated with between 4 and 55 repeat units.

The presence of AF(G)Ps in both arctic and antarctic fish species raised interest in exploring their evolutionary origins⁴¹ with a general consensus that AF(G)Ps in arctic and antarctic specimens arose by convergent evolution⁴² and how this was driven by ancient climatic changes.⁴³ A vast number of AF(G)Ps have now been identified and subcategorised according to their MW into 8 different groups.

Larger AF(G)Ps with MW values between 20 kDa and 34 kDa are categorised into AF(G)P groups 1-4 and small AF(G)Ps under 20 kDa into groups 5-8 with the smallest identified AF(G)P (AF(G)P8) just 2.4 kDa corresponding to tripeptide repeat units of between 4 and 55 in number.^{22,44,45}

As the prevalence of AF(G)Ps grew as did interest in their native expression and in their responsiveness to different thermal stimuli with seasonal changes in AF(G)P expression attributed to hormonal changes as hypophysectomised specimens lost the ability to modulate expression with changing surface water temperature.⁴⁶ AF(G)P expression has also been studied in depth in a controlled environment showing how the concentration of all AF(G)Ps decreases over a 16 week period with specimens incubated at the comparatively high temperature of +4 °C.⁴⁷ AF(G)Ps have also been confirmed to be distributed in numerous body fluids with the highest concentration detected in blood plasma but with notable amounts in peritoneal, pericardial and extradural fluids also.⁴⁸

Understanding the interaction of AF(G)Ps with water and ice and how this is related to AF(G)P structure, which may elucidate clues as to their mechanistic functionality (Section 1.3.), soon became a popular avenue of interest. Numerous techniques have been utilised to investigate the primary, secondary and tertiary structure of AF(G)Ps.⁴⁹ The primary structure of AF(G)Ps has been elaborated in brief prior and consists principally of a tripeptide (AAT) backbone with nearly all AF(G)Ps having a C-terminal sequence ending in two alanine residues. A notable exception however has been identified though in an AF(G)P isolated from *Eleginus gracilis* with a penultimate arginine residue.⁵⁰ Arginine residues have in addition to this been identified to rarely substitute for threonine residues within the peptide backbone.⁵¹ Proline residues have also been observed in low MW AF(G)Ps substituting for alanine residues with a consequence on secondary

structure elements.⁵² One of the first investigatory studies using circular dichroism (CD) pertained that AF(G)Ps contain minimal α -helical and β -sheet content.³² Raman spectroscopy and proton NMR (90 MHz) studies from around the same period tended to support this also.^{53,54} Advancements in both proton NMR (300 MHz)⁵⁵ and carbon NMR (68 MHz)⁵⁶ have driven a better understanding of the solution conformation of AF(G)P supporting a random coil configuration. However even more recent experiments using a combination of infra red (IR) spectroscopy and proton NMR (500 MHz) that focused on a short chain (14 residue) proline containing AF(G)P8 showed local ordering that aided to induce a type II polyproline helical conformation. Using the same parameters a mixture of AF(G)Ps 1-5 elicited no local ordering, supporting a random coil conformer, with no long range ordering present in either AF(G)P8 or AF(G)P 1-5 subsets.^{57,58} Molecular dynamics (MD) simulations further supported the formation of a type II polyproline helical conformer in the same proline containing AF(G)P8 but stressed that several other conformations are attainable with energetically equal minima.⁵⁹ Carbon NMR (100 MHz) and fourier transform infra red spectroscopy (FTIR) experiments further support the highly flexible structure of AF(G)Ps.⁶⁰ Therefore AF(G)Ps do not share many secondary structure elements typical of most proteins. As a consequence there is no well defined three dimensional model or precise tertiary structure.⁶¹ The structure of AF(G)Ps is no doubt influenced heavily by the presence of the disaccharide moieties, the majority of modifications of which are known to completely negate antifreeze activity.^{32,62} The comparatively high density of carbohydrates makes conventional structural biology approaches more difficult also.⁶³

1.2.2. Antifreeze Proteins (AFPs).

Soon after the discovery of AF(G)Ps, serum proteins with similar properties including an ability to induce a non-colligative freezing point depression were identified from the arctic fish species *Pseudeopluronectes americanus*⁶⁴ but lacked any carbohydrate content. These proteins were termed as antifreeze proteins (AFPs) and are more akin to traditional globular proteins. From this point to the present day many AFPs have been identified in a vast array of organisms. Along with numerous fish species, AFPs have been isolated from insects^{65,66}, plants⁶⁷⁻⁷¹, fungi⁷², yeast⁷³ and bacterium⁷². However unlike with AF(G)Ps that have a uniform primary structure bar for a few select proline and arginine substitutions, AFPs comprising a wide variety of primary and by virtue secondary and tertiary structures have been categorized. In fish species alone four significantly different variants of AFP (type I-IV)⁷⁴⁻⁷⁷ have been classified with instances of some species expressing more than one type.⁷⁸ AFPs present within insects are also structurally diverse.⁷⁹⁻⁸¹ AFP diversity is emphasized in a recent review by Haridas and Naik that highlights 11 distinct AFP variants.⁸² As AFPs lack the structural complexities caused by the carbohydrate content of AF(G)Ps and have MWs from as low as 2.7 kDa many AFP structures have been solved by both NMR and x-ray crystallography (Figure 1.2.). Structural biology has therefore elucidated the diversity in AFP structures giving a much more complicated view of their functionality (and the functionality of AF(G)Ps additionally). Therefore AFP structures containing predominantly an α -helical, β -sheet, random coil arrangement or even a combination of all three have been reported.

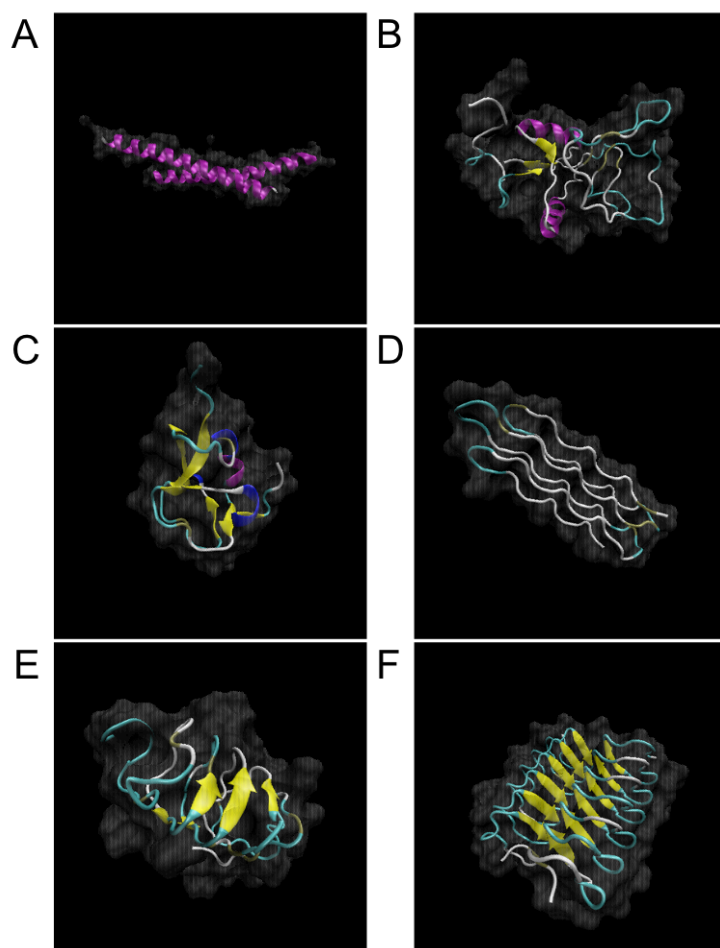


Figure 1.2. Structural representations of various AFPs highlighting secondary structure motifs and structural diversity. (A) AFP type I⁷⁴, (B) AFP type II⁷⁵, (C) AFP type III⁷⁶, (D) AFP (*Hypogastrura harveyi* (Snow Flea))⁸¹, (E) AFP (*Choristoneura fumiferana* (Spruce budworm))⁸⁰ and (F) AFP (*Tenebrio molitor* (Yellow mealworm beetle))⁸³.

The lack of available material from source due to the logistical problems in attaining specimens in addition to refining AFPs and AF(G)Ps of a suitable purity has always been a bottleneck. However in the present day many groups are able to express various AFPs from recombinant systems.^{84,85} and perform site-direct mutagenesis experiments which has helped to improve mechanistic understanding.⁸⁵ AF(G)Ps however have yet to be expressed in traditional unicellular recombinant systems due to the complexities of glycosylation which is a posttranslational modification typically seen in higher eukaryotes. However an

insect AF(G)P from *Ixodus scapularis* has been successfully incorporated into *Drosophila melanogaster* that then displayed an improved freeze tolerance.⁴⁰ Therefore the application of AFPs and AF(G)Ps could be promising as expression systems improve further, though the use of non-native proteins could raise immunogenicity problems.⁸⁶ In spite of these improvements there is an overwhelming issue concerning the application of AFPs and AF(G)Ps in cryopreservation in that they have been shown to have significant cytotoxic effect in *in vitro* models.⁸⁷ More importantly AFPs and AF(G)Ps failed *in vitro* and *ex vivo* to improve the cryopreservation of biological materials on several occasions.^{88,89} The details and reasoning of which are highlighted in Section 1.5. and emphasize the need for mimics that eliminate any detrimental effects or properties.

1.2.3. Non-protein based strategies of cold acclimatization.

A final area of interest is in non-protein based strategies that have been observed frequently in terrestrial organisms but predominately in insects and amphibians.^{90,91} These approaches were first described even before the discovery of AF(G)Ps or AFPs in the late 1950s.^{92,93} These strategies have focused on both freeze avoidance and freeze tolerance whilst AFPs and AF(G)Ps only enable the former and not latter⁹⁴ though behavioral adaptations have also been recorded in these organisms to aid thermoregulation.⁹⁵ These freeze tolerance and freeze avoidance mechanisms have allowed several organisms to survive in harsher environments even at temperatures as low as -60 °C.⁹⁶ Non-protein based strategies tend to work by the perturbation of metabolic pathways in response to cold stimuli induced by seasonal changes to produce very high concentrations of a single small organic molecule be it either glycerol, sorbitol, glucose, trehalose or one of several other polyols in conjunction with anti ice

nucleating factors (Figure 1.3.).⁹⁷ This is a very energy intensive process and such polyols can constitute up to 10 % of dry weight and therefore this process is only undertaken annually with the onset of winter.⁹⁸

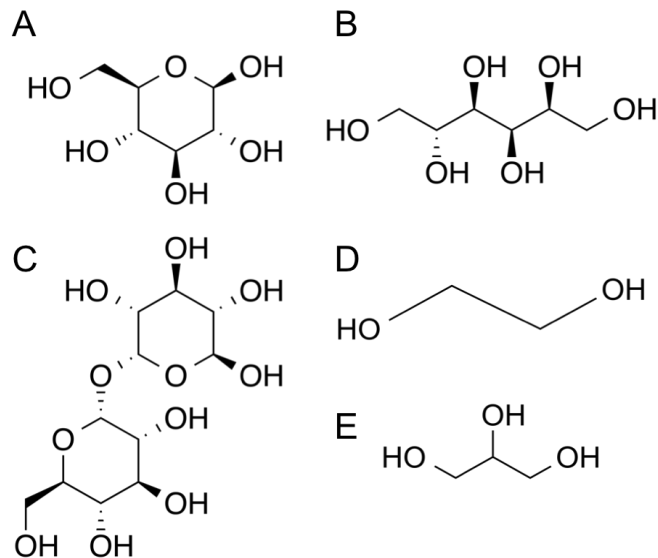


Figure 1.3. Representative non-protein based low MW weight cryoprotectants (non-exhaustive list).⁹⁴ (A) Glucose, (B) Sorbitol, (C) Trehalose, (D) Ethylene Glycol and (E) Glycerol.

In addition to this such organisms often suppress metabolic functions (undergo diapause) and promote extensive dehydration thereby increasing solute concentration in any remaining water content and causing a lowering of the supercooling point⁹⁸ though this has not been observed in all cases.⁹⁹ The rate of ice formation (if any) is then very gradual and occurs over a period of hours or even days, though most ice formation is extracellular even extensive intracellular ice formation that is typically more injurious has been reported to be reasonably well tolerated.¹⁰⁰ As a consequence organisms have been frequently reported to pertain an ice content of 65 % of total body water.¹⁰¹ Though values as high as 82 % have been documented.¹⁰² More recently however the isolation of a xylomannan¹⁰³ from the Alaskan insect *Upis ceramoides* akin to AFPs and AF(G)Ps is the first non-protein compound to be isolated from nature with similar properties and therefore hypothesized to have an analogous cryoprotective

effect¹⁰⁴ with other antifreeze xylomannans recently verified in 8 other species including the plant *Solanum dulcamara* and frog *Rana lessonae*.¹⁰⁵ The identification of a diverse number of solutions that nature has evolved inspires a great number of potential applications for clinical benefit. The precise understanding of the mechanisms and activities of AFPs and AF(G)Ps in particular as these are present at low concentrations could elucidate improved strategies for the cryopreservation of cells, tissues and organs.¹⁰⁶

1.3. MOLECULAR INTERACTIONS OF AFPs AND AF(G)Ps WITH ICE.

The properties that enable AFPs and AF(G)Ps to confer antifreeze activity *in vivo* has been of interest in order to attain whether or not such properties can be translated *in vitro* for use in cryopreservation.¹⁰⁷ As AF(G)Ps were discovered it was quickly documented that they were able to depress the freezing point of a solution by an amount far greater than expected for their given concentration (colligative effect). Therefore another process must be taking place in order to explain this pronounced lowering of the freezing point transition or non-colligative effect that accounted for approximately 30 % of the freezing point depression seen in these organisms.^{29,32} Currently three distinctive properties have been attributed to AFPs and AF(G)Ps that describe and explain their antifreeze properties and remain measures for quantifying the effectiveness of AFP and AF(G)P mimics.²⁴

1.3.1. Ice Recrystallization Inhibition (IRI).

One property of AFPs and AF(G)Ps is the ability to prevent or impede the kinetic growth or ripening of ice crystals during thawing in a process termed ice recrystallization inhibition (IRI). Importantly this does not alter the freezing point or alter probability of nucleation (the formation of ice crystals). The process of ice recrystallization is where by larger ice crystals grow at the expense of small adjacent ice crystals in order to minimize the total surface energy in a process similar to ostwald ripening.¹⁰⁸⁻¹¹⁰ AF(G)Ps and AFPs are able to reduce this process in a concentration dependant manner such it almost becomes indistinguishable over a reasonable time period.¹¹¹ A physical measure with suitable reproducibility of IRI activity was first described by Knight *et al.* who

developed the now commonplace standard for measuring IRI activity the “splat” assay.¹¹² The development of the “splat” assay was driven by the inadequacies of prior methods that involved the freezing and annealing of supercooled solutions. Previous techniques used a small volume of a supercooled solution between two thin glass slides in which grain (ice crystal) size determination was driven by both the spontaneous rate of nucleation in addition to growth, with the unpredictability of nucleation limiting satisfactory replication. The “splat” assay (Section 2.5.3.) overcomes this by impacting a small droplet ($\approx 10 \mu\text{L}$) from a height of approximately 2 m on to a pre-cooled surface ($> -50 \text{ }^\circ\text{C}$) forming a polycrystalline wafer (thereby removing the rate of nucleation as a variable) comprising of very small ice crystals ($< 10 \mu\text{m } \varnothing$) of a thickness typically less than $50 \mu\text{m}$. That is then annealed at a constant temperature between $-6 \text{ }^\circ\text{C}$ and $-8 \text{ }^\circ\text{C}$ for a desired period of time (normally 30 minutes) before quantifying grain size. The value reported is frequently the mean value of the largest dimension of the ten largest ice crystals within a significant field of view (Figure 1.4.) and termed the mean largest grain size (MLGS). An isotonic control is often used as a positive control (100 %) by which IRI activity is compared. Domain recognition tools have also been developed that aim to improve and hasten image analysis.¹¹³ Several modifications have been developed since that use solutions consisting of a high proportion of solutes (up to 30 % (w/v)) such as sucrose or hydroxyethyl starch (HES) in addition to the analyte of interest.^{114,115} Another method that uses capillary tubes for the simultaneous measurement of multiple samples has also been reported.¹¹⁶ The splat assay has been widely used to report relative IRI values for many AFPs, AF(G)Ps and their mimics.¹¹⁷⁻¹²⁰ IRI is the property of AFPs and AF(G)Ps that is understood to be of the most benefit in cryopreservation by attenuating damage arising from ice crystal growth.

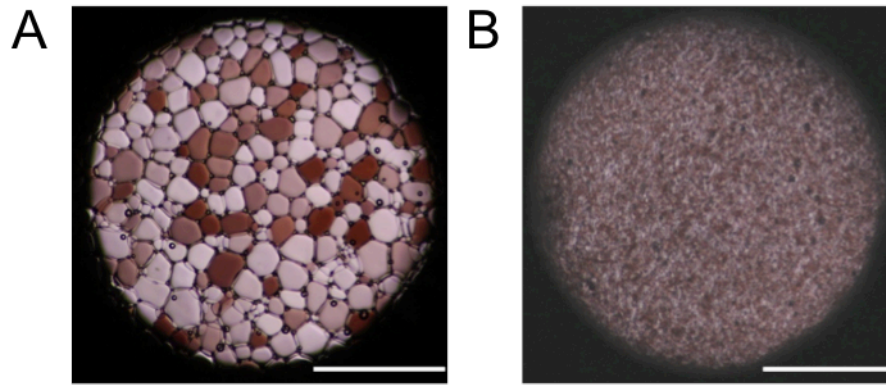


Figure 1.4. Example micrographs taken from “splat” IRI measurements. (A) Positive control (PBS) exemplifying ice recrystallization over a 30 minute period at -6 °C and (B) ice recrystallization in the presence of a IRI active compound under the same experimental conditions (scale bar = 400 μm).

1.3.2. Thermal Hysteresis (TH).

The second property that AFPs and AF(G)Ps exhibit is thermal hysteresis (TH). Thermal hysteresis is where by the freezing point of a solution is lowered but the melting point of the same solution is unchanged. This as a result creates a gap between the freezing and melting points. An important observation is that any ice crystals held isothermally within this gap will neither shrink nor grow henceforth leading to the term thermal hysteresis (TH) and was among the first characteristics of AF(G)Ps identified.¹⁰⁷ The size of the TH gap varies with different AFPs, AF(G)Ps and mimics giving different values but the highest TH gaps observed tend not to be greater than 1.5 °C with the majority lower than 0.5 °C.^{61,72,121} However a few exceptional “hyper-active” AFPs have been isolated that generate a TH gap in excess of 2 °C.¹²²⁻¹²⁴ TH is typically measured at precise temperature intervals using a nanolitre osmometer to accurately monitor changes in ice crystal size indicating the upper and lower TH gap boundaries.¹²⁵

TH activity has been strongly associated with the final property of AFPs and AF(G)Ps the ability to alter ice crystal morphology.

1.3.3. Dynamic Ice Shaping (DIS).

The third and final property that AFPs and AF(G)Ps exhibit on the freezing and thawing process is dynamic ice shaping (DIS). DIS is a phenomenon that results in the alteration of the ice crystal growth habitat resulting in its extreme the formation of ice crystals with a hexagonal bipyramidal “needle-like” morphology (Figure 1.5.A). The onset of DIS has been studied in great depth with the following mechanistic understanding. A starting point is to consider the 1977 article by Raymond *et al.* who first described an adsorption inhibition model for the binding and interaction of AF(G)Ps to ice and links adsorption to TH activity and discusses how adsorption leads to DIS.¹²⁶ Later an article by Knight *et al.* who observed that an (α -helical) AFP interacted and bound to a single specific plane of ice only termed the (6) prism faces (A-axis). Binding to the prism faces leaves only the opposing perpendicular (2) basal planes (C-axis) unbound and able to expand (Figure 1.5.B)¹²⁷ giving rise to a step-pinning model that supports these observations (Figure 1.5.C).^{24,128} This adsorption inhibition process can further explain the freezing point depression leading to TH as growth on the prism faces forms a surface with a highly convex curvature (Figure 1.5.C) that is energetically unfavourable (Kelvin effect).²² NMR studies have further supported the adsorption inhibition model showing the complementary fit of AF(G)Ps to the ice crystal lattice.¹²⁹ Houston *et al.* explored the adsorption inhibition process further and showed how the modification of an oligopeptide derived from a type I α -helical AFP resulted in a reduction in DIS activity inciting a milder change in ice crystal morphology indicating that binding to the ice crystal lattice is not a on/off behaviour.¹³⁰ Ice shaping events with a range of AFPs, AF(G)Ps and mimics

have since been shown^{77,131,132} in a concentration dependant manner and it is this property that is thought to create a prohibitive effect for the application of native AFPs and AF(G)Ps as cryopreservatives. The formation of hexagonal bipyramidal “needle-like” structures has been shown to increase mechanical damage, a property that AFP and AF(G)P mimics attempt to suppress, whilst retaining the beneficial effect of IRI.

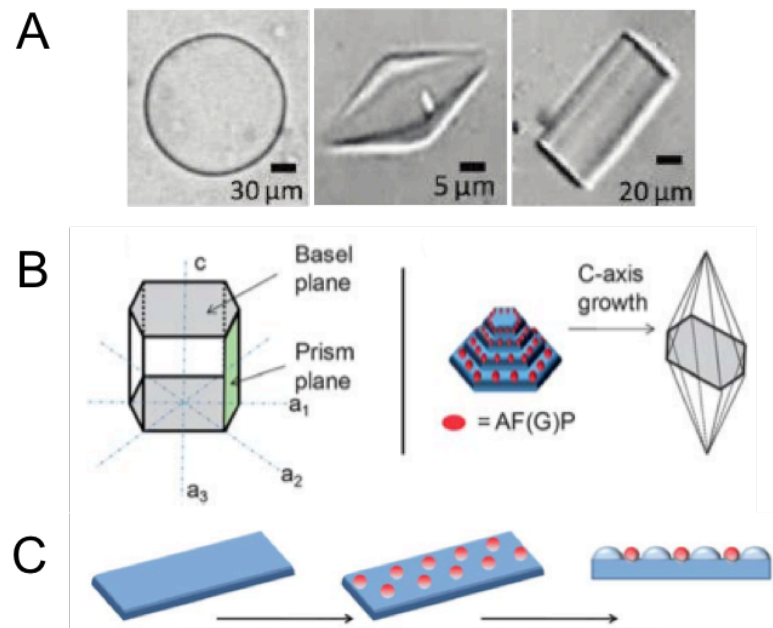


Figure 1.5. Mechanisms and consequences of DIS. (A) Representative micrographs of ice crystal morphologies (and sizes) arising from left to right no ice shaping, strong DIS effect and a mild DIS effect (adapted from Peltier *et al.*, 2010).¹³¹ (B) Illustration of the prism and basal planes showing how AF(G)P binding to the prism plane enables growth in the basal plane only and thereby adopting a hexagonal bipyramidal structure. (C) Depiction of the step pinning model showing AFP/AF(G)P (red) binding to the ice crystal lattice and the formation of a curved surface (Kelvin effect) forming between each binding site. (adapted from Gibson, M.I., 2010).²⁴

1.4. SYNTHETIC MIMICS OF AFPs AND AF(G)Ps.

Given the complexities of isolating AFPs and AF(G)Ps from primary sources and recombinant systems in addition to problems typically associated with the application of non-host proteins many synthetic mimics principally close derivatives of AF(G)Ps have been developed.¹³³ Synthetic strategies have many benefits in that synthetic mimics allow the impact of single tailored made modifications on the aforementioned properties of IRI, TH and DIS to be assessed. These alterations have created an improved understanding on how AF(G)Ps interact and manipulate ice. AFP variants through site-specific mutagenesis with reduced activities have elucidated the importance of key residues but tend to be too large to be synthesized by solid phase peptide synthesis (SPPS) limiting throughput. Progressive improvements have begun to lead to the rational design of synthetic mimics that are more synthetically accessible, scalable with greater biochemical stability and that are less likely to cause immunogenicity concerns. These mimics tend to be biosynthetically inaccessible to natural expression systems but with further refinement could perhaps be produced artificially on a significantly sufficient scale.

The work of Ben *et al.* has arguably contributed the most substantial progress over the last decade in this regard beginning in 1999 with the synthesis of a AF(G)P mimic that consisted of a tripeptide backbone with three repeat units using SPPS.^{134,135} Following on a single β -D-galactose per tripeptide unit was conjugated by a C-linkage that is less likely to be susceptible to biochemical degradation (Figure 1.6.A).¹³⁶ Soon after more complex longer chain C-linked derivatives were synthesised.^{137,138} However it was not until 2005 that several C-linked AF(G)P derivatives (Figure 1.6.B) were tested and reported to have IRI activity in a concentration dependant manner with no TH activity successfully

separating these two properties. A critical observation was that IRI activity was strongly influenced by the linkage length that separated the galactoside moiety from the peptide backbone. A longer linkage length (Figure 1.6.B (n=2,3)) corresponded to a dramatic reduction in IRI activity whilst the shortest linker the most representative of AF(G)Ps had a much higher IRI activity. (Figure 1.6.B (n=1)).¹²⁰ This IRI activity was then found to be comparable to freshly isolated AFGP8^{87,113} with the effect of AFGP8 aggregation induced at higher concentrations and corresponding effect on TH activity also explored.¹³⁹ Later in 2008 Czechura *et al.* showed that substituting galactose for either glucose, mannose and talose monosaccharide moieties negated IRI activity emphasizing the importance of retaining a galactose moiety in synthetic preparations which further supports the prevalence of the naturally occurring β -D-galactosyl(1 \rightarrow 3)- α -N-acetyl-D-galactosamine disaccharide moiety.¹⁴⁰ The variation in IRI activity between each of these monosaccharides in addition to several disaccharides was then attributed to differences in their hydration index which was reflected by their (weak) IRI activities as stand alone entities.¹⁴¹

Following on, a more extensive investigation into linkage length using derivatives of Figure 1.6.A and Figure 1.6.B highlighted a preferred separation distance corresponding to differences in solution conformation as ascertained by CD and MD. CD studies failed to illustrate any significant differences in secondary structure composition but using a model compound of an IRI active mimic in MD simulations a unique orientation resulting in a hydrophobic pocket that interacts favourably with the quasi liquid layer (QLL) of the ice crystal lattice was identified.¹⁴² The development of a triazole containing C-linked AF(G)P caused a dramatic reduction in IRI activity regardless of the linkage length employed (Figure 1.6.C) so that the chemical composition (bulkiness) of the linker is as important as the separation distance.¹⁴³ A similar loss of IRI activity was

additionally identified in fluorinated mimics and in mimics with increasing carbohydrate hydrophobicity.¹⁴⁴ The differences in the IRI activities of several monosaccharides and disaccharides as cryoprotectants (at high concentrations) has since been investigated with human embryonic liver cells (WRL-68)¹⁴⁵ and umbilical cord blood¹⁴⁶. A beneficial cryoprotective effect was also shown decisively with active C-linked AF(G)P mimics and WRL-68 cells.¹⁴⁷

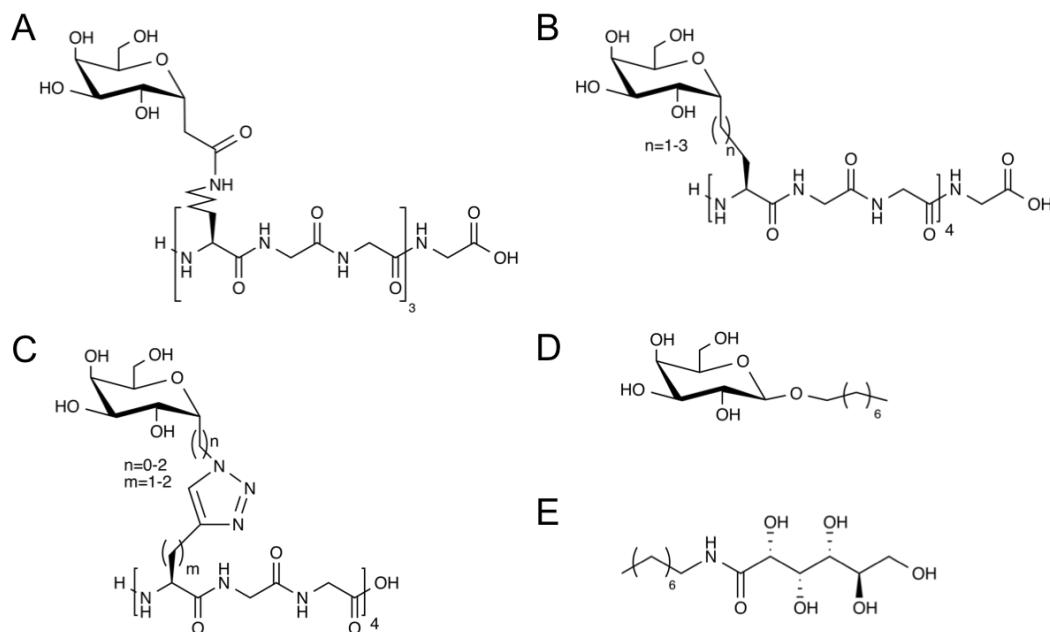


Figure 1.6. AF(G)P analogues developed by Ben and co-workers. (A) Original C-linked serine derivative¹³⁶, (B) C-linked galactosyl serine derivative¹²⁰, (C) C-linked triazole serine derivative (inactive)¹⁴³, (D) *n*-octyl- β -D-galactopyranoside¹⁴⁸ and (E) *N*-octyl-D-gluconamide.¹⁴⁸

In 2012 Wilkinson *et al.* reported a complete synthesis of AF(G)P with 2, 4, 8, 12, 16 and 32 repeat units (1.2 kDa – 19.5 kDa) with 8 repeat units or greater giving significantly high IRI activity similar to AF(G)P8 where as the shorter 2 and 4 repeat unit polypeptides had no significant activity even at concentrations 100x higher. Notable TH values were also reported in each compound that displayed significant IRI activity.¹⁴⁹ However the largest 19.5 kDa AF(G)P prepared also

represents the largest AF(G)P synthesised to date and indeed one of the largest native glycoproteins of any kind. Soon after it was reported that *n*-octyl- β -D-galactopyranoside possessed a strong IRI activity where as *n*-octyl- β -D-glucopyranoside did not with this relationship reversed when examining *N*-octyl-D-aldoamides, though in each instance it was the presence of the large hydrophobic alkyl chain that proved critical (Figure 1.6.D and Figure 1.6.E.).¹⁴⁸ Finally Corcilius *et al.* synthesised a range of peptides and glycopeptides with type II polyproline helical topology though only two derivatives displayed significant IRI activity.¹⁵⁰

Several other research groups have also synthesised AF(G)P mimics including Miller *et al.* who synthesised O-linked triazole containing mimics using microwave assisted SPPS.¹⁵¹ Within the same group Peltier *et al.* investigated the effect of substitutions in the peptide backbone (with select proline for alanine replacements) and saccharide moiety (β -galactose and α -*N*-acetyl-galactosamine) compared to AF(G)P8 with respect to DIS and TH activity. Whilst galactose containing analogues had no DIS activity except at the highest concentration tested of 80 mg/mL, those containing α -*N*-acetyl-galactosamine did have a profound influence on DIS with either peptide backbone configuration in a concentration dependant manner forming hexagonal rods at 20 mg/mL. At higher concentrations (80 mg/mL) morphology changed to the widely observed hexagonal bipyramidal structure (Figure 1.5.A), where as this structure was observed with native AF(G)P8 (β -D-galactosyl(1 \rightarrow 3)- α -*N*-acetyl-D-galactosamine disaccharide) at a much lower concentration of 20 mg/mL.¹³¹ These studies show how alterations in the conjugated saccharide can have profound influence on ice crystal morphology with the formation of hexagonal bipyramidal structures. Hexagonal bipyramidal structures have been deemed to be detrimental to cells as “needle-like” morphologies incite greater mechanical damage during

cryopreservation negating any beneficial IRI activity. Using proton NMR they were able to determine the importance of the appropriate solution conformation, how the *N*-acetyl-amine group and α -linkage were key features of any interacting conformation that modified the ice crystal growth habitat. Eliminating DIS effects whilst maintaining IRI activity would be highly desirable. Ben *et al.* showed with similar monosaccharide containing analogues (Figure 1.6.B) that did display an IRI activity a lack of TH activity successfully separating these properties.¹²⁰ Tachibana *et al.* showed that the removal of the *N*-acetylamine group from *N*-acetylgalactosamine resulted in a loss of both TH and DIS activity highlighting how these two properties are linked.¹⁵² In the same study Tachibana *et al.* who successfully produced a variety of AF(G)P mimics alongside an earlier reported synthesis (one of only three) of AF(G)P (8 repeat units)¹⁵³ also showed the importance of the *N*-acetyl-amine motif and α -configuration of the O-linked glycosidic linkage and further concluded that a type II polyproline helical like conformation is required for antifreeze activity.¹⁵⁴

Many others have also investigated synthetic methodologies for the production of AF(G)P mimics including Garner *et al.* who used a native chemical ligation-desulphurization strategy to produce α -*N*-acetyl-galactosamine peptides containing up to six repeat units.¹⁵⁵ Heggemann *et al.* have also reported the use of a microwave enhanced synthetic strategy to produce a range of short chain AF(G)P mimics with various backbone substitutions including serine and glycine that are not seen in any native AF(G)Ps in addition to proline containing polypeptides. These mimics closely resemble those seen elsewhere in literature (i.e. O-linked α -*N*-acetyl-galactosamine peptides without backbone modifications) that displayed potent IRI activity. The work of Heggemann *et al* further supports how the α -*N*-acetyl-galactosamine moiety is critical for activity as discussed prior with a fully acetylated galactoside containing mimic (lowering its hydration index)

possessing a significantly reduced IRI activity. Three mimics that contained altered peptide backbone structures had minimal IRI activity at the highest concentration studied of 4 mg/mL. 4 mg/mL is low by comparison to some other studies but up to three and one hundred times greater than the concentrations of other mimics in the same study that possessed potent activity. The lack of activity was despite the presence of the critical α -*N*-acetyl-galactosamine monosaccharide moiety. The only exception to this (Figure 1.7.A) is a proline containing analogue that in contrast to others is able to adopt a regular periodic (type II polyproline helix) secondary structure whereas those with substituted glycine and serine residues plus irregularly placed proline residues are not and henceforth accounts for the difference in IRI activity.¹⁵⁶ Periodicity highlights the importance of AF(G)P mimics being able to adopt consistent and regular conformations that are inhibited by residues that promote flexibility such as glycine or greater steric hindrance such as (unconjugated) serine residues. Periodicity is an important conjecture in the rational design of AF(G)P mimics. The same group soon after reported the synthesis of small AF(G)P molecules and that these synthetically derived AF(G)Ps had comparable properties to naturally derived AF(G)P8. These short chain mimics further clarified the importance of chain length with increasing chain length purporting to a higher activity with CD data supplementing the likelihood of a type II polyproline helical conformation.¹⁵⁷ However oligoproline peptides with triazole conjugated α -*N*-acetyl-galactosamine and β -D-galactosyl(1 \rightarrow 3)- α -*N*-acetyl-D-galactosamine moieties (Figure 1.7.C) did not illicit strong IRI activity despite the formation of type II polyproline helical secondary structure elements as noted by CD.¹⁵⁸ This lack of activity is presumed to be due to the presence of the large triazole functional group as a spacer agreeing with findings (Figure 1.6.C) by Capicciotti *et al.*¹⁴³ Finally the work of Nishimura *et al.* has to be reviewed with regards to improving the synthetic pathways of attaining relevant glycopeptide mimics^{159,160}

and in understanding AF(G)P function.¹⁵² However interestingly a 2009 publication that details the production of cyclic AF(G)P mimics consisting of 2,3 and 4 repeat units (Figure 1.7.B) that do not possess the typical secondary structure elements due to this cyclization with a characteristic shift in CD spectra do have equivalent TH and DIS characteristics (IRI was not measured). The synthesis of cyclic AF(G)Ps represent the first instance of AF(G)P like glycopeptides with antifreeze properties that do not have the otherwise necessary type II polyproline helical conformation seen elsewhere.¹⁶¹

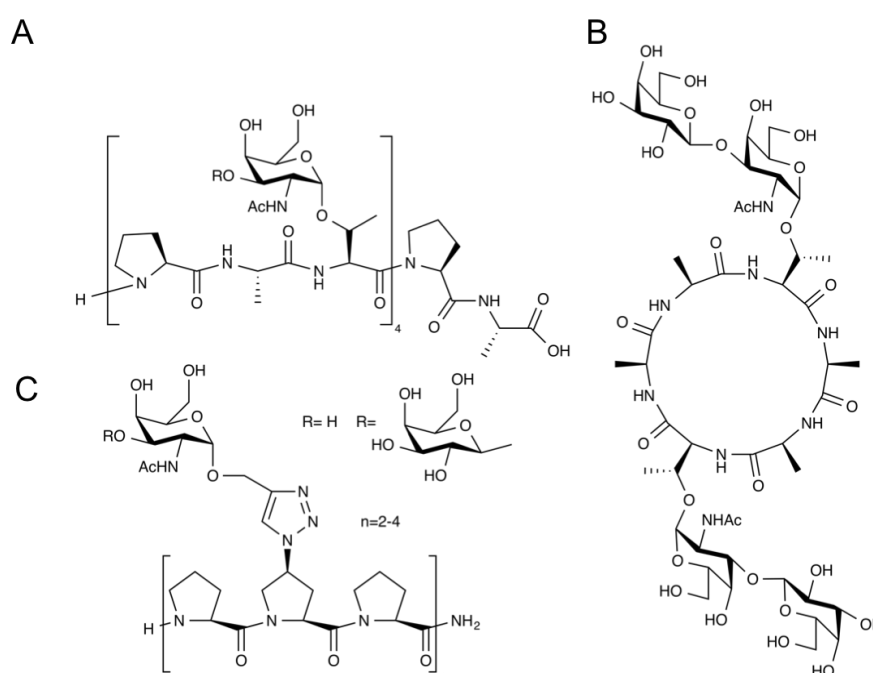


Figure 1.7. Other AF(G)P mimics. (A) Antifreeze active proline containing AF(G)P mimic with a *N*-acetyl-galactosamine monosaccharide moiety, activity is only conserved with periodic proline substitutions.¹⁵⁶ (B) Example of an antifreeze active cyclic (2 repeat units) AF(G)P mimic that does not form a typical type II polyproline helical conformation¹⁶¹ and (C) an antifreeze inactive AF(G)P mimic that does form a type II polyproline helical conformation but the presence of the comparatively bulky triazole spacer inhibits antifreeze activity.¹⁵⁸

A high number of the previously discussed AF(G)P mimics have identified a relatively strict criterion for antifreeze activity, though in some instances IRI

activity has been successfully separated from TH and DIS activity. However despite the production of many AF(G)Ps, several non-protein like molecules have been identified that have minimal resemblance to any of the mimics discussed (Figure 1.6. and Figure 1.7.) but strong antifreeze properties. The first of these is the synthetically simple and commercially available polymer poly(vinyl alcohol) (PVA) (Figure 1.8.A) that has been shown to have a strong IRI activity even over prolonged periods of time.¹¹⁷ PVA has also been demonstrated to have a strong concentration and MW dependence with regards to IRI potency.^{118,162} However IRI activity is reduced and eventually lost with decreasing MW and with the gradual acetylation of the polymer backbone¹⁶³ highlighting the importance of hydration which is consistent with other AF(G)P mimics and their corresponding IRI activities.¹⁴¹ This is further emphasized with observations that neither poly(ethylene glycol) (PEG) (Figure 1.8.B) which is isomeric to PVA, poly(vinyl pyrrolidone) (PVP) (Figure 1.8.C) or poly(acrylic acid) (PAA) (Figure 1.8.D) have IRI activity consistent with their lack of hydroxyl groups.¹⁶⁴ Furthermore DIS has been shown with unusually high concentrations (10 mg/mL) of a large MW PVA (27 kDa)¹⁶⁵ and only a mild TH effect even at 50 mg/mL and a MW of 13 kDa.¹⁶⁶ Further characterization of PVA and its interactions with ice in addition to different arrangements of PVA such as branched or star polymers is also of interest as well as analyzing PVA and these variants by CD for the formation of secondary structure like motifs akin to glycopeptide mimics. With the use of MD to help gauge further its interactions with ice. Exploring a range of periodic and block copolymers comprising in part PVA would also be attractive.¹⁶⁷ The use of polymeric macromolecules has many advantages. Firstly the controlled synthesis of PVA on a large scale is regularly employed on a financially viable basis which is advantageous with respect to other AF(G)P mimics that are synthetically intensive with a comparatively small return. Furthermore PVA has excellent biocompatibility¹⁶⁸, biodegradability¹⁶⁹ and already has FDA approval as a foodstuff therefore the translation to a clinically employed preparation would have

reduced risk compared to glycopeptide mimics that may have unknown biological interactions often associated with non-host proteins.^{86,170,171} However the administration of an AFP III (referenced as ice structuring protein (ISP) III) preparation orally to 42 healthy volunteers failed to identify any adverse effects.¹⁷² As a consequence of this AFP III is now used commercially in ice cream preparations in numerous products within the Unilever PLC portfolio as reducing ice recrystallization improves quality, longevity and eases logistics.

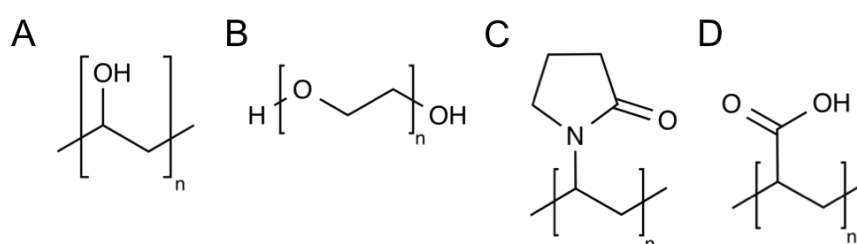


Figure 1.8. Select polymeric compounds assessed for antifreeze activities.^{118,164} (A) antifreeze active poly(vinyl alcohol) (PVA) and antifreeze inactive polymers (B) poly(ethylene glycol) (PEG), (C) poly(vinyl pyrrolidone) (PVP) and (D) poly(acrylic acid) (PAA).

A final and recently recognized ice interaction phenomena has been reported by Deville *et al.* who observed that zirconium acetate complexes (Figure 1.9.A) had a strong ice structuring tendency reporting similarities to many other AF(G)P mimics and polymers. However zirconium acetate has a low MW (327 g/mol) and a financially non-restrictive availability and Deville *et al.* later elucidated on a possible mechanism corresponding with these observations.¹⁷³ Mizrahy *et al.* have very recently reported however that neither zirconium acetate or zirconium acetate hydroxide (Figure 1.9.B) possesses notable TH activity but yet still demonstrate DIS which is contradictory to other observations that TH and DIS are intrinsically linked but given the vast structural differences from AF(G)Ps and AFPs an alternative mechanism could be at play.^{174,175} However the use of zirconium acetate complexes would likely be undesirable with biological materials

due to the higher molar concentrations that would be required and thus may be better suited as an antifreeze from a materials science perspective as opposed to usage in clinical applications.

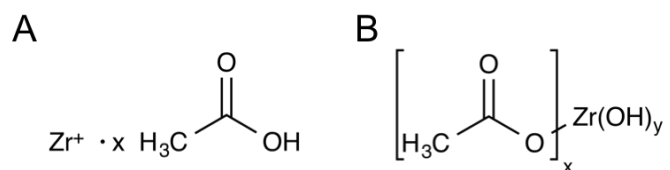


Figure 1.9. Antifreeze active Zirconium compounds. (A) Zirconium acetate and (B) Zirconium acetate hydroxide.

1.5. CURRENT STORAGE STRATEGIES OF BIOLOGICAL MATERIALS.

The field of cryobiology and preservation science has diversified extensively over the last 60 years with the preservation of a wide range of biomaterials now undertaken. Concurrent advances in the areas of haematology, reproduction medicine and transplantation science have accelerated the demand for technologies that improve the storage of these materials *ex vivo* to prolong their clinical viability. In parallel, improvements in biocatalysis, biotechnology and a range of molecular biology techniques have also incentivized the development of novel methodologies that extend the longevity of therapeutics and biochemical reagents. Preservation science can be broadly categorized into four areas. Hypothermic storage (above 0 °C), non-vitrifying (ice present) cryopreservation, vitrifying (ice absent) cryopreservation and lyophilisation (freeze drying).

1.5.1. Haematology.

The demand for blood products is enormous and can be emphasized by the number of units (1 unit \approx 470 mL) required daily. The vast majority of blood products required clinically are red blood cells (RBCs) also referred to as erythrocytes, though there is also a significant demand for blood plasma and platelets. For example approximately 44,000 units in the USA and 6,000 units in the UK are needed every day with equivalent per capita quantities required across the developed world. Long-term, the demand for blood products is increasing as the mean population age continues to rise.^{176,177} The majority of transfusions at present are for chronic illnesses as opposed to acute emergencies meaning overall (UK) demand is reasonably predictable and consistent as shown in table 1.1.¹⁷⁸

Uses of Donated Blood	%
Surgical	30%
Haematology	18%
Gastro-intestinal Bleeding	11%
Anaemia	30%
Maternity	6%
Other	5%

Table 1.1. Breakdown of the clinical use of donated blood units in the UK.¹⁷⁹

However donations are not provided uniformly across the year with numerous instances highlighting a significant drop in donations at times of adverse weather and during large sporting or cultural events. Fluctuations are exemplified in Figure 1.10 and summarized in Table 1.2 that detailing centralized UK blood stocks over a 14 week period highlighting instances where demand outstrips supply and how different blood groups (ABO/Rh) are more at risk at attaining dangerously low supply levels depending on their different compatibilities.

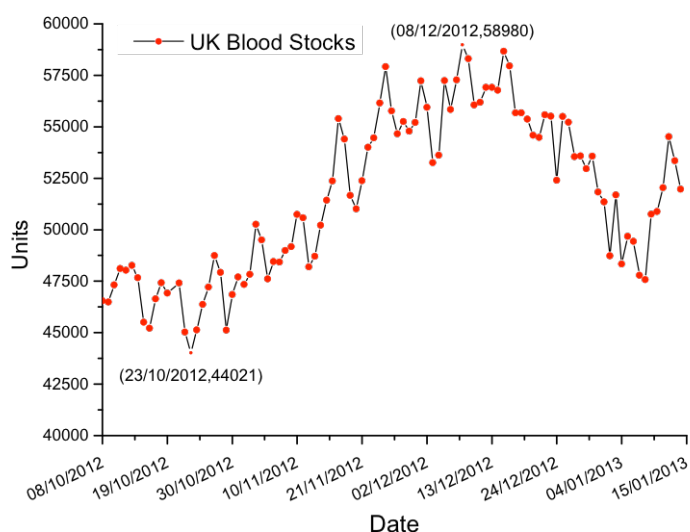


Figure 1.10. UK blood stocks over a 14-week period. Highlighting the inconsistency of donations with over a 14,000 (unit) difference between the highest and lowest quantities recorded.¹⁷⁹

Blood Group	Mean Day Supply	Mean Unit Supply	% of total (Mean Unit Supply)	Units Demanded Per Day (fixed)	% of total (Units Demanded Per Day (fixed))	Ratio (Demand/Supply)
O+	9.70	21409	41.49%	2206	37.31%	0.899
O ⁻	5.03	3101	6.01%	616	10.43%	1.735
A+	9.10	17199	33.33%	1890	31.96%	0.959
A-	8.22	3759	7.29%	457	7.73%	1.061
B+	8.07	3632	7.04%	450	7.61%	1.082
B-	5.92	719	1.39%	121	2.05%	1.473
AB+ [‡]	11.00	1408	2.73%	128	2.16%	0.793
AB-	8.50	377	0.73%	44	0.75%	1.026
Total		51604	100.00%	5914.0	100.00%	

Table 1.2. Detailed breakdown of UK blood stocks over a 14 week period.

Highlighting the relative demands of each blood group (ABO/Rh) in particular the high demand for O⁻ blood (universal donor*) and comparatively low demand for AB⁺ (universal recipient[‡]) blood.

A fundamental issue is that RBCs only have a functional life span between 100 and 120 days *in vivo*. However *ex vivo*, RBCs can only be routinely stored for between 35 and 42 days hypothermically before being deemed clinically unviable.¹⁸⁰ Hypothermic storage is defined as the preservation of biological material at temperatures significantly lower than normal physiological temperatures but above the freezing point of the storage solution (usually around 4 °C). Many storage solutions have been developed with a variety of solutes that prevent coagulation such as ethylenediaminetetraacetic acid (EDTA), citrate and heparin as well as solutes to help maintain a compatible osmotic pressure.¹⁸¹⁻¹⁸³ Several issues have been identified in the hypothermic storage of RBCs *ex vivo* including a reduction in ATP and 2,3-DPG concentration.¹⁸⁴ A reduction in 2,3-DPG a key regulator of oxygen affinity in haemoglobin causes a reduction in oxygen release though this change is reversible with 2,3-DPG levels recovering approximately 3 days after transfusion, however this may still have clinical repercussions in certain scenarios.¹⁸⁵ A reduction in ATP is linked with an overall

reduction in RBC metabolic activity, many other metabolites are also suppressed as lower temperatures inhibit biochemical processes with a 97 % reduction observed at storage temperatures of between 1 °C and 6 °C.¹⁸⁶ Another issue in storing RBCs hypothermically *ex vivo* is alterations in cell deformability caused in part by changes such as those mentioned above that can alter membrane composition but additionally changes in physiochemical properties that alter membrane plasticity. Hypothermic storage increases the likelihood of membrane lesions and irreparable injuries and has been associated with changes to aggregability, adhesiveness, volume, flexibility and internal viscosity in addition to other rheological properties.^{187,188} Many additives have been studied to maintain RBC survival *ex vivo* and maximize posttransfusion viability including the addition of saline, adenine, glucose and mannitol (SAGM) to help retain favourable metabolic activity.¹⁸⁹ Plus inorganic phosphates that act as both a pH buffer as other additives tend to incite acidity and as a substrate for 2,3-DPG production. However cumulatively these additives accelerate decay limiting storage to a legal maximum of 42 days defined by a minimum 24 hour posttransfusional (*in vivo*) survival rate of 75 %. *In vitro*, unviable samples are defined as haemolysis exceeding 0.8 % (EU) or 1.0 % (USA).^{190,191} However even at this level of viability the immune system may be temporarily compromised as non-viable RBCs are identified and removed from the body, a clinical detriment. Continuing research is focused upon not only extending the maximum storage limits but also improving the quality of hypothermically stored RBCs, which would improve logistics and avoid secondary transfusions and disorders associated from the transfusion of non-viable cells, though no dramatic improvements or changes have been implemented over the previous 20 years.

Another technique that aims to retain the long-term viability of RBCs is cryopreservation that can be defined in this context as the storage of RBCs at

low or ultra low temperatures such that RBCs are not freely in suspension but frozen. The cryopreservation of RBCs is advantageous in that it has no upper limit on storage duration and cellular energetics are minimized. However even though such storage conditions are not inherently damaging both the freezing and thawing process can inflict significant damage by a variety of mechanisms, the prevalence and impact of which is dependant upon the rates of freezing and thawing amongst an array of other factors.¹⁹² The freezing rate of RBCs can have a significant impact on viability. Slow freezing promotes the formation of extracellular ice that as a consequence creates an osmotic gradient that favours the efflux of water from the cell, which is influenced by other additives that alter osmolarity. The rate at which water exchange occurs is highly dependant on the rate of ice formation that is in turn dependant upon the cooling rate. If the rate of efflux is sustainable such that RBCs can control the rate of water loss then the cell will slowly become dehydrated.¹⁹³ However if the rate of dehydration is too high then membrane lesions and excessive cell shrinkage may occur and in conjunction, the levels of some solutes may reach localized concentrations that may have a consequential cytotoxicity.¹⁹⁴ The exact effect of solute cytotoxicity however remains a contested topic and it is believed that membrane lesions may alter permeability allowing the entry of previous impermeable molecules shifting osmolarity detrimentally.¹⁹⁵⁻¹⁹⁷ The presence of extracellular ice can also depending upon the density (haematocrit) of RBCs have a significant impact with regards to inciting significant mechanical damage.^{198,199} A rapid cooling rate which there by limits the duration with which RBCs are exposed to the potentially damaging effects experienced at slow cooling rates is offset by an increased probability in the development of intracellular ice. Intracellular ice formation occurs during rapid cooling as the efflux of water in addition to changes in membrane permeability associated with low temperatures allow an undesirable retention of water within the cytoplasm. Intracellular ice formation can occur by 3 different mechanisms.²⁰⁰ The formation of intracellular ice is hypothesized to

incite greater mechanical damage and to be avoided where possible.²⁰¹ Once frozen RBCs are often kept at temperatures below -150 °C indefinitely until required though an array of storage conditions have been employed that have no significantly detrimental effects.^{180,202,203} The thawing of RBCs is a process that is just as critical as freezing. However it is more difficult to precisely thaw cells in a controlled manner, as implementing a high thaw rate requires the use of temperatures that exceed tolerable levels. The problems associated with controlled thawing are more prevalent with RBCs as they are stored and transfused in large volumes (470 mL) meaning that they cannot be thawed homogeneously. Heterogeneous thawing would result in exposing a substantially high proportion of RBCs to undesirably high temperatures. As a consequence RBCs must be thawed at a comparatively slow rate. Slow thawing results in allowing ice recrystallization that is highly detrimental and a significant cause of cryoinjury. Aside from a financial and practical perspective, ice recrystallization damage is one of the main reasons as to why RBCs are not routinely cryopreserved.

The cryopreservation of RBCs requires a complex array of cryoprotective agents (CPAs) and at substantially higher concentrations than those used in hypothermic storage solutions in order to best mitigate against the damaging effects listed previously. CPAs can be broadly categorized into membrane permeable and membrane impermeable additives.^{180,204,205} Membrane permeable additives including glycerol and DMSO are often necessary at exceptionally high concentrations.²⁰² Standard RBC cryopreservation uses glycerol at high concentrations up to 40 wt% with significant discrepancies between the techniques employed in Western Europe and North America. The removal of glycerol prior to transfusion is a necessity as glycerol can induce posttransfusional intravascular haemolysis.²⁰⁶ Early efforts in the 1950s to

translate glycerol cryopreservation into a clinical setting were dampened by the inability to remove glycerol (deglycerolisation) sterilely as bacterial contamination of blood products was and is, if now only a minor issue a continual concern.²⁰⁷ However the frequency of bacterial contamination occurring in platelet transfusions is far higher.²⁰⁸ The development of continuous flow centrifugation in the 1960s allowed the clinical use of glycerol as a cryoprotectant with two different methodologies now fully developed. European blood banks tend to use a comparatively low glycerol (15 – 20 wt%) concentration and rapid cooling (<100 °C per minute) technique storing at a temperature between -165 °C and -196 °C and thawing at between 42 °C – 45 °C.²⁰⁹ Conversely North American blood banks use a higher glycerol (40 wt%) concentration and slow cooling (1 °C per minute) technique storing at -80 °C and thawing at 37 °C.²¹⁰ The addition and removal of glycerol though must be highly controlled in order to limit osmotic damage and prevent patient exposure to glycerol and thus requires specialized equipment and training increasing expense and processing time, which is often incompatible with clinical requirements demanding immediacy. The viability of RBCs after deglycerolisation is limited to 24 hours and thus poses another significant limitation, meaning that the cryopreservation of RBCs is typically limited to rare blood types for autologous transfusion and military applications where by logistics can limit the availability of donations.^{211,212} Therefore current research is predominantly focused on the improving the speed of postthaw processing and extending the shelf life of RBCs after deglycerolisation.²⁰⁶

Other cryopreservation techniques focus on the application of membrane impermeable (and henceforth extracellular) CPAs which include poly(vinyl pyrrolidone) (PVP), hydroxyethyl starch (HES), and dextran. However PVP and HES can lead to posttransfusional intravascular haemolysis at concentrations between 15 – 25 wt%.²¹³⁻²¹⁵ Several of these were used clinically as acute

plasma expanders albeit at concentrations lower than those used to attain a cryoprotective effect that offset hypovolemia in instances of severe trauma,²¹⁶ though HES has been shown to interfere with coagulation which may have clinical repercussions.²¹⁷ Instances of Pruritus have also been associated with prolonged exposure at high doses.²¹⁸ Furthermore recent studies conducted by Boldt *et al* are under intense scrutiny for fraudulent claims regarding studies and trials into the efficacy and safety of HES that strongly supported the use of HES in intravascular fluid replacement therapy.²¹⁹ These factors have contributed to the recent and immediate withdrawal within the EU (14/06/13) and limited application in the US (24/06/13) of HES in intravascular fluid replacement therapy.²²⁰ HES is the most widely studied extracellular CPA and can be synthesised relatively easily on a large scale at various molecular weights and is readily metabolized and excreted (fragments smaller than 40 kDa)²²¹ from the body.^{222,223} The cryoprotective mechanism of HES and other extracellular CPAs differs from glycerol. HES serves to alter viscosity²²⁴ and is known to strongly interact with water and as changes in viscosity occur it increases the rate of water efflux promoting faster dehydration enabling more rapid cooling and lowering the likelihood of intracellular ice formation upon cooling and thawing.²⁰⁴ Patients whom were transfused with RBCs cryopreserved with HES had an elevated incidence of haemoglobinuria indicative of possible renal toxicity when HES was not removed prior to transfusion.²²⁵ The absence of clinical data evaluating patients subjected to multiple HES cryopreserved RBC transfusions in addition to the reasons aforementioned have limited the clinical application of HES and in general extracellular CPAs in RBC cryopreservation.

Vitrification is the freezing of an aqueous solution at ultrahigh cooling rates such that ice formation is circumvented and instead an “ice-free” amorphous glass solid is attained.²²⁶ The obvious benefits of vitrification include the complete elimination of ice formation and the corresponding damage associated with it.

The cooling rates required to attain a vitrified state are often very high. For example pure water can attain a vitrified state at -138 °C but ice crystal formation often occurs at temperature much higher than this. In order to avoid ice formation cooling at 10^6 °C/min is necessary therefore being impractical for all but the smallest volumes and certainly not feasible for the cryopreservation of RBCs clinically.²²⁷ Devitrification and consequential ice crystal formation can occur upon thawing or suboptimal storage conditions.²²⁸ The addition of PVP, HES and dextran have been shown to lower the freezing rates required to attain a vitrified state and improve overall recovery rates.¹⁸⁰ Monosaccharides and disaccharides also have a similar effect.²²⁹ However subsequent haemolysis after transfusion was undesirably high plus the concentrations of these CPAs needed is excessively high and cytotoxic.²² The addition of membrane impermeable monosaccharides and disaccharides has shown to alleviate some of the toxicological consequences of using high concentrations of short chain diols as RBC cryoprotectants.^{230,231} Nonetheless an implementable cryopreservation strategy of RBCs using vitrification has yet to be successfully applied but remains an active area of investigation.

A final area of research into the storage of RBCs is lyophilisation. Lyophilisation or freeze drying is the sublimation of ice under vacuum removing a vast majority of the water content.²³² The lyophilisation of RBCs would be beneficial as it would harbour significant logistical benefits as the overall weight of the lyophilized product prior to rehydration is minimized and it has been suggested that lyophilised RBCs could be stored at room temperature possibly indefinitely if kept sterile.²³³ The addition of PVP, PEG and dextran was able to improve overall recovery during freezing after lyophilisation, cryostorage and rehydration and even though lyophilised RBCs initially showed acceptable recovery a high frequency of membrane lesions were later identified limiting their application.

Even though desiccation (i.e. the removal of water) has been frequently observed in nature it has yet to be successfully replicated by others by lyophilisation or otherwise with RBCs.²³⁴

Ice recrystallization upon thawing as aforementioned is a key mechanism of cryoinjury¹⁹² during cryopreservation and to a lesser extent during thawing of vitrified samples as a consequence of devitrification.^{228,235} However none of the previously identified methodologies aim principally at eliminating ice recrystallization, though thawing cells rapidly can reduce ice recrystallization, this is problematic with RBCs due to the large volume and number of cells required for transfusions. IRI may therefore provide a means of limiting damage arising from extracellular ice crystal growth and improve the cryopreservation of RBCs by increasing the number of cells recovered subsequent to freezing. Efforts at improving the cryopreservation of RBCs by inhibiting ice recrystallization has been attempted previously.⁸⁸ The work of Carpenter and Hansen demonstrated the use of a type I recombinant AFP isolated from winter flounder (*Pseudopleuronectes americanus*) in decreasing the level of haemolysis in RBCs supplemented with 30 wt% HES (MW 450 kDa, 0.7 degree of substitution). A decrease in haemolysis was observed at concentrations as low as 8 µg/mL, though maximum protection was conferred at 62 µg/mL. Increasing the concentration of AFP, which resulted in a more profound IRI activity, actually elicited a reduction in cryoprotection. At the maximum concentration tested of 1.54 mg/mL the level of haemolysis was higher than when RBCs were cryopreserved in the complete absence of AFP, which the authors attributed to the presence of hexagonal bipyramidal “needle-like” ice crystal structures caused by DIS. Reductions in haemolysis were the most apparent when slow thawing (20 °C, air) conditions were used that greatly promote ice recrystallization, though the addition of AFP could not reduce haemolysis to levels observed when an

optimal fast thawing (45 °C, water) technique was applied that minimized ice recrystallization. Continuing studies by Carpenter *et al* expanded on these findings by comparing type I, II and III AFPs and their ability to improve the cryopreservation of RBCs. Using a similar freezing and thawing regime each AFP was found to convey a cryoprotective effect in a similar concentration dependant manner, though the loss of cryoprotection at higher concentrations was far less apparent with AFP II and AFP III but speculated that on a molar basis the loss could be comparable. Continuing on several mutant variants of AFP III were generated using site-directed mutagenesis. One mutant (P29A) which had a reduced (50 %) thermal hysteresis activity that the authors attribute as a measure of beneficial “antifreeze” activity in addition to observations by cryomicroscopy of substantially greater ice crystal growth did confer a significantly reduced level of cryoprotection.²³⁶ These findings highlight that the inhibition of ice recrystallization can confer beneficial cryoprotection but that the exact mechanism by which cryoprotection is conveyed *in vitro* remains elusive as simply increasing IRI activity does not yield improved cryopreservation. This highlights a balance between the properties of IRI and DIS and its importance in identifying a candidate IRI active compound with beneficial cryoprotection to RBCs.

1.5.2. Reproductive medicine.

Substantial differences exist between the storage strategies used with RBCs (Section 1.5.1) and in reproductive medicine, which is fundamentally due to the differences in their biology in which these cells are donated and required, subcategorized broadly into spermatozoa, oocytes and embryos. Also RBCs are anuclear and required in substantially larger volumes where as in reproductive medicine the volumes and number of gametes and embryos is minute by

comparison.²³⁷ One of the first successful cryopreservation strategies of any biological tissue was demonstrated by Polge *et al.* in 1949 who were able to cryopreserve (frog and fowl) spermatozoa using a high concentration of the vitrifying organic solvent glycerol and attained a statistically significant amount of functional spermatozoa upon revival but were unable to produce any viable offspring.²³⁸ Since then a variety of techniques that principally utilize glycerol but also DMSO²³⁹ and raffinose²⁴⁰ as cryoprotectants have been applied to a range of spermatozoa, oocytes and embryos and revolutionized selective breeding capabilities and improved assisted reproduction (artificial insemination) especially with cattle with the first successfully conceived calf occurring in 1951 and is in the present, commonplace.²⁴¹ The application of such protocols soon drew notable success with human spermatozoa despite morphological and size dissimilarities as well as differences in membrane composition.²⁴² The storage of spermatozoa is also of increasing importance in the conservation of mammalian species but significant optimization is often required in order to attain the highest yields.²⁴³ The cryopreservation of certain species such as members of the rodent, marsupial and porcine families still remains difficult not only in their ability to successfully undergo cryopreservation but also in their sensitivities to the concentrations of glycerol required for successful cryopreservation.²⁴⁴ However unlike any other biological materials the (acceptable) survival rate of motile and viable spermatozoa is typically only between 50 % - 60 % at best, which is clearly unacceptable for most other cell types but still of practical use.^{245,246} This is in part due to the high osmosensitivity of spermatozoa.^{247,248} Few studies have investigated the application of AFPs and AF(G)Ps to aid the cryopreservation of spermatozoa. In particular the work of Payne, *et al.* reported that both AFP I and AF(G)Ps 1-8 decreased the motility of ram spermatozoa prior to freezing indicative of a cytotoxic effect even at a concentrations of 0.1 µg/mL that offset their beneficial effects during thawing except with the use of AFP I at the highest

concentration tested, 10 µg/mL.²⁴⁹ However in contrast to this Koshimoto *et al.* showed that whilst ice recrystallization is a detrimental consequence of slow thawing and lowered the recovery of mouse spermatozoa the addition AFP I, AFP III or AF(G)P at concentrations up to 100 µg/mL did not induce cytotoxicity. However the impact of each of these as additives during the cryopreservation process was highly disadvantageous with each additive, with each increase in concentration tested lowering recovery progressively in comparison to the complete absence of AFP I, AFP III or AF(G)P. Reductions in recovery were hypothesized to be as a result of DIS.²⁵⁰ A similar effect had been reported elsewhere with chimpanzee spermatozoa using AFP III.²⁵¹ A comparable experiment again investigating AFP I, AFP III and AF(G)P but using bull spermatozoa by Prathalingam *et al.* in contrast showed a mild benefit by the addition of either cryoprotectants irrespective of the concentration used (0.1 µg/mL – 100 µg/mL).²⁵² A positive effect upon AFP I and AFP III addition was also reported by Beirão *et al.* albeit with fish spermatozoa that are substantially different to their mammalian counterparts.²⁵³

The cryopreservation of unfertilized mammalian oocytes is a unique problem as oocytes are large cells often stored individually with a low membrane permeability to water and thus this increases the probability of intracellular ice formation (due to greater water retention) and ice crystal growth during thawing both of which are highly destructive processes.²⁵⁴ Though live births from cryopreserved oocytes were reported over 35 years ago in mice²⁵⁵ and then following on from rabbits²⁵⁶, cows²⁵⁷, horses²⁵⁸ and even humans,²⁵⁹ though success rates still remain very low with between 1 % and 5 % of cryopreserved human oocytes resulting in a live birth.^{260,261} Two different approaches have been used to prolong the storage of human oocytes (neither of which contain additives with IRI activity). A slow freezing strategy (2 °C/min) that uses a high

concentration of propan-1,2-diol (membrane permeable) and sucrose (membrane impermeable) with a 10 minute pause at -7 °C to ensure ice nucleation before cooling down to a temperature greater than -150 °C. A rapid thawing strategy is then used when required with the controlled and gradual removal of both propan-1,2-diol and sucrose subsequent.²⁶² The second technique uses a combination of DMSO and PEG to achieve a vitrification state by rapid cooling, though the high concentration of DMSO means that significant exposure to DMSO at physiological temperatures (37 °C) can lower fertilization rates.^{263,264}

A study by O'Neil *et al.* that undertook human oocyte cryopreservation with and without the addition of 1 mg/mL AF(G)P showed that the addition of AF(G)P at room temperature as opposed to 4 °C reduced fertilization rates compared to the absence of AF(G)P. However when AF(G)P was added at 4 °C an improvement in recovery and the resulting downstream measures (fertilization and blastocyst formation) was attained.²⁶⁵ An earlier study by Arav *et al.* agrees with the benefits (though with swine as opposed to human oocytes) of AFP I, AFP II, AFP III and AF(G)P addition (at a high concentration of 20 mg/mL) by assessing morphology post freezing but did not investigate whether or not these oocytes were then able to undergo fertilization successfully.²⁶⁶ A recent article by Jo *et al.* also showed that the addition of 0.5 µg/mL AFP III also led to an improvement in the post thaw survival and development of mouse oocytes.²⁶⁷

The final area of reproductive medicine to consider is the cryopreservation of fertilized (pre-implantation) embryos with discrepancies in the preferred cryopreservation method depending upon the stage of blastocyst development at which cryopreservation is performed. Again two approaches similar to those undertaken with oocyte cryopreservation focusing on either slow cooling or vitrification are the standard methodologies utilized. A slow cooling strategy with

an early stage embryo (8-cell maximum) uses propan-1,2-diol and sucrose as before as the CPAs preferred.²⁶⁸ Embryos isolated at a later stage of development however, utilize glycerol instead of propan-1,2-diol. However the first successful cryopreservation of (mouse) embryos was attained using a slow thawing strategy but with DMSO as the CPA of choice and resulted in the production of a significant proportion of viable offspring.²⁶⁹ DMSO based cryopreservation has been replicated in several other species since including humans aided by concurrent improvements in *in vitro* manipulation.²⁷⁰ Vitrification approaches using several different additives at high concentrations have also been successfully implemented.^{271,272} A few studies have investigated the use of AFPs in improving the viabilities of cryopreserved embryos. An example of which is an article by Baguisi *et al.* who investigated the addition of AFP I or AFP III to ovine embryos and showed no significant impact on recovery or pregnancy rates when these were stored hypothermically (i.e. no ice formation) over a period of 4 days.²⁷³ Robles *et al.* showed that AFP I had a similar benefit improving the storage of fish embryos, though these have an inherently different developmental biology.²⁷⁴ Overall however few reports have investigated the use of AFPs and AF(G)Ps as cryoprotective agents presumably due to the lack of readily available materials and the ethical concerns arising from such experiments.

1.5.3. Transplantation medicine.

Transplantation medicine is the final area in which cryobiology continues to have a positive impact but is vastly different in comparison to haematology and reproductive medicine. Firstly the diversity of cell biologies within the umbrella of transplantation medicine means that no one strategy or solution will likely be applicable. A successful strategy will in part depend on whether or not the transplanted material is simply a single cell type, a tissue containing a few cell

varieties or an entire organ with increasing complexities understandably applicable with each, in terms of volume, structure and biology. Especially as the procurement of such materials is often non-ideal.^{275,276} Furthermore transplanted material often has to retain a proliferative capacity in order to have a long-term clinical benefit (where as RBCs do not). Overall however as the demand for transplantable material is increasing year on year especially with the development of new transplant procedures that further diversify the types of cells and tissues that require transit and storage *ex vivo* in addition to an aging populace the importance of minimizing wastage is pivotal.^{277,278}

The storage of hepatocytes that constitute the primary cell type within the liver is one most pressing concerns at present with over 100,000 liver transplants successfully conducted between 2009-2012 in the USA and over 16,500 on current waiting lists according to the organ procurement and transplantation network.²⁷⁹ Understanding the idealized cryopreservation technique for hepatocytes and other hepatic cell types would no doubt translate to clinical benefits and hasten post-operative recovery.²⁸⁰ Furthermore the use of hepatocytes from more readily available (non-human) sources has great importance in the field of pharmacokinetics and pharmacodynamics in assessing novel xenobiotics and in quantifying potential drug-drug interactions.^{281,282} Current long-term storage strategies are reliant on the cryopreservation of fresh hepatocytes as opposed to hypothermic strategies which are only effective in the short term.^{283,284} The cryopreservation medium of choice for hepatocytes for transplantation is often University of Wisconsin (UW) solution (an isotonic solution principally consisting of lactobionate and raffinose as osmotic stabilizers and dexamethasone as a membrane stabilizer) supplemented with between 10 % (v/v) and 20.5 % (v/v) DMSO depending on the specific cooling rates and cell densities used²⁸⁵⁻²⁸⁷ and is usually undertaken as soon as possible after isolation.²⁸⁸ Critically all cryopreservation medium has to be devoid of animal

material in order to minimize the risk of zoonosis (animal to human disease transfer) and immunogenicity issues such as fetal calf serum that is commonplace in *in vitro* cell culture preparations. Hepatocytes are then cryopreserved slowly (1 °C/min – 2 °C/min) as opposed to rapid freezing (vitrification) to minimize osmotic shock and the probability of intracellular ice formation. The final storage temperature has also been shown to be of importance with the optimal temperature being -150 °C or lower with a reduction in viability with prolonged storage at temperatures greater than this.²⁸⁹ The thawing of hepatocytes is undertaken rapidly (37 °C, water) in order to minimize the damaging effects of ice recrystallization.²⁹⁰ However once thawed hepatocytes are then cooled back to 4 °C to lessen the cytotoxic impact of DMSO observed at 37 °C, with the removal of DMSO of critical importance to avoid the adverse effects of DMSO infusion to patients. Despite DMSO removal at the low temperature of 4 °C, the maintenance of hepatic function after cryopreservation remains a challenging problem.^{291,292} Several studies have investigated the use of several additives in improving the cryopreservation process. Rubinsky *et al.* showed that the supplementation of 1 mg/mL AF(G)P (predominately AF(G)P8) to a glycerol (as opposed to DMSO) based cryopreservative mixture had a benefit on whole rat liver cryopreservation (2 °C/min) albeit preparations were only cooled down to a maximum of -3 °C for 6 hours though this was still sufficient time for prolific ice formation.²⁹³ Miyamoto *et al.* investigated the use of a range of oligosaccharides which have mild IRI activity¹⁶² with benefits shown in a concentration dependant manner with both rat and human hepatocytes in terms of viability and attachment rate, which is of importance in plating *in vitro* and in the adherence to the hepatic sinusoidal endothelium after engraftment *in vivo*.²⁹⁴ However these improvements were not attributed to a reduction in ice recrystallization.²⁹⁵ Finally Soltys *et al.* showed that a combination of 2,3-butandiol (serving as a mimic for DMSO) and AFP I had little impact on the

cryopreservation of hepatocytes or sinusoidal (another cell type within the liver) cells.²⁹⁶

Another primary cell type that has importance in the field of transplantation are islet cells, especially given the rate at which the incidence of type II diabetes (diabetes mellitus) is increasing in the developed world. The demand for islet cells for transplantation is therefore likely to see substantial increases alongside.^{297,298} Islet transplantation has been shown to eliminate dependence on insulin supplementation in type I diabetic patients in a landmark study by Shapiro *et al.* and thus is a real therapeutic possibility if sufficient material is available²⁹⁹ and has been replicated in other transplant centers since.³⁰⁰ Cell lines derived from pancreatic islets are also gaining more prominence as models for diabetic activity and metabolic homeostasis.³⁰¹ Current strategies to islet cryopreservation follow a similar methodology to that used with hepatocytes in the application of a slow cooling rate, with cells supplemented with high concentrations of DMSO (investigations using HES have also been described).³⁰² When required cells are thawed rapidly prior to the removal of DMSO.^{303,304} Various other (faster) freezing rates have been investigated but a slow freezing rate predominates in current protocols.³⁰⁵ A vitrification approach has additionally been reviewed but acknowledges that further progress is required if this is to compete with established methodologies.³⁰⁶ The use of IRI additives to improve the cryopreservation of islet cells has been documented by Matsumoto *et al.* who demonstrated the effect of a synthetic AF(G)P analogue¹⁵² on RBC and islet cryopreservation. The effect on RBCs was of a similar beneficial value to those seen elsewhere with native AFP I, AFP II and AFP III.^{88,236} The synthetic AF(G)P analogue showed an initial benefit in terms of cell recovery, which was then lost at higher concentrations due to DIS. This effect also occurred when applied to the cryopreservation of islet cells using standard procedures, supplemented with 0.5 mg/mL of the AF(G)P analogue providing beneficial effects but at a higher

concentration of 1 mg/mL this benefit was negated due to DIS.³⁰⁷ Another area of interest in this regard includes the cryopreservation of cardiac tissue and cardiomyocytes³⁰⁸ that again uses similar protocols to islets and hepatocytes for use in transplantation.³⁰⁹ However the addition of AF(G)P at 0.5 mg/mL in this instance proved to be detrimental and lowered significantly, cardiac output⁸⁹ which was attributed again to the effects of DIS.³¹⁰

Stem cells whether it be haematopoietic, mesenchymal or embryonic stem cells have a great potential to revolutionize medicine in the 21st century, particularly in the field of regenerative medicine.³¹¹⁻³¹³ The cryopreservation of stem cells therefore is of exceptional interest. Current cryopreservation strategies tend to focus on the use of DMSO as aforementioned.³¹⁴⁻³¹⁷ However strategies that aim to reduce the current reliance upon DMSO have been developed, with the use of other CPAs such as trehalose, sucrose and HES substituting for a substantial part of the DMSO content used in traditional methodologies.^{318,319} Plus the use of vitrifying strategies enabling DMSO free preparations to be successfully cryopreserved.³²⁰ No strategies have been reported however that focuses on enhancing the cryopreservation of stem cells by attenuating ice recrystallization. The cryopreservation of scarcely available and poorly understood biomaterials could be argued as one of the key challenges in advancing transplantation, therefore even minute benefits many translate into substantial clinical gains.

1.5.4. Pharmaceuticals and biotechnology.

A final area of interest to briefly touch upon is the storage of pharmaceuticals and other biological preparations, the preservation of proteins, drugs, vaccines and genetic constructs such as plasmids in addition to numerous microorganisms (viruses, bacteria, protozoa, fungi and algae). The relative instability at

physiological temperatures of these often warrants the need for cryopreservation³²¹ or lyophilisation³²² strategies, to limit their degradation or unwarranted proliferation. Of particular importance is the storage of transgenic (protein) products for therapeutic use or proteins that having been extensively mutated for structural studies and thus may have a less stable tertiary structure. The continuous propagation of microorganisms is also undesirable especially those that may be pathogenic or highly virulent. However these processes must be carefully undertaken, as the removal of water by ice crystallization or sublimation will produce high but localized salt concentrations (originating from the buffers required at physiological temperatures) or create pH shifts, which can cause denaturation or aggregation in proteins that cannot be reversed upon reconstitution. Such issues are especially apparent with membrane bound proteins. Numerous excipients have been shown to improve the storage of proteins over the long term including sugars (e.g. trehalose), polyols (e.g. glycerol), polymers (e.g. PVP), amino acids, organic salts and inorganic salts.^{323,324} As with most other storage strategies, the concentration and storage temperatures of the preparations is influential on the relative recovery rates.³²⁵

One of the most commonly utilized protectants for protein (enzyme) storage is the osmolyte, trehalose (Figure 1.3.C) that has no reactivity with proteins but has advantageous effects on protein stabilization allowing suitable catalytic activity upon reconstitution and has been demonstrated with a variety of proteins.³²⁶⁻³²⁸ Other studies have shown the effectiveness of a trehalose glycopolymer conjugation in the aiding lyophilisation.^{329,330} However there are no reports of the use of AFPs or AF(G)Ps in aiding the cryopreservation or lyophilisation of protein preparations presumably due to the difficulties in separating such mixtures. The cryopreservation of microorganisms and genetic constructs however tends to rely upon the use of high concentrations of glycerol or DMSO principally though a range of penetrating and non-penetrating CPAs have been used depending upon

the organism or preparation of interest.^{205,321} Lyophilisation strategies have also been successfully implemented.^{331,332} The use of AFPs and AF(G)Ps in this capacity is limited but an interesting study that may be of use elsewhere was conducted by McKown *et al.* who successfully incorporated an AFP I gene (*Psudeopluronectes americanus*) into yeast that then displayed improved survival rates subsequent to cryopreservation due to AFP expression.³³³ Overall there has been little progress on improving the cryopreservation or lyophilisation protocols currently used within the pharmaceutical sciences and in molecular biology. The use of more elaborate molecular biology tools and an increasing shift away from small molecule xenobiotics towards therapeutic biologics emphasizes the importance of understanding the interactions of ice with AFPs and AF(G)Ps. This will become more important with time and is an area that requires extensive monitoring in the future.

1.6. REFERENCES.

1. Hewitt, G. M. Some genetic consequences of ice ages, and their role in divergence and speciation. *Biol J Linn Soc* **58**, 247–276 (2008).
2. Hewitt, G. The genetic legacy of the Quaternary ice ages. *Nature* **405**, 907–913 (2000).
3. Forster, P. Ice Ages and the mitochondrial DNA chronology of human dispersals: a review. *Philos T R Soc B* **359**, 255–264 (2004).
4. Clarke, A. *et al.* A Low Temperature Limit for Life on Earth. *PLoS one* **8**, e66207 (2013).
5. Berezovsky, I. N. & Shakhnovich, E. I. Physics and evolution of thermophilic adaptation. *Proc Natl Acad Sci USA* **102**, 12742–12747 (2005).
6. Horikoshi, K. Barophiles: deep-sea microorganisms adapted to an extreme environment. *Curr Opin Microbiol* **1**, 291–295 (1998).
7. Fütterer, O. *et al.* Genome sequence of *Picrophilus torridus* and its implications for life around pH 0. *Proc Natl Acad Sci USA* **101**, 9091–9096 (2004).
8. Zhang, L.-M., Wang, M., Prosser, J. I., Zheng, Y.-M. & He, J.-Z. Altitude ammonia-oxidizing bacteria and archaea in soils of Mount Everest. *FEMS Microbiol Ecol* **70**, 208–217 (2009).
9. Vieille, C. & Zeikus, G. J. Hyperthermophilic Enzymes: Sources, Uses, and Molecular Mechanisms for Thermostability. *Microbiol Mol Bio Rev* **65**, 1–43 (2001).
10. Takami, H. *et al.* Thermoadaptation trait revealed by the genome sequence of thermophilic *Geobacillus kaustophilus*. *Nucleic Acids Res* **32**, 6292–6303 (2004).
11. Henne, A. *et al.* The genome sequence of the extreme thermophile *Thermus thermophilus*. *Nat Biotechnol* **22**, 547–553 (2004).
12. Fahy, G. M. The relevance of cryoprotectant ‘toxicity’ to cryobiology. *Cryobiology* **23**, 1–13 (1986).
13. Arakawa, T., Carpenter, J. F., Kita, Y. A. & Crowe, J. H. The basis for toxicity of certain cryoprotectants: A hypothesis. *Cryobiology* **27**, 401–415 (1990).
14. Da Violante, G. *et al.* Evaluation of the Cytotoxicity Effect of Dimethyl Sulfoxide (DMSO) on Caco2/TC7 Colon Tumor Cell Cultures. *Biol Pharm Bull* **25**, 1600–1603 (2002).
15. Lynch, F. T. & Khodadoust, A. Effects of ice accretions on aircraft aerodynamics. *Prog Aerosp Sci* **37**, 669–767 (2001).
16. Gao, H. & Rose, J. L. Ice detection and classification on an aircraft wing with ultrasonic shear horizontal guided waves. *IEEE Trans Ultrason Ferroelectr Freq Control* **56**, 334–344 (2009).
17. Ryerson, C. C. Ice protection of offshore platforms. *Cold Reg Sci Technol* **65**, 97–110 (2011).
18. Carriveau, R., Edrisy, A., Cadieux, P. & Mailloux, R. Ice Adhesion Issues in

- Renewable Energy Infrastructure. *J Adhes Sci Technol* **26**, 447–461 (2012).
19. Frankenstein, S. & Tuthill, A. M. Ice Adhesion to Locks and Dams: Past Work; Future Directions? *J Cold Reg Eng* **16**, 83–96 (2002).
 20. Parent, O. & Ilinca, A. Anti-icing and de-icing techniques for wind turbines: Critical review. *Cold Reg Sci Technol* **65**, 88–96 (2011).
 21. Wareing, J. B. The effects of wind, snow and ice on optical fibre systems on overhead line conductors. in *14th International Conference and Exhibition on Electricity Distribution* **438**, v3–35 (IEE, 1997).
 22. Bouvet, V. & Ben, R. N. Antifreeze glycoproteins: structure, conformation, and biological applications. *Cell Biochem Biophys* **39**, 133–144 (2003).
 23. Davies, P. L. & Sykes, B. D. Antifreeze proteins. *Curr Opin Struct Biol* **7**, 828–834 (1997).
 24. Gibson, M. I. Slowing the growth of ice with synthetic macromolecules: beyond antifreeze(glyco) proteins. *Polym Chem* **1**, 1141–1152 (2010).
 25. Somero, G. N. & Devries, A. L. Temperature Tolerance of Some Antarctic Fishes. *Science* **156**, 257–258 (1967).
 26. Scholander, P. F., van Dam, L., Kanwisher, J. W., Hammel, H. T. & Gordon, M. S. Supercooling and osmoregulation in arctic fish. *J Cell Comp Physiol* **49**, 5–24 (1957).
 27. Potts, D. C. & Morris, R. W. Some body fluid characteristics of the Antarctic fish, *Trematomus bernacchii*. *Marine Biol* **1**, 269–276 (1968).
 28. Klingenberg, C. P. & Ekau, W. A combined morphometric and phylogenetic analysis of an ecomorphological trend: pelagization in Antarctic fishes (Perciformes: Nototheniidae). *Biol J Linn Soc* **59**, 143–177 (2008).
 29. Devries, A. L. & Wohlschlag, D. E. Freezing resistance in some Antarctic fishes. *Science* **163**, 1073–1075 (1969).
 30. Anderson, C. Blagden Papers at the Royal Society. *Notes Rec Roy Soc* **61**, 237–238 (2007).
 31. Husa, W. J. & Rossi, O. A. A study of isotonic solutions. *J Pharm Sci* **31**, 270–277 (1942).
 32. Devries, A. L., Komatsu, S. K. & Feeney, R. E. Chemical and physical properties of freezing point-depressing glycoproteins from Antarctic fishes. *J Biol Chem* **245**, 2901–2908 (1970).
 33. Shier, W. T., Lin, Y. & De Vries, A. L. Structure and mode of action of glycoproteins from an antarctic fish. *Biochimica et Biophysica Acta (BBA)* **263**, 406–413 (1972).
 34. Lin, Y., Duman, J. G. & Devries, A. L. Studies on the structure and activity of low molecular weight glycoproteins from an antarctic fish. *Biochem Biophys Res Commun* **46**, 87–92 (1972).
 35. van den Akker, F., Steensma, E. & Hol, W. G. Tumor marker disaccharide D-Gal-beta 1, 3-GalNAc complexed to heat-labile enterotoxin from Escherichia coli. *Protein Sci* **5**, 1184–1188 (1996).

36. Raymond, J. A., Lin, Y. & Devries, A. L. Glycoprotein and protein antifreezes in two Alaskan fishes. *J Exp Zool* **193**, 125–130 (1975).
37. Feeney, R. E. & Osuga, D. T. Antifreeze glycoproteins from Arctic fish. *J Biol Chem* **253**, 5338–5343 (1978).
38. Scholander, P. F. & Maggert, J. E. Supercooling and ice propagation in blood from arctic fishes. *Cryobiology* **8**, 371–374 (1971).
39. Neelakanta, G., Sultana, H., Fish, D., Anderson, J. F. & E, F. *Anaplasma phagocytophilum* induces *Ixodes scapularis* ticks to express an antifreeze glycoprotein gene that enhances their survival in the cold. *J Clin Inv* **120**, 3179–3190 (2010).
40. Neelakanta, G., Hudson, A., Sultana, H. & Cooley, L. Expression of *Ixodes scapularis* Antifreeze Glycoprotein Enhances Cold Tolerance in *Drosophila melanogaster*. *PloS one* **7**, e33447 (2012).
41. Scott, G. K., Fletcher, G. L. & Davies, P. L. Fish antifreeze proteins: recent gene evolution. *Can J Fish Aquat Sci* **43**, 1028–1034 (1986).
42. Chen, L., Devries, A. L. & Cheng, C. H. C. Convergent evolution of antifreeze glycoproteins in Antarctic notothenioid fish and Arctic cod. *Proc Natl Acad Sci USA* **94**, 3817–3822 (1997).
43. Near, T. J. *et al.* Ancient climate change, antifreeze, and the evolutionary diversification of Antarctic fishes. *Proc Natl Acad Sci USA* **109**, 3434–3439 (2012).
44. Devries, A. L. Antifreeze peptides and glycopeptides in cold-water fishes. *Annu Rev Physiol* **45**, 245–260 (1983).
45. Devries, A. L. The role of antifreeze glycopeptides and peptides in the freezing avoidance of Antarctic fishes. *Comp Biochem Physiol B* **90**, 611–621 (1988).
46. Fletcher, G. L. The effects of hypophysectomy and pituitary replacement on the plasma freezing point depression, Cl⁻, glucose and protein antifreeze in the winter flounder (*Pseudopleuronectes americanus*). *Comp Biochem Physiol A* **63**, 535–537 (1979).
47. Jin, Y. & Devries, A. L. Antifreeze glycoprotein levels in Antarctic notothenioid fishes inhabiting different thermal environments and the effect of warm acclimation. *Comp Biochem Physiol B* **144**, 290–300 (2006).
48. Ahlgren, J. A., Cheng, C. C., Schrag, J. D. & Devries, A. L. Freezing avoidance and the distribution of antifreeze glycopeptides in body fluids and tissues of Antarctic fish. *J Exp Biol* **137**, 549–563 (1988).
49. Yeh, Y. & Feeney, R. E. Antifreeze Proteins: Structures and Mechanisms of Function. *Chem Rev* **96**, 601–618 (1996).
50. Feeney, R. E., Burcham, T. S. & Yeh, Y. Antifreeze Glycoproteins from Polar Fish Blood. *Annu Rev Biophys Biophys Chem* **15**, 59–78 (1986).
51. Ben, R. N. Antifreeze Glycoproteins—Preventing the Growth of Ice. *ChemBioChem* **2**, 161–166 (2001).
52. Morris, H. R. *et al.* Antifreeze glycoproteins from the blood of an antarctic fish. The structure of the proline-containing glycopeptides. *J Biol Chem* **253**, 5155–5162

- (1978).
53. Franks, F. & Morris, E. R. Blood glycoprotein from antarctic fish possible conformational origin of antifreeze activity. *Biochimica et Biophysica Acta (BBA)* **540**, 346–356 (1978).
 54. Tomimatsu, Y., Scherer, J. R., Yeh, Y. & Feeney, R. E. Raman spectra of a solid antifreeze glycoprotein and its liquid and frozen aqueous solutions. *J Biol Chem* **251**, 2290–2298 (1976).
 55. Bush, C. A. & Feeney, R. E. Conformation of the glycotriptide repeating unit of antifreeze glycoprotein of polar fish as determined from the fully assigned proton n.m.r. spectrum. *Int J Peptide Protein Res* **28**, 386–397 (1986).
 56. Berman, E., Allerhand, A. & Devries, A. L. Natural abundance carbon 13 nuclear magnetic resonance spectroscopy of antifreeze glycoproteins. *J Biol Chem* **255**, 4407–4410 (1980).
 57. Lane, A. N., Hays, L. M., Crowe, L. M., Crowe, J. H. & Feeney, R. E. Conformational and dynamic properties of a 14 residue antifreeze glycopeptide from antarctic cod. *Protein Sci* **7**, 1555–1563 (1998).
 58. Lane, A. N. *et al.* Comparison of the Solution Conformation and Dynamics of Antifreeze Glycoproteins from Antarctic Fish. *Biophys J* **78**, 3195–3207 (2000).
 59. Nguyen, D. H., Colvin, M. E., Yeh, Y., Feeney, R. E. & Fink, W. H. The Dynamics, Structure, and Conformational Free Energy of Proline-Containing Antifreeze Glycoprotein. *Biophys J* **82**, 2892–2905 (2002).
 60. Tsvetkova, N. M. *et al.* Dynamics of Antifreeze Glycoproteins in the Presence of Ice. *Biophys J* **82**, 464–473 (2002).
 61. Harding, M. M., Anderberg, P. I. & Haymet, A. D. J. 'Antifreeze' glycoproteins from polar fish. *Eur J Biochem* **270**, 1381–1392 (2003).
 62. Ahmed, A. I., Osuga, D. T. & Feeney, R. E. Antifreeze Glycoprotein from an Antarctic Fish: Effects of chemical modifications of carbohydrate residues on antifreeze and antilectin activities. *J Biol Chem* **248**, 8524–8527 (1973).
 63. Seeberger, P. H. Chemical glycobiology: why now? *Nat Chem Biol* **5**, 368–372 (2009).
 64. Duman, J. G. & Devries, A. L. Freezing resistance in winter flounder *Pseudopleuronectes americanus*. *Nature* **247**, 237–238 (1974).
 65. Duman, J. G., Bennett, V., Sformo, T., Hochstrasser, R. & Barnes, B. M. Antifreeze proteins in Alaskan insects and spiders. *J Insect Physiol* **50**, 259–266 (2004).
 66. Clark, M. & Worland, M. R. How insects survive the cold: molecular mechanisms - a review. *J Comp Physiol B* **178**, 917–933 (2008).
 67. Bravo, L. & Griffith, M. Characterization of antifreeze activity in Antarctic plants. *J Exp Biol* **56**, 1189–1196 (2005).
 68. Griffith, M. & Yaish, M. W. F. Antifreeze proteins in overwintering plants: a tale of two activities. *Trends Plant Sci.* **9**, 399–405 (2004).
 69. Jarzabek, M., Pukacki, P. M. & Nuc, K. Cold-regulated proteins with potent

- antifreeze and cryoprotective activities in spruces (*Picea* spp.). *Cryobiology* **58**, 268–274 (2009).
70. Lauersen, K. J., Brown, A., Middleton, A., Davies, P. L. & Walker, V. K. Expression and characterization of an antifreeze protein from the perennial rye grass, *Lolium perenne*. *Cryobiology* **62**, 194–201 (2011).
 71. Griffith, M. *et al.* Antifreeze proteins modify the freezing process in planta. *Plant Physiol* **138**, 330–340 (2005).
 72. Duman, J. & Olsen, T. M. Thermal Hysteresis Protein Activity in Bacteria, Fungi and Phylogenetically Diverse Plants. *Cryobiology* **30**, 322–328 (1993).
 73. Lee, J. K. *et al.* An extracellular ice-binding glycoprotein from an Arctic psychrophilic yeast. *Cryobiology* **60**, 222–228 (2010).
 74. Sicheri, F. & Yang, D. S. C. Ice-binding structure and mechanism of an antifreeze protein from winter flounder. *Nature* **375**, 427–431 (1995).
 75. Gronwald, W. *et al.* The Solution Structure of Type II Antifreeze Protein Reveals a New Member of the Lectin Family. *Biochemistry* **37**, 4712–4721 (1998).
 76. Jia, Z., DeLuca, C. I., Chao, H. & Davies, P. L. Structural basis for the binding of a globular antifreeze protein to ice. *Nature* **384**, 285–288 (1996).
 77. Gauthier, S. Y. *et al.* A re-evaluation of the role of type IV antifreeze protein. *Cryobiology* **57**, 292–296 (2008).
 78. Low, W. K. *et al.* Isolation and Characterization of Skin-type, Type I Antifreeze Polypeptides from the Longhorn Sculpin, *Myoxocephalus octodecemspinosus*. *J Biol Chem* **276**, 11582–11589 (2001).
 79. Liou, Y. C., Tocilj, A., Davies, P. L. & Jia, Z. Mimicry of ice structure by surface hydroxyls and water of a beta-helix antifreeze protein. *Nature* **406**, 322–324 (2000).
 80. Davies, P. L. *et al.* Beta-Helix structure and ice-binding properties of a hyperactive antifreeze protein from an insect. *Nature* **406**, 325–328 (2000).
 81. Pentelute, B. L. *et al.* X-ray Structure of Snow Flea Antifreeze Protein Determined by Racemic Crystallization of Synthetic Protein Enantiomers. *J Am Chem Soc* **130**, 9695–9701 (2008).
 82. Haridas, V. & Naik, S. Natural macromolecular antifreeze agents to synthetic antifreeze agents. *RSC Adv* **3**, 14199–14218 (2013).
 83. Liou, Y. C. *et al.* Folding and structural characterization of highly disulfide-bonded beetle antifreeze protein produced in bacteria. *Protein expression and purification* **19**, 148–157 (2000).
 84. Chao, H., Davies, P. L., Sykes, B. D. & Sönnichsen, F. D. Use of proline mutants to help solve the NMR solution structure of type III antifreeze protein. *Protein Sci* **2**, 1411–1428 (1993).
 85. Garnham, C. P., Natarajan, A. & Middleton, A. J. Compound ice-binding site of an antifreeze protein revealed by mutagenesis and fluorescent tagging. *Biochemistry* **49**, 9063–9071 (2010).
 86. De Groot, A. S. & Scott, D. W. Immunogenicity of protein therapeutics. *Trends*

- Immunol* **28**, 482–490 (2007).
87. Liu, S. *et al.* *In vitro* studies of antifreeze glycoprotein (AFGP) and a C-linked AFGP analogue. *Biomacromolecules* **8**, 1456–1462 (2007).
 88. Carpenter, J. F. & Hansen, T. N. Antifreeze protein modulates cell survival during cryopreservation: mediation through influence on ice crystal growth. *Proc Natl Acad Sci USA* **89**, 8953–8957 (1992).
 89. Wang, T., Zhu, Q., Yang, X., Layne, J. R., Jr & Devries, A. L. Antifreeze glycoproteins from antarctic notothenioid fishes fail to protect the rat cardiac explant during hypothermic and freezing preservation. *Cryobiology* **31**, 185–192 (1994).
 90. Schmid, W. Survival of frogs in low temperature. *Science* **215**, 697–698 (1982).
 91. Danks, H. V. Seasonal Adaptations in Arctic Insects. *Integr Comp Biol* **44**, 85–94 (2004).
 92. Salt, R. W. Natural Occurrence of Glycerol in Insects and Its Relation to Their Ability to Survive Freezing. *Can Entomol* **89**, 491–494 (1957).
 93. Chino, H. Conversion of Glycogen to Sorbitol and Glycerol in the Diapause Egg of the Bombyx Silkworm. *Nature* **180**, 606–607 (1957).
 94. Brockbank, K. G. M., Campbell, L. H., Greene, E. D., Brockbank, M. C. G. & Duman, J. G. Lessons from nature for preservation of mammalian cells, tissues, and organs. *In Vitro Cell Dev Biol* **47**, 210–217 (2010).
 95. Kukal, O., Heinrich, B. & Duman, J. Behavioural thermoregulation in the freeze-tolerant Arctic caterpillar, *Gynaephora groenlandica*. *J Exp Biol* **138**, 181–193 (1988).
 96. Worland, M. R., Block, W. & Grubor-Lajsic, G. Survival of *Heleomyza borealis* (Diptera, Heleomyzidae) larvae down to -60°C. *Physiol Entomol* **25**, 1–5 (2000).
 97. Duman, J. G. Insect antifreezes and ice-nucleating agents. *Cryobiology* **19**, 613–627 (1982).
 98. Worland, M. R., Grubor-Lajsic, G. & Montiel, P. O. Partial desiccation induced by sub-zero temperatures as a component of the survival strategy of the Arctic collembolan *Onychiurus arcticus* (Tullberg). *J Insect Physiol* **44**, 211–219 (1998).
 99. Hayward, S. A. L., Rinehart, J. P., Sandro, L. H., Lee, R. E. & Denlinger, D. L. Slow dehydration promotes desiccation and freeze tolerance in the Antarctic midge *Belgica antarctica*. *J Exp Biol* **210**, 836–844 (2007).
 100. Wharton, D. & Ferns, D. Survival of intracellular freezing by the Antarctic nematode *Panagrolaimus davidi*. *J Exp Biol* **198**, 1381–1387 (1995).
 101. Wharton, D. A. & Block, W. Differential Scanning Calorimetry Studies on an Antarctic Nematode (*Panagrolaimus davidi*) Which Survives Intracellular Freezing. *Cryobiology* **34**, 114–121 (1997).
 102. Sinclair, B. J., Worland, M. R., and Wharton, D. A. Ice nucleation and freezing tolerance in New Zealand alpine and lowland weta, *Hemideina* spp. (Orthoptera; Stenopelmatidae). *Physiol Entomol* **24**, 56–63 (1999).
 103. Ishiwata, A., Sakurai, A., Nishimiya, Y., Tsuda, S. & Ito, Y. Synthetic study and

- structural analysis of the antifreeze agent xylomannan from *Upis ceramboides*. *J Am Chem Soc* **133**, 19524–19535 (2011).
104. Walters, K. R., Serianni, A. S., Sformo, T., Barnes, B. M. & Duman, J. G. A nonprotein thermal hysteresis-producing xylomannan antifreeze in the freeze-tolerant Alaskan beetle *Upis ceramboides*. *Proc Natl Acad Sci USA* **106**, 20210–20215 (2009).
 105. Walters, K. R. *et al.* A thermal hysteresis-producing xylomannan glycolipid antifreeze associated with cold tolerance is found in diverse taxa. *J Comp Physiol B* **181**, 631–640 (2011).
 106. Karlsson, J. O. M. & Toner, M. Long-term storage of tissues by cryopreservation: critical issues. *Biomaterials* **17**, 243–256 (1996).
 107. Devries, A. L. Glycoproteins as biological antifreeze agents in antarctic fishes. *Science* **172**, 1152–1155 (1971).
 108. Marqusee, J. A. & Ross, J. Theory of Ostwald ripening: Competitive growth and its dependence on volume fraction. *J Chem Phys* **80**, 536–543 (1984).
 109. Pronk, P., Ferreira, C. I. & Witkamp, G. J. A dynamic model of Ostwald ripening in ice suspensions. *J Cryst Growth* **275**, 1355–1361 (2005).
 110. Kraska, T. Direct Observation of Single Ostwald Ripening Processes by Molecular Dynamics Simulation. *J Phys Chem B* **112**, 12408–12413 (2008).
 111. Knight, C. A., Devries, A. L. & Oolman, L. D. Fish antifreeze protein and the freezing and recrystallization of ice. *Nature* **308**, 295–296 (1984).
 112. Knight, C. A., Hallett, J. & Devries, A. L. Solute effects on ice recrystallization: an assessment technique. *Cryobiology* **25**, 55–60 (1988).
 113. Jackman, J. *et al.* Assessing antifreeze activity of AFGP 8 using domain recognition software. *Biochem Biophys Res Commun* **354**, 340–344 (2007).
 114. Smallwood, M. *et al.* Isolation and characterization of a novel antifreeze protein from carrot (*Daucus carota*). *Biochem J* **340**, 385–391 (1999).
 115. Hansen, T. N. & Carpenter, J. F. Calorimetric determination of inhibition of ice crystal growth by antifreeze protein in hydroxyethyl starch solutions. *Biophys J* **64**, 1843–1850 (1993).
 116. Tomczak, M. M., Marshall, C. B., Gilbert, J. A. & Davies, P. L. A facile method for determining ice recrystallization inhibition by antifreeze proteins. *Biochem Biophys Res Commun* **311**, 1041–1046 (2003).
 117. Inada, T. & Lu, S.-S. Inhibition of recrystallization of ice grains by adsorption of poly (vinyl alcohol) onto ice surfaces. *Cryst Growth Des* **3**, 747–752 (2003).
 118. Gibson, M. I., Barker, C. A., Spain, S. G., Albertin, L. & Cameron, N. R. Inhibition of ice crystal growth by synthetic glycopolymers: implications for the rational design of antifreeze glycoprotein mimics. *Biomacromolecules* **10**, 328–333 (2009).
 119. Yu, S. O. *et al.* Ice restructuring inhibition activities in antifreeze proteins with distinct differences in thermal hysteresis. *Cryobiology* **61**, 327–334 (2010).
 120. Liu, S. & Ben, R. N. C-linked galactosyl serine AFGP analogues as potent recrystallization inhibitors. *Org Lett* **7**, 2385–2388 (2005).

121. Urrutia, M. E., Duman, J. G. & Knight, C. A. Plant thermal hysteresis proteins. *Biochimica et Biophysica Acta (BBA)* **1121**, 199–206 (1992).
122. Marshall, C. B., Fletcher, G. L. & Davies, P. L. Hyperactive antifreeze protein in a fish. *Nature* **429**, 153 (2004).
123. Scotter, A. J. *et al.* The basis for hyperactivity of antifreeze proteins. *Cryobiology* **53**, 229–239 (2006).
124. Graham, L. A., Liou, Y. C., Walker, V. K. & Davies, P. L. Hyperactive antifreeze protein from beetles. *Nature* **388**, 727–728 (1997).
125. Chakrabarty, A., Yang, D. & Hew, C. L. Structure-function relationship in a winter flounder antifreeze polypeptide. II. Alteration of the component growth rates of ice by synthetic antifreeze polypeptides. *J Biol Chem* **264**, 11313–11316 (1989).
126. Raymond, J. A. & Devries, A. L. Adsorption inhibition as a mechanism of freezing resistance in polar fishes. *Proc Natl Acad Sci USA* **74**, 2589–2593 (1977).
127. Knight, C. A., Cheng, C. C. & Devries, A. L. Adsorption of alpha-helical antifreeze peptides on specific ice crystal surface planes. *Biophys J* **59**, 409–418 (1991).
128. Strom, C. S., Liu, X. Y. & Jia, Z. Ice surface reconstruction as antifreeze protein-induced morphological modification mechanism. *J Am Chem Soc* **127**, 428–440 (2005).
129. Knight, C. A., Driggers, E. & Devries, A. L. Adsorption to ice of fish antifreeze glycopeptides 7 and 8. *Biophys J* **64**, 252–259 (1993).
130. Houston, M. E. *et al.* Binding of an oligopeptide to a specific plane of ice. *J Biol Chem* **273**, 11714–11718 (1998).
131. Peltier, R. *et al.* Growth habit modification of ice crystals using antifreeze glycoprotein (AFGP) analogues. *Cryst Growth Des* **10**, 5066–5077 (2010).
132. Deville, S. *et al.* Ice Shaping Properties, Similar to That of Antifreeze Proteins, of a Zirconium Acetate Complex. *PLoS one* **6**, 1–6 (2011).
133. Peltier, R. *et al.* Synthesis and antifreeze activity of fish antifreeze glycoproteins and their analogues. *Chem Sci* **1**, 538–551 (2010).
134. Merrifield, R. B. Solid Phase Peptide Synthesis. I. The Synthesis of a Tetrapeptide. *J Am Chem Soc* **85**, 2149–2154 (1963).
135. Larsen, K., Thygesen, M. B., Guillaumie, F., Willats, W. G. T. & Jensen, K. J. Solid-phase chemical tools for glycobiology. *Carbohydr Res* **341**, 1209–1234 (2006).
136. Ben, R. N., Eniade, A. A. & Hauer, L. Synthesis of a C-linked Antifreeze Glycoprotein (AFGP) Mimic: Probes for Investigating the Mechanism of Action. *Org Lett* **1**, 1759–1762 (1999).
137. Eniade, A. & Ben, R. N. Fully convergent solid phase synthesis of antifreeze glycoprotein analogues. *Biomacromolecules* **2**, 557–561 (2001).
138. Eniade, A., Murphy, A. V., Landreau, G. & Ben, R. N. A general synthesis of structurally diverse building blocks for preparing analogues of C-linked antifreeze glycoproteins. *Bioconjugate Chem* **12**, 817–823 (2001).
139. Bouvet, V. R., Lorello, G. R. & Ben, R. N. Aggregation of antifreeze glycoprotein

- fraction 8 and its effect on antifreeze activity. *Biomacromolecules* **7**, 565–571 (2006).
140. Czechura, P., Tam, R. Y., Dimitrijevic, E., Murphy, A. V. & Ben, R. N. The Importance of Hydration for Inhibiting Ice Recrystallization with C-Linked Antifreeze Glycoproteins. *J Am Chem Soc* **130**, 2928–2929 (2008).
141. Tam, R. Y., Ferreira, S. S., Czechura, P., Chaytor, J. L. & Ben, R. N. Hydration Index-A Better Parameter for Explaining Small Molecule Hydration in Inhibition of Ice Recrystallization. *J Am Chem Soc* **130**, 17494–17501 (2008).
142. Tam, R. Y. *et al.* Solution conformation of C-linked antifreeze glycoprotein analogues and modulation of ice recrystallization. *J Am Chem Soc* **131**, 15745–15753 (2009).
143. Capicciotti, C. J., Trant, J. F., Leclere, M. & Ben, R. N. Synthesis of C-linked triazole-containing AFGP analogues and their ability to inhibit ice recrystallization. *Bioconjugate Chem* **22**, 605–616 (2011).
144. Chaytor, J. L. & Ben, R. N. Assessing the ability of a short fluorinated antifreeze glycopeptide and a fluorinated carbohydrate derivative to inhibit ice recrystallization. *Bioorg Med Chemistry Lett* **20**, 5251–5254 (2010).
145. Chaytor, J. L. *et al.* Inhibiting ice recrystallization and optimization of cell viability after cryopreservation. *Glycobiology* **22**, 123–133 (2012).
146. Wu, L. K. *et al.* Carbohydrate-mediated inhibition of ice recrystallization in cryopreserved human umbilical cord blood. *Carbohydr Res* **346**, 86–93 (2011).
147. Leclere, M., Kwok, B. K., Wu, L. K., Allan, D. S. & Ben, R. N. C-linked antifreeze glycoprotein (C-AFGP) analogues as novel cryoprotectants. *Bioconjugate Chem* **22**, 1804–1810 (2011).
148. Capicciotti, C. J. *et al.* Potent inhibition of ice recrystallization by low molecular weight carbohydrate-based surfactants and hydrogelators. *Chem Sci* **3**, 1408–1416 (2012).
149. Wilkinson, B. L. *et al.* Total Synthesis of Homogeneous Antifreeze Glycopeptides and Glycoproteins. *Angew Chem Int Edit* **51**, 3606–3610 (2012).
150. Corcilus, L. *et al.* Synthesis of peptides and glycopeptides with polyproline II helical topology as potential antifreeze molecules. *Bioorg Med Chem* **21**, 3569–3581 (2013).
151. Miller, N., Williams, G. M. & Brimble, M. A. Synthesis of fish antifreeze neoglycopeptides using microwave-assisted 'click chemistry'. *Org Lett* **11**, 2409–2412 (2009).
152. Tachibana, Y. *et al.* Antifreeze glycoproteins: elucidation of the structural motifs that are essential for antifreeze activity. *Angew Chem Int Edit* **116**, 874–880 (2004).
153. Tachibana, Y., Matsubara, N., Nakajima, F. & Tsuda, T. Efficient and versatile synthesis of mucin-like glycoprotein mimics. *Tetrahedron* **58**, 10213–10224 (2002).
154. Garner, J. & Harding, M. M. Design and synthesis of antifreeze glycoproteins and

- mimics. *ChemBioChem* **11**, 2489–2498 (2010).
155. Garner, J., Jolliffe, K. A., Harding, M. M. & Payne, R. J. Synthesis of homogeneous antifreeze glycopeptides via a ligation-desulfurisation strategy. *Chem Comm* 6925–6927 (2009).
 156. Heggemann, C. *et al.* Antifreeze glycopeptide analogues: microwave-enhanced synthesis and functional studies. *Amino Acids* **38**, 213–222 (2010).
 157. Nagel, L. *et al.* Synthesis and characterization of natural and modified antifreeze glycopeptides: glycosylated foldamers. *Amino Acids* **41**, 719–732 (2011).
 158. Nagel, L. *et al.* Influence of Sequential Modifications and Carbohydrate Variations in Synthetic AFGP Analogues on Conformation and Antifreeze Activity. *Chemistry* **18**, 12783–12793 (2012).
 159. Tsuda, T. & Nishimura, S.-I. I. Synthesis of an antifreeze glycoprotein analogue: efficient preparation of sequential glycopeptide polymers. *Chem Comm* 2779–2780 (1996).
 160. Matsushita, T., Hinou, H., Kuroguchi, M., Shimizu, H. & Nishimura, S.-I. I. Rapid microwave-assisted solid-phase glycopeptide synthesis. *Org Lett* **7**, 877–880 (2005).
 161. Hachisu, M. *et al.* One-pot synthesis of cyclic antifreeze glycopeptides. *Chem Comm* 1641–1643 (2009).
 162. Deller, R. *et al.* Ice recrystallization inhibition by polyols: comparison of molecular and macromolecular inhibitors and role of hydrophobic units. *Biomater Sci* **1**, 478–485 (2013).
 163. Congdon, T., Notman, R. & Gibson, M. I. Antifreeze (Glyco)protein Mimetic Behavior of Poly(vinyl alcohol): Detailed Structure Ice Recrystallization Inhibition Activity Study. *Biomacromolecules* **14**, 1578–1586 (2013).
 164. Modak, P. & Inada, T. Growth control of ice crystals by poly (vinyl alcohol) and antifreeze protein in ice slurries. *Chem Eng Sci* **61**, 3149–3158 (2006).
 165. Budke, C. & Koop, T. Ice recrystallization inhibition and molecular recognition of ice faces by poly(vinyl alcohol). *ChemPhysChem* **7**, 2601–2606 (2006).
 166. Inada, T. & Lu, S.-S. Thermal hysteresis caused by non-equilibrium antifreeze activity of poly (vinyl alcohol). *Chem Phys Lett* **394**, 361–365 (2004).
 167. Mastai, Y., Rudloff, J., Cölfen, H. & Antonietti, M. Control over the Structure of Ice and Water by Block Copolymer Additives. *ChemPhysChem* **1**, 119–123 (2002).
 168. Jiang, Y. *et al.* In-vivo studies on intraperitoneally administered poly(vinyl alcohol). *J Biomed Mater Res Part B* **93**, 275–284 (2010).
 169. Matsumura, S., Kurita, H. & Shimokobe, H. Anaerobic biodegradability of polyvinyl alcohol. *Biotechnol Lett* **15**, 749–754 (1993).
 170. Schellekens, H. Immunogenicity of therapeutic proteins: Clinical implications and future prospects. *Clin Ther* **24**, 1720–1740 (2002).
 171. DeMerlis, C. & Schoneker, D. Review of the oral toxicity of polyvinyl alcohol (PVA). *Food Chem Toxicol* **41**, 319–326 (2003).
 172. Crevel, R. W. R. *et al.* Lack of immunogenicity of ice structuring protein type III

- HPLC12 preparation administered by the oral route to human volunteers. *Food Chem Toxicol* **45**, 79–87 (2007).
173. Deville, S., Viazzi, C. & Guizard, C. Ice-Structuring Mechanism for Zirconium Acetate. *Langmuir* **28**, 14892–14898 (2012).
 174. Mizrahy, O., Bar-Dolev, M., Guy, S. & Braslavsky, I. Inhibition of ice growth and recrystallization by zirconium acetate and zirconium acetate hydroxide. *PloS one* **8**, e59540 (2013).
 175. Deville, S. Ice-templating, freeze casting: Beyond materials processing. *J Mater Res* **28**, 2202–2219 (2013).
 176. Ali, A., Auvinen, M.-K. & Rautonen, J. The aging population poses a global challenge for blood services. *Transfusion* **50**, 584–588 (2010).
 177. Benjamin, R. J. & Whitaker, B. I. Boom or bust? Estimating blood demand and supply as the baby boomers age. *Transfusion* **51**, 670–673 (2011).
 178. Give Blood - How Blood is used. *blood.co.uk* at <<http://www.blood.co.uk/about-blood/how-blood-is-used/>>
 179. *nhsbt.nhs.uk.* at <<http://www.nhsbt.nhs.uk>>
 180. Scott, K. L., Lecak, J. & Acker, J. P. Biopreservation of red blood cells: past, present, and future. *Transfus Medicine Rev* **19**, 127–142 (2005).
 181. Solomon, A. K., Toon, M. R. & Dix, J. A. Osmotic properties of human red cells. *J Membrane Biol* **91**, 259–273 (1986).
 182. Liu, J., Christian, J. A. & Critser, J. K. Canine RBC osmotic tolerance and membrane permeability. *Cryobiology* **44**, 258–268 (2002).
 183. Meryman, H. T. Osmotic stress as a mechanism of freezing injury. *Cryobiology* **8**, 489–500 (1971).
 184. Wood, L. & Beutler, E. The viability of human blood stored in phosphate adenine media. *Transfusion* **7**, 401–408 (1967).
 185. Beutler, E., Meul, A. & Wood, L. A. Depletion and Regeneration of 2,3-diphosphoglyceric Acid in Stored Red Blood Cells. *Transfusion* **9**, 109–114 (1969).
 186. Meyer, E. K., Dumont, D. F., Baker, S. & Dumont, L. J. Rejuvenation capacity of red blood cells in additive solutions over long-term storage. *Transfusion* **51**, 1574–1579 (2011).
 187. Hovav, T., Yedgar, S., Manny, N. & Barshtein, G. Alteration of red cell aggregability and shape during blood storage. *Transfusion* **39**, 277–281 (2002).
 188. Holovati, J. Emerging Role for Use of Liposomes in the Biopreservation of Red Blood Cells. *Transfus Med Hemother* **38**, 99–106 (2011).
 189. Hess, J. R. & Greenwalt, T. G. Storage of red blood cells: New approaches. *Transfus Medicine Rev* **16**, 283–295 (2002).
 190. Acker, J. P. & Croteau, I. An analysis of the bias in red blood cell hemolysis measurement using several analytical approaches. *Clin Chim Acta* **413**, 1746–1752 (2012).
 191. Hess, J. R. *et al.* Blood Components: Red blood cell hemolysis during blood bank

- storage: using national quality management data to answer basic scientific questions. *Transfusion* **49**, 2599–2603 (2009).
192. Mazur, P. Freezing of living cells: mechanisms and implications. *Am J Physiol* C125–C142 (1984).
 193. Fowler, A. & Toner, M. Cryo-Injury and Biopreservation. *Ann NY Acad Sci* **1066**, 119–135 (2005).
 194. Meryman, H. T. The Relationship between Dehydration and Freezing Injury in the Human Erythrocyte. *Cellular Injury and Resistance in Freezing Organisms* **2**, 231–244 (1967).
 195. Lovelock, J. E. The mechanism of the protective action of glycerol against haemolysis by freezing and thawing. *Biochimica et Biophysica Acta (BBA)* **11**, 28–36 (1953).
 196. Pegg, D. E. & Diaper, M. P. On the mechanism of injury to slowly frozen erythrocytes. *Biophys J* **54**, 471–488 (1988).
 197. Pegg, D. E. & Diaper, M. P. The effect of initial tonicity on freeze/thaw injury to human red cells suspended in solutions of sodium chloride. *Cryobiology* **28**, 18–35 (1991).
 198. Pegg, D. E. The effect of cell concentration on the recovery of human erythrocytes after freezing and thawing in the presence of glycerol. *Cryobiology* **18**, 221–228 (1981).
 199. Nei, T. Mechanism of freezing injury to erythrocytes: Effect of initial cell concentration on the post-thaw hemolysis. *Cryobiology* **18**, 229–237 (1981).
 200. Meryman, H. T. Cryopreservation of living cells: principles and practice. *Transfusion* **47**, 935–945 (2007).
 201. Muldrew, K. & McGann, L. E. Mechanisms of intracellular ice formation. *Biophys J* **57**, 525–532 (1990).
 202. Sputtek, A., Kuhn, P. & Rowe, A. W. Cryopreservation of Erythrocytes, Thrombocytes, and Lymphocytes. *Trans Med Hemother* **34**, 262–267 (2007).
 203. Valeri, C. R. & Runck, A. H. Long Term Frozen Storage of Human Red Blood Cells: Studies *in vivo* and *in Vitro* of Autologous Red Blood Cells Preserved up to Six Years with High Concentrations of Glycerol. *Transfusion* **9**, 5–14 (1969).
 204. McGann, L. E. Differing actions of penetrating and nonpenetrating cryoprotective agents. *Cryobiology* **15**, 382–390 (1978).
 205. Meryman, H. T. Cryoprotective agents. *Cryobiology* **8**, 173–183 (1971).
 206. Lelkens, C., Noorman, F., Koning, J. & Lange, R. Stability after thawing of RBCs frozen with the high-and low-glycerol method. *Transfusion* **43**, 157–164 (2003).
 207. Brecher, M. E. & Hay, S. N. Bacterial Contamination of Blood Components. *Clin. Microbiol. Rev.* **18**, 195–204 (2005).
 208. Palavecino, E. L., Yomtovian, R. A. & Jacobs, M. R. Detecting bacterial contamination in platelet products. *Clin Lab* **52**, 443–456 (2006).
 209. Rowe, A., Eyster, E. & Kellner, A. Liquid nitrogen preservation of red blood cells

- for transfusion. A low glycerol-Rapid freeze procedure. *Cryobiology* **5**, 119–128 (1968).
210. Meryman, H. T. & Hornblower, M. A simplified procedure for deglycerolizing red blood cells frozen in a high glycerol concentration. *Transfusion* **17**, 438–442 (1977).
 211. Johnson, V. V. & Swiatkowski, S. A. Scientific aspects of supplying blood to distant military theaters. *Curr Opin Hematol* **14**, 694–699 (2007).
 212. Klein, H. G., Spahn, D. R. & Carson, J. L. Red blood cell transfusion in clinical practice. *Lancet* **370**, 415–426 (2007).
 213. Pellerin-Mendes, C., Million, L. & Marchand-Arvier, M. *In vitro* study of the protective effect of trehalose and dextran during freezing of human red blood cells in liquid nitrogen. *Cryobiology* **35**, 20–30 (1997).
 214. Quan, G. *et al.* Intracellular Sugars Improve Survival of Human Red Blood Cells Cryopreserved at -80°C in the Presence of Polyvinyl Pyrrolidone and Human Serum Albumin. *Cryo Lett* **28**, 95–108 (2007).
 215. Takahashi, T., Hirsh, A., Erbe, E. & Williams, R. J. Mechanism of cryoprotection by extracellular polymeric solutes. *Biophys J* **54**, 509–518 (1988).
 216. Treib, J., Baron, J., Grauer, M. & Strauss, R. G. An international view of hydroxyethyl starches. *Intens Care Med* **25**, 258–268 (1999).
 217. Kozek-Langenecker, S. Effects of hydroxyethyl starch solutions on hemostasis. *Anesthesiology* **103**, 654–660 (2005).
 218. Bork, K. Pruritus precipitated by hydroxyethyl starch: a review. *Brit J Dermatol* **152**, 3–12 (2005).
 219. Reinhart, K. & Takala, J. Hydroxyethyl starches: what do we still know? *Anesth Analg* **112**, 507–511 (2011).
 220. Nolan, J. P. & Mythen, M. G. I. Hydroxyethyl starch: here today, gone tomorrow. *Brit J Anaesth* **111**, 321–324 (2013).
 221. Stolzing, A., Naaldijk, Y., Fedorova, V. & Sethe, S. Hydroxyethyl starch in cryopreservation - mechanisms, benefits and problems. *Transfus Apher Sci* **46**, 137–147 (2012).
 222. Westphal, M. *et al.* Hydroxyethyl starches: different products-different effects. *Anesthesiology* **111**, 187–202 (2009).
 223. Jungheinrich, C. & Neff, T. A. Pharmacokinetics of Hydroxyethyl Starch. *Clin Pharmacokinet* **44**, 681–699 (2005).
 224. Neff, T. A., Fischler, L., Mark, M., Stocker, R. & Reinhart, W. H. The Influence of Two Different Hydroxyethyl Starch Solutions (6% HES 130/0.4 and 200/0.5) on Blood Viscosity. *Anesth Analg* **100**, 1773–1780 (2005).
 225. Sputtek, A., Singbartl, G. & Langer, R. Cryopreservation of red blood cells with the non-penetrating cryoprotectant hydroxyethyl starch. *Cryo Lett* **16**, 283–288 (1995).
 226. Fahy, G. M., MacFarlan, D. R., Angell, C. A. & Meryman, H. T. Vitrification as an approach to cryopreservation. *Cryobiology* **21**, 407–426 (1984).
 227. Fahy, G. M., Saur, J. & Williams, R. J. Physical problems with the vitrification of

- large biological systems. *Cryobiology* **27**, 492–510 (1990).
228. Macfarlane, D. R. Devitrification in glass-forming aqueous solutions. *Cryobiology* **23**, 230–244 (1986).
229. Kuleshova, L. L., Macfarlane, D. R. & Trounson, A. O. Sugars Exert a Major Influence on the Vitrification Properties of Ethylene Glycol-Based Solutions and Have Low Toxicity to Embryos and Oocytes. *Cryobiology* **38**, 119–130 (1999).
230. Mehl, P. & Boutron, P. Cryoprotection of red blood cells by 1,3-butanediol and 2,3-butanediol. *Cryobiology* **25**, 44–54 (1988).
231. Boutron, P. & Peyridieu, J. F. Reduction in Toxicity for Red Blood Cells in Buffered Solutions Containing High Concentrations of 2,3-Butanediol by Trehalose, Sucrose, Sorbitol, or Mannitol. *Cryobiology* **31**, 367–373 (1994).
232. Han, Y. *et al.* Improved preservation of human red blood cells by lyophilization. *Cryobiology* **51**, 152–164 (2005).
233. Goodrich, R. P., Sowemimo-Coker, S. O., Zerez, C. R. & Tanaka, K. R. Preservation of metabolic activity in lyophilized human erythrocytes. *Proc Natl Acad Sci USA* **89**, 967–971 (1992).
234. Spieles, G., Heschel, I. & Rau, G. An attempt to recover viable human red blood cells after freeze-drying. *Cryo Lett* **17**, 43–52 (1996).
235. Karlsson, J. O. M. A Theoretical Model of Intracellular Devitrification. *Cryobiology* **42**, 154–169 (2001).
236. Chao, H., Davies, P. L. & Carpenter, J. F. Effects of antifreeze proteins on red blood cell survival during cryopreservation. *J Exp Biol* **199**, 2071–2076 (1996).
237. Liebermann, J., Nawroth, F., Isachenko, V., Isachenko, E. & Rahimi, R. Potential Importance of Vitrification in Reproductive Medicine. *Biol Reprod* **67**, 1671–1680 (2002).
238. Polge, C., Smith, A. U. & Parkes, A. S. Revival of Spermatozoa after Vitrification and Dehydration at Low Temperatures. *Nature* **164**, 666 (1949).
239. Wales, R. The deep freezing of rabbit spermatozoa. *Aust J Biol Sci* **21**, 831–833 (1968).
240. Koshimoto, C. & Mazur, P. The effect of the osmolality of sugar-containing media, the type of sugar, and the mass and molar concentration of sugar on the survival of frozen-thawed mouse sperm. *Cryobiology* **45**, 80–90 (2002).
241. Curry, M. Cryopreservation of semen from domestic livestock. *Rev Reprod* **5**, 46–52 (2000).
242. Bunge, R. G. & Sherman, J. K. Fertilizing Capacity of Frozen Human Spermatozoa. *Nature* **172**, 767–768 (1953).
243. Andrabi, S. M. H. & Maxwell, W. M. C. A review on reproductive biotechnologies for conservation of endangered mammalian species. *Anim Reprod Sci* **99**, 223–243 (2007).
244. Holt, W. V. Fundamental aspects of sperm cryobiology: The importance of species and individual differences. *Theriogenology* **53**, 47–58 (2000).
245. Parks, J. E. & Graham, J. K. Effects of cryopreservation procedures on sperm

- membranes. *Theriogenology* **38**, 209–222 (1992).
246. Morris, G. J., Acton, E. & Avery, S. A novel approach to sperm cryopreservation. *Hum Reprod* **14**, 1013–1021 (1999).
 247. Willoughby, C. E., Mazur, P., Peter, A. T. & Critser, J. K. Osmotic tolerance limits and properties of murine spermatozoa. *Biol Reprod* **55**, 715–727 (1996).
 248. Songsasen, N. & Leibo, S. P. Cryopreservation of mouse spermatozoa. II. Relationship between survival after cryopreservation and osmotic tolerance of spermatozoa from three strains of mice. *Cryobiology* **35**, 255–269 (1997).
 249. Payne, S. R., Oliver, J. E. & Upreti, G. C. Effect of antifreeze proteins on the motility of ram spermatozoa. *Cryobiology* **31**, 180–184 (1994).
 250. Koshimoto, C. & Mazur, P. Effects of warming rate, temperature, and antifreeze proteins on the survival of mouse spermatozoa frozen at an optimal rate. *Cryobiology* **45**, 49–59 (2002).
 251. Younis, A., Rooks, B., Khan, A. & Gould, K. K. The Effects of Antifreeze Peptide III (AFP) and Insulin Transferrin Selenium (ITS) on Cryopreservation of Chimpanzee (*Pan troglodytes*) Spermatozoa. *J Androl* **19**, 207–214 (1998).
 252. Prathalingam, N. S. *et al.* Impact of antifreeze proteins and antifreeze glycoproteins on bovine sperm during freeze-thaw. *Theriogenology* **66**, 1894–1900 (2006).
 253. Beirão, J. *et al.* Improving sperm cryopreservation with antifreeze proteins: effect on gilthead seabream (*Sparus aurata*) plasma membrane lipids. *Biol Reprod* **86**, 1–9 (2012).
 254. Seki, S. & Mazur, P. Effect of warming rate on the survival of vitrified mouse oocytes and on the recrystallization of intracellular ice. *Biol Reprod* **79**, 727–737 (2008).
 255. Whittingham, D. G. Fertilization in vitro and development to term of unfertilized mouse oocytes previously stored at -196 degrees C. *J Reprod Fertil* **49**, 89–94 (1977).
 256. al-Hasani, S. *et al.* Successful embryo transfer of cryopreserved and in-vitro fertilized rabbit oocytes. *Hum Reprod* **4**, 77–79 (1989).
 257. Fuku, E., Kojima, T., Shioya, Y., Marcus, G. J. & Downey, B. R. *In vitro* fertilization and development of frozen-thawed bovine oocytes. *Cryobiology* **29**, 485–492 (1992).
 258. Maclellan, L. J. *et al.* Pregnancies from vitrified equine oocytes collected from super-stimulated and non-stimulated mares. *Theriogenology* **58**, 911–919 (2002).
 259. Chen, C. Pregnancy after human oocyte cryopreservation. *Lancet* **1**, 884–886 (1986).
 260. Chen, C. Pregnancies after Human Oocyte Cryopreservation. *Ann NY Acad Sci* **541**, 541–549 (1988).
 261. Paynter, S. J. Current status of the cryopreservation of human unfertilized oocytes. *Hum Reprod Update* **6**, 449–456 (2000).
 262. Konc, J., Kanyo, K., Varga, E., Kriston, R. & Cseh, S. Births resulting from oocyte

- cryopreservation using a slow freezing protocol with propanediol and sucrose. *Syst Biol Reprod Med* **54**, 205–210 (2008).
263. Pickering, S. J., Braude, P. R. & Johnson, M. H. Cryoprotection of human oocytes: inappropriate exposure to DMSO reduces fertilization rates. *Hum Reprod* **6**, 142–143 (1991).
 264. Boldt, J. Current results with slow freezing and vitrification of the human oocyte. *Reprod BioMed Online* **23**, 314–322 (2011).
 265. O'neil, L., Paynter, S., Fuller, B. & Shaw, R. Vitrification of mature mouse oocytes in a 6 M Me₂SO solution supplemented with antifreeze glycoproteins: the effect of temperature. *Cryobiology* **37**, 59–66 (1998).
 266. Arav, A., Rubinsky, B., Fletcher, G. L. & Seren, E. Cryogenic protection of oocytes with antifreeze proteins. *Mol Reprod Dev* **36**, 488–493 (1993).
 267. Jo, J. W., Jee, B. C., Suh, C. S. & Kim, S. H. The beneficial effects of antifreeze proteins in the vitrification of immature mouse oocytes. *PloS one* **7**, e37043 (2012).
 268. Byrd, W. Cryopreservation, thawing, and transfer of human embryos. *Semin Reprod Med* **20**, 37–43 (2002).
 269. Whittingham, D. G., Leibo, S. P. & Mazur, P. Survival of mouse embryos frozen to -196 degrees and -269 degrees C. *Science* **178**, 411–414 (1972).
 270. Tucker, M. J., Morton, P. C., Sweitzer, C. L. & Wright, G. Cryopreservation of human embryos and oocytes. *Curr Opin Obstet Gynecol* **7**, 188–192 (1995).
 271. Nowshari, M. Effect of cryoprotectants and their concentration on post-thaw survival and development of expanded mouse blastocysts frozen by a simple rapid-freezing procedure. *Theriogenology* **50**, 1001–1013 (1998).
 272. Cseh, S. *et al.* Vitrification of mouse embryos in two cryoprotectant solutions. *Theriogenology* **52**, 103–113 (1999).
 273. Baguisi, A., Arav, A., Crosby, T. F., Roche, J. F. & Boland, M. P. Hypothermic storage of sheep embryos with antifreeze proteins: development *in vitro* and *in vivo*. *Theriogenology* **48**, 1017–1024 (1997).
 274. Robles, V., Barbosa, V., Herráez, M. P., Martínez-Páramo, S. & Cancela, M. L. The antifreeze protein type I (AFP I) increases seabream (*Sparus aurata*) embryos tolerance to low temperatures. *Theriogenology* **68**, 284–289 (2007).
 275. Hauptman, P. J. & O'Connor, K. J. Procurement and Allocation of Solid Organs for Transplantation. *N Engl J Med* **336**, 422–431 (1997).
 276. Gridelli, B. & Remuzzi, G. Strategies for Making More Organs Available for Transplantation. *N Engl J Med* **343**, 404–410 (2000).
 277. Opar, A. As demand for organs expands, so does transplant technology. *Nat Med* **14**, 225 (2008).
 278. Orlando, G. *et al.* Regenerative medicine and organ transplantation: past, present, and future. *Transplantation* **91**, 1310–1317 (2011).
 279. OPTN: Organ Procurement and Transplantation Network. optn.transplant.hrsa.gov (2013). at <<http://optn.transplant.hrsa.gov/data/>>

280. Wolfe, R. A., Roys, E. C. & Merion, R. M. Trends in organ donation and transplantation in the United States, 1999-2008. *Am J Transplant* **10**, 961–972 (2010).
281. Ubeaud, G., Schiller, C. D., Hurbin, F., Jaeck, D. & Coassolo, P. Comparison of the stability of some major cytochrome p450 and conjugation reactions in rat, dog and human hepatocyte monolayers. *Eur J Drug Metab Ph* **26**, 37–45 (2001).
282. McGinnity, D. F., Soars, M. G., Urbanowicz, R. A. & Riley, R. J. Evaluation of fresh and cryopreserved hepatocytes as *in vitro* drug metabolism tools for the prediction of metabolic clearance. *Drug Metab Dispos* **32**, 1247–1253 (2004).
283. Pahernik, S. A., Thasler, W. E., Mueller-Hoecker, J. & Schildberg, F. W. Hypothermic Storage of Pig Hepatocytes: Influence of Different Storage Solutions and Cell Density. *Cryobiology* **33**, 552–566 (1996).
284. Fuller, B. J. & Lee, C. Y. Hypothermic perfusion preservation: The future of organ preservation revisited? *Cryobiology* **54**, 129–145 (2007).
285. Stephenne, X., Najimi, M. & Sokal, E. M. Hepatocyte cryopreservation: Is it time to change the strategy? *World J Gastroenterol* **16**, 1–14 (2010).
286. Coundouris, J. A., Grant, M. H., Engeset, J., Petrie, J. C. & Hawksworth, G. M. Cryopreservation of human adult hepatocytes for use in drug metabolism and toxicity studies. *Xenobiotica* **23**, 1399–1409 (1993).
287. Chesné, C. & Guillouzo, A. Cryopreservation of isolated rat hepatocytes: A critical evaluation of freezing and thawing conditions. *Cryobiology* **25**, 323–330 (1988).
288. Terry, C., Dhawan, A., Mitry, R. R., Lehec, S. C. & Hughes, R. D. Optimization of the cryopreservation and thawing protocol for human hepatocytes for use in cell transplantation. *Liver Transpl* **16**, 229–237 (2010).
289. Kusano, M., Ebata, H., Onishi, T. & Saito, T. Transplantation of cryopreserved isolated hepatocytes into the rat spleen. *Transplant P* **13**, 848–854 (1981).
290. Karlsson, J. O. *et al.* Nucleation and growth of ice crystals inside cultured hepatocytes during freezing in the presence of dimethyl sulfoxide. *Biophys J* **65**, 2524–2536 (1993).
291. Terry, C., Dhawan, A., Mitry, R. R. & Hughes, R. D. Cryopreservation of isolated human hepatocytes for transplantation: State of the art. *Cryobiology* **53**, 149–159 (2006).
292. Fowler, A., Tompkins, R. & Toner, M. Cryopreservation of isolated primary rat hepatocytes: enhanced survival and long-term hepatospecific function. *Ann Surg* **241**, 125–133 (2005).
293. Rubinsky, B., Arav, A., Hong, J. S. & Lee, C. Y. Freezing of Mammalian Livers with Glycerol and Antifreeze Proteins. *Biochem Biophys Res Commun* **200**, 732–741 (1994).
294. Watts, P. & Grant, M. H. Cryopreservation of rat hepatocyte monolayer cultures. *Hum Exp Toxicol* **15**, 30–37 (1996).
295. Miyamoto, Y., Suzuki, S., Nomura, K. & Enosawa, S. Improvement of hepatocyte viability after cryopreservation by supplementation of long-chain oligosaccharide

- in the freezing medium in rats and humans. *Cell Transplantation* **15**, 911–919 (2006).
296. Soltys, K. A., Batta, A. K. & Koneru, B. Successful nonfreezing, subzero preservation of rat liver with 2,3-butanediol and type I antifreeze protein. *J Surg Res* **96**, 30–34 (2001).
 297. Imperatore, G. *et al.* Projections of Type 1 and Type 2 Diabetes Burden in the U.S. Population Aged <20 Years Through 2050. *Diabetes* **35**, 2515–2520 (2012).
 298. Nolan, C. J., Damm, P. & Prentki, M. Type 2 diabetes across generations: from pathophysiology to prevention and management. *Lancet* **378**, 169–181 (2011).
 299. Shapiro, A. M. *et al.* Islet transplantation in seven patients with type 1 diabetes mellitus using a glucocorticoid-free immunosuppressive regimen. *N Engl J Med* **343**, 230–238 (2000).
 300. Matsumoto, S. *et al.* Insulin independence after living-donor distal pancreatectomy and islet allotransplantation. *Lancet* **365**, 1642–1644 (2005).
 301. Hohmeier, H. & Newgard, C. B. Cell lines derived from pancreatic islets. *Mol Cell Endocrinol* **228**, 121–128 (2004).
 302. Kenmochi, T. *et al.* Cryopreservation of Human Pancreatic Islets From Non-Heart-Beating Donors Using Hydroxyethyl Starch and Dimethyl Sulfoxide as Cryoprotectants. *Cell Transplantation* **17**, 61–67 (2008).
 303. Warnock, G. L. & Rajotte, R. V. Effects of precryopreservation culture on survival of rat islets transplanted after slow cooling and rapid thawing. *Cryobiology* **26**, 103–111 (1989).
 304. Rajotte, R. V. Islet cryopreservation protocols. *Ann NY Acad Sci* **875**, 200–207 (1999).
 305. Foreman, J., Moriya, H. & Taylor, M. J. Effect of cooling rate and its interaction with pre-freeze and post-thaw tissue culture on the in vitro and in vivo function of cryopreserved pancreatic islets. *Transplant Int* **6**, 191–200 (1993).
 306. Taylor, M. J. & Baicu, S. Review of vitreous islet cryopreservation: Some practical issues and their resolution. *Organogenesis* **5**, 155–166 (2009).
 307. Matsumoto, S. *et al.* Effects of synthetic antifreeze glycoprotein analogue on islet cell survival and function during cryopreservation. *Cryobiology* **52**, 90–98 (2006).
 308. Yokomuro, H. *et al.* Transplantation of cryopreserved cardiomyocytes. *J Thorac Cardiovasc Sur* **121**, 98–107 (2001).
 309. Yokomuro, H., Mickle, D. A. G., Weisel, R. D. & Li, R.-K. Optimal conditions for heart cell cryopreservation for transplantation. *Mol Cell Biochem* **242**, 109–114 (2003).
 310. Mugnano, J. A., Wang, T., Layne, J. R., Jr, Devries, A. L. & Lee, R. E. Antifreeze glycoproteins promote intracellular freezing of rat cardiomyocytes at high subzero temperatures. *Am J Physiol* **269**, R474–R479 (1995).
 311. Kurtzberg, J., Laughlin, M. & Graham, M. Placental blood as a source of hematopoietic stem cells for transplantation into unrelated recipients. *N Engl J Med* (1996).

312. Olausson, M. *et al.* Transplantation of an allogeneic vein bioengineered with autologous stem cells: a proof-of-concept study. *Lancet* **380**, 230–237 (2012).
313. Hipp, J. & Atala, A. Sources of Stem Cells for Regenerative Medicine. *Stem Cell Rev* **4**, 3–11 (2008).
314. Abbruzzese, L. *et al.* Long term cryopreservation in 5% DMSO maintains unchanged CD34(+) cells viability and allows satisfactory hematological engraftment after peripheral blood stem cell transplantation. *Vox Sang* **105**, 77–80 (2013).
315. Windrum, P. *et al.* Variation in dimethyl sulfoxide use in stem cell transplantation: a survey of EBMT centres. *Bone Marrow Transpl* **36**, 601–603 (2005).
316. Hubel, A. Parameters of cell freezing: implications for the cryopreservation of stem cells. *Transfus Medicine Rev* **11**, 224–233 (1997).
317. Hunt, C. J. Cryopreservation of Human Stem Cells for Clinical Application: A Review. *Transfus Med Hemother* **38**, 107–123 (2011).
318. Naaldijk, Y., Staude, M., Fedorova, V. & Stolzing, A. Effect of different freezing rates during cryopreservation of rat mesenchymal stem cells using combinations of hydroxyethyl starch and dimethylsulfoxide. *BMC Biotechnol* **12**, 49 (2012).
319. Rodrigues, J. P. *et al.* Evaluation of trehalose and sucrose as cryoprotectants for hematopoietic stem cells of umbilical cord blood. *Cryobiology* **56**, 144–151 (2008).
320. Wang, H.-Y., Lun, Z.-R. & Lu, S.-S. Cryopreservation of umbilical cord blood-derived mesenchymal stem cells without dimethyl sulfoxide. *Cryo Lett* **32**, 81–88 (2011).
321. Hubalek, Z. Protectants used in the cryopreservation of microorganisms. *Cryobiology* **46**, 205–229 (2003).
322. Wang, W. Lyophilization and development of solid protein pharmaceuticals. *Int J Pharm* **203**, 1–60 (2000).
323. Carpenter, J. F. & Crowe, J. H. The mechanism of cryoprotection of proteins by solutes. *Cryobiology* **25**, 244–255 (1988).
324. Arakawa, T., Kita, Y. & Carpenter, J. F. Protein–Solvent Interactions in Pharmaceutical Formulations. *Pharm Res* **08**, 285–291 (1991).
325. Jiang, S. & Nail, S. L. Effect of process conditions on recovery of protein activity after freezing and freeze-drying. *Eur J Pharm Biopharm* **45**, 249–257 (1998).
326. Jain, N. & Roy, I. Effect of trehalose on protein structure. *Protein Sci* **18**, 24–36 (2009).
327. Teramoto, N., Sachinvala, N. D. & Shibata, M. Trehalose and Trehalose-based Polymers for Environmentally Benign, Biocompatible and Bioactive Materials. *Molecules* **13**, 1773–1816 (2008).
328. Lins, R., Pereira, C. & Hunenberger, P. H. Trehalose–protein interaction in aqueous solution. *Proteins* **55**, 177–186 (2004).
329. Lee, J., Maynard, H. & Mancini, R. J. Trehalose Glycopolymers for Stabilization of Protein Conjugates to Environmental Stressors. *J Am Chem Soc* **134**, 8474–8479 (2012).

330. Lee, J. *et al.* Trehalose Glycopolymers as Excipients for Protein Stabilization. *Biomacromolecules* **14**, 2561–2569 (2013).
331. Manzanera, M., Vilchez, S. & Tunnacliffe, A. High survival and stability rates of *Escherichia coli* dried in hydroxyectoine. *FEMS Microbio Lett* **233**, 347–352 (2004).
332. Louis, P. & Trüper, H. Survival of *Escherichia coli* during drying and storage in the presence of compatible solutes. *Appl Microbiol Biot* **41**, 684–688 (1994).
333. McKown, R. L. & Warren, G. J. Enhanced survival of yeast expressing an antifreeze gene analogue after freezing. *Cryobiology* **28**, 474–482 (1991).

CHAPTER 2.

2. ICE RECRYSTALLIZATION INHIBITION ACTIVITIES OF CARBOHYDRATES, SMALL MOLECULES AND POLYMERS.

2.1. CHAPTER SUMMARY.

The importance of identifying novel IRI compounds as potential cryopreservatives has been extensively iterated (Chapter 1). The IRI activity of a range of monosaccharides, disaccharides, oligosaccharides, low molecular weight (MW) polyols and natural and synthetic polymers was assessed with poly(vinyl alcohol) (PVA) having potent IRI activity. All of the compounds examined except PVA displayed a comparable decrease in the mean largest grain size (MLGS) of ice with increasing [OH]_L with no observable multivalent effect. PVA had an anomalously high IRI activity attributed to a hydrophobic and surfactant character, though few hydrophobic molecules and surfactants have IRI activity. Furthermore the impact of freezing rates on ice crystal growth and the concentration of the cryoprotectant DMSO on ice crystal formation was assessed by cryomicroscopy. A slower freezing rate enabled greater ice crystal growth and significant amounts of DMSO incited vitrification under conditions that mimic rapid cryopreservation protocols. Differential scanning calorimetry (DSC) further supported this and emphasized the minimal impact of PVA at concentrations with IRI activity. This work forms the basis of the publication. Deller, R. *et al.* Ice

recrystallization inhibition by polyols: comparison of molecular and macromolecular inhibitors and role of hydrophobic units. *Biomater Sci* **1**, 478–485 (2013).

2.2. INTRODUCTION.

Nature has continually battled to limit the detrimental effects of ice across the natural world, developing a variety of mechanisms to combat both its presence and growth allowing a diverse number of organisms to inhabit every landscape and ocean on earth.¹ The life science revolution over the last century has led to the notion of cryopreservation, the low temperature storage of clinically relevant cells, tissues and organs leading to advances in transfusion and transplantation science.² The importance of cryopreservation is escalating alongside the ever-increasing rates of transplantation caused by an aging population and in parallel the continuing advances in the emerging field of regenerative medicine.³⁻⁶ However despite recent advances many unanswered questions remain about the properties and interactions of ice especially within biological systems.⁷ One of the main exceptions is that it is well documented that the presence and growth of ice in biological systems is highly destructive and to be avoided where possible.^{8,9} Few strategies are available at present for manipulating the presence and growth of ice, fewer still in a clinical context.¹⁰ The evolution of antifreeze proteins (AFPs) and antifreeze (glyco)proteins (AF(G)Ps) has since their discovery over 40 years ago in the circulatory systems of arctic and antarctic fish species proven to be one of the principal molecular mechanisms by which organisms can thrive in sub-zero environments.^{11,12} However the isolation of AFPs and AF(G)Ps from primary sources has proven difficult on a large and financially viable scale (Chapter 1).¹³ The synthesis of AFPs and AF(G)Ps using both recombinant and synthetic strategies is another challenging limitation that does not need reiterating here.¹⁴

Soon after their discovery it was hypothesized that AFPs and AF(G)Ps could have clinical application as cryoprotectants for isolated cells, tissues and organs

both *in vitro* and *ex vivo*.¹⁵ The rationale for hypothesizing that AFPs and AF(G)Ps could be applied as cryopreservatives can be put into perspective by considering their ice interacting properties, which are three-fold. The first property is ice recrystallization inhibition (IRI) that is the kinetic inhibition (slowing) of ice crystal growth. AF(G)Ps and AFPs successfully arrest ice crystal growth such that almost no appreciable increase in ice crystal size occurs.^{16,17} Ice crystal growth is a result of a form of ostwald ripening that aims to limit the total surface energy and therefore large ice crystals will grow at the expense of small ones via the transfer of water molecules in the liquid phase of adjacent and interfacing ice crystals.^{18,19} The inhibition of H₂O transfer is believed to be due to the interaction or binding of AF(G)Ps and AFPs along a particular plane of the ice crystal lattice.²⁰ The second property is dynamic ice shaping (DIS). As AF(G)Ps preferentially bind a single (prism) plane of the developing ice crystal lattice any ice crystal growth (albeit significantly reduced) will occur only in the opposing unbound (basal) plane. As such the adsorption-inhibition mechanism will incite explosive ice crystal growth in the single unbounded plane changing the overall morphology dramatically. In the extreme DIS can generate “needle like” hexagonal bipyramidal ice crystal structures.²¹ The final property is thermal hysteresis (TH). TH is whereby the freezing point of a solution decreases to an extent greater than colligative effects alone without any corresponding change in melting point, creating a thermal hysteresis gap between these two temperatures. Thus ice crystals held isothermally within this thermal hysteresis gap will neither shrink nor grow as they are neither freezing or melting.²² The intensity of each property is highly influenced by concentration. The mechanisms behind all these observed behaviours is not fully understood but growing evidence is supporting the importance of the quasi-liquid layer (QLL) and how AF(G)Ps modulate the interactions of ice with the surrounding bulk water.²³ Understanding these properties in more depth may allow the development of molecules that manipulate or separate these properties and improve current cryopreservation

techniques²⁴ or from an engineering perspective prevent ice accumulation that can result in structural failures.²⁵⁻²⁸

The aforementioned limitations in accumulating native AFPs and AF(G)Ps however has led to extensive investigations using simpler structural mimics that are synthetically more accessible.²⁹ Figure 2.1. highlights some key modifications undertaken in order to replicate native AF(G)P behaviour but additionally improve and simplify synthesis as well as addressing some of the negative concerns regarding the use of non-native proteins such as biochemical stability and immunogenicity.³⁰ However in many cases the beneficial ice recrystallization inhibition (IRI) property of AF(G)Ps has been negatively affected but successfully separated from TH and DIS activities.^{14,31-38}

Modifications include the use of short chain AF(G)P (principally AF(G)P8) mimics as AF(G)Ps have been identified with a range of chain lengths from between 4 (2.6 kDa) and 55 (33 kDa) tripeptide (AAT) repeat units and classified according to their MW into 8 distinct groups with AF(G)P1 containing the largest and AF(G)P8 the smallest.¹⁶ However the efficiency of even the current state of the art SPPS^{39,40} techniques limits the production of polypeptides to approximately 70 residues (e.g. even with 99% efficiency for each coupling step the final yield of a 70 residue polypeptide would be lower than 50%) restricting overall length. The susceptibility of the glycosidic bond to hydrolysis also limits downstream modifications.

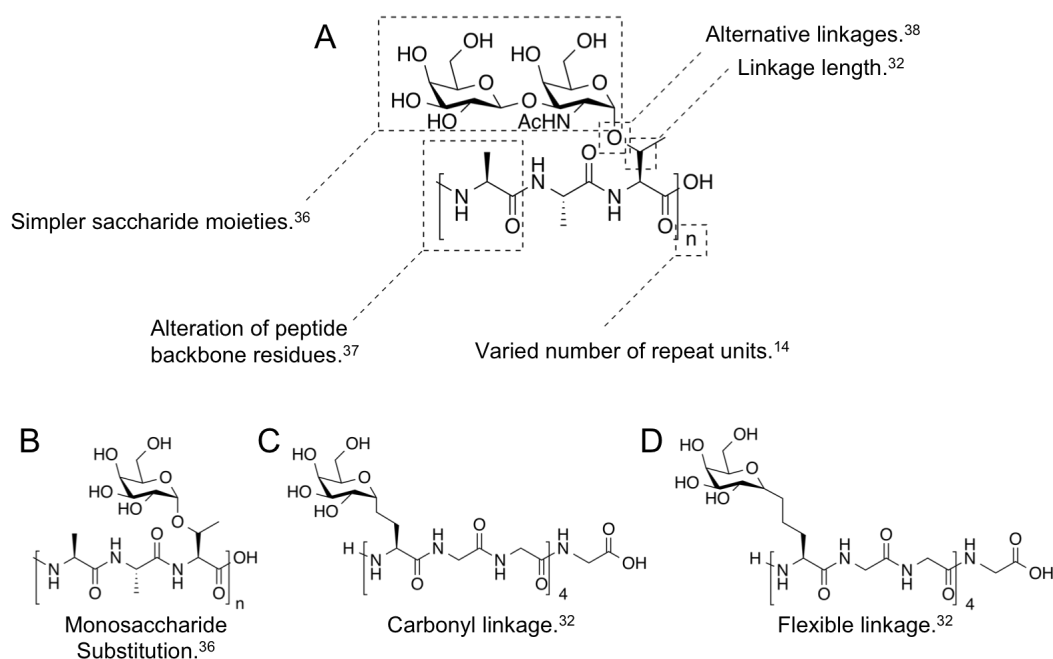


Figure 2.1. Strategies for the rationale design of AF(G)P mimics. (A) Native AF(G)P structure with targeted alterations in composition and structure undertaken in many studies aiming to reduced synthetic complexity and improve scalability whilst retaining or improving control over IRI, DIS and TH activity with examples from literature showing a (B) monosaccharide substitution, (C) carbonyl linkage and (D) linkage extension.

A second obvious area of interest that has been readily exploited is the substitution of the relatively complex β -D-galactosyl(1→3)- α -N-acetyl-D-galactosamine disaccharide moiety to a simpler and more accessible (mono)saccharide moiety. For example Liu *et al.* developed a set of (C-linked and serine substituted) analogues of AF(G)P8 with glucose, mannose and talose carbohydrate moieties but these had poor IRI activity.³⁶ A (C-linked and serine substituted) AF(G)P8 analogue with galactose though had a reasonably strong concentration dependant IRI activity and was tolerated by WRL-68 cells (*in vitro*) at a concentration of 5 mg/mL even after a period of 20 hours^{36,41}. The work of Peltier *et al.* illustrated the differences between an AF(G)P8 analogue containing

either a glucose or *N*-acetyl-galactosamine monosaccharide moiety. They revealed a lack of DIS activity with the glucose moiety but a profound effect remained with the *N*-acetyl-galactosamine moiety, though the resulting ice crystal morphology was different to that induced by native AF(G)P8.⁴² Finally the work of Matsumoto *et al.* that utilized a *N*-acetyl-galactosamine monosaccharide moiety on larger (32 to 48 residues) peptide backbone was able to improve the recovery of red blood cells (RBCs) and islet cells was attributed to its IRI activity.⁴³ Therefore even subtle changes in glycosylation can have large and detrimental effects on IRI, DIS and TH activity but retain antifreeze activity that translates into a beneficial cryopreservative effect. Understanding and rationalizing what differences these saccharide moieties have is an important task as well as their activities independent of the peptide backbone as stand alone entities.

Alterations to the peptide backbone-saccharide conjugation principally carbonyl (C-linked) ligations using serine as opposed to threonine as aforementioned have been undertaken for synthetic ease.^{33,38} The synthesis of thio (S-linked) glycopeptides is also possible but it is understood that thio linkages have not yet been incorporated into AF(G)P analogues.⁴⁴ Synthetic modifications have produced mimics that may be more biochemically stable compared to the native O-linked glycosylated AF(G)Ps that are more susceptible to degradation by naturally occurring protein degradation pathways.⁴⁵ An extension of which is the introduction of spacers altering the distance and flexibility of the saccharide moiety from the peptide backbone and its consequential effect on IRI activity. The early work of Liu and Ben showed that increasing the distance between the peptide backbone and a (non-native) monosaccharide moiety resulted in a dramatic reduction in IRI activity rationalizing the need to maintain a distance between these features comparable to native AF(G)Ps.³² Finally subtle changes in the composition of the peptide backbone have been identified and isolated in some naturally occurring AF(G)P family members. The most significant of which

is the substitution of alanine for proline⁴⁶ and threonine for arginine⁴⁷ in low MW AF(G)Ps with the widely investigated AF(G)P8 a notable example.⁴⁸

None of these AF(G)P derivatives have IRI activity that is truly comparable to native AF(G)P, though some do lack any detectable TH activity successfully separating these properties. The removal of DIS activity (linked to TH) is particularly desirable as this has been shown to be detrimental in cryopreservation.^{49,50} A range of synthetic polymers that loosely resemble AF(G)P structure have been evaluated and several studies have identified that the simple, scalable and biocompatible polymer, poly(vinyl alcohol) (PVA) has a potent IRI activity.^{51,52} It has been shown that the activity of PVA is strongly affected by the degree of hydrolysis, with stepwise reductions in hydrolysis by controlled acetylation lowering IRI activity. With hydrolysis less than 80% having adverse effects on IRI potency. Chain length has also been shown to be important with a higher chain length corresponding with a stronger IRI activity, though improvements in IRI activity are offset by a reduction in aqueous solubility lowering the final obtainable concentration.⁵³ Efforts at improving the understanding of AF(G)Ps and ice as well as the investigation of small non-peptide molecules as IRI active molecules is therefore key and an ongoing aim going forward. The work of Tam *et al.* first investigated a small selection of carbohydrates (monosaccharides and disaccharides) as IRI active compounds in an attempt to define how subtle differences in structure that affect hydration number may relate to their potential as IRI active compounds.⁵⁴ Hydration number is defined as the number of H₂O molecules strongly associated to each carbohydrate molecule and differences in hydration number have been postulated to be as a consequence of differences in carbohydrate stereochemistry.^{55,56} The hydration number of many monosaccharides, their respective methyl derivatives and disaccharides have been defined accurately in literature.⁵⁷ Several other descriptors including the anomeric effect, hydrophobic

index and hydrophilic volume amongst others are also important in resolving how carbohydrate structure can affect H₂O interactions and together characterize the hydration layer.^{58,59} The hydration layer is the region of H₂O molecules affected by the presence and interaction of a molecule in an aqueous system.⁶⁰ Therefore extending the preliminary findings of Tam *et al.* and investigating how a diverse variety of carbohydrates and low MW polyols affect IRI activity was undertaken as several studies have already highlighted the importance of the interaction between ice and bulk water via the quasi liquid layer (QLL).^{61,62} How carbohydrates modulate this process may allow the rationale design or identification of potent IRI active molecules.

2.3. RESULTS AND DISCUSSION.

2.3.1. IRI activity of monosaccharides, disaccharides and oligosaccharides.

The standard method to determine IRI activity was proposed by Knight *et al.* who developed the “splat” test (Section 2.5.3.).⁶³ In brief the splat test involves the release of a small (10 μ L) droplet from approximately 2 m on to a pre-cooled aluminum plate (> -50 °C) causing an instantaneous phase change resulting in the formation of a single layer of ice crystals as a result of this impact. The consequent annealing of this layer at -6 °C (other studies have used annealing temperatures as low as -8 °C) promotes ice crystal growth. The rate of ice crystal growth is therefore in turn determined by the composition and IRI activity of the sample. Annealing for a period of 30 minutes allows for accurate and quantifiable differences to be measured. The mean largest grain size (MLGS) is the value commonly reported, which is the mean value of the largest single dimension of the ten largest ice crystals across a reasonably sized viewing field (1.33 mm²). This value is usually then expressed as a percentage of a non-IRI active (isotonic) control such as PBS. It is necessary to emphasize that the volume of each inhibited ice crystal would be significantly lower (as a % value). The splat assay can therefore be used to accurately measure IRI activity and provide an initial screen for identifying novel cryopreservatives as IRI activity as been implicated as being a mechanism that may reduce cryodamage during freezing and thawing processes (Chapter 1). To begin with a range of naturally occurring monosaccharides (including aldopentoses and aldohexoses) and a methyl- β -D-galactopyranoside derivative (Figure 2.2.) were assessed for IRI activity over an extensive concentration range (Figure 2.3.).

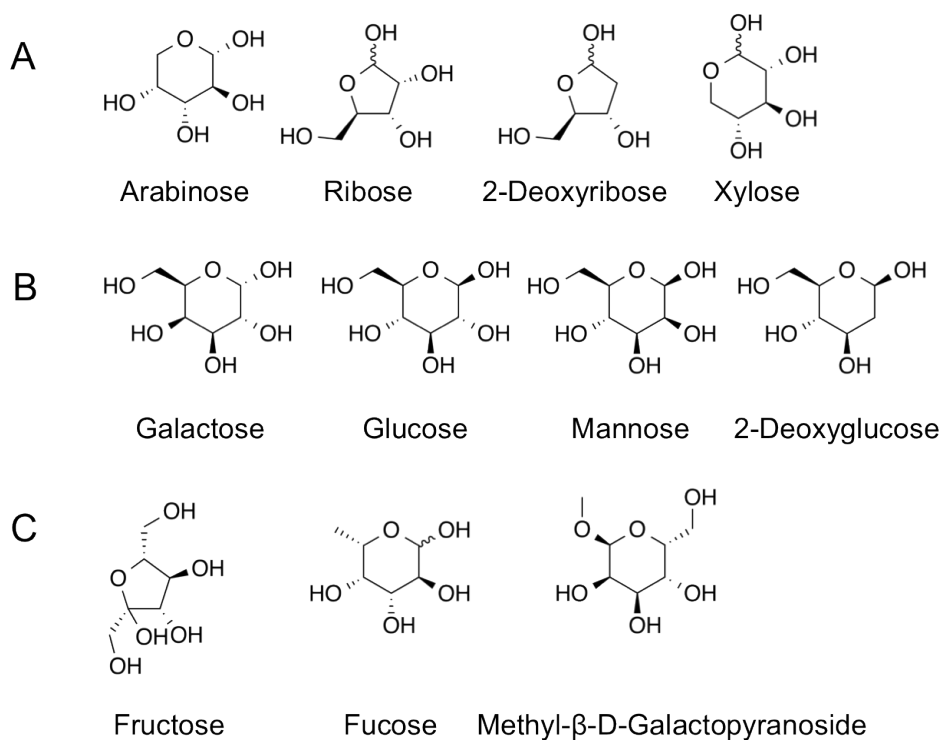


Figure 2.2. Structures of various monosaccharides investigated for IRI activity. (A) Aldopentoses, (B) Aldoexes and (C) Other monosaccharides.

The immediate benefits of using monosaccharides are that they are readily available from a variety of natural sources, biocompatible and highly soluble in aqueous solutions. Deliberately high concentrations (up to 50 mg/mL) of monosaccharides were eventually used in order to help emphasize and resolve their weak IRI activity. However high concentrations can lead to a significant colligative freezing point depression which should not be ignored when high concentrations of cryopreservatives are used.⁶⁴ Estimations of freezing point depression can be easily calculated for concentrations that constitute a near ideal solution.⁶⁵ For example the composition of PBS (Section 2.5.1.) leads to a colligative freezing point depression approximating 0.58 °C and a 50 mg/mL solution of glucose in PBS (the highest concentration tested) tends to a freezing point depression of 1.1 °C. Carbohydrates (unlike AF(G)Ps) have no reported non-colligative effects on freezing point depression (TH activity), which is important given the perceived benefits of separating IRI from DIS and TH. Even

though the solubility of glucose and other monosaccharides permits solutions as high as 400 mg/mL this would cause a drastic lowering of the freezing point (≈ -4.74 °C) that would affect the rate of ice crystal growth regardless of any IRI activity. Furthermore the precipitation upon cooling/freezing would tend to non-representative and erroneous IRI results. In addition to this, these high concentrations of solute would reduce the molar fraction of H₂O and possibly cause vitrification as opposed to ice crystal formation, given the high rate of cooling samples are subjected to during the “splat” assay.

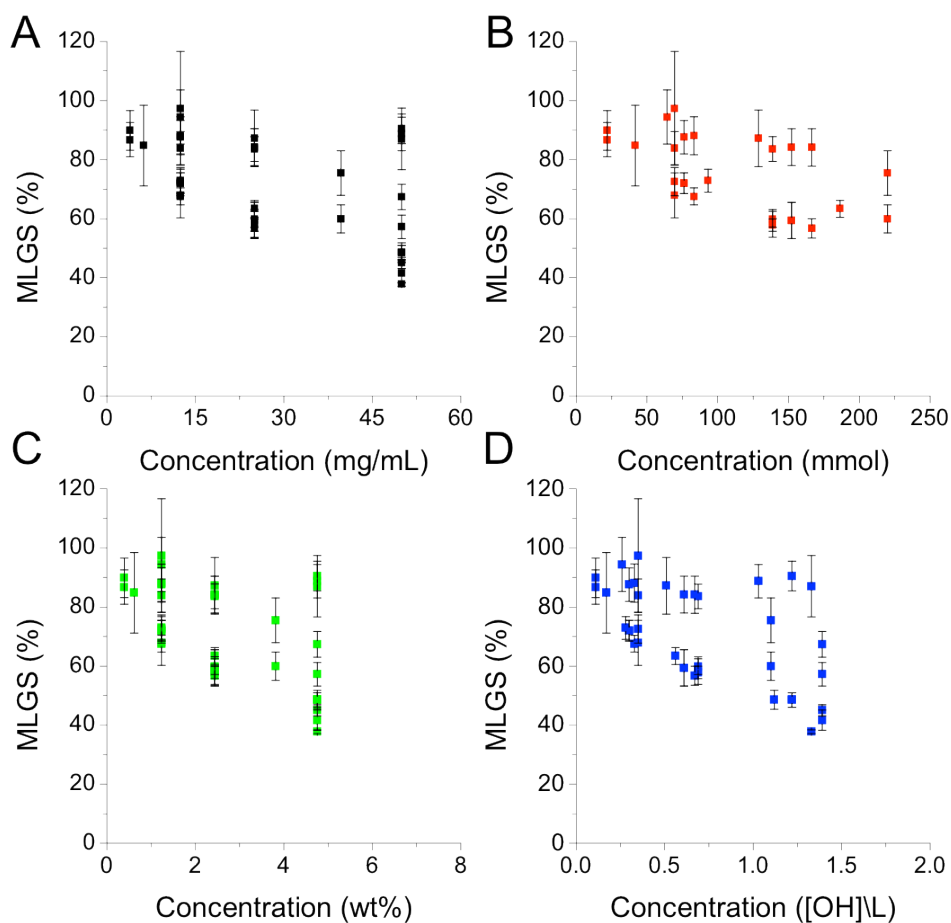


Figure 2.3. IRI activity of (11) monosaccharides. IRI activity of monosaccharides listed in Figure 2.2. Each measurement represents the MLGS (%) of 10 crystals with error bars representing \pm standard deviation; (A) MLGS (%) vs. Concentration (mg/mL); (B) MLGS (%) vs. Concentration (mmol); (C) MLGS (%) vs. Concentration (wt %); (D) MLGS (%) vs. Concentration ([OH]/L). Error bars represent \pm standard deviation.

In order to best resolve any differences between each molecule, the IRI data set is displayed in terms of MLGS (%) against concentration in mg/mL (Figure 2.3.A), mmol (Figure 2.3.B), wt % (Figure 2.3.C) and [OH]/L (Figure 2.3.D). Figure 2.3. shows that no monosaccharide possessed a high level of IRI activity over this concentration range (Figure 2.27.). A weak correlation can be seen in each

representation with the MLGS (%) decreasing (i.e. increasing IRI activity) with rising monosaccharide concentration. The highest concentration tested with the greatest but still only moderate IRI activity would induce significant changes in osmolarity. This could be detrimental to many biological tissues for example spermatozoa^{66,67} and RBCs.⁶⁸ Therefore the use of disaccharides that in general retain reasonable solubility and biocompatibility whilst reducing changes in osmotic pressure when compared on a mass basis were assessed for IRI activity (Figure 2.4. and Figure 2.5.). As with the assessment of monosaccharides a diverse range of subtle structural differences that give a varied hydration number were investigated (Figure 2.27.).

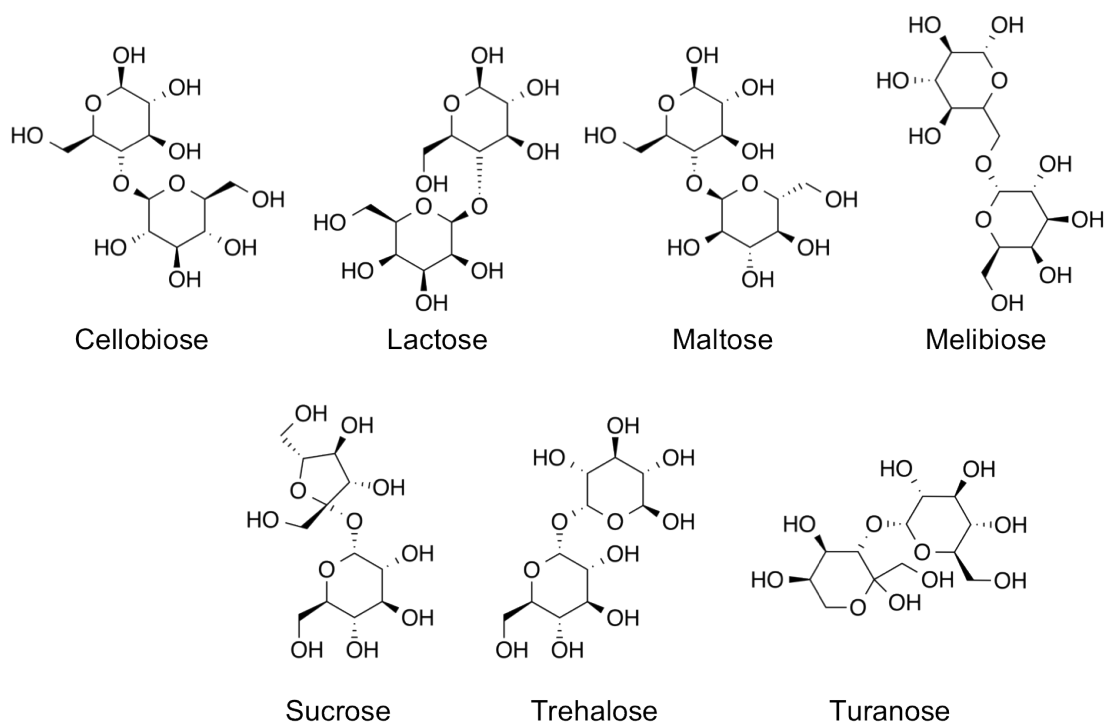


Figure 2.4. Structures of various disaccharides investigated for IRI activity.

(Clockwise from top left); Cellobiose (Glucose $\beta(1\rightarrow4)$ Glucose), Lactose (Galactose $\beta(1\rightarrow4)$ Glucose), Maltose (Glucose $\alpha(1\rightarrow4)$ Glucose), Melibiose (Galactose $\alpha(1\rightarrow6)$ Glucose), Turanose (Glucose $\alpha(1\rightarrow3)$ Fructose), Trehalose (Glucose $\alpha(1\rightarrow1)$ Glucose) and Sucrose (Glucose $\beta(1\rightarrow2)$ Fructose).

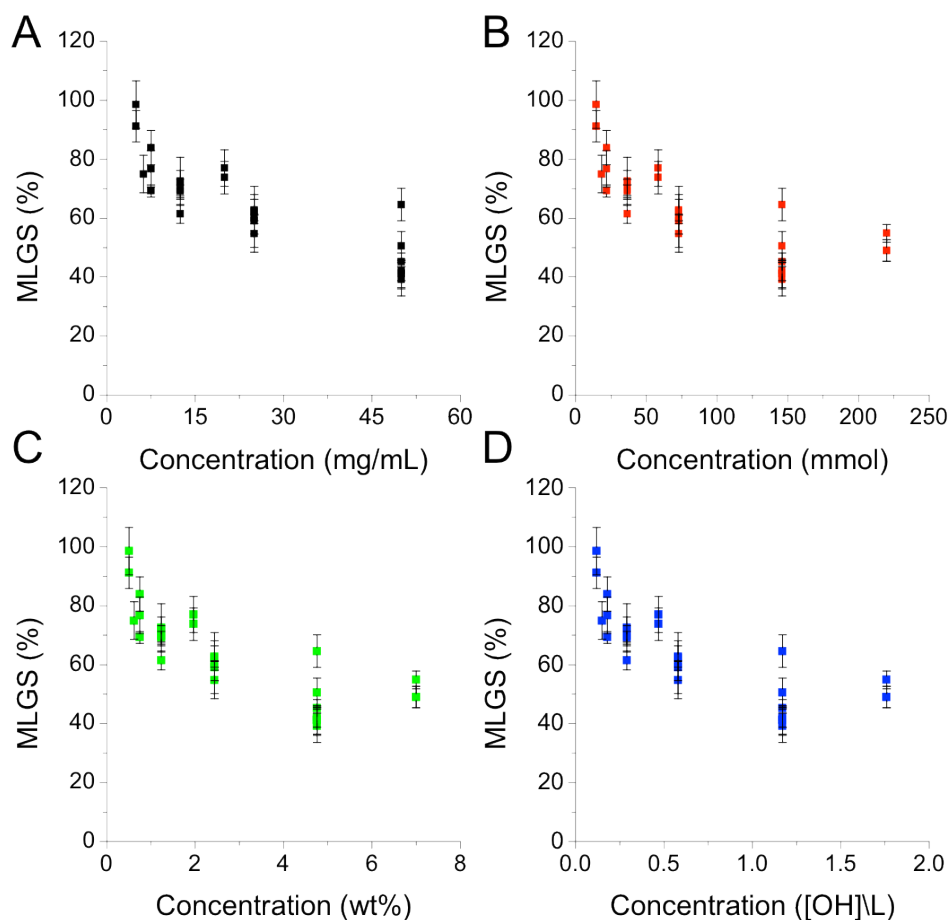


Figure 2.5. IRI activity of (7) disaccharides. IRI activity of disaccharides listed in Figure 2.4. Each measurement represents the MLGS (%) of 10 crystals with error bars representing \pm standard deviation; (A) MLGS (%) vs. Concentration (mg/mL); (B) MLGS (%) vs. Concentration (mmol); (C) MLGS (%) vs. Concentration (wt %); (D) MLGS (%) vs. Concentration ([OH]/L). Error bars represent \pm standard deviation.

The range of disaccharides tested shows a similar level of IRI activity to monosaccharides when compared on a mass basis (mg/mL) that again increases weakly with increasing concentration (Figures 2.3.A and 2.5.A). However to further refine any differences between any of the individual disaccharides it is possible to relate the MLGS (%) of each disaccharide to its hydration number and

hydration index. Hydration number is defined as the number of H₂O molecules strongly associated with a single carbohydrate molecule (Figure 2.6.) and hydration index as the hydration number divided by the partial molar volume (Figure 2.7.) as defined and previously investigated by Tam *et al.*^{54,57} The concentration at which MLGS (%) was measured was deliberately chosen as 50 mg/mL in order to maximise any potential differences in IRI activity and minimise the influence of the inherent variability associated with IRI measurements.⁶³ Incidentally as each disaccharide tested was of equal MW and possessed the same number of hydroxyl functional groups (8) both the molar (mmol) and hydroxyl ([OH]L) concentrations were consistent at 146 mmol and 1.17 [OH]L. The range of monosaccharides tested display significant discrepancies (due to their differing MWs) with respect to these values and thus has not been compared in this regard here. The findings of Tam *et al.* highlighted a good correlation between hydration number (Adj-R² = 0.758) and hydration index (Adj-R² = 0.791) with MLGS (%).⁵⁴ In contrast to this as shown in Figures 2.6. and 2.7. that use a greater number of disaccharides (7 as opposed to 4) a weaker correlation is derived (Adj-R² = 0.441 (hydration number) and Adj-R² = 0.287 (hydration index)) that essentially shows a non linear relationship. Improvements to defining more accurate MLGS (%) values may help⁶⁹ but critically a larger data set would be required in order to confidently define any correlation and generate a model to predict the MLGS (%) of a carbohydrate from its respective hydration index (that accounts for differences in the number of saccharide units). This would still only be for a single (and high) concentration that at best would likely have only moderate IRI activity given the observations recorded to date. Furthermore observations with this albeit rather limited data set do not reflect the advantages of using the hydration index as opposed to hydration number as a more accurate predictor of IRI activity that the authors ascribe to (i.e. the strength and significance of the correlation). The main benefit of the hydration index is the ability to normalise the relative unit number of monosaccharides and

disaccharides (plus other oligosaccharides) by dividing through with the partial molar volume giving a more extensive data set and compares different compounds on a molar as opposed to mass basis.

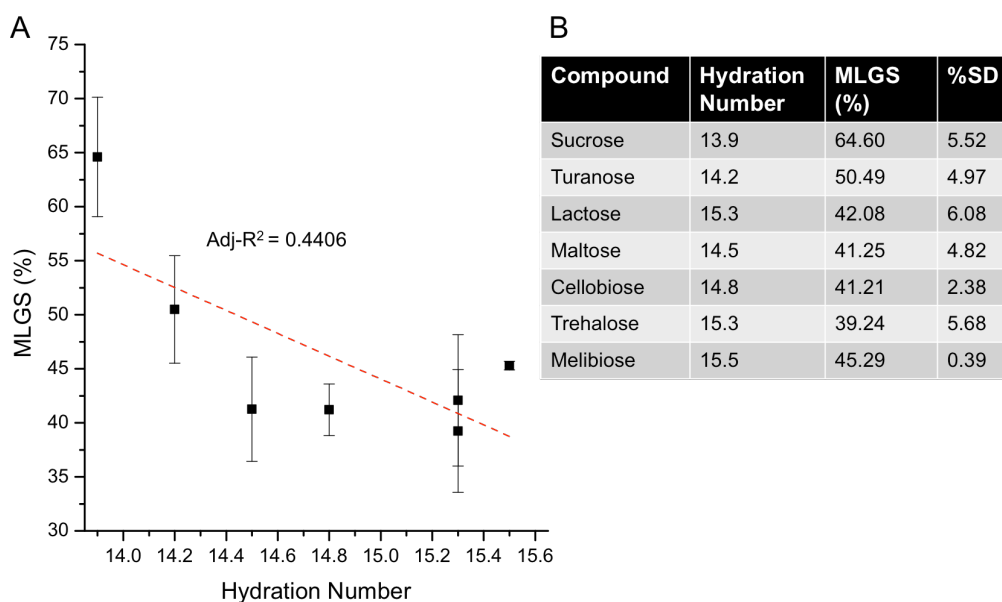


Figure 2.6. IRI activity of (7) disaccharides against hydration number. Using a concentration 50 mg/mL (146 mmol/1.17 [OH]L) comparing (A) MLGS (%) against hydration number and (B) table illustrating hydration number values and MLGS (%) for each disaccharide assessed.

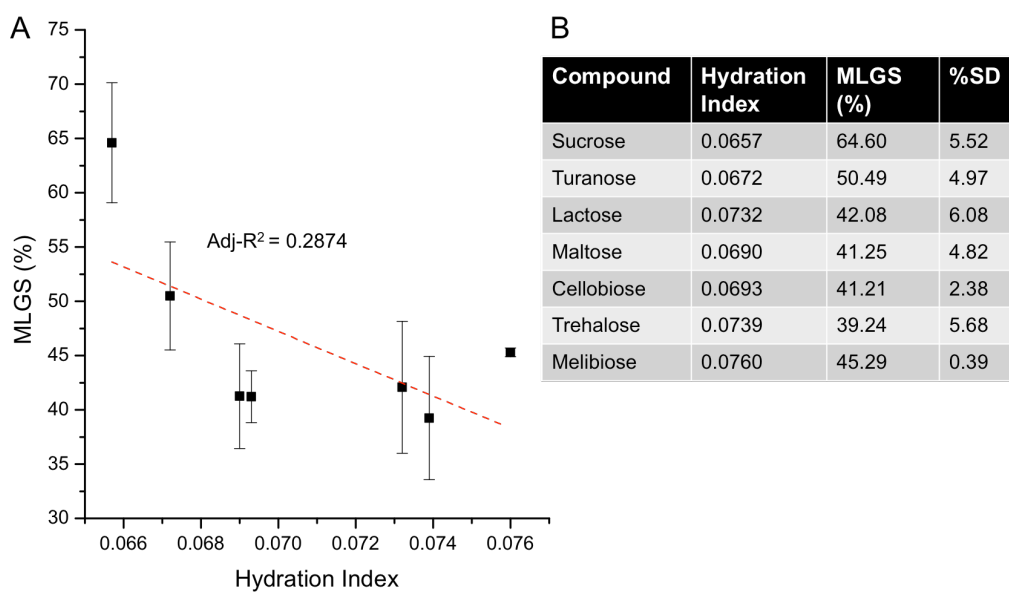


Figure 2.7. IRI activity of (7) disaccharides against hydration index. Using a concentration 50 mg/mL (146 mmol/1.17 [OH]L) comparing (A) MLGS (%) against hydration index and (B) table illustrating hydration index values and MLGS (%) for each disaccharide assessed.

One final set of saccharides were assessed for IRI activity. A small collection (4) of oligosaccharides (Figure 2.8.) are illustrated under the same criteria as both the monosaccharides and disaccharides prior (Figure 2.2. and Figure 2.4.) and again (Figure 2.9.) follow a similar concentration dependant relationship (Figure 2.28.).

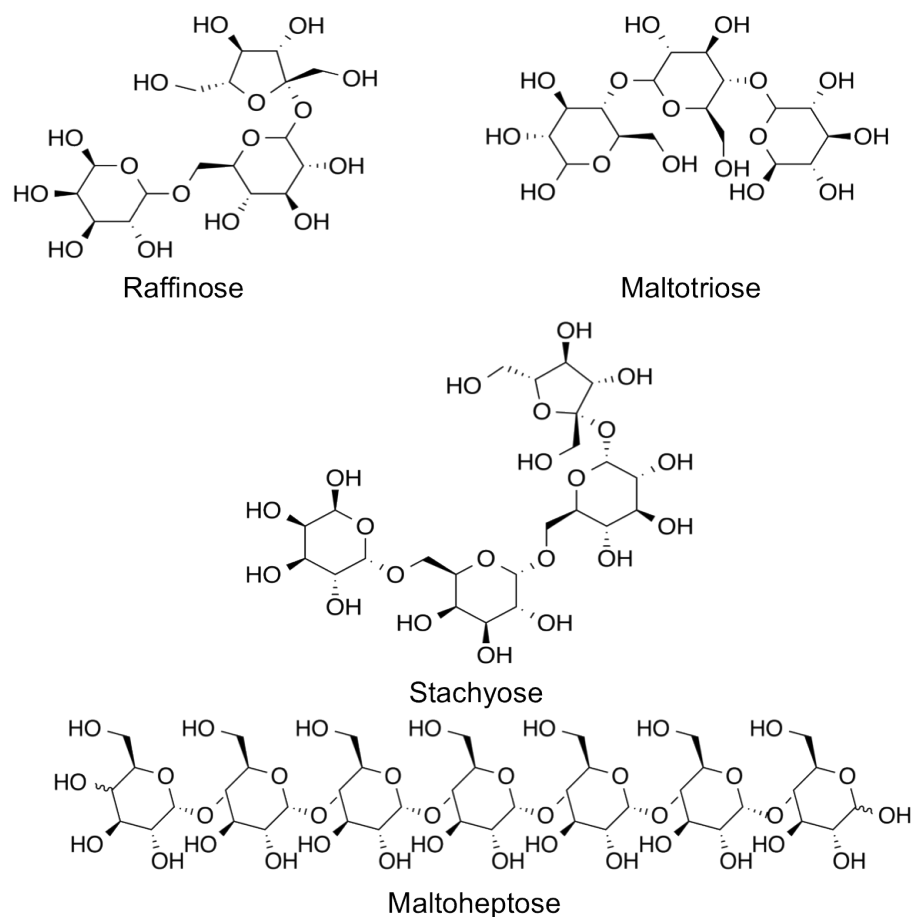


Figure 2.8. Structures of various oligosaccharides investigated for IRI activity. (Clockwise from top left); Raffinose (Galactose $\alpha(1\rightarrow4)$ Glucose $\beta(1\rightarrow2)$ Fructose), Maltotriose (Glucose $\alpha(1\rightarrow4)$ Glucose $\alpha(1\rightarrow4)$ Glucose), Stachyose (Galactose $\alpha(1\rightarrow6)$ Galactose $\alpha(1\rightarrow6)$ Glucose $\beta(1\rightarrow2)$ Fructose) and Maltoheptose (Glucose $\alpha(1\rightarrow4)$ Glucose (6x)).

To best highlight these similarities to other saccharides, each data set was combined into a single figure comparing MLGS (%) against concentration (mmol) (Figure 2.10.A) showing that on a molar basis that oligosaccharides outperform disaccharides that in turn outperform monosaccharides. However as these compounds all have a varied valency (i.e. number of hydroxyl groups) and there may be a beneficial multivalent effect in a similar manner to that observed with for example carbohydrate recognition proteins and thus a molar comparison may be unrepresentative and misleading.^{70,71} To probe the relative activity of each set

an alternative measure ($[OH]_L$) was used (Figure 2.10.B). Using the $[OH]_L$ measure it can be concluded that no significant differences are apparent between monosaccharides, disaccharides and oligosaccharides. However the impact of $[OH]_L$ is profoundly different when comparing the saccharide moieties and IRI activities of synthetic mimics. This means that the IRI activity of two maltotriose (Glucose $\alpha(1\rightarrow4)$ Glucose $\alpha(1\rightarrow4)$ Glucose) molecules is roughly equivalent to three maltose (Glucose $\alpha(1\rightarrow4)$ Glucose) molecules or six glucose molecules. Simply increasing concentration does influence (albeit weak given the wide concentration range) IRI activity but with no benefits from multivalency. Therefore the use of oligosaccharides as IRI additives would be preferred in a biological context in terms of limiting changes in osmotic pressure and are less susceptible to metabolic degradation and is the main rationale for their inclusion in hypothermic storage solutions.^{72,73}

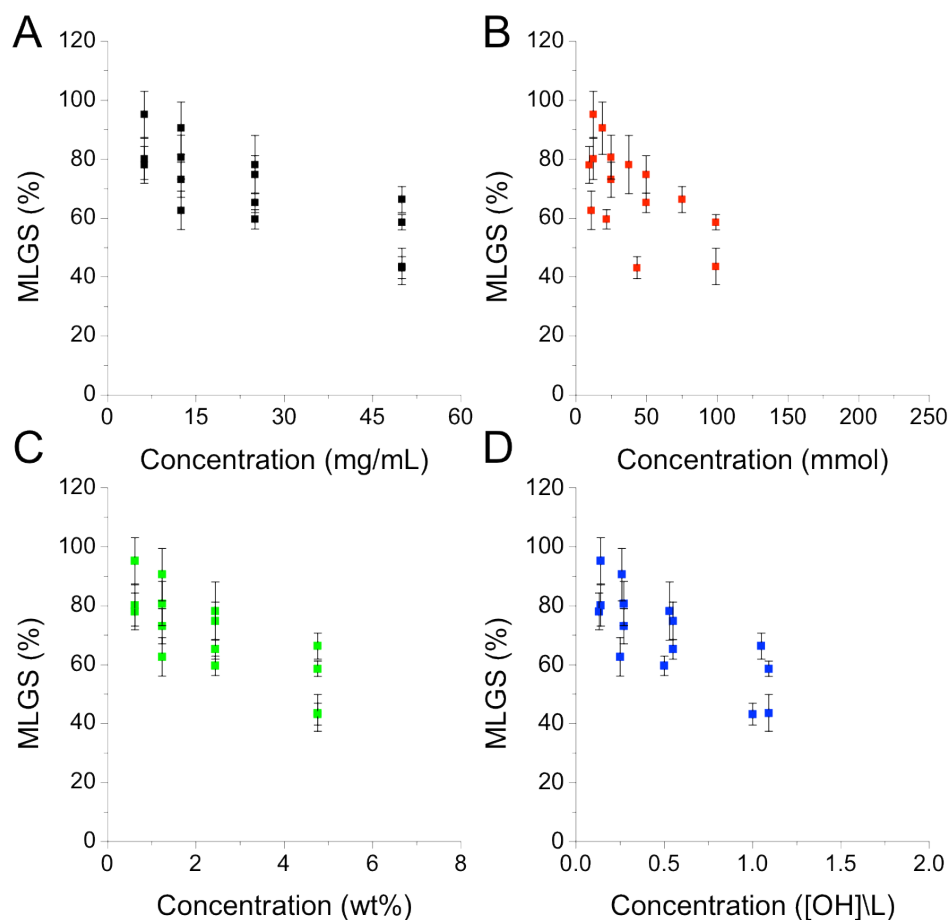


Figure 2.9. IRI activity of (4) oligosaccharides. IRI activity of oligosaccharides listed in Figure 2.8. Each measurement represents the MLGS (%) of 10 crystals with error bars representing \pm standard deviation; (A) MLGS (%) vs. Concentration (mg/mL); (B) MLGS (%) vs. Concentration (mmol); (C) MLGS (%) vs. Concentration (wt %); (D) MLGS (%) vs. Concentration ([OH]/L). Error bars represent \pm standard deviation.

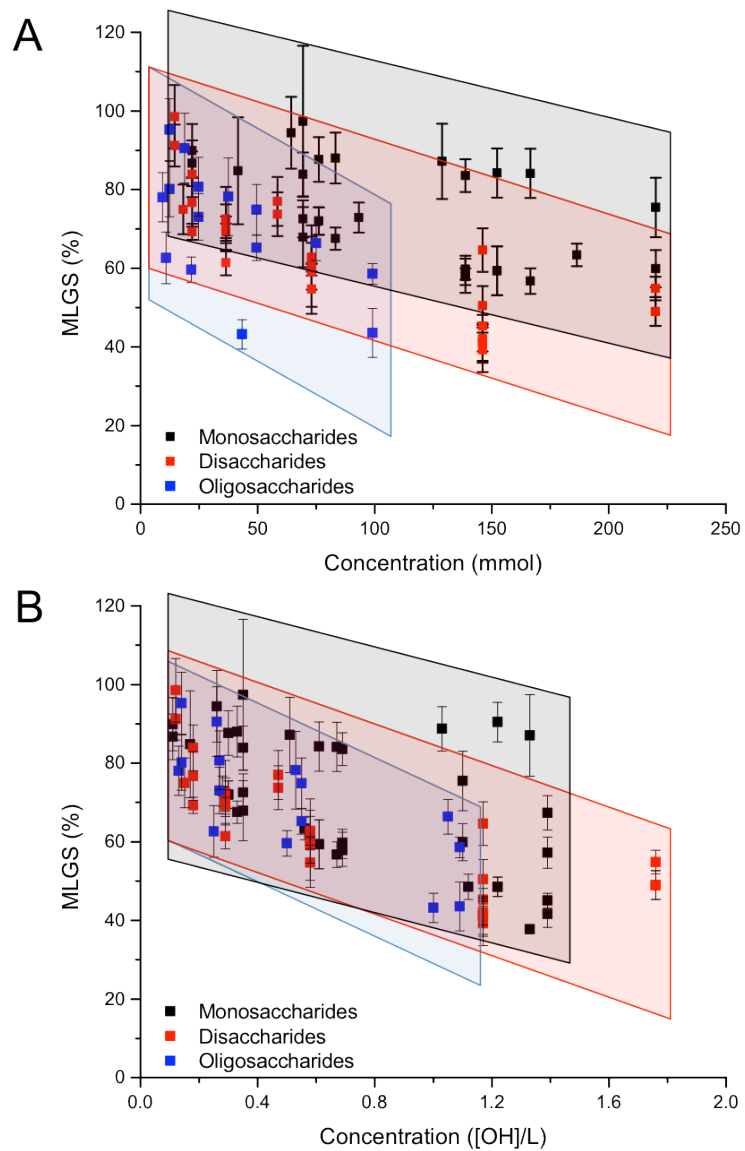


Figure 2.10. Comparative IRI activity of monosaccharides, disaccharides and oligosaccharides. (A) MLGS (%) vs. concentration (mmol) and (B) MLGS (%) vs. concentration ([OH]/L). Each measurement represents the MLGS (%) of 10 crystals with error bars representing \pm standard deviation.

2.3.2. IRI activity of low MW polyols.

Given the importance of hydration and the interactions that hydroxyl groups may have with ice and water a vast array of low MW polyols were investigated for IRI activity. Low MW polyols including an extensive range of aliphatic, nitro and benzyl compounds (Figure 2.11.). IRI activity was investigated to examine if any of these polyols had activity similar to saccharides of a comparable MW. The only stipulation being that they contain at least one hydroxyl group regardless of their cytotoxicity that would limit their application *in vitro*, *ex vivo* and *in vivo* as the main rationale is to attempt to identify and analyse structural motifs conducive to IRI activity. Several of the low MW molecules were deliberately chosen as such to analyse the impact (if any) of minor differences in their corresponding structure such as hydroxyl group positioning (nitro derivatives) and hydroxylation (ectoine and hydroxyectoine). These differences have profound effects on their physicochemical properties, such as solubility and phase transition temperatures. No significant differences in IRI activity could however be derived due to differences in either hydroxyl group placement or extent of hydroxylation.

Figure 2.12. shows a similar concentration dependant relationship to the saccharides examined previously (Figure 2.10.) and thus it can be concluded that a reduction in MLGS (%) can be initiated simply by increasing the concentrations of a polyol in an aqueous system as all the low MW polyols tested fit within the range of the previously tested saccharides on a [OH]_L basis (appendicized in full in Figure 2.28.). No notable differences were apparent between the aliphatic, benzyl and nitro derivatives and other polyols. However these conditions are unattractive due to the physiologically high concentrations required to have significant impact that may incite unwarranted changes in osmotic pressure and would have profound effects chemically and biochemically.

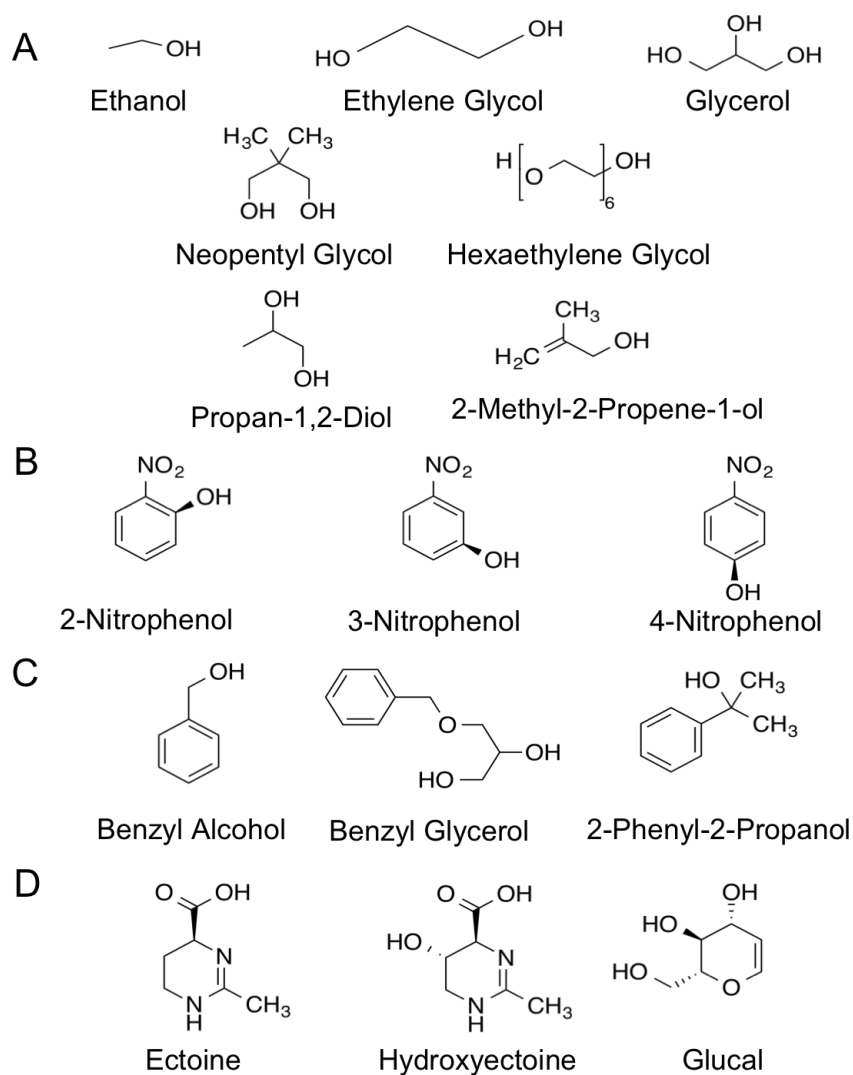


Figure 2.11. Structures of various small non-carbohydrate derived polyols investigated for IRI activity. (A) Aliphatic derivatives, (B) Nitro derivatives, (C) Benzyl derivatives and (D) Other Polyols.

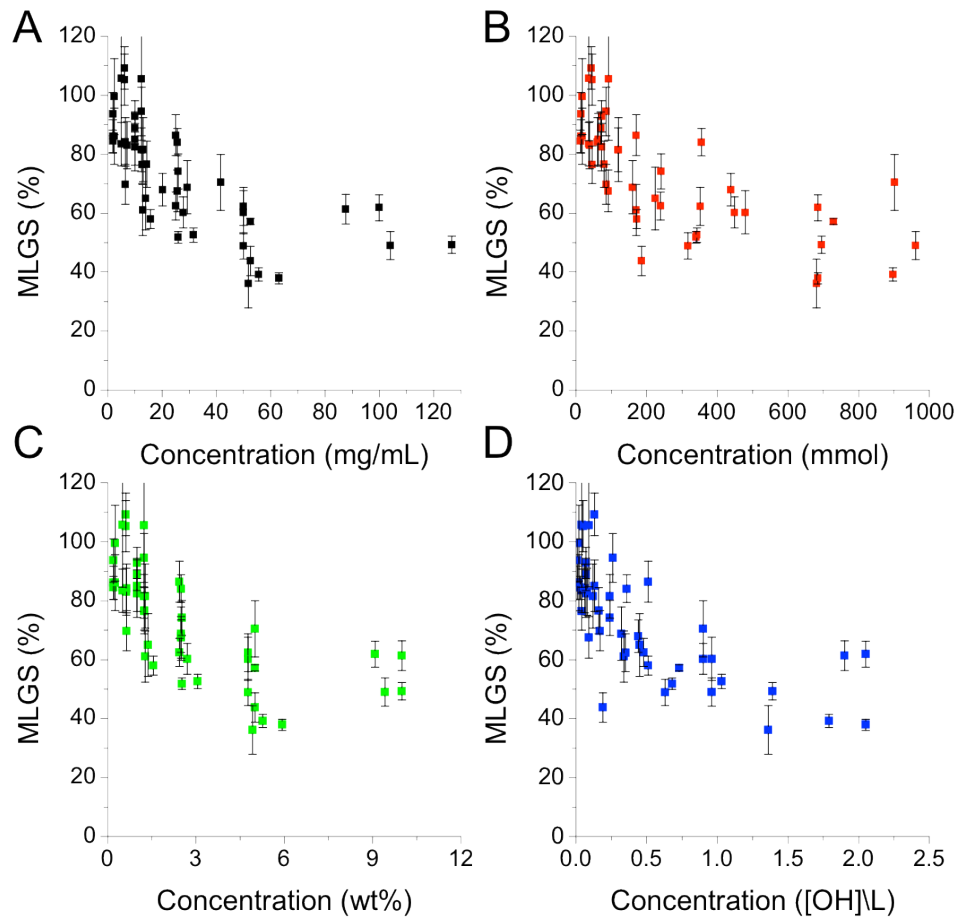


Figure 2.12. IRI activity of (16) small molecule polyols. Each measurement represents the MLGS (%) of 10 crystals with error bars representing \pm standard deviation; (A) MLGS (%) vs. Concentration (mg/mL); (B) MLGS (%) vs. Concentration (mmol); (C) MLGS (%) vs. Concentration (wt %); (D) MLGS (%) vs. Concentration ([OH]/L). Error bars represent \pm standard deviation.

Extreme changes in osmotic pressure would necessitate their careful addition and removal (assuming their moderate IRI activity translates into cryoprotection), which is further complicated by their varied membrane permeability to different cell types and other pharmacodynamic and pharmacokinetic properties. These are all undesirable qualities, as cryopreservation usually demands the immediate storage of biological tissues after isolation in order to maintain maximal viability

and clinical scenarios are often unpredictable and demand rapid availability and therefore cryopreserved samples would require swift or no post-thaw processing.²⁴ Therefore alternative IRI active compounds would be desirable though as aforementioned simply isolating or synthesizing the compounds utilised by nature is not possible due to a myriad of reasons. The molecular mechanisms of cold acclimatisation regularly observed in biological systems are not typically small molecules but are predominantly macromolecules^{13,74}. However a limited number of small molecules most notably glycerol and trehalose have been identified in the natural world to behave as desiccants in a few select freeze protective insect species as well as in a number of bacterium in response to low temperatures.^{75,76} Desiccation in this context aims to minimize water content and in cold acclimatised organisms limiting the formation and presence of ice entirely (freeze prevention) thus allowing these species to remain dormant (diapause) and inactive for prolonged periods of time⁷⁷ and differs from other (freeze tolerance) mechanisms. More specifically these macromolecules are either AFPs which are typical globular proteins forming four distinctive families (in fish species for instance)⁷⁸ or AF(G)Ps that are proteins with a repeat and (semi)regular tripeptide (AAT) structure consistently glycosylated with a single disaccharide moiety per tripeptide.¹¹ Closely related mimics of AF(G)Ps have yielded mixed results in terms of comparable IRI activity.^{32,33,42} Convergent evolution that is whereby two different species independently by geographical separation or otherwise develop similar or near-identical mechanisms to a common problem (i.e. freeze tolerance) has been observed with the development of AF(G)Ps in arctic and antarctic fish species.^{79,80} Therefore it is unsurprising that a biosynthetically simpler but similar mimic or glycoprotein with comparable IRI activity has not been successfully identified, otherwise it is possible that separate structures would of arisen in nature rather than on the convergence of a single structure. The conservation of AF(G)P structure can be exemplified by the

diversity of AFPs with for instance AFP type I proteins have a high α -helical content where as AFP type II proteins have mainly β -sheet and random coil secondary structure motifs, yet they both have similar properties.⁸¹ Exploring macromolecules that are synthetically inaccessible to nature and have modest similarity but take into account what is currently understood about the interaction of AF(G)Ps and AFPs with water/ice is the next step. The rationale of which leads towards the exploration and examination of synthetically derived (glyco)polymers as IRI active compounds and potential AFP and AF(G)P mimics.

2.3.3. IRI activity of synthetic and natural polymeric macromolecules.

Previous studies by Inada *et al.*, Budke *et al.* and Gibson *et al.* have investigated the IRI activity of several synthetic polymers and macromolecules.^{51,52,82} These are appealing as even at a high mass concentration their molar concentration is not sufficient to significantly alter osmolarity detrimentally. Additionally from a synthetic perspective polymers are not inhibited in terms of chain length to same extent as SPPS derived mimics have been and can be fine tuned or modified by several established chemistries.^{83,84} However polydispersity especially at low degrees of polymerisation can be problematic in ensuring batch-to-batch replication. The physicochemical properties of polymers vary widely and as such their application may be limited by for example their aqueous solubility and photo and thermal stability. A variety of (glyco)polymers with a range of complexities have been investigated in literature but the relatively simple polymer poly(vinyl alcohol) (PVA) has repeatedly showed a potent IRI activity. The IRI potency of many other (glyco)polymers is significantly reduced in comparison except at high concentrations (40 mg/mL) where high MW (105 kDa) Poly(methyl-6-O-methacryloyl- α -D-glucopyranoside) (PMAMGlc) had significant IRI activity,

though activity was reduced with a PMAMGlc of MW 56.5 kDa and lost completely at lower MW values (18 kDa and 37 kDa) that are akin to the MW of even the largest AF(G)Ps.⁸² It is understood that PVA is the synthetic derivative with the most comparable IRI activity to native AF(G)Ps.^{29,85} To probe this activity further a selection of PVA molecules (Section 2.5.2.) amongst a collection of other high MW polymers were investigated for IRI activity (Figure 2.13.). One of the other polymers examined was poly (ethylene glycol) (PEG) as it is isomeric to PVA but only contains a single terminal hydroxyl group and has excellent aqueous solubility and commercial availability. Examining PEG allows the importance of hydroxylation (hydration) to be further clarified. Both hydroxyethyl starch (HES) (140 kDa) and dextran (40 kDa) were chosen as these naturally derived branched chain polysaccharides have been shown to have cryoprotective properties when applied to biological materials at high concentrations^{86,87} though not without adverse clinical side effects.⁸⁸

PVA from 3 commercially available preparations were chosen and purified with MWs of 9 kDa (80 % hydrolysis), 31 kDa (98-99 % hydrolysis) and 85 kDa (99 %+ hydrolysis). The aqueous solubility of 85 kDa PVA however was extremely low and precluded its analysis and was not examined. Literature findings suggest PVA molecules of reasonable size may gelate easily at low temperatures preventing their application successfully.⁸⁹ The IRI activity of PVA (9 kDa and 31 kDa), PEG (8 kDa and 100 kDa), HES and dextran at 10 mg/mL in PBS is illustrated in Figure 2.14. It is immediately apparent that both 9 kDa and 31 kDa PVA possess a strong IRI activity with a MLGS (%) of $33.7 \% \pm 1.8 \%$ and $16.8 \% \pm 24.4 \%$ respectively with 8 kDa and 100 kDa PEG having values much larger at $90.4 \% \pm 5.7 \%$ and $73.6 \% \pm 6.9 \%$. Furthermore the cryoprotectants HES and dextran have low IRI activity with values of $87.9 \% \pm 6.0 \%$ and $90.1 \% \pm 5.9 \%$, implying their cryoprotective properties are independent of any IRI effect.

Micrographs of polynucleated ice crystals subsequent to annealing at -6 °C for 30 minutes assist to visualize the clear difference between inhibited (5 mg/mL 9 kDa PVA) and uninhibited ice crystal growth and are the basis from which MLGS (%) values are derived (Figure 2.15.).

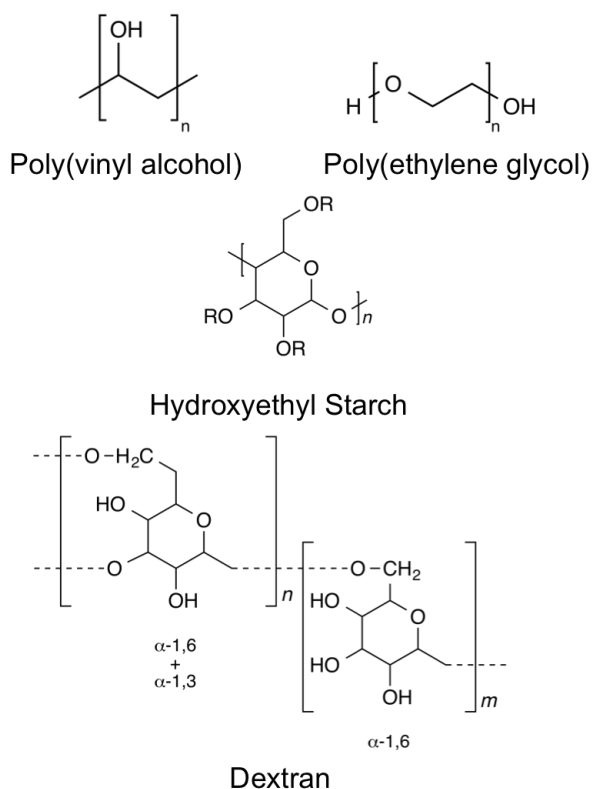


Figure 2.13. Structures of various high molecular weight polymers assessed for IRI activity. (Clockwise from top left); Poly(vinyl alcohol) (PVA), Poly(ethylene glycol) (PEG), Hydroxyethyl Starch and Dextran (α (1→6) glucose and α (1→6) and α (1→3) glucose units).

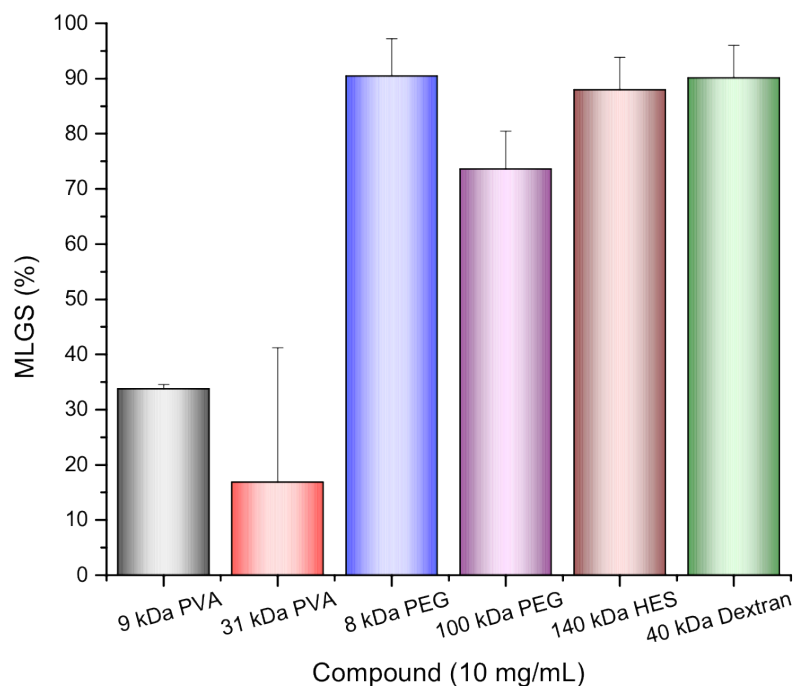


Figure 2.14. IRI activity of different polymers of various molecular weights and polydispersities. Each polymer was tested at a concentration of 10 mg/mL. All measurements represent the MLGS (%) of 10 crystals with error bars representing \pm standard deviation.

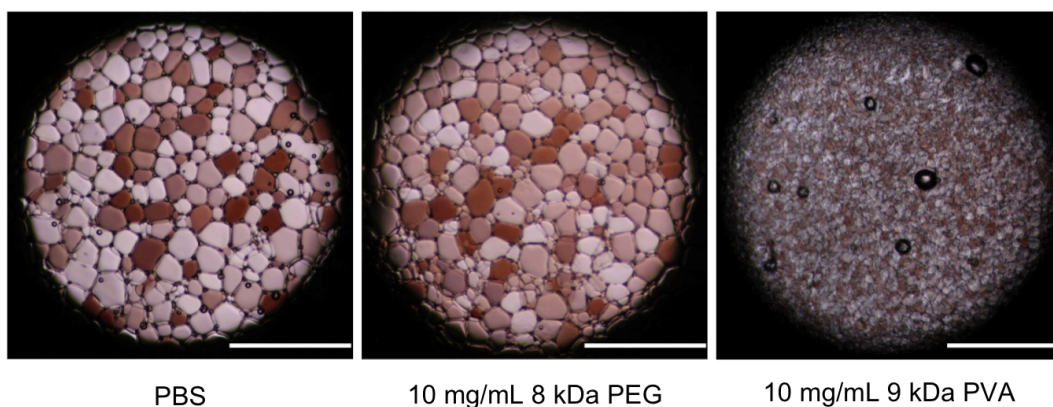


Figure 2.15. Micrographs of polynucleated ice crystal wafers. Illustrating ice recrystallization (growth) of various solutions annealed at $-6\text{ }^{\circ}\text{C}$ for 30 minutes; From left to right; PBS, 10 mg/mL 8 kDa PEG and 10 mg/mL 9 kDa PVA. Scale bar = 400 μm .

The low % MLGS of PVA is astonishing and PVA possesses a significantly greater IRI activity than any other polymers, (mono-, di- and oligo-) saccharides and low MW molecules tested. The %MLGS is also lower than the majority of those reported elsewhere with no immediate explanation (i.e. hydration index) for this anomalously high IRI activity (Figure 2.16.). Two other compounds that have similar properties but vastly different structures from AFPs and AF(G)Ps include a (lipo)xylomannan polysaccharide from the freeze tolerant Alaskan beetle *Upis ceramboides* identified by Walters *et al.* that additionally has strong TH activity. The IRI activity of (lipo)xylomannan is significant as it is the first compound to be isolated from nature that has no protein component.^{90,91} Studies by Deville *et al.* have also shown that preparations of zirconium acetate influence ice crystal structure though its properties with respect to ice recrystallization remain unknown but nonetheless continues to be an intriguing prospect (Section 1.4.).^{92,93}

Expanding the concentration range further the IRI activity of 9 kDa PVA and 31 kDa PVA between 0.0125 mg/mL and 1.5 mg/mL was assessed with significant activity observed at concentrations as low as 0.2 mg/mL (0.0048 [OH]/L) 9 kDa PVA (84.3 % ± 6.4 %) and 0.05 mg/mL (0.0012 [OH]/L) 31 kDa PVA (53.3 % ± 11.3 %) (Figure 2.17.) highlighting the potency of PVA as an IRI active compound and its potential to mitigate cryodamage caused by ice recrystallization.

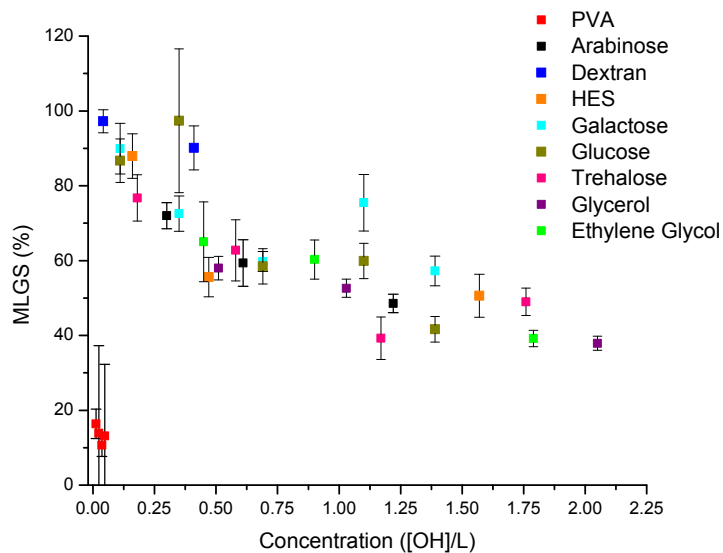


Figure 2.16. Selection of low MW compounds tested for IRI activity compared to 31 kDa PVA, 40 kDa Dextran and 140 kDa HES. Measurement of MLGS (%) vs. concentration ([OH]/L) highlighting the anomalously high IRI activity of PVA. Each measurement represents the (%) MLGS of 10 crystals with error bars representing \pm standard deviation.

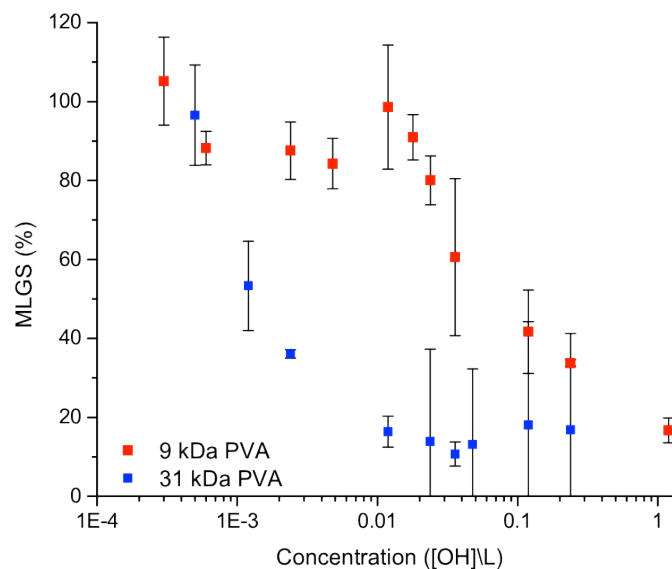


Figure 2.17. IRI activity of a range of concentrations of 9 kDa and 31 kDa PVA. Measurement of MLGS (%) vs. Concentration ([OH]/L). Each measurement represents the MLGS (%) of 10 crystals in triplicate with error bars representing \pm standard deviation.

2.3.4. IRI activity of PVA over an extended time frame.

The definition of IRI is the kinetic inhibition (slowing) of ice crystal growth, but a low rate of ice crystal growth will persist regardless, therefore it is important to assess IRI activity over a longer period as larger volume samples (e.g. organs) would be subjected to sufficiently long thawing times that would under normal circumstances promote extensive ice recrystallization. As a result some ice crystals may reach sizes that cause cryodamage at concentrations that only have a partial and inadequate inhibitory effect. Figure 2.18. shows the IRI activity (MLGS (μm)) of 9 kDa PVA and 31 kDa PVA over a 120-minute period at 20-minute intervals at 0.2 mg/mL, 2 mg/mL and for 9 kDa PVA 20 mg/mL also (31 kDa PVA was not soluble at this concentration). These measurements were calculated using MLGS (μm) as opposed to MLGS (%) in order to not give the impression of shrinking ice crystals (i.e. decreasing MLGS (%)) and to gain values for the overall ice crystal size, which is a more important measure over a prolonged period. It must be noted that over a prolonged period at concentrations where IRI activity starts to decrease (e.g. 0.2 mg/mL 31 kDa PVA and 2 mg/mL 9 kDa PVA) that a few significantly large ice crystals (as a consequence of Ostwald ripening) appeared and persisted skewing the size distribution and giving a large standard deviation (Figure 2.19). Importantly even the presence of a few large ice crystals such as these may prove detrimental to cells, a consideration to undertake with all IRI compounds both natural and synthetic. Pleasingly though the presence of moderately low concentrations of both 9 kDa and 31 kDa PVA appear to dramatically arrest significant ice recrystallization within this extended time frame, with MLGS values of $90.1 \mu\text{m} \pm 19.9 \mu\text{m}$ ($44.9 \% \pm 9.9 \%$) and $36.4 \mu\text{m} \pm 3.2 \mu\text{m}$ ($18.2 \% \pm 1.6 \%$) for 2 mg/mL solutions of 9 kDa and 31 kDa PVA respectively compared to a value of $200.5 \mu\text{m} \pm 20.5 \mu\text{m}$ for PBS after 120 minutes.

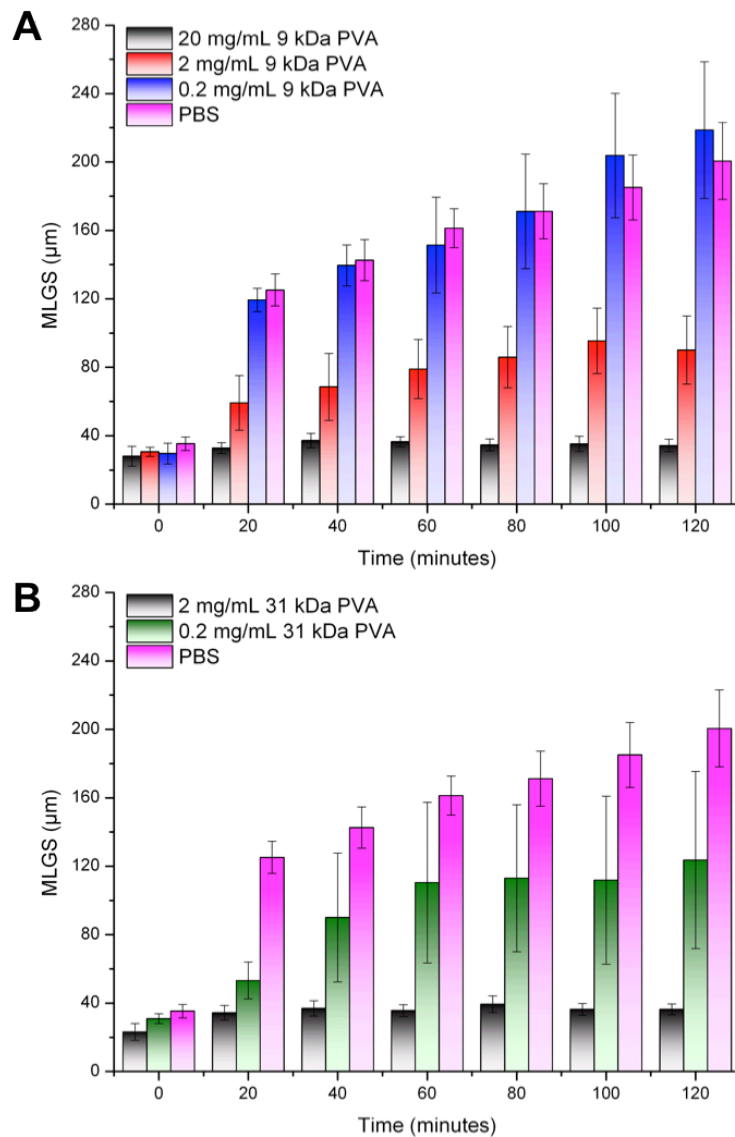


Figure 2.18. IRI activity of 9 kDa PVA and 31 kDa PVA at various concentrations over a 120-minute period. MLGS (μm) of (A) 9 kDa PVA and (B) 31 kDa PVA at 20-minute intervals relative to PBS. Each measurement represents the MLGS (μm) of 10 crystals with error bars representing \pm standard deviation.

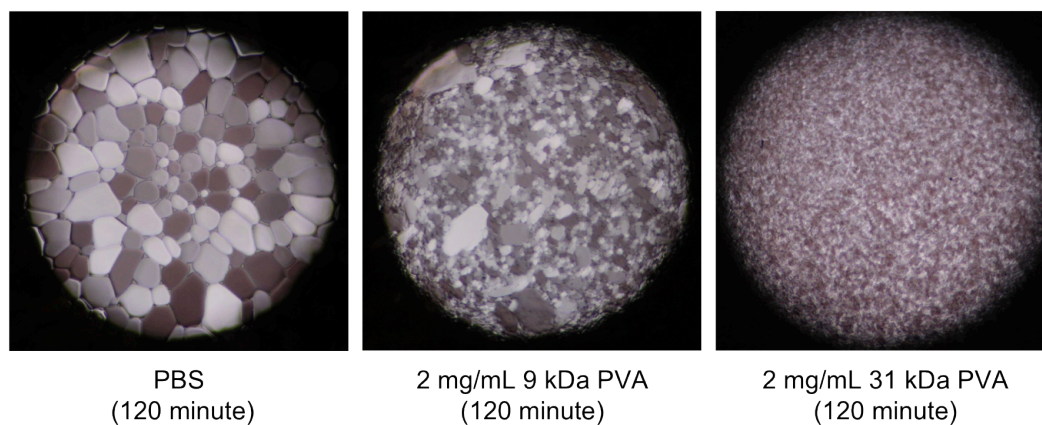


Figure 2.19. Micrographs of polynucleated ice crystal wafers after 120 minutes. Illustration of ice recrystallization (growth) of various solutions annealed at -6 °C for 120 minutes; From left to right; PBS, 2 mg/mL 9 kDa PVA (note the presence of a few persistently large ice crystals) and 2 mg/mL 31 kDa PVA.

2.3.5. Investigation of the hydrophobic and surfactant characteristics of PVA underlying its anomalously high IRI activity.

Considering all the data thus far, PVA clearly has an anomalously high activity and requires further investigation to identify any properties that may rationalise its IRI potency. The work of Capicciotti *et al.* has identified the potent IRI activity of two low MW carbohydrate derivatives, the non-ionic surfactant n-octyl- β -D-galactopyranoside and related IRI to its critical micelle concentration (CMC) in addition to the high potency of the hydrogelator n-octyl-D-gluconamide. Though they also showed that the ability to form micelles or promote gelation did not necessarily correlate with an appreciable IRI activity but did hypothesize the importance of hydration as n-octyl- β -D-galactopyranoside lacked an appreciable IRI activity.⁹⁴ Such findings correlated with galactose, n-methyl- β -D-galactopyranoside and n-methyl- α -D-galactopyranoside having higher hydration

number values than glucose, n-methyl- β -D-glucopyranoside and n-methyl- α -D-glucopyranoside respectively.⁵⁷ Balcerzak *et al.* expanded on the work of Capicciotti *et al.* and showed the importance of hydrophobicity in IRI activity.⁹⁵ This work focuses on the use of small MW lysine based surfactants, which have been previously investigated as anti-ice nucleating agents as potent IRI active compounds.^{96,97} These findings highlighted that the presence of a hydrophobic long chain alkyl group (decyl) at the C-terminus of a lysine residue permitted potent IRI activity. Alkyl chains longer than decyl resulted in a loss of IRI activity but shorter chain alkyl groups tended to a reduction in IRI activity correlating with shortening chain length, though the shortest chain length (butyl) examined still retained moderate IRI activity. Continuing on from this they investigated a range of double alkyl-substituted compounds (amino side chain and N-terminus) that again had IRI activity with potency varying with chain length and substitution applied. A simple comparison between PVA and these compounds is not easily possible, though it is important to assess whether or not PVA has any hydrophobic characteristics as suggested by these findings. However as aforementioned the ability to form micelles should not be considered a definite indicator of IRI activity but the formation of micelles is indicative of amphiphilicity.^{98,99} To probe whether or not PVA can form micelles indicative of amphiphilicity and therefore hydrophobicity, a dye inclusion assay with fluorescent 1,2-diphenyl-1,3,5-hexatriene (DPH) was performed (Section 2.5.5).¹⁰⁰ Dye inclusion assays are often used to determine the self-assembly of block copolymers in water.¹⁰¹ The organic dye DPH is only sparingly soluble in water and only fluoresces in a hydrophobic environment and therefore fluorescence will be detected as a consequence of aggregation. For that reason a range of concentrations of 9 kDa PVA and for comparison 8 kDa PEG, 40 kDa dextran, glucose, sucrose and trehalose were evaluated for micelle formation and define (if any) a corresponding critical micelle concentration (CMC) (Figure 2.20).

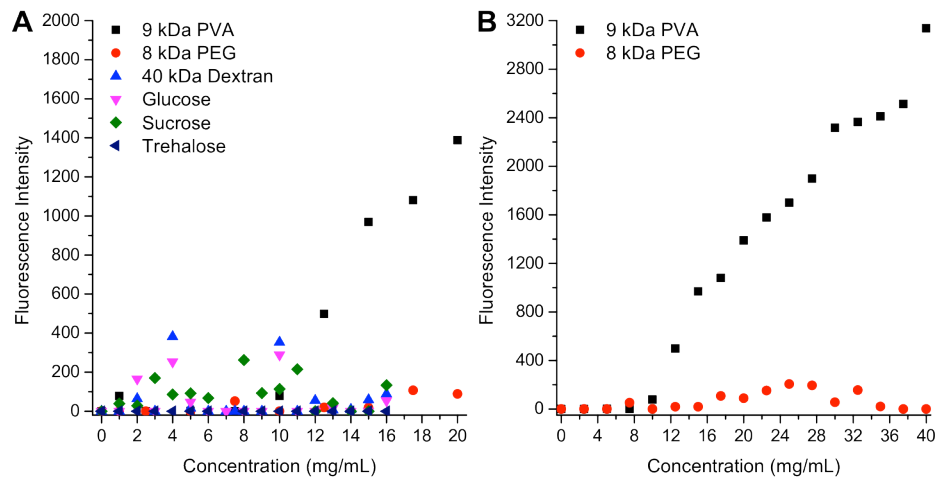


Figure 2.20. Assessment of critical micelle concentration (mg/mL) using fluorescence spectroscopy. Investigation of several different polymers and small molecules and the fluorophore DPH that fluoresces significantly (+1000) only in hydrophobic environments, indicative of aggregation. (A) All compounds assessed at concentrations between 0-20 mg/mL; (B) 9 kDa PVA and 8 kDa PEG assessed at a wider concentration range between 0-40 mg/mL.

Only 9 kDa PVA (the least IRI activity PVA identified) shows any significant fluorescence and only at concentrations above 10 mg/mL (CMC) where as all other materials tested were negative including 8 kDa PEG even up to a concentration of 40 mg/mL. The detection of fluorescence implies that 9 kDa PVA is capable of forming micelles. However experiments undertaken by colleagues demonstrated an absence of micelles (typically on the scale of 100Å) at comparable concentrations using dynamic light scattering (lower limit of approximately 1 nm). The lack of particle detection by dynamic light scattering is contradictory to the notion of micelle formation and therefore implies that PVA has the capability to form local hydrophobic domains and incorporate DPH without the onset of micelle formation. A finding that correlates well with the work of Capicciotti *et al.* as n-octyl-β-D-galactopyranoside, which has a CMC

approximating 30 mM defined by MD¹⁰² and a range of biophysical methods¹⁰³ is higher than the concentration (11 mM) with potent IRI activity. A similar trend observed with 9 kDa PVA that has IRI activity at concentrations (0.2 mg/mL) far lower than the perceived CMC here of 10 mg/mL. These findings tend to the hypothesis that PVA is able to present a local hydrophobic domain important to its anomalously high IRI activity though the abundance of hydroxyl groups will understandably play a part in IRI and other water/ice interactions, which is contrary to majority of surfactants that self assemble into micelles in aqueous solutions.¹⁰⁴ The lack of IRI activity in other (glyco)polymers may be due to their greater conformational flexibility causing inability to present this characteristic hydrophobic domain.⁸² The step-wise increase in the moderate IRI activity of methyl-glucopyranoside, ethyl-glucopyranoside and octyl-glucopyranoside compared to glucose and arabinose (same valency as allyl-glucose derivatives) is attributed to presence of a hydrophobic domain, though this IRI activity is still significantly below that of PVA. The CMC of octyl-glucopyranoside is 25 mM and at concentrations higher than this the allyl chain (hydrophobic domain) is sequestered into the micelle core and not available to interact in the surrounding hydration layer.¹⁰⁵ The CMC of octyl-glucopyranoside advocates that the dye inclusion assay is able to detect the presence of hydrophobic domains but not able to separate hydrophobicity from IRI activity.⁸⁵ The very high IRI activity of PVA though does excitingly suggest that PVA maybe able to improve cryopreservation by modulating ice crystal growth at biocompatible concentrations to reduce or alleviate ice recrystallization cryodamage (Chapters 3, 4 and 5). However to best understand the effect that PVA may have it is necessary to assess how ice crystal growth in the presence and absence of PVA is affected by various fast and slow freezing rates.^{106,107}

2.3.6. The effect of freezing rates and DMSO content on ice crystal formation and growth.

The freezing and thawing of cells, tissues and organs is a complex process (Chapter 1) and does not need reexamining here. Understanding nucleation (ice crystal formation) and ice crystal growth during the freezing process in an absence of cryoprotective additives is important as current cryopreservation strategies utilize an expansive array of freezing rates,²⁴ therefore understanding these properties may allow the rational design and implementation of novel cryopreservatives including PVA.

To probe any differences in ice crystal size and overall morphology, an assortment of cooling rates were used to freeze PBS (no cryoprotective effect) precisely from +2 °C to -78 °C at rates ranging from 0.5 °C/min to 150 °C/min by cryomicroscopy (Section 2.5.6.). Figure 2.21. illustrates micrographs of PBS taken at -78 °C with a clear indication that decreasing the freezing rate increases ice crystal size, with dramatically large differences between the slowest and fastest rates examined. How ice crystal size changes with freezing rate has obvious relevance to ice crystal growth during freezing and thawing, particularly slow thawing. To further investigate ice formation during freezing, cryomicroscopy was used to examine how solutions containing differing concentrations of the organic solvent, DMSO behave when cooled at a constant cooling rate of 40 °C/min down to -78 °C. Figure 2.22. illustrates a micrograph at -78 °C of a PBS solution containing 10 % (v/v) DMSO (Figure 2.22.A) which has clear ice crystal formation under these conditions and is akin to the concentrations used to cryopreserve immortalized mammalian cell lines as well as numerous primary cell types.¹⁰⁸ However these solutions are often far more complex and comprise high concentrations of FBS (> 5% (v/v)) in an isotonic cell

medium in addition to DMSO and thus may behave differently. In contrast to this a PBS solution with 50% (v/v) DMSO (Figure 2.22.B) inhibits ice formation under identical conditions, even when cooled further down to -150 °C (the lowest temperature attainable) no ice crystals were detected (Figure 2.22.C). The freezing point depressions of water/DMSO mixtures have been widely documented¹⁰⁹ as well as MD simulations attempting to model this phenomena.¹¹⁰ These freezing point depressions may be responsible for an absence of immediate ice formation at -80 °C but would be anticipated at -150 °C, this is suggestive therefore of a vitrified (ice crystal free) state. The presence of nucleators is also known to affect the probability of ice crystal formation and alter freezing points.¹¹¹ To put the effect of nucleators into the context of cryopreservation a review by Morris & Acton highlights the impact of ice nucleation¹¹² while Vigier & Vassoille describe ice nucleation and crystallization in water and glycerol (another commonly used organic cryoprotectant) mixtures as a consequence of devitrification upon thawing.¹¹³ Cryomicroscopy while enabling an accurate qualitative indication of ice crystal formation (nucleation) a more powerful tool for assessing phase transitions (i.e. nucleation/freezing or vitrification) is differential scanning calorimetry (DSC).¹¹⁴

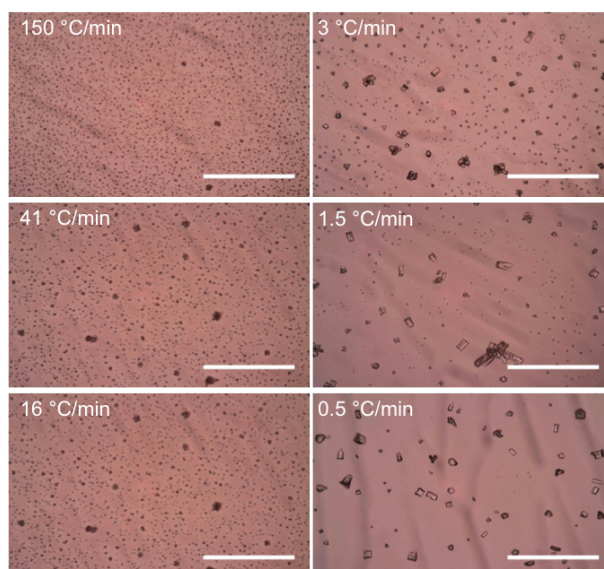


Figure 2.21. Micrographs illustrating ice crystal growth during freezing at various cooling rates. Highlighting increasing ice crystal size with decreasing freezing rate. (Scale bar = 200 μm) All samples (200x magnification) were cooled to $-78\text{ }^{\circ}\text{C}$ at the indicated rate, and images taken once that temperature had been reached.

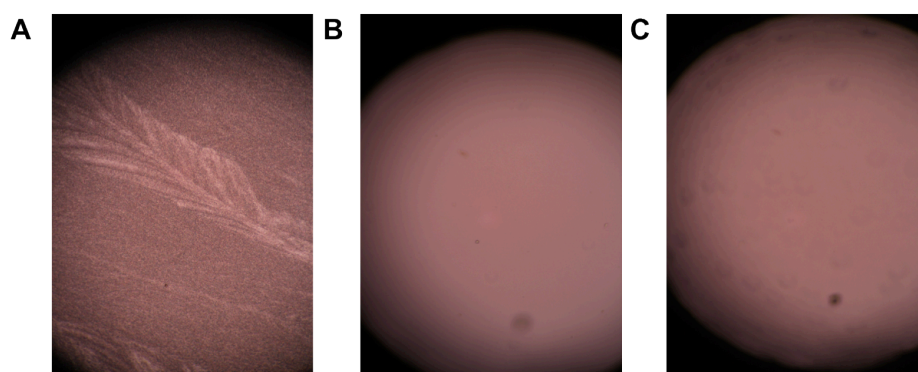


Figure 2.22. Micrographs of DMSO solutions cooled to $-80\text{ }^{\circ}\text{C}$ at $40\text{ }^{\circ}\text{C}/\text{min}$. (A) 10 % (v/v) solution of DMSO showing ice crystal formation; (B) 50 % (v/v) DMSO and (C) 50 % (v/v) DMSO cooled further to $-150\text{ }^{\circ}\text{C}$. Each showing an absence of ice crystal formation (100x magnification).

2.3.7. Investigation of freezing and thawing by Differential Scanning Calorimetry.

DSC is a thermoanalytical technique that precisely measures the differences in energy required between a reference and sample of interest to maintain a preprogrammed shift in temperature and is distinct from the similar technique of thermogravimetric analysis (TGA), though both techniques are used widely in materials science. TGA simply measures the mass loss of a sample with respect to increases in temperature and can be used to describe and define a range of physical and chemical phenomena including vaporization, desolvation and decomposition.¹¹⁵ DSC however can be used to detect exothermic and endothermic events (presented as peaks) and therefore phase transitions. The onset, asymmetry and broadness of these peaks are commonly used to assess purity. Impurities tend to shift and broaden phase transitions and can be used to consequently detect and approximate for example freezing point depressions.¹¹⁶ A liquid to solid phase transition is typically observed by a large exothermic event and these are distinct from glass transition events that evidential in this context of vitrification.¹¹⁷ Vitrification is a consequence of a rapid decrease in temperature causing a liquid to undergo a glass transition, which is the instantaneous switch from the liquid phase to an amorphous solid with abrupt changes in several material properties including viscosity and heat capacity.¹¹⁸ These changes can also be implemented by high pressure and a high solute concentration and therefore circumvent ice formation.¹¹⁹ The potential benefits for cryopreservation are enormous and were first identified by Polge *et al.* over 60 years ago with the use of high concentrations of glycerol to cryopreserve spermatozoa.¹²⁰ Despite early promise numerous problems have been encountered including devitrification.¹²¹ Devitrification caused by inadequate storage conditions or as a consequence of the thawing process results in ice crystal formation, which then

inflicts sufficient cryodamage due to recrystallization.¹¹⁹ The cooling rates required to typically incite vitrification are very high and therefore difficult to achieve with all but the smallest volumes even after the addition of large amounts of solute that reduce the absolute temperature and the cooling rates required.¹²² Additionally the concentration of cryoprotectant often DMSO or glycerol necessary can be cytotoxic and difficult to eliminate postthaw.¹²³ In recent years though progress have been made, difficulties remain in overcoming the aforementioned challenges.^{124,125} Using DSC it is therefore possible to investigate the processes of freezing and vitrification as separate events and assess how increases in DMSO concentration promotes either ice crystal formation or vitrification when cooled rapidly to -78 °C at 40 °C/min which mimics the conditions used in cryomicroscopy.

Figure 2.23. illustrates the DSC traces (Figure 2.23.A) attained for a range (0.5 % (v/v) – 15 % (v/v)) of DMSO solutions highlighting freezing transitions due to the presence of exotherms (+ve peaks), though these do not correlate strongly (Adj- $R^2 = 0.3857$) in a linear fashion indicative of the spontaneous nature of nucleation (Figure 2.23.C). Such findings are consistent with those demonstrated by cryomicroscopy. Concentrations of DMSO at 20, 30, 40 and 50 % (v/v) however did not elicit any exothermic peaks suggestive of no ice crystal formation (Figure 2.23.B). Understanding the effect of solute concentration upon thawing is equally of importance and thus each sample once cooled to -78 °C was warmed slowly at 2.5 °C/min until a final temperature of +2 °C. Melting is observed as a consequence of a large endothermic event during thawing and Figure 2.24.A shows the effect of DMSO concentration on the onset (1 °C thermal lag) and duration of melting with higher concentrations having broader and less pronounced peaks at lower temperatures. Interestingly both 20 % (v/v) and 30 % (v/v) DMSO while showing no ice crystal formation during freezing appear to have endothermic events indicative of melting which may be as a consequence

of devitrification leading to subsequent ice formation. Figure 2.24.B highlights that melting correlates strongly ($\text{Adj-R}^2 = 0.973$) with concentration which agrees well with existing literature.¹²⁶ From these findings it can be postulated that solute concentration affects the duration and onset of melting which is significant because this will have a consequence on the onset and duration at which ice recrystallization can occur especially at 10 % (v/v) DMSO that is the concentration most prevalent in cryobiology.²⁴

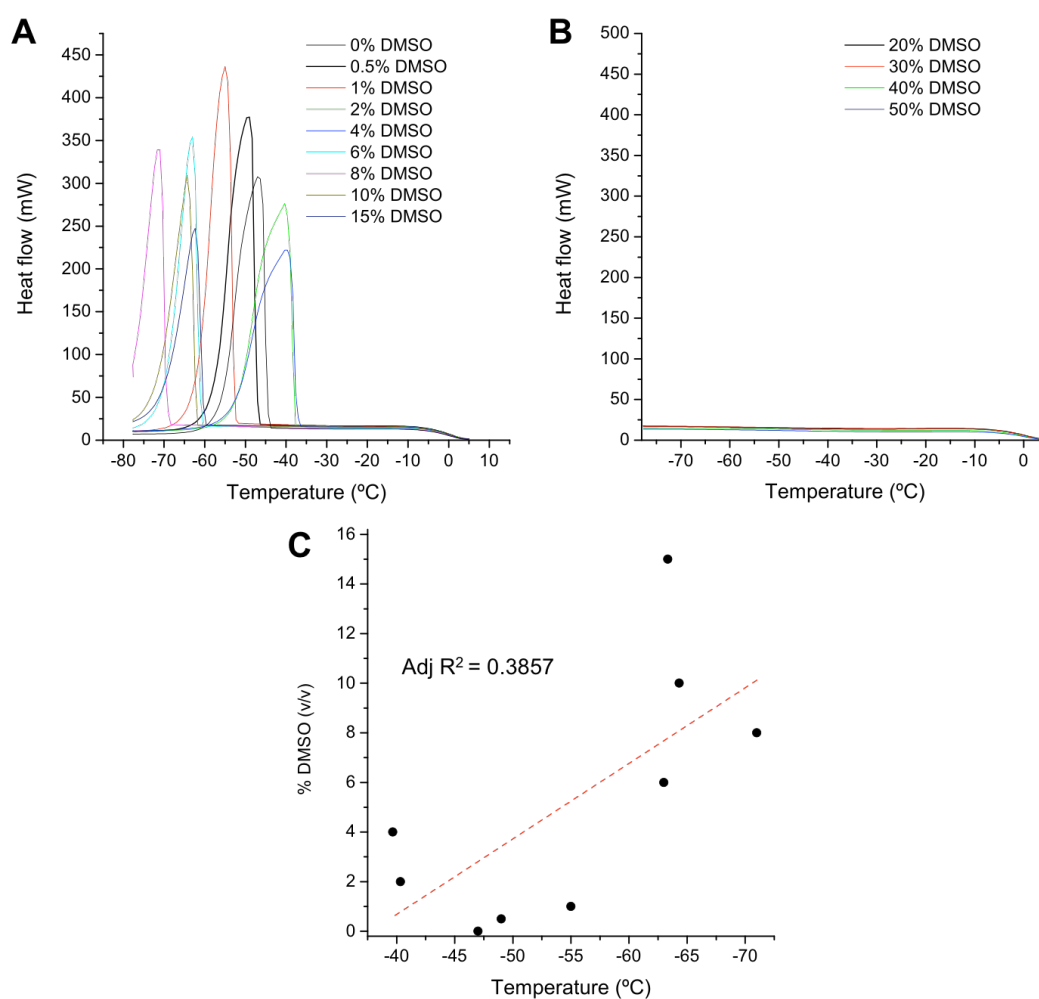


Figure 2.23. DSC traces upon cooling various concentrations (% (v/v)) of DMSO. (A) DSC traces (heat flow (mW)) assessing the freezing point of DMSO solutions between 0.5 % (v/v) and 15 % (v/v) (indicated by large exothermic peaks) down to a temperature of $-78\text{ }^{\circ}\text{C}$ at $40\text{ }^{\circ}\text{C}/\text{min}$; (B) Solutions greater than or equal to 20 % (v/v) DMSO that failed to freeze under identical conditions; (C) Temperature ($^{\circ}\text{C}$) at Peak_{Max} vs DMSO (v/v).

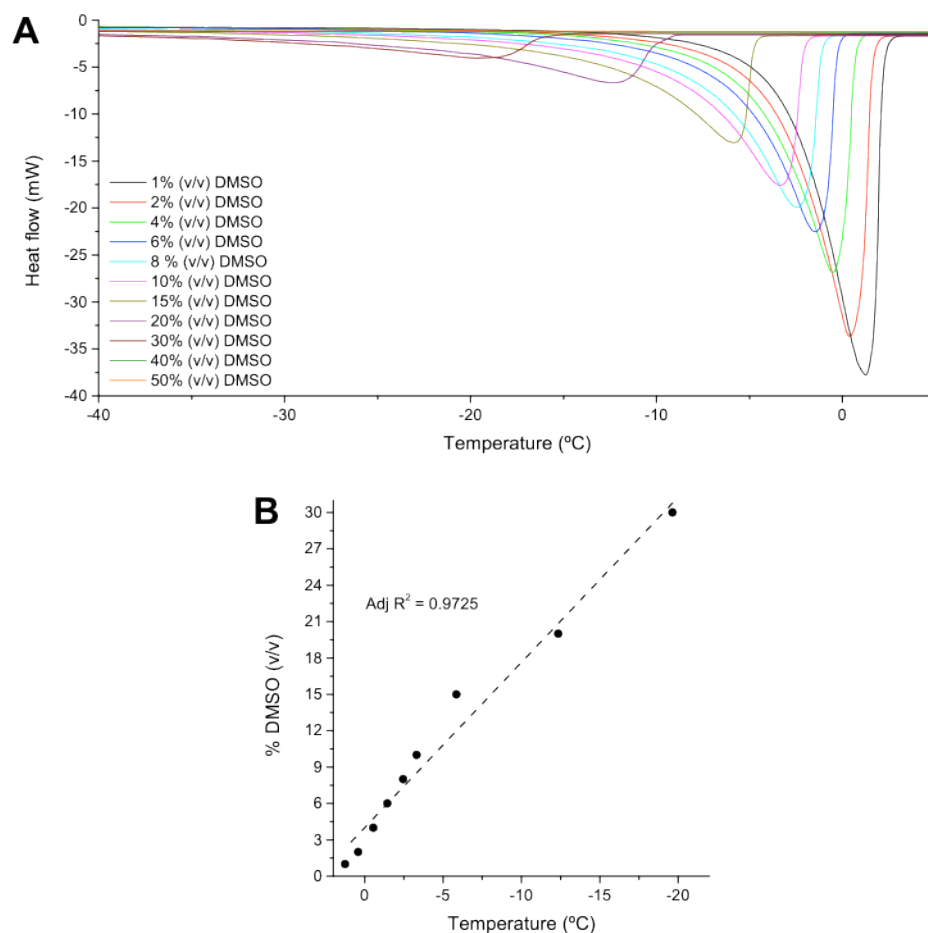


Figure 2.24. DSC traces upon thawing various concentrations (% (v/v)) of DMSO. DSC traces (heat flow (mW)) of (A) DMSO solutions heated from -78 °C to +5 °C at a rate of 2.5 °C/min exemplifying endothermic (thawing) transitions and the effect of DMSO concentration and (B) temperature at each peak minimum vs. DMSO concentration (% (v/v)) for the DSC traces presented in (A) demonstrating a strong linear relationship.

Several studies have investigated the impact and role of PVA and other polymers as inhibitors of heterogeneous ice nucleation in conjunction with high concentrations of organic solvents to help promote vitrification and evade ice formation.¹²⁷⁻¹³⁰ PVA is able to strongly inhibit ice nucleation events and reduce the concentrations of DMSO and glycerol required to incite vitrification and is available as a commercial preparation (Super cool X1000™, 21st century medicine, CA, USA) for this purpose.¹³¹ However our aims are not to prevent ice

formation, as the high concentrations of organic solvents required for vitrification (even with the addition of PVA) limit their application in cryobiology due to their cytotoxicity and in the difficulties in removing these membrane permeable solvents. Instead here we focus on the impact of 9 kDa PVA in an aqueous system to detect any effects it may have during the freezing and thawing process using DSC. Figure 2.25. illustrates the DSC traces attained from a wide range of 9 kDa PVA concentrations (0.2 mg/mL – 50 mg/mL). In each instance a large exothermic event is detected indicative of ice nucleation even at the highest concentration tested (50 mg/mL) with the no significant correlation between the onset of each exothermic event and PVA concentration. The absence of a significant correlation is suggestive of no anti-nucleating activity in these preparations. In contrast to this Ogawa *et al.* demonstrated a positive change in nucleation temperature, with a maximum shift of almost 3 °C using PVA (22 kDa) at a concentration of 1 mmol. At concentrations higher than this the nucleation temperature began to revert, corresponding with a decrease in the (colligative) melting point though the rate at which this reversion occurred was approximately 4.3 times greater, a constant that varies between different additives.¹²⁹ This effect was not detected in our experiments with 9 kDa PVA but the freezing rate used in our experiments (40 °C/min) were far greater than the (5 °C/min) used in this study which may account for this difference. A 40 °C/min freezing rate was chosen in order to mimic the rapid freezing rate used in several cryopreservation protocols. Interestingly the increase in nucleation temperature was found to be independent of MW when compared on a mass basis in the same study which differs with respect to the IRI activities of PVA which have a strong MW dependant activity over a similar MW range.⁵³ Analogous relationships involving changes (though depressions as opposed to increases) in nucleation temperature in aqueous systems have been documented elsewhere with non-IRI active polymers and small MW polyols including PEG and glycerol.^{132,133} The addition of PVA (13 kDa) to a vitrified system consisting of 35 % (v/v) 1,2-

propandiol that is cooled at 5 °C/min does cause a significant freeze point depression with the addition 3 % (w/w) PVA (the highest tested) producing a 50 °C depression, though under the same conditions and concentrations PEG induced a 30 °C shift.¹³⁴ Therefore under non-vitrifying conditions there is no significant effect on ice formation during rapid freezing that is detrimental to the potential application of PVA as a cryoprotectant.

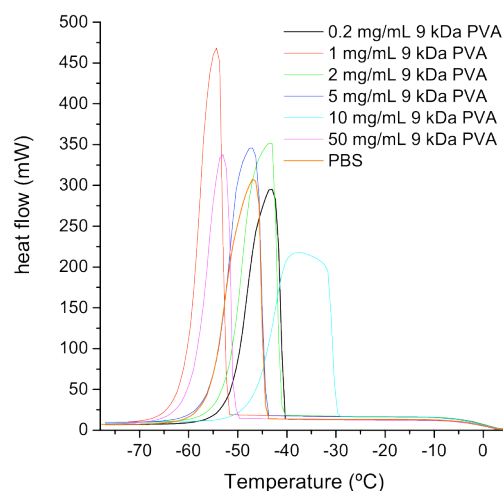


Figure 2.25. DSC traces upon cooling various concentrations (mg/mL) of 9 kDa PVA. DSC analysis (heat flow (mW)) assessing the freezing point of 9 kDa PVA solutions (indicated by large exothermic peaks) down to a temperature of -78 °C at 40 °C/min. No significant freezing point alteration that correlated with concentration was observed even with the addition of up to 50 mg/mL 9 kDa PVA.

However our focus is principally upon the effect (IRI) of PVA during thawing as opposed to freezing and assessing if PVA incites any large-scale changes during thawing especially slow thawing. Figure 2.26.A shows the DSC traces of aqueous 9 kDa PVA solutions at the same concentration range and with a slow thawing rate of 2.5 °C/min. It is clear that the concentration of PVA does not affect the onset or duration of melting (≈ -6 °C), though it is worth noting the apparent thermal lag in this system equating to about 1 °C. No exothermic events

indicative of recrystallization (though the magnitude of these cannot be predicted) are apparent¹³⁵ but these may be simply offset and therefore hidden by the endothermic melting process over the same time period. Upon closer inspection however an interesting endothermic event is recorded at around -22 °C (Figure 2.26.B). The magnitude and integral value is though far smaller meaning less energy is required for this event when compared to the melting process, but this is lessened and even negated (50 mg/mL) with increasing concentrations of 9 kDa PVA. This event is not seen either in solutions containing DMSO even at comparable mass concentrations (though the molar concentration will be significantly higher) nor is it reported elsewhere in literature though not many studies have been undertaken with most analysing PVA in conjunction with vast amounts of organic solvent which would mask this event anyway.^{130,134} Investigating further how this secondary minor peak may alter the freezing or thawing process remains a tantalising area for future investigation but under scenarios where by PVA would be used as a cryoprotectant is unlikely to have detrimental effects.

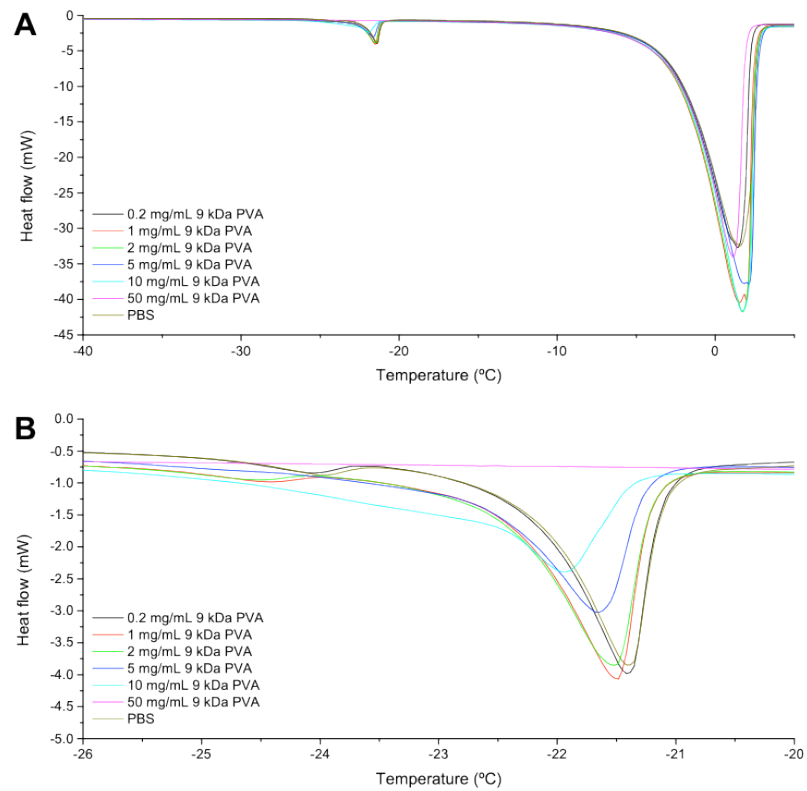


Figure 2.26. DSC traces upon thawing various concentrations (mg/mL) of 9 kDa PVA. DSC traces (heat flow (mW)) of (A) 9 kDa PVA solutions heated from -78 °C to +5 °C at a rate of 2.5 °C/min exemplifying two endothermic peaks and the effect of PVA concentration and (B) detailed view of the minor endothermic event depicted in (A).

2.4. CONCLUSION.

The IRI activities of a diverse set of monosaccharides, disaccharides, oligosaccharides, low MW molecules, natural and synthetic polymers have been defined. IRI studies have highlighted that increasing the concentration of hydroxyl groups ($[OH]/L$) tends to an increased IRI activity. However even at high concentrations the level of IRI is moderate at best with no discernable differences between these polyols even when considering variations in hydration number and hydration index. The polymer PVA is an exception and possesses exceptionally high IRI activity even at comparatively low concentrations with 31 kDa PVA having greater IRI activity than 9 kDa PVA but inferior aqueous solubility. A significant level of IRI activity with both PVA molecules is retained even over extended time periods and considerably longer than the durations required to successfully thaw small biological samples. Cryomicroscopy and DSC studies also showed the impact of freezing rates on ice crystal growth and how the presence of the cryoprotectant DMSO can inhibit ice formation and promote vitrification though at concentrations that are decidedly cytotoxic. Furthermore the presence of 9 kDa PVA at concentrations with significant IRI activity had no fundamental impact on the freezing or thawing processes that mimic conditions used in some cryopreservation protocols.

2.5. MATERIALS AND METHODS.

2.5.1. Preparation of Phosphate Buffered Saline.

A single phosphate buffered saline (PBS) tablet (Sigma-Aldrich Company Ltd, Dorset, UK) was placed in 200 mL of ultrahigh purity (18.2 mΩ cm (resistivity) at 25 °C) H₂O_(l) and stirred until the tablet dissolved fully. This yielded a solution of 137 mM (8.01 g/L) NaCl_(aq), 2.7 mM (0.20 g/L) KCl_(aq), 10 mM (1.78 g/L) Na₂HPO₄ · 2H₂O_(aq) and 2.0 mM (0.27 g/L) KH₂PO_{4(aq)} at pH 7.4 (303 mOsm/L). The solution could then be stored for a period of 3 months at 23 °C until required.

2.5.2. IRI compounds and the purification of HES, PVA, PEG and Dextran.

All monosaccharides, disaccharides, oligosaccharides and small MW polyols were of the highest attainable quality and sourced from various suppliers (Sigma-Aldrich Company Ltd, Dorset, UK; Fisher Scientific UK Ltd, Leicestershire, UK; Carbosynth Ltd, Berkshire, UK;) and used as supplied without further purification. 9 kDa PVA (average MW 9,000-10,000, 80 % hydrolyzed), 31 kDa PVA (average MW 31,000-50,000, 98-99 % hydrolyzed), 85 kDa PVA (average MW 85,000 - 124,000, 99+ % hydrolyzed), 8 kDa PEG (average MW 8,000), 100 kDa PEG (average MW 100,000) and 40 kDa dextran (average MW 40,000 obtained from *Leuconostoc spp*) were of the highest attainable quality available (Sigma-Aldrich Company Ltd, Dorset, UK). Purified (130 kDa) hydroxyethyl starch (0.4 degree of substitution) was isolated from the plasma expander, Volulyte® (Fresenius Kabi Ltd, Cheshire, UK) that comprises of 6 % (v/v) HES is an isotonic medium. Each polymer and polysaccharide was purified by dialysis as follows using ultrahigh

quality water with a resistance of 18.2 M Ω cm (25 °C) obtained from a Millipore Milli-Q gradient machine fitted with a 0.22 μ m filter and MWCO = 1000 dialysis membranes (Spectrum Laboratories Inc, CA, USA) and frequent 4 L H₂O(l) changes. Each sample was then freeze-dried overnight. Samples could then be stored for a period of 1 year at 23 °C and diluted with PBS when required.

2.5.3. Assessment of ice recrystallization inhibition (IRI) activity.

Determination of IRI activity was achieved using a modified “splat” assay.⁶³ Determination of IRI activity involved the expulsion of a 10 μ L droplet of analyte in PBS using a Hamilton gastight 1750 syringe (Hamilton Bonaduz AG, GR, Switzerland) coupled with a BD microlance 3 21G needle (BD, Oxfordshire, UK) from a fixed height of 2 m on to a 22x22 mm no.1 thickness glass cover slip (Fisher Scientific UK Ltd, Leicestershire, UK) on a CO_{2(s)} cooled aluminium plate (> -50 °C). The resulting impact generated a polynucleated ice crystal wafer with numerous ice crystals approximately 10 μ m in diameter. This wafer was then immediately transferred onto a pre-cooled (-6 °C) cryostage (either a nanolitre osmometer (Otago Osmometers Ltd, Dunedin, New Zealand) or Linkam BCS196 cryostage (Linkam Scientific Instruments Ltd, Guildford, Surrey, UK)) and allowed to anneal for 30 minutes (or longer if necessary). Photographs at all magnifications were taken using a Canon EOS 500D SLR digital camera (Canon (UK) Ltd, Surrey, UK) after 0 and 30 minutes (or longer in case of Figure 2.18.) coupled to an Olympus CX41 microscope equipped with UIS-2 20x/0.45/ ∞ /0-2/FN22, UIS-2 4x/0.1/ ∞ /-/FN22 and UIS-2 10x/0.2/ ∞ /-/FN22 lenses (Olympus Ltd, Essex, UK) through cross polarisers. At least 3 fields of view (1.33 mm²) were photographed (exemplified in Figure 2.15.) for each compound at each concentration, forming an extensive library. The 10 largest ice crystals from each image were then measured (40x magnification = 1.44 pixels per μ m; 100x

magnification = 3.6 pixels per μm ; 200x magnification = 7.2 pixels per μm ;) using the freely available image analysis software image J (<http://imagej.nih.gov/ij/>)¹³⁶ and the mean (μm) and standard deviation calculated and plotted in Origin 8.5 (OriginLab Corp, MA, USA) allowing the mean largest grain size (MLGS (μm)) with a resolution of up to 0.2 μm (200x magnification) to be defined. Each value was then contrasted against a positive PBS control (no IRI), which was taken as 100 % and the MLGS (%) \pm standard deviation reported (Equation 2.1.).

Equation 2.1: Calculation of MLGS (%) from MLGS (μm) of compound and MLGS (μm) of PBS.

$$MLGS (\%) = 100 \% \left(\frac{MLGS (\mu m)_{\text{compound}}}{MLGS (\mu m)_{\text{PBS}}} \right)$$

2.5.4. Assessment of ice formation in PBS solutions at various cooling rates.

The rate of ice crystal formation and growth at various freezing rates with a PBS solution was achieved using a Linkam BCS196 cryostage (Linkam Scientific Instruments Ltd, Guildford, Surrey, UK) coupled to an Olympus CX41 microscope equipped with a UIS-2 20x/0.45/ ∞ /0-2/FN22 lens (Olympus Ltd, Essex, UK) and a Canon EOS 500D SLR digital camera (Canon (UK) Ltd, Surrey, UK). A 5 μL droplet of PBS was placed between two No.0 thickness 19 mm diameter cover slips (Fisher Scientific UK Ltd, Leicestershire, UK) and cooled to +2 $^{\circ}\text{C}$. The sample was then cooled to -78 $^{\circ}\text{C}$ at one of a variety of cooling rates (Figure 2.21.) and images taken (200x magnification) at the focal plane showing ice formation. The same sample was used for each freeze/thaw cycle and heated rapidly (150 $^{\circ}\text{C}/\text{min}$) to +10 $^{\circ}\text{C}$ for 2 minutes to ensure all ice was melted between cooling cycles.

2.5.5. Assessment of Critical Micelle Concentration (CMC).

Several polymers including 9 kDa PVA, 8 kDa PEG and 40 kDa Dextran as well as several small carbohydrates including glucose, sucrose and trehalose were assessed by fluorescence spectrometry using a Synergy HT multi-mode microplate reader (BioTek UK, Bedfordshire, UK) for their potential to form micelles/undergo aggregation in aqueous solutions at 25 °C. Aqueous 80 µL aliquots of analyte ranging from 0-20 mg/mL were added to a clear flat-bottom 96-well plate (Bibby-Sterlin Ltd, Staffordshire, UK) and 20 µL of 0.01 mg/mL 1,2-diphenyl-1,3,5-hexatriene (DPH) added prior to vigorous mixing and incubation at 25 °C for a minimum of 3 minutes in absence of light giving a final concentration between 0 – 16 mg/mL (or higher in the case of 9 kDa PVA and 8 kDa PEG). The fluorescence of each sample was then measured with excitation at 360/40 nm and emission of 460/40 nm (sensitivity 35). The CMC was then defined as the lowest concentration (mg/mL) with an appreciable level (1000+) of fluorescence.

2.5.6. Assessment of vitrification by cryomicroscopy.

Ice crystal formation was assessed with PBS solutions containing various concentrations of DMSO up to 40 % (v/v) using a Linkam BCS196 cryostage (Linkam Scientific Instruments Ltd, Guildford, Surrey, UK) coupled to an Olympus CX41 microscope equipped with a UIS-2 20x/0.45/∞/0-2/FN22 lens (Olympus Ltd, Essex, UK) and a Canon EOS 500D SLR digital camera (Canon (UK) Ltd, Surrey, UK). A 5 µL droplet of PBS was placed between two No.0 thickness 19 mm diameter cover slips (Fisher Scientific UK Ltd, Leicestershire, UK) and cooled to +2 °C. Samples were then cooled at 40 °C/min down to a final temperature of -78 °C and ice crystal formation was examined at a range of focal planes and the results photographed highlighting the presence or absence of ice

crystals (Figure 2.22.). If no ice crystal formation was apparent then samples were cooled even further down to $-150\text{ }^{\circ}\text{C}$ the lowest attainable temperature with this instrumentation.

2.5.7. Preparation of samples for differential scanning calorimetry (DSC).

Samples were prepared by weighing standard $40\text{ }\mu\text{L}$ aluminum crucibles (Mettler Toledo, Leicestershire, UK) and adding $15\text{ }\mu\text{L}$ of analyte before sealing (hermetically) and reweighing in order to quantify the exact mass of sample. Each sample was then transferred to a liquid nitrogen cooled DSC 1 STAR® system (Mettler Toledo, Leicestershire, UK) differential scanning calorimeter. The mass of the aluminum crucible and sample mass was inputted into the complimentary STAR® thermal analysis software to retain a digital record and aid analysis.

2.5.8. Freezing and thawing of DSC samples and evaluation of DSC spectra.

Each DSC sample was individually cooled from $+5\text{ }^{\circ}\text{C}$ to $-78\text{ }^{\circ}\text{C}$ at a rate of $40\text{ }^{\circ}\text{C}/\text{min}$ whilst concurrently monitoring the heat flow (mW) of the system to detect any endothermic or exothermic transitions. When samples were cooled to $-78\text{ }^{\circ}\text{C}$ each sample was then immediately warmed at a rate of $2\text{ }^{\circ}\text{C}/\text{min}$ from $-78\text{ }^{\circ}\text{C}$ to $+5\text{ }^{\circ}\text{C}$. Raw data from each experiment was exported and plotted in Origin 8.5 (OriginLab Corp, MA, USA) and individual peaks highlighted for comparison using the in built modeling functions for linear curve fitting when required.

2.6. APPENDIX.

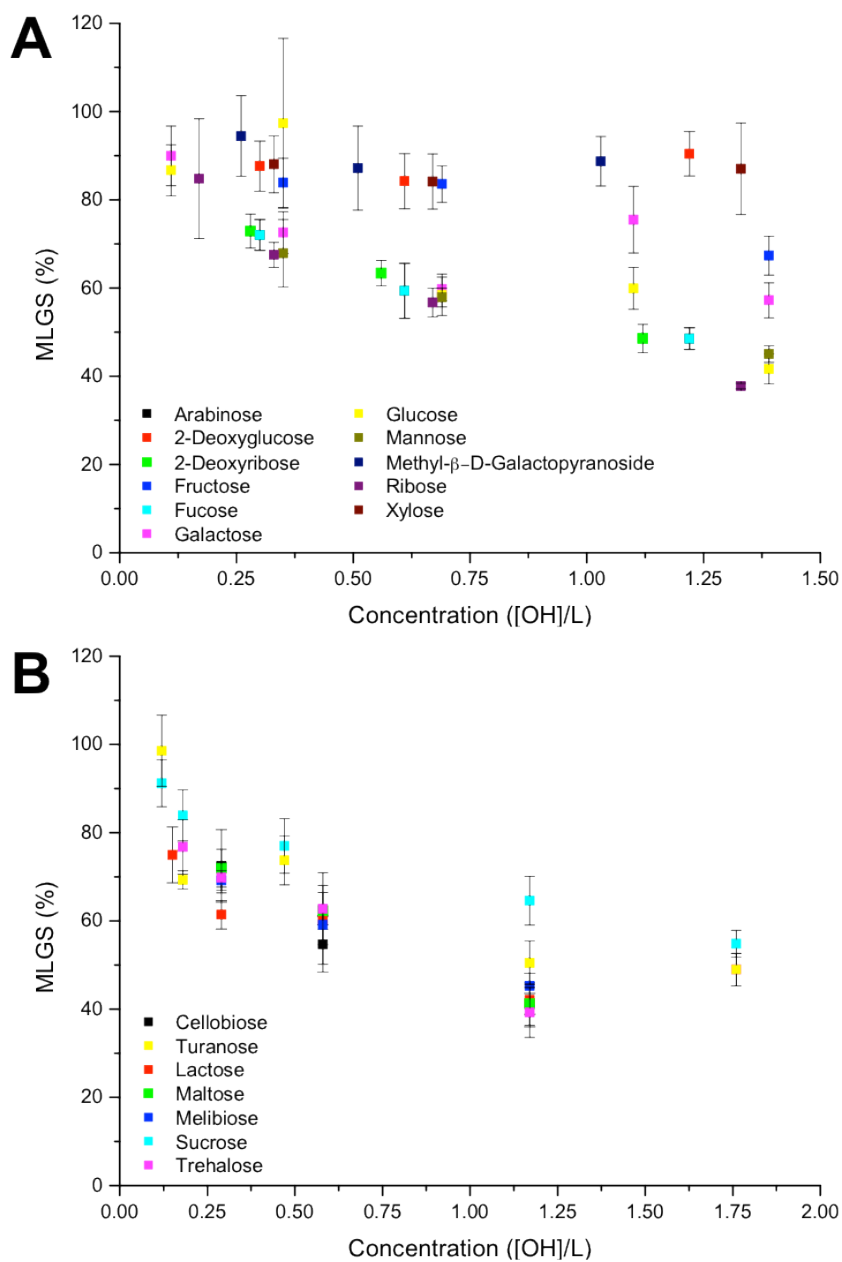


Figure 2.27. Comprehensive overview of the IRI activities of all investigated monosaccharides and disaccharides. (A) monosaccharides and (B) disaccharides. Each measurement represents the MLGS (%) of 10 crystals with error bars representing \pm standard deviation.

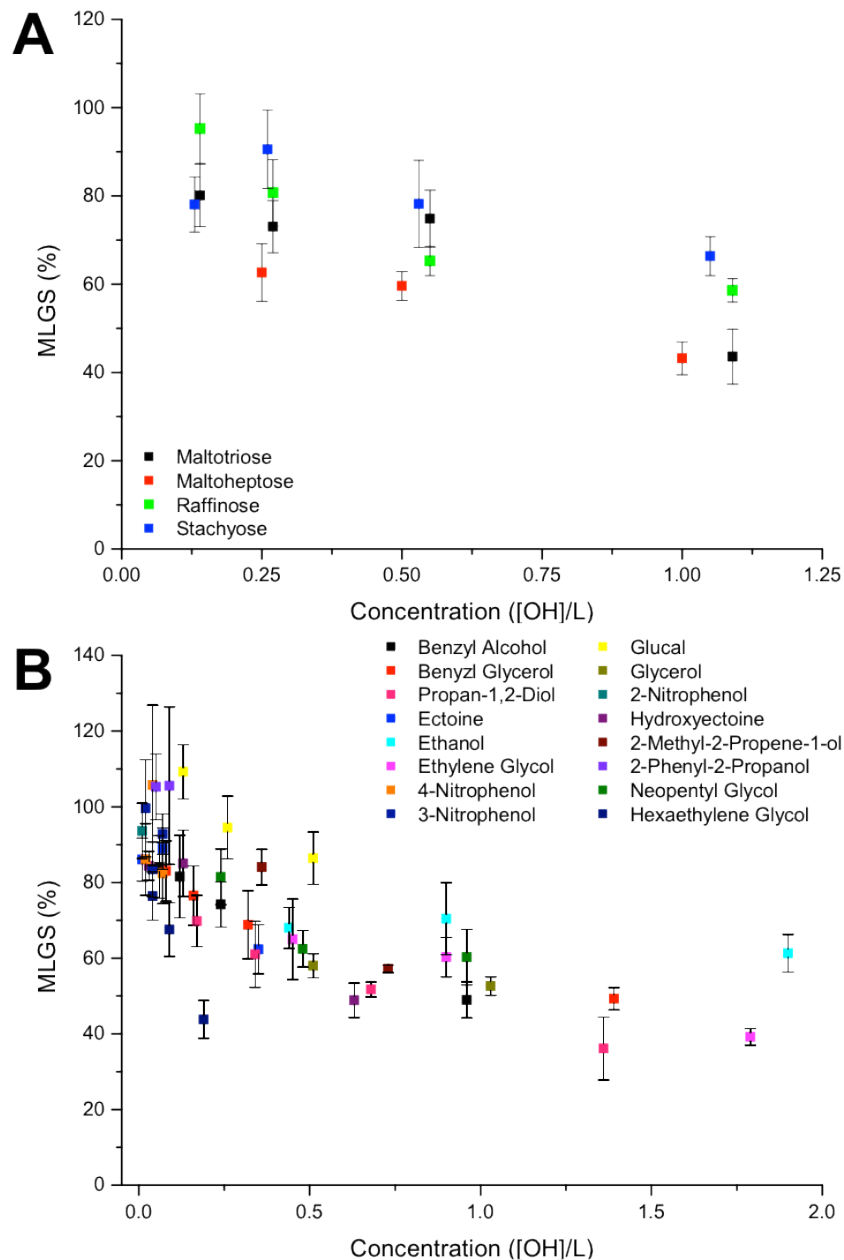


Figure 2.28. Comprehensive overview of the IRI activities of all investigated oligosaccharides and low MW polyols. (A) oligosaccharides and (B) low MW molecules. Each measurement represents the MLGS (%) of 10 crystals with error bars representing \pm standard deviation.

2.7. REFERENCES.

1. Mora, C., Tittensor, D. P., Adl, S., Simpson, A. G. B. & Worm, B. How Many Species Are There on Earth and in the Ocean? *PLoS Biol* **9**, 1–8 (2011).
2. Orlando, G. *et al.* Regenerative medicine and organ transplantation: past, present, and future. *Transplantation* **91**, 1310–1317 (2011).
3. Mason, C. & Dunnill, P. A brief definition of regenerative medicine. *Regen Med* **3**, 1–5 (2008).
4. Opar, A. As demand for organs expands, so does transplant technology. *Nat Med* **14**, 225 (2008).
5. Ringe, J., Kaps, C., Burmester, G.-R. & Sittinger, M. Stem cells for regenerative medicine: advances in the engineering of tissues and organs. *Naturwissenschaften* **89**, 338–351 (2002).
6. Orlando, G. *et al.* Regenerative medicine as applied to solid organ transplantation: current status and future challenges. *Transplant Int* **24**, 223–232 (2011).
7. Mazur, P. Cryobiology: the freezing of biological systems. *Science* **168**, 939–949 (1970).
8. Meryman, H. T. Freezing Injury and its Prevention in Living Cells. *Annu Rev Biophys Bioeng* **3**, 341–363 (1974).
9. Acker, J. P. & McGann, L. E. Membrane damage occurs during the formation of intracellular ice. *Cryo Lett* **22**, 241–254 (2001).
10. Rubinsky, B. Cryosurgery. *Annu Rev Biomed Eng* **2**, 157–187 (2000).
11. Devries, A. L. & Wohlschlag, D. E. Freezing resistance in some Antarctic fishes. *Science* **163**, 1073–1075 (1969).
12. Devries, A. L., Komatsu, S. K. & Feeney, R. E. Chemical and physical properties of freezing point-depressing glycoproteins from Antarctic fishes. *J Biol Chem* **245**, 2901–2908 (1970).
13. Harding, M. M., Anderberg, P. I. & Haymet, A. D. J. 'Antifreeze' glycoproteins from polar fish. *Eur J Biochem* **270**, 1381–1392 (2003).
14. Wilkinson, B. L. *et al.* Total Synthesis of Homogeneous Antifreeze Glycopeptides and Glycoproteins. *Angew Chem Int Edit* **51**, 3606–3610 (2012).
15. Devries, A. L. Glycoproteins as biological antifreeze agents in antarctic fishes. *Science* **172**, 1152–1155 (1971).
16. Ben, R. N. Antifreeze Glycoproteins—Preventing the Growth of Ice. *ChemBioChem* **2**, 161–166 (2001).
17. Davies, P. L. & Sykes, B. D. Antifreeze proteins. *Curr Opin Struct Biol* **7**, 828–834 (1997).
18. Marqusee, J. A. & Ross, J. Theory of Ostwald ripening: Competitive growth and its dependence on volume fraction. *J Chem Phys* **80**, 536–543 (1984).
19. Pronk, P., Ferreira, C. I. & Witkamp, G. J. A dynamic model of Ostwald ripening in ice suspensions. *J Cryst Grow* **275**, 1355–1361 (2005).

20. Houston, M. E. *et al.* Binding of an oligopeptide to a specific plane of ice. *J Biol Chem* **273**, 11714–11718 (1998).
21. Chao, H., DeLuca, C. I. & Davies, P. L. Mixing antifreeze protein types changes ice crystal morphology without affecting antifreeze activity. *FEBS Lett* **357**, 183–186 (1995).
22. Kristiansen, E. & Zachariassen, K. E. The mechanism by which fish antifreeze proteins cause thermal hysteresis. *Cryobiology* **51**, 262–280 (2005).
23. Gibson, M. I. Slowing the growth of ice with synthetic macromolecules: beyond antifreeze(glyco) proteins. *Polym Chem* **1**, 1141–1152 (2010).
24. Meryman, H. T. Cryopreservation of living cells: principles and practice. *Transfusion* **47**, 935–945 (2007).
25. Lynch, F. T. & Khodadoust, A. Effects of ice accretions on aircraft aerodynamics. *Prog Aerosp Sci* **37**, 669–767 (2001).
26. Ryerson, C. C. Ice protection of offshore platforms. *Cold Reg Sci Technol* **65**, 97–110 (2011).
27. Carriveau, R., Edrisy, A., Cadieux, P. & Mailloux, R. Ice Adhesion Issues in Renewable Energy Infrastructure. *J Adhes Sci Technol* **26**, 447–461 (2012).
28. Frankenstein, S. & Tuthill, A. M. Ice Adhesion to Locks and Dams: Past Work; Future Directions? *J Cold Reg Eng* **16**, 83–96 (2002).
29. Garner, J. & Harding, M. M. Design and synthesis of antifreeze glycoproteins and mimics. *ChemBioChem* **11**, 2489–2498 (2010).
30. De Groot, A. S. & Scott, D. W. Immunogenicity of protein therapeutics. *Trends Immunol* **28**, 482–490 (2007).
31. Peltier, R. *et al.* Synthesis and antifreeze activity of fish antifreeze glycoproteins and their analogues. *Chem Sci* **1**, 538–551 (2010).
32. Liu, S. & Ben, R. N. C-linked galactosyl serine AFGP analogues as potent recrystallization inhibitors. *Org Lett* **7**, 2385–2388 (2005).
33. Leclere, M., Kwok, B. K., Wu, L. K., Allan, D. S. & Ben, R. N. C-linked antifreeze glycoprotein (C-AFGP) analogues as novel cryoprotectants. *Bioconjugate Chem* **22**, 1804–1810 (2011).
34. Balcerzak, A., Ferreira, S., Trant, J. F. & Ben, R. N. Structurally diverse disaccharide analogs of antifreeze glycoproteins and their ability to inhibit ice recrystallization. *Bioorg Med Chemistry Lett* **22**, 1719–1721 (2012).
35. Corcilius, L. *et al.* Synthesis of peptides and glycopeptides with polyproline II helical topology as potential antifreeze molecules. *Bioorg Med Chem* **21**, 3569–3581 (2013).
36. Czechura, P., Tam, R. Y., Dimitrijevic, E., Murphy, A. V. & Ben, R. N. The Importance of Hydration for Inhibiting Ice Recrystallization with C-Linked Antifreeze Glycoproteins. *J Am Chem Soc* **130**, 2928–2929 (2008).
37. Heggemann, C. *et al.* Antifreeze glycopeptide analogues: microwave-enhanced synthesis and functional studies. *Amino Acids* **38**, 213–222 (2010).
38. Capicciotti, C. J., Trant, J. F., Leclere, M. & Ben, R. N. Synthesis of C-linked

- triazole-containing AFGP analogues and their ability to inhibit ice recrystallization. *Bioconjugate Chem* **22**, 605–616 (2011).
39. Merrifield, R. B. Solid Phase Peptide Synthesis. I. The Synthesis of a Tetrapeptide. *J Am Chem Soc* **85**, 2149–2154 (1963).
 40. Eniade, A. & Ben, R. N. Fully convergent solid phase synthesis of antifreeze glycoprotein analogues. *Biomacromolecules* **2**, 557–561 (2001).
 41. Liu, S. *et al.* *In vitro* studies of antifreeze glycoprotein (AFGP) and a C-linked AFGP analogue. *Biomacromolecules* **8**, 1456–1462 (2007).
 42. Peltier, R. *et al.* Growth habit modification of ice crystals using antifreeze glycoprotein (AFGP) analogues. *Cryst Growth Des* **10**, 5066–5077 (2010).
 43. Matsumoto, S. *et al.* Effects of synthetic antifreeze glycoprotein analogue on islet cell survival and function during cryopreservation. *Cryobiology* **52**, 90–98 (2006).
 44. Zhu, X., Pachamuthu, K. & Schmidt, R. R. Synthesis of S-Linked Glycopeptides in Aqueous Solution. *J Org Chem* **68**, 5641–5651 (2003).
 45. Wang, J., Kováč, P., Sinaÿ, P. & Glaudemans, C. P. J. Synthetic C-oligosaccharides mimic their natural, analogous immunodeterminants in binding to three monoclonal immunoglobulins. *Carbohydr Res* **308**, 191–193 (1998).
 46. Morris, H. R. *et al.* Antifreeze glycoproteins from the blood of an antarctic fish. The structure of the proline-containing glycopeptides. *J Biol Chem* **253**, 5155–5162 (1978).
 47. Davies, P. L. & Hew, C. L. Biochemistry of fish antifreeze proteins. *FASEB J* **4**, 2460–2468 (1990).
 48. Nguyen, D. H., Colvin, M. E., Yeh, Y., Feeney, R. E. & Fink, W. H. The Dynamics, Structure, and Conformational Free Energy of Proline-Containing Antifreeze Glycoprotein. *Biophys J* **82**, 2892–2905 (2002).
 49. Carpenter, J. F. & Hansen, T. N. Antifreeze protein modulates cell survival during cryopreservation: mediation through influence on ice crystal growth. *Proc Natl Acad Sci USA* **89**, 8953–8957 (1992).
 50. Chao, H., Davies, P. L. & Carpenter, J. F. Effects of antifreeze proteins on red blood cell survival during cryopreservation. *J Exp Biol* **199**, 2071–2076 (1996).
 51. Inada, T. & Lu, S.-S. Inhibition of recrystallization of ice grains by adsorption of poly(vinyl alcohol) onto ice surfaces. *Cryst Growth Des* **3**, 747–752 (2003).
 52. Budke, C. & Koop, T. Ice recrystallization inhibition and molecular recognition of ice faces by poly(vinyl alcohol). *ChemPhysChem* **7**, 2601–2606 (2006).
 53. Congdon, T., Notman, R. & Gibson, M. I. Antifreeze (Glyco)protein Mimetic Behavior of Poly(vinyl alcohol): Detailed Structure Ice Recrystallization Inhibition Activity Study. *Biomacromolecules* **14**, 1578–1586 (2013).
 54. Tam, R. Y., Ferreira, S. S., Czechura, P., Chaytor, J. L. & Ben, R. N. Hydration Index-A Better Parameter for Explaining Small Molecule Hydration in Inhibition of Ice Recrystallization. *J Am Chem Soc* **130**, 17494–17501 (2008).
 55. Gaïda, L. B., Dussap, C. G. & Gros, J. B. Variable hydration of small carbohydrates for predicting equilibrium properties in diluted and concentrated

- solutions. *Food Chem* **96**, 387–401 (2006).
56. Franks, F., Reid, D. S. & Suggett, A. Conformation and Hydration of Sugars and Related Compounds in Dilute Aqueous Solution. *J Solution Chem* **2**, 99–118 (1973).
 57. Galema, S. & Hoiland, H. Stereochemical aspects of hydration of carbohydrates in aqueous solutions. 3. Density and ultrasound measurements. *J Phys Chem* **95**, 5321–5326 (1991).
 58. Lee, S. L., Debenedetti, P. G. & Errington, J. R. A computational study of hydration, solution structure, and dynamics in dilute carbohydrate solutions. *J Chem Phys* **122**, 204511 (2005).
 59. Pomata, M. H. H., Sonoda, M. T., Skaf, M. S. & Elola, M. D. Anomalous Dynamics of Hydration Water in Carbohydrate Solutions. *J Phys Chem B* **113**, 12999–13006 (2009).
 60. Galema, S. A., Engberts, J., Hoiland, H. & M, F. G. Informative thermodynamic properties of the effect of stereochemistry on carbohydrate hydration. *J Phys Chem* **97**, 6885–6889 (1993).
 61. Uda, Y., Zepeda, S., Kaneko, F., Matsuura, Y. & Furukawa, Y. Adsorption-induced conformational changes of antifreeze glycoproteins at the ice/water interface. *J Phys Chem B* **111**, 14355–14361 (2007).
 62. Zepeda, S., Yokoyama, E., Uda, Y., Katagiri, C. & Furukawa, Y. In Situ Observation of Antifreeze Glycoprotein Kinetics at the Ice Interface Reveals a Two-Step Reversible Adsorption Mechanism. *Cryst Growth Des* **8**, 3666–3672 (2008).
 63. Knight, C. A., Hallett, J. & Devries, A. L. Solute effects on ice recrystallization: an assessment technique. *Cryobiology* **25**, 55–60 (1988).
 64. Ross, H. K. Cryoscopic Studies - Concentrated Solutions of Hydroxy Compounds. *Ind Eng Chem* **46**, 601–610 (1954).
 65. Goldberg, R. N. & Tewari, Y. B. Thermodynamic and transport properties of carbohydrates and their monophosphates: the pentoses and hexoses. *J Phys Chem Ref Data* **18**, 809–880 (1989).
 66. Willoughby, C. E., Mazur, P., Peter, A. T. & Critser, J. K. Osmotic tolerance limits and properties of murine spermatozoa. *Biol Reprod* **55**, 715–727 (1996).
 67. Guthrie, H. D. Osmotic Tolerance Limits and Effects of Cryoprotectants on Motility of Bovine Spermatozoa. *Biol Reprod* **67**, 1811–1816 (2002).
 68. Liu, J., Christian, J. A. & Critser, J. K. Canine RBC osmotic tolerance and membrane permeability. *Cryobiology* **44**, 258–268 (2002).
 69. Jackman, J. *et al.* Assessing antifreeze activity of AFGP 8 using domain recognition software. *Biochem Biophys Res Commun* **354**, 340–344 (2007).
 70. Richards, S.-J., Jones, M. W., Hunaban, M., Haddleton, D. M. & Gibson, M. I. Probing Bacterial-Toxin Inhibition with Synthetic Glycopolymers Prepared by Tandem Post-Polymerization Modification: Role of Linker Length and Carbohydrate Density. *Angew Chem Int Edit* **51**, 7812–7816 (2012).

71. Lee, Y. C. & Lee, R. T. Carbohydrate-Protein Interactions: Basis of Glycobiology. *Acc Chem Res* **28**, 321–327 (1995).
72. Langer, F. & Mittermayer, C. Preservation solutions for transplantation. *Transplant P* **31**, 2069–2070 (1999).
73. Busza, A. L., Fuller, B. J. & Proctor, E. The response of liver to lactobionate/raffinose (University of Wisconsin--UW) solution during hypothermic preservation: a study using ³¹phosphorus nuclear magnetic resonance. *Cryobiology* **26**, 273–276 (1989).
74. Fletcher, G. L., Hew, C. L. & Davies, P. L. Antifreeze proteins of teleost fishes. *Annu Rev Physiol* **63**, 359–390 (2001).
75. Hayward, S. A. L., Rinehart, J. P., Sandro, L. H., Lee, R. E. & Denlinger, D. L. Slow dehydration promotes desiccation and freeze tolerance in the Antarctic midge *Belgica antarctica*. *J Exp Biol* **210**, 836–844 (2007).
76. Zhang, Q. & Yan, T. Correlation of intracellular trehalose concentration with desiccation resistance of soil *Escherichia coli* populations. *Appl Environ Microb* **78**, 7407–7413 (2012).
77. Clark, M. S. *et al.* Surviving extreme polar winters by desiccation: clues from Arctic springtail (*Onychiurus arcticus*) EST libraries. *BMC Genomics* **8**, 475 (2007).
78. Ewart, K. V., Lin, Q. & Hew, C. L. Structure, function and evolution of antifreeze proteins. *Cell Mol Life Sci* **55**, 271–283 (1999).
79. Chen, L., Devries, A. L. & Cheng, C. H. C. Convergent evolution of antifreeze glycoproteins in Antarctic notothenioid fish and Arctic cod. *Proc Natl Acad Sci USA* **94**, 3817–3822 (1997).
80. Near, T. J. *et al.* Ancient climate change, antifreeze, and the evolutionary diversification of Antarctic fishes. *Proc Natl Acad Sci USA* **109**, 3434–3439 (2012).
81. Yeh, Y. & Feeney, R. E. Antifreeze Proteins: Structures and Mechanisms of Function. *Chem Rev* **96**, 601–618 (1996).
82. Gibson, M. I., Barker, C. A., Spain, S. G., Albertin, L. & Cameron, N. R. Inhibition of ice crystal growth by synthetic glycopolymers: implications for the rational design of antifreeze glycoprotein mimics. *Biomacromolecules* **10**, 328–333 (2009).
83. Binder, W. H. & Sachsenhofer, R. 'Click' Chemistry in Polymer and Materials Science. *Macromol Rapid Commun* **28**, 15–54 (2007).
84. Hawker, C. J. The Convergence of Synthetic Organic and Polymer Chemistries. *Science* **309**, 1200–1205 (2005).
85. Deller, R. *et al.* Ice recrystallisation inhibition by polyols: comparison of molecular and macromolecular inhibitors and role of hydrophobic units. *Biomater Sci* **1**, 478–485 (2013).
86. Knorpp, C. T., Merchant, W. R., Gikas, P. W., Spencer, H. H. & Thompson, N. W. Hydroxyethyl starch: extracellular cryophylactic agent for erythrocytes. *Science* **157**, 1312–1313 (1967).
87. Pellerin-Mendes, C., Million, L. & Marchand-Arvier, M. *In vitro* study of the

- protective effect of trehalose and dextran during freezing of human red blood cells in liquid nitrogen. *Cryobiology* **35**, 20–30 (1997).
88. Korttila, K. *et al.* Effect of hydroxyethyl starch and dextran on plasma volume and blood hemostasis and coagulation. *J Clin Pharmacol* **24**, 273–282 (1984).
 89. Liu, M., Cheng, R. & Qian, R. Effect of solution concentration on the gelation of aqueous polyvinyl alcohol solution. *J Polym Sci Polym Phys* **33**, 1731–1735 (1995).
 90. Walters, K. R., Serianni, A. S., Sformo, T., Barnes, B. M. & Duman, J. G. A nonprotein thermal hysteresis-producing xylomannan antifreeze in the freeze-tolerant Alaskan beetle *Upis ceramoides*. *Proc Natl Acad Sci USA* **106**, 20210–20215 (2009).
 91. Ishiwata, A., Sakurai, A., Nishimiya, Y., Tsuda, S. & Ito, Y. Synthetic study and structural analysis of the antifreeze agent xylomannan from *Upis ceramoides*. *J Am Chem Soc* **133**, 19524–19535 (2011).
 92. Deville, S. *et al.* Ice Shaping Properties, Similar to That of Antifreeze Proteins, of a Zirconium Acetate Complex. *PloS one* **6**, 1–6 (2011).
 93. Deville, S., Viazzi, C. & Guizard, C. Ice-Structuring Mechanism for Zirconium Acetate. *Langmuir* **28**, 14892–14898 (2012).
 94. Capicciotti, C. J. *et al.* Potent inhibition of ice recrystallization by low molecular weight carbohydrate-based surfactants and hydrogelators. *Chem Sci* **3**, 1408–1416 (2012).
 95. Balcerzak, A. K., Febbraro, M. & Ben, R. N. The importance of hydrophobic moieties in ice recrystallization inhibitors. *RSC Adv* **3**, 3232–3236 (2013).
 96. Inada, T., Koyama, T., Goto, F. & Seto, T. Inactivation of ice nucleating activity of silver iodide by antifreeze proteins and synthetic polymers. *J Phys Chem B* **116**, 5364–5371 (2012).
 97. Zachariassen, K. E. & Kristiansen, E. Ice nucleation and antinucleation in nature. *Cryobiology* **41**, 257–279 (2000).
 98. Reiss-Husson, F. & Luzzati, V. The Structure of the Micellar Solutions of Some Amphiphilic Compounds in Pure Water as Determined by Absolute Small-Angle X-Ray Scattering Techniques. *J Phys Chem* **68**, 3504–3511 (1964).
 99. Dendukuri, D., Hatton, T. A. & Doyle, P. S. Synthesis and self-assembly of amphiphilic polymeric microparticles. *Langmuir* **23**, 4669–4674 (2007).
 100. Zhang, X., Jackson, J. & M, B. H. Determination of surfactant critical micelle concentration by a novel fluorescence depolarization technique. *J Biochem Biophys Methods* **31**, 145–150 (1996).
 101. Ma, N., Zhang, H., Song, B., Wang, Z. & Zhang, X. Polymer Micelles as Building Blocks for Layer-by-Layer Assembly: An Approach for Incorporation and Controlled Release of Water-Insoluble Dyes. *Chem Mater* **17**, 5065–5069 (2005).
 102. Chong, T. T., Hashim, R. & Bryce, R. A. Molecular dynamics simulation of monoalkyl glycoside micelles in aqueous solution: influence of carbohydrate headgroup stereochemistry. *J Phys Chem B* **110**, 4978–4984 (2006).

103. Haller, J. & Kaatze, U. Monomer Exchange and Rotational Isomerization of Alkyl Monoglycosides in Water. *J Phys Chem B* **113**, 12283–12292 (2009).
104. Zana, R. Critical Micellization Concentration of Surfactants in Aqueous Solution and Free Energy of Micellization. *Langmuir* **12**, 1208–1211 (1996).
105. Shinoda, K., Yamaguchi, T. & Hori, R. The Surface Tension and the Critical Micelle Concentration in Aqueous Solution of β -D-Alkyl Glucosides and their Mixtures. *Bull Chem Soc Jpn* **34**, 237–241 (1961).
106. Stephenson, J. L. Ice crystal growth during the rapid freezing of tissues. *J Biophysic Biochem Cytol* **2**, 45–52 (1956).
107. Ohtomo, M. & Wakahama, G. Growth rate of recrystallization in ice. *J Phys Chem* **87**, 4139–4142 (1983).
108. Grout, B., Morris, J. & McLellan, M. Cryopreservation and the maintenance of cell lines. *Trends Biotechnol.* **8**, 293–297 (1990).
109. Havemeyer, R. N. Freezing point curve of dimethyl sulfoxide–water solutions. *J Pharm Sci* **55**, 851–853 (1966).
110. Kirchner, B. & Reiher, M. The Secret of Dimethyl Sulfoxide–Water Mixtures. A Quantum Chemical Study of 1DMSO– nWater Clusters. *J Am Chem Soc* **124**, 6206–6215 (2002).
111. Wilson, P. W., Heneghan, A. F. & Haymet, A. Ice nucleation in nature: supercooling point (SCP) measurements and the role of heterogeneous nucleation. *Cryobiology* **46**, 88–98 (2003).
112. Morris, G. & Acton, E. Controlled Ice nucleation in cryopreservation – a review. *Cryobiology* **66**, 85–92 (2012).
113. Vigier, G. & Vassouille, R. Ice nucleation and crystallization in water-glycerol mixtures. *Cryobiology* **24**, 345–354 (1987).
114. Charoenrein, S. & Reid, D. S. The use of DSC to study the kinetics of heterogeneous and homogeneous nucleation of ice in aqueous systems. *Thermochimica Acta* **156**, 373–381 (1989).
115. Coats, A. W. & Redfern, J. P. Thermogravimetric analysis. A review. *Analyst* **88**, 906–924 (1963).
116. Plato, C. & Glasgow, A. R. Differential Scanning Calorimetry as a General Method for Determining the Purity and Heat of Fusion of High-Purity Organic Chemicals. Application to 95 Compounds. *Anal Chem* **41**, 330–336 (1969).
117. Wowk, B. Thermodynamic aspects of vitrification. *Cryobiology* **60**, 11–22 (2010).
118. Chang, Z. H. & Baust, J. G. Physical aging of glassy state: DSC study of vitrified glycerol systems. *Cryobiology* **28**, 87–95 (1991).
119. Yavin, S. & Arav, A. Measurement of essential physical properties of vitrification solutions. *Theriogenology* **67**, 81–89 (2007).
120. Polge, C., Smith, A. U. & Parkes, A. S. Revival of Spermatozoa after Vitrification and Dehydration at Low Temperatures. *Nature* **164**, 666 (1949).
121. Macfarlane, D. R. Devitrification in glass-forming aqueous solutions. *Cryobiology* **23**, 230–244 (1986).

122. Fahy, G. M., Saur, J. & Williams, R. J. Physical problems with the vitrification of large biological systems. *Cryobiology* **27**, 492–510 (1990).
123. Fahy, G. M. The relevance of cryoprotectant 'toxicity' to cryobiology. *Cryobiology* **23**, 1–13 (1986).
124. Fahy, G. M. *et al.* Cryopreservation of organs by vitrification: perspectives and recent advances. *Cryobiology* **48**, 157–178 (2004).
125. Fahy, G. M. Cryoprotectant toxicity neutralization. *Cryobiology* **60**, 545–553 (2010).
126. Bryant, G. DSC measurement of cell suspensions during successive freezing runs: implications for the mechanisms of intracellular ice formation. *Cryobiology* **32**, 114–128 (1995).
127. Wowk, B. & Fahy, G. M. Inhibition of bacterial ice nucleation by polyglycerol polymers. *Cryobiology* **44**, 14–23 (2002).
128. Mastai, Y., Rudloff, J., Cölfen, H. & Antonietti, M. Control over the Structure of Ice and Water by Block Copolymer Additives. *ChemPhysChem* **1**, 119–123 (2002).
129. Ogawa, S., Koga, M. & Osanai, S. Anomalous ice nucleation behavior in aqueous polyvinyl alcohol solutions. *Chem Phys Lett* **480**, 86–89 (2009).
130. Wang, H.-Y., Lu, S.-S. & Lun, Z.-R. Glass transition behavior of the vitrification solutions containing propanediol, dimethyl sulfoxide and polyvinyl alcohol. *Cryobiology* **58**, 115–117 (2009).
131. Rasch, C. M. *et al.* Vitrification enhancement by synthetic ice blocking agents. *Cryobiology* **40**, 228–236 (2000).
132. Zobrist, B., Weers, U. & Koop, T. Ice nucleation in aqueous solutions of poly[ethylene glycol] with different molar mass. *J Chem Phys* **118**, 10254 (2003).
133. Kanno, H., Miyata, K., Tomizawa, K. & Tanaka, H. Additivity Rule Holds in Supercooling of Aqueous Solutions. *J Phys Chem A* **108**, 6079–6082 (2004).
134. Wang, H.-Y., Inada, T., Funakoshi, K. & Lu, S.-S. Inhibition of nucleation and growth of ice by poly(vinyl alcohol) in vitrification solution. *Cryobiology* **59**, 83–89 (2009).
135. Alvarez, V. A., Kenny, J. M. & Vazquez, A. A. Isothermal crystallization of poly(vinyl alcohol-co-ethylene). *J Appl Polym Sci* **89**, 1071–1077 (2003).
136. Abràmoff, M., Magalhaes, P. & Ram, S. J. Image processing with ImageJ. *Biophotonics Int* **7**, 36–44 (2004).

CHAPTER 3.

3. ICE RECRYSTALLIZATION INHIBITORS IMPROVE THE CRYOPRESERVATION OF RED BLOOD CELLS.

3.1. CHAPTER SUMMARY.

The application of poly(vinyl alcohol) (PVA) that has been previously identified (Chapter 2) as a potent ice recrystallization inhibition (IRI) active compound is explored as a cryoprotectant for improving the cryopreservation of red blood cells (RBCs). RBCs are robust and relatively simple (non-nucleated) compared to many other cell types yet there is a strong clinical need for prolonging their storage. PVA is applied as separate entity and in conjunction with the non-IRI active cryoprotectant hydroxyethyl starch (HES) to both ovine (sheep) and human RBCs. The addition of PVA is shown to improve recovery rates of RBCs that are subjected to slow and consequently detrimental thawing rates with this property attributed to the ability of PVA to attenuate ice crystal growth and forms the basis of the recently accepted publication in the interdisciplinary journal *Nature Communications* entitled; Synthetic Polymers Enable Non-Vitreous Cellular Cryopreservation by Reducing Ice Crystal Growth During Thawing).

3.2. INTRODUCTION.

Human red blood cells (RBCs) can only be stored currently *ex vivo* for a maximum of 42 days hypothermically. Hypothermic storage requires RBCs to be kept in complex (saline, adenine, glucose and mannitol (SAGM)) solutions between 1 °C and 6 °C. The most popular options in order to retain acceptable viability (<1 % haemolysis) and posttransfusion survival (75 % after 24 hours) as defined by the American Association of Blood Banks being Adsol, Nutricel and Optisol.¹⁻⁴ A decline in the critical metabolites ATP and 2,3-DPG in addition to decreases in K⁺ concentration and pH have been well documented during this period. In addition to metabolite depletion there are significant changes in metabolism and energetics. The latter of which is reduced by 97 % when compared to that at physiological temperatures⁵ though these effects are usually reversed posttransfusion without consequence.⁶ The likelihood of a myriad of clinical consequences however increases with transfusion volume (mean transfusion volume approximately 1.4 L) and in neonatal and pediatric medicine.⁷ These complications are predominantly of a non-infectious nature, though even these are still considered as rare events.⁸ Increased haemovigilance and screening means that bacterial contamination and viral transmission account for a minute proportion of adverse reactions.⁹ A technique that aims to retain and extend the viability of RBCs beyond current limits is cryopreservation, which can be defined in this context as the storage of RBCs at low or ultra low temperatures such that RBCs are not freely in suspension but frozen. The cryopreservation of RBCs is advantageous in that it has no upper limit on storage duration and cellular energetics are minimized, limiting degradation and eryptosis. However even though such storage conditions are not inherently damaging both the freezing and thawing process can inflict significant damage by a variety of mechanisms, the prevalence and impact of which is dependant upon the rates of

freezing and thawing amongst an array of other factors (e.g. haematocrit).¹⁰ The freezing rate of RBCs can have a significant impact on viability. Slow freezing promotes the formation of extracellular ice that as a consequence creates an osmotic gradient that favours the efflux of water from the cell. The rate at which this occurs is highly dependant on the rate of ice formation that is in turn dependant upon the cooling rate. If the rate of efflux is sustainable such that RBCs can control the rate of water loss then the cell will slowly become dehydrated.¹¹ However if the rate of dehydration is too high then membrane lesions and excessive cell shrinkage may occur and in conjunction with this the levels of some solutes may reach localized concentrations that may have a consequential cytotoxicity.¹² The exact mechanism however remains a contested topic and it is believed that membrane lesions may alter permeability allowing the entry of previous impermeable molecules shifting osmolarity detrimentally.¹³⁻¹⁵ The presence of extracellular ice can also, depending upon the density (haematocrit) of RBCs, have a significant impact with regards to mechanical damage.^{16,17} A rapid cooling rate which there by limits the duration with which RBCs are exposed to the potentially damaging effects experienced at slow cooling rates is offset by an increased probability in the development of intracellular ice. Intracellular ice formation occurs during rapid cooling as the efflux of water in addition to changes in membrane permeability associated with low temperatures allow an undesirable retention of water within the cytoplasm and can occur by 3 different mechanisms.¹⁸ The formation of intracellular ice is hypothesized to incite greater mechanical damage and to be avoided where possible.¹⁹ Once frozen RBCs are often kept at temperatures below -150 °C indefinitely until required though an array of storage conditions have been employed that have no significantly detrimental effects.^{1,20,21} The thawing of RBCs is a process that is just as critical as freezing. However it is more difficult to precisely thaw cells in a controlled manner, as implementing a high thaw rate

requires the use of temperatures that exceed tolerable levels. The controlled of RBCs is especially true as they are stored and transfused in large volumes (470 mL) meaning that they cannot be thawed homogeneously. Heterogeneous thawing results in exposing a substantially high proportion of RBCs to undesirably high temperatures. As a consequence RBCs must be thawed at a comparatively slow rate. Slow thawing results in allowing ice recrystallization (Chapter 2) that is highly detrimental and a significant cause of cryoinjury. Aside from a financial and practical perspective, ice recrystallization damage is one of the main reasons as to why RBCs are not routinely cryopreserved as current methodologies fail to address the problems arising from ice recrystallization.²² Therefore the use of an affordable, biocompatible and IRI active additive that can be used at low concentrations and easily removed is highly desirable. The presence of PVA would limit ice recrystallization, which could limit cryoinjury and thus improve the overall yield of intact RBCs recovered after cryopreservation. Our aim is for that reason to apply PVA, which has a demonstrable IRI activity (Chapter 2) to RBCs in order to reduce the dependency of detrimental organic solvents such as glycerol and determine its potential as a novel cryoprotectant to limit an otherwise neglected mechanism of cryodamage.

3.3. RESULTS AND DISCUSSION.

3.3.1. Degradation of Ovine RBCs stored at 4 °C and 23 °C.

To demonstrate the challenges of the hypothermic storage of ovine RBCs in simple isotonic solutions, 25 mL aliquots were prepared and stored statically at 4 °C and 23 °C in PBS, with haemolysis assessed by quantifying the relative levels of haemoglobin leakage over a prolonged period (Figure 3.1. and Section 3.5.4.). In brief haemoglobin leakage was assessed by diluting RBCs 2-fold in PBS then at the desired time point taking a 20 µL aliquot, diluting in 200 µL PBS prior to centrifugation (1950 x g), transferring 50 µL of the supernatant to 150 µL PBS and measuring absorbance in a 96-well plate at 450 nm and referenced against 100 % haemolysed controls. Ovine RBCs stored at 4 °C had a haemolysed content exceeding 5 % after 15 days (6.6 % ± 0.7 %), which following 42 days at 4 °C exceeded 50 % (55.5 % ± 2.2 %). Comparable rates of haemolysis were mirrored when RBCs were stored at 23 °C which, after 15 days also exceeded 5 % (5.4 % ± 0.8 %) and after 35 days exceeded 35 % (39.4 % ± 3 %) with essentially no differences in haemolysis rates apparent using either storage temperature. These values are clearly unacceptable and greatly exceed legal limits, helping to emphasize the inadequacies of hypothermic storage for the long-term preservation of RBCs and indeed other types of clinically relevant biomaterials that tend to have greater fragility and susceptibility. The rates of haemolysis highlight the need for a clinically effective cryopreservation strategy, as hypothermic techniques are insufficient beyond the short and mid term. More effective strategies are of particular importance when rare blood products are collected for future autologous transfusion or in instances whereby logistical difficulties inhibit the regular and continuous resupply of blood products such as

in the recent conflicts in Iraq and Afghanistan, though issues in maintaining cryopreservation temperatures would be expected.^{23,24}

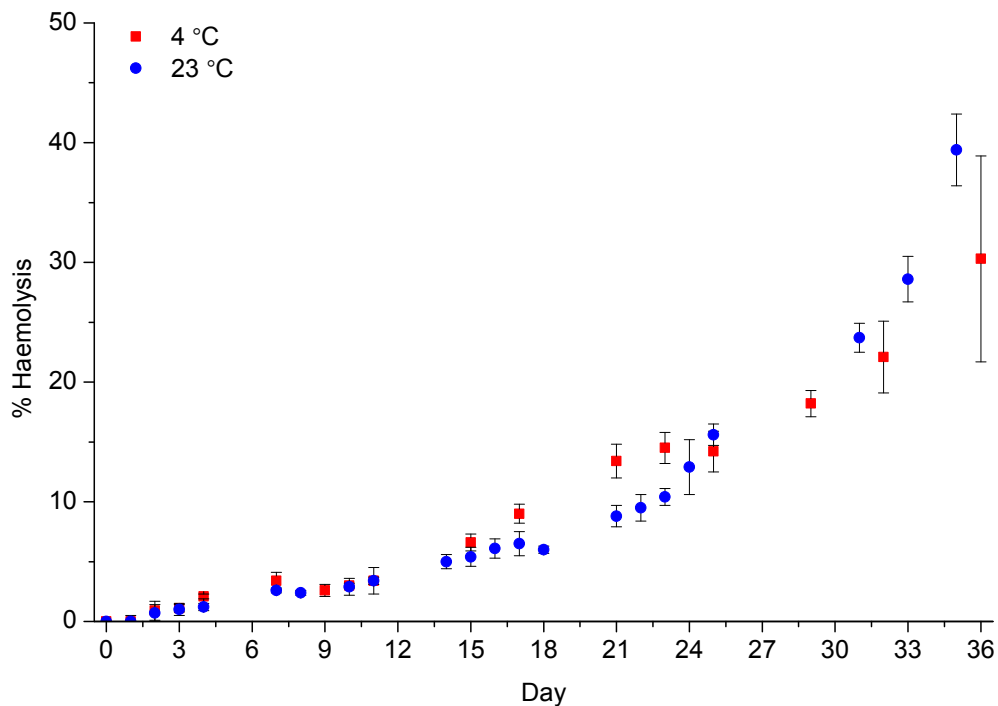


Figure 3.1. Hypothermic storage of ovine RBCs. Static storage of ovine RBCs at 4 °C over a 42 day period and static storage of ovine RBCs at 23 °C over a 35 day period in simple (PBS) isotonic solutions. Samples were taken at frequent intervals and each data point was measured (mean) in triplicate with the error bars representing \pm standard deviation.

3.3.2. Cytotoxicity of current cryopreservatives to Ovine and Human RBCs.

Cryopreservation provides a demonstrable alternative to the predominating hypothermic storage techniques and enables almost indefinite storage.²⁰ However to highlight the demand for novel cryopreservatives it is necessary to exemplify the inadequacies of commonly utilized cryopreservatives namely the

organic solvents glycerol and DMSO. Glycerol is the principal cryoprotective agent (CPA) used in the cryopreservation of RBCs but is required at extremely high concentrations (15 % (v/v) – 40 % (v/v)).^{1,25,26} Glycerol is membrane permeable and thus can promote rapid changes in osmotic pressure *in vitro* among a wide variety of cell types and is time-consuming and difficult to eliminate postthaw, which is critical as glycerol can incite posttransfusional intravascular haemolysis.²⁷ Membrane permeable CPAs²⁸ can result in extensive membrane damage (osmotic shock) if changes in osmotic pressure are sufficiently rapid and abrupt.¹¹ The distinctive membrane composition of RBCs means its membrane permeability differs from most other cell types²⁹ and varies extensively between different mammalian species.^{30,31} Therefore RBCs are possibly more susceptible to membrane lesions and as a consequence haemolysis, though haemolysis may also be dependant upon the thermoelasticity of the RBC membrane.^{32,33} Figure 3.2.A demonstrates how the direct addition and mixing (vortex) of glycerol at 23 °C to a final concentration of 5 % (v/v) glycerol (that is 3-fold lower than the minimum used in current cryopreservation protocols) leads to significant haemolysis of ovine RBCs. Even after the shortest time interval of 1 minute a clinically intolerable level of haemolysis (23.9 % ± 2.8 %) is observed and after a period of 15 minutes haemolysis has risen to near totality (93.9 % ± 3.8 %). The susceptibility of human RBCs to haemolysis with the addition of 5 % (v/v) glycerol was much lower even after a period of 60 minutes (12.1 % ± 1.9 %) but is still unacceptably high. However as shown in Figure 3.2.B haemolysis does not increase over this time period unlike observations with ovine RBCs that show an increase in haemolysis with time (Figure 3.2.A). The Plateauing of haemolysis is probably as a consequence of human RBCs attaining an equilibrium state faster than ovine RBCs due to their differences in membrane permeability with human RBCs having greater permeability (57-fold) than ovine RBCs. The robustness of human RBCs is contrary to literature findings that reveal that human RBCs were

more susceptible than ovine RBCs which were the second most robust from eight mammalian species tested where as human RBCs ranked seventh, however an essential difference is that such findings were determined using a lower glycerol concentration of 2.1 % (v/v) and at a temperature of 37 °C. Susceptibilities to haemolysis in this study correlated strongly with decreasing glycerol permeability though all species showed appreciable (> 50 %) haemolysis within 10 minutes.^{34,35} Another determinant may be that the level of haemolysis might also vary with haematocrit, the rationale being that studies examining the impact of haematocrit on the postthaw recovery of human RBCs when cryopreserving with a fixed concentration of glycerol showed dramatic and significant discrepancies between the highest (83 %) and lowest (4 %) haematocrits examined. Once haematocrits exceeded 50 % substantial increases in haemolysis were observed,^{16,17} additionally differences in tonicity (osmolarity) have been proven to considerably influence postthaw recoveries,¹⁵ therefore various membrane permeable CPAs are likely to have dissimilar and hard to define cryoprotective properties between different cell types and species.

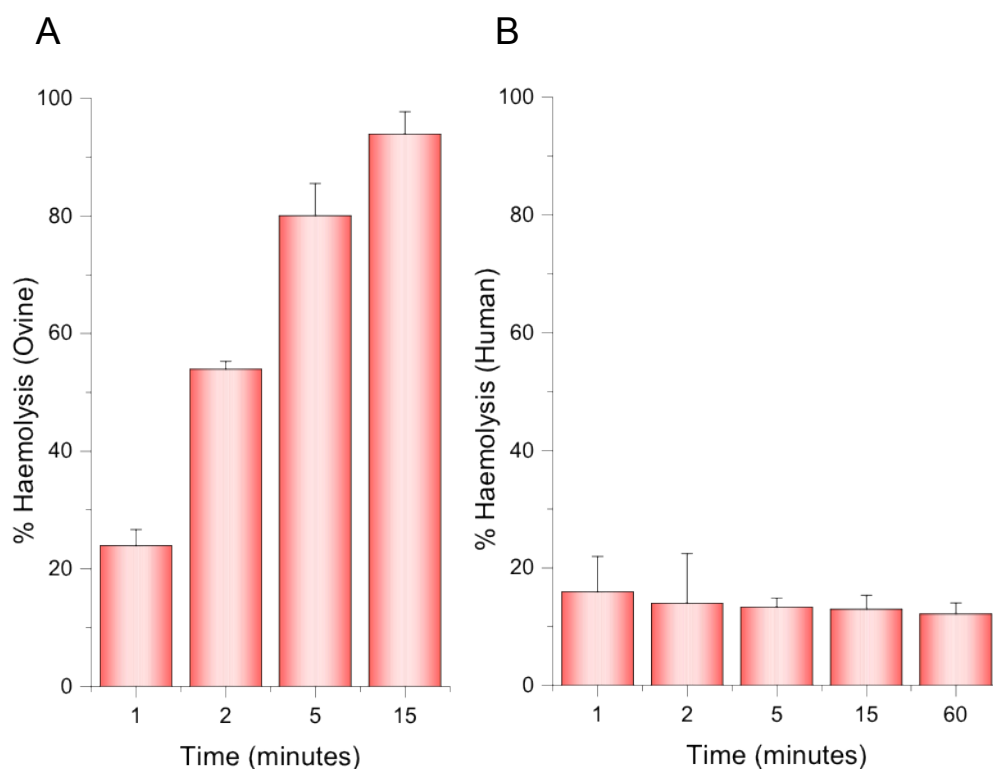


Figure 3.2. Cytotoxicity of the cryoprotectant glycerol to RBCs. (A) (%) Haemolysis of ovine RBCs (1 mL) incubated with glycerol (direct addition) over 15 minutes at 23 °C. (B) (%) Haemolysis of human RBCs (200 μ L) incubated with glycerol (direct addition) over 60 minutes at 23 °C. Each data point was measured (mean) in quintuplicate with the error bars representing \pm standard deviation.

The susceptibility of ovine and human RBCs to another commonly used cryoprotectant DMSO, was also evaluated using a similar methodology (Figure 3.3.). After a period of 60 minutes at 23 °C a dramatic level of haemolysis with ovine RBCs (40.3 % \pm 20.7 %) was detected at concentrations as low as 1.5 % (v/v) with haemolysis at the highest concentration tested of 4 % (v/v) equaling 77.1 % \pm 17.9 %. Extending the incubation time further to 150 minutes significant (63.8 % \pm 14.5 %) haemolysis at the lower concentration of 0.75 % (v/v) was detected. Analogous with glycerol a difference in the susceptibility of human RBCs to DMSO was observed. Only the highest concentration tested of 4 % (v/v)

elicited significant haemolysis in human RBCs ($23.2 \% \pm 0.7 \%$) after a period of 60 minutes at $23\text{ }^{\circ}\text{C}$, extending further at this concentration to 150 minutes resulted in greater haemolysis ($68.3 \% \pm 18.6 \%$), similar to ovine RBCs with $0.75\text{ } \%$ (v/v) DMSO. Human RBCs exposed to concentrations lower than $4\text{ } \%$ (v/v) demonstrated no significant haemolysis even after a period of 300 minutes (Figure 3.3.C). Though it has been reported that DMSO can cryoprotect human and bovine RBCs it is not routinely used.³⁶ This cryoprotective effect is understood to be due to its high membrane permeability³⁷ which is enhanced compared to glycerol especially with respect to bovine RBCs.³⁸ In spite of the cryoprotective effect of DMSO it has been shown that DMSO can have detrimental effects at physiological temperatures in a range of biological systems in *in vitro*^{39,40} and *ex vivo*^{41,42} models as well as clinically with the transfusion or transplantation of cells (including platelets) cryopreserved with DMSO.⁴³⁻⁴⁵ Compared to DMSO and glycerol, HES (membrane impermeable) incites minimal haemolysis in ovine RBCs by simple addition after 120 minutes ($0.66 \% \pm 0.45 \%$) at a concentration ($17.7\text{ wt}\%$ (low molar concentration)) that has a proven cryoprotective effect.⁴⁶⁻⁴⁸ Therefore going forward HES was the established cryoprotectant used in future experimentation. The HES preparation selected in this instance was isolated from the previously clinically utilized plasma expander, Volulyte[®] (Fresenius Kabi Ltd, Cheshire, UK) which was used to combat hypovolemia which is the reduction in blood volume often as a consequence of severe trauma.⁴⁹ Volulyte[®] is provided as a $6\text{ wt}\%$ isotonic solution (composition and structure in Figure 3.4.A and Figure 3.4.B) hence necessitating its purification and concentration (Section 3.5.1.). HES is prepared as a polydispersed compound and frequently characterized by its average MW (130 kDa), degree of substitution (0.4) and C_2/C_6 substitution ratio ($\approx 9:1$). Numerous preparations ranging from 70 kDa and 670 kDa with degrees of substitution from 0.4 to 0.75 are available. These different preparations have assorted efficacies

and varied pharmacodynamic and pharmacokinetic profiles with the latest generation of HES products have tended to focus on lower MWs.⁵⁰ HES is a non-IRI active and non-membrane permeable compound at reasonably low concentrations with a % MLGS of 87.9 % \pm 6.0 % at 10 mg/mL (0.157 [OH]L) (Figure 3.4.C). At the concentrations used in cryopreservation (> 30 mg/mL), HES alters viscosity⁵¹ and at higher concentrations limits ice crystal formation forming gel like particles (Figure 3.4.D),⁵² though these changes in solubility are likely to be influenced by MW.^{53,54}

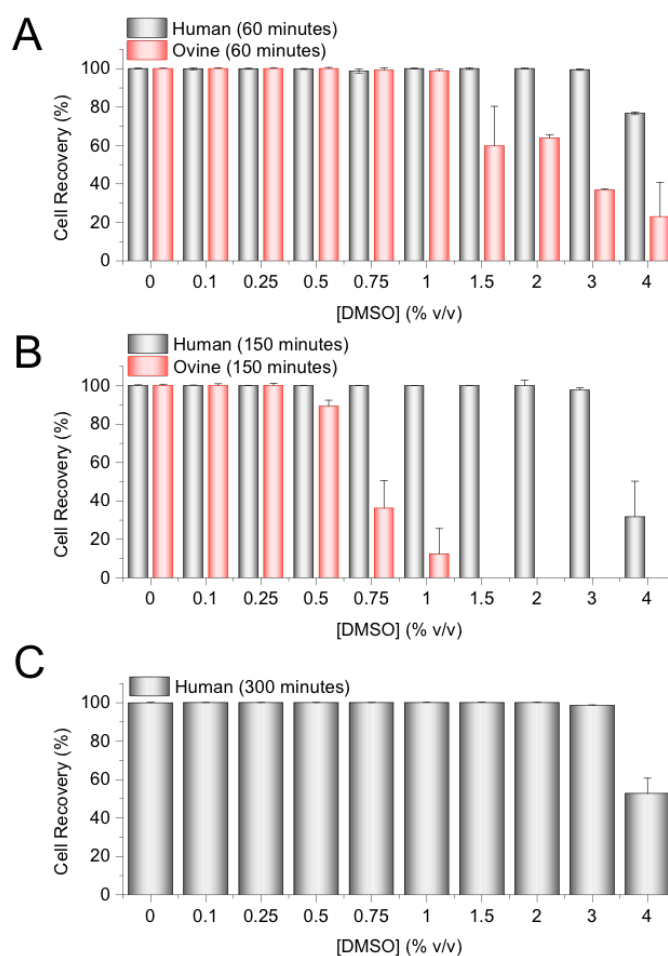


Figure 3.3. Cytotoxicity of the cryoprotectant DMSO to human and ovine RBCs. (%) Cell recovery of cells (human (200 μ L) and ovine (1mL)) incubated with varying concentrations of DMSO for 60 minutes (A), 150 minutes (B) and 300 minutes (human only) (C) at 23 °C. Each data point was measured (mean) in quintuplicate with the error bars representing \pm standard deviation.

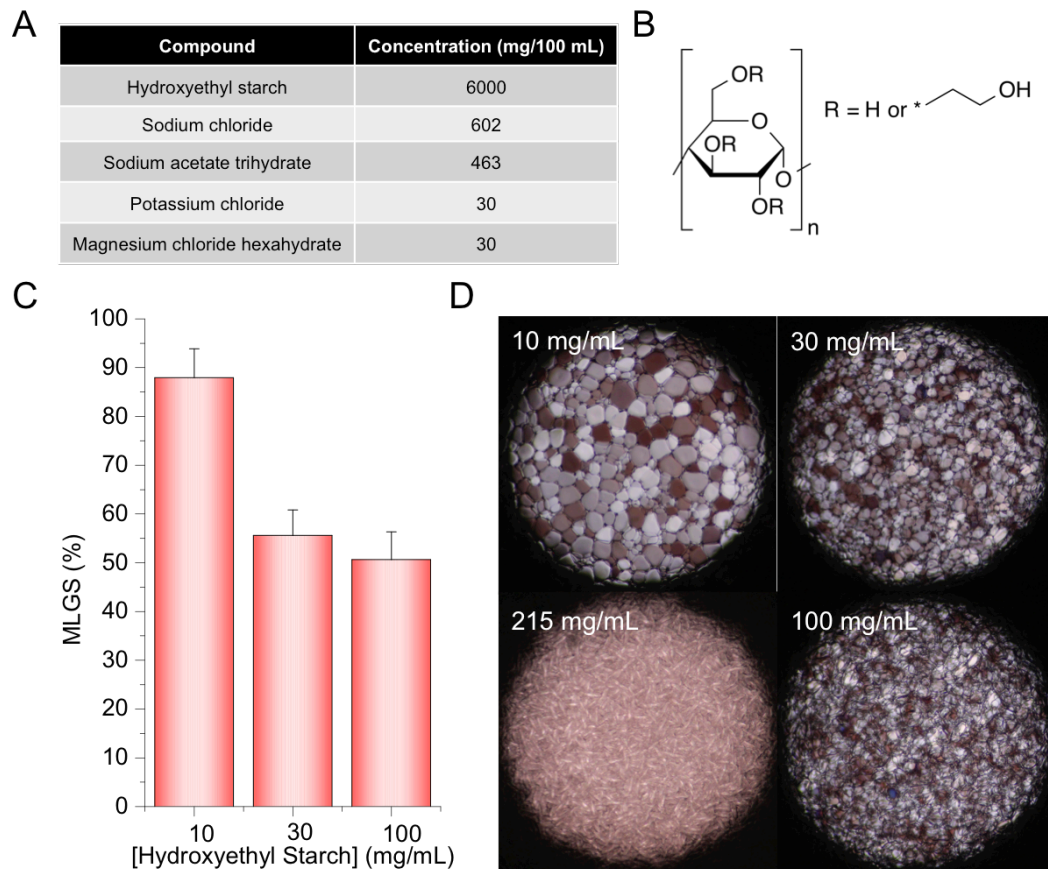


Figure 3.4. Ice recrystallization inhibition activity and composition of HES.

A) Composition of Volulyte[®] solution. B) Structure of HES derived from Volulyte[®].

C) Quantitative assessment of IRI activity of HES, relative to PBS solution alone.

D) Cryomicroscopic images showing influence of HES on ice crystal growth, following 30 minutes at -6°C , highlighting at high concentrations the inhibition of ice crystal formation from top left clockwise 10 mg/mL, 30 mg/mL, 100 mg/mL and 215 mg/mL HES. Data presented as (N=3) % mean largest grain size relative to PBS. Error bars represent \pm SD.

3.3.3. Cryopreservation of Ovine RBCs with HES.

To reiterate literature statements and to form a basis upon which improvements in cell recovery could be established, HES was utilized in its capacity as a cryoprotectant of RBCs.^{54,55} Several studies have examined the use of HES

(albeit with different HES preparations) in the cryopreservation of human and canine RBCs at concentrations ranging from 2.5 wt% to 22.5 wt% with notable success even with large volumes of clinical relevance (470 mL).^{47,48,56} Furthermore it has been demonstrated in a small clinical trial that HES cryopreserved human RBCs can be successfully transfused autologously.⁴⁶ Small (100 μ L) suspensions of RBCs diluted two-fold with HES at final concentrations between 46 mg/mL – 215 mg/mL (4.4 wt% - 17.7 wt%) were frozen rapidly ($N_{2(l)}$ (-196 °C) for 180 seconds) from 23 °C. The use of a high freezing rate promoted the rapid nucleation of many small yet tolerable extracellular ice crystals, which were uninfluenced by the presence of HES (i.e. not vitrified). RBCs were then thawed rapidly (45 °C water, 600 seconds) limiting ice recrystallization and cryodamage. Cell recovery was measured against untreated RBCs (100 % cell recovery) and RBCs frozen without HES in (inciting osmotic shock) $H_2O_{(l)}$ (0 % cell recovery). A concentration dependant relationship was observed with ovine cell recovery highest (51.4 % \pm 13.2 %) at 215 mg/mL decreasing with concentration to effectively no recovery at 46 mg/mL (1.8 % \pm 5.1 %) the lowest concentration examined (Figure 3.5.A). The cryopreservation of human RBCs was performed using an identical cryopreservation strategy albeit with a different range of HES concentrations ranging from 70 – 215 mg/mL (6.5 wt % - 17.7 wt%) and larger volumes (200 μ L). A similar concentration dependency is observed but the maximal level of cell recovery is even higher than with ovine RBCs when using 215 mg/mL HES (81.8 % \pm 5.7 %) (Figure 3.5.B). Microscopy studies of the ultrastructure of human RBCs from literature suggests the absence of intracellular ice with cryopreservation again more effective at higher concentrations (14 wt%).⁵⁷ However for the prolonged storage (5 days) of human RBCs using HES (12 wt%) a strong and significant factor determining cell recovery was storage temperature with the lowest storage temperature of -16 °C inciting a near complete loss of cell recovery after 120

hours where as with storage at $-75\text{ }^{\circ}\text{C}$ cell recovery was approximately 80%, which is only slightly lower than the short term recoveries (85%) observed under similar conditions. Intermediate storage temperatures were shown to have cell recoveries between these values.⁵⁸ The effect of storage temperature on cell recovery provides further evidence that HES does not limit ice crystal growth and prevent the associated damage it causes. Demonstrating that HES does not limit ice crystal growth is key as there is a continual importance in reducing cryopreservation storage temperatures. Reducing storage temperature is important, as the demand for and volumes of clinically relevant blood products is significantly higher than other biological materials especially in environments with logistical difficulties. The scale of which can be emphasized by the transfusion of over 140,000 units of fresh RBCs in both Afghanistan and Iraq between November 2001 and December 2010 by the US military necessitating twice weekly flights of fresh blood products sourced and collected from the continental US.²³ Currently only the Netherlands Armed Forces routinely cryopreserves RBCs and other blood products in such scenarios but using glycerol and DMSO (platelets) as opposed to HES.²⁴ The recent withdrawal of HES⁵⁹ as a plasma expander and controversy⁶⁰ regarding several studies investigating the safety of HES means it is unlikely to be developed further as a clinically utilized cryoprotectant in the near future, thus alternatives that reduce or eliminate the dependency of organic solvents remains a difficult task but would yield far spread benefits.

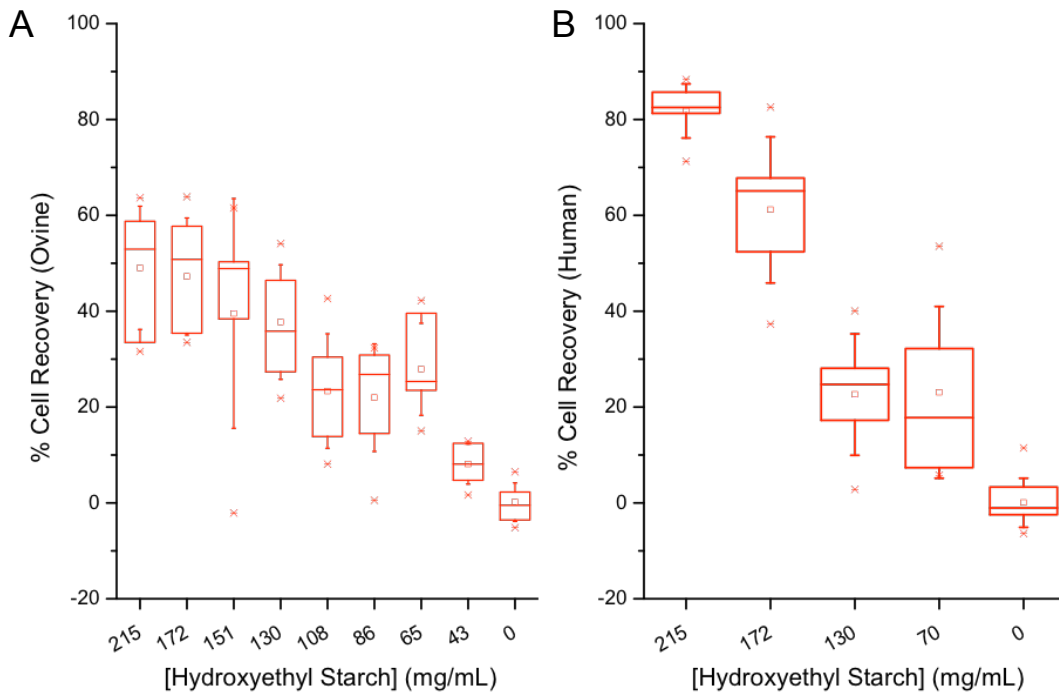


Figure 3.5. Cryopreservation of RBCs using HES. (A) (%) Cell recovery of ovine RBCs (100 μ L) supplemented with various concentrations (46 – 215 mg/mL) of HES. (B) (%) Cell recovery of human RBCs (200 μ L) supplemented with various concentrations (70 mg/mL – 215 mg/mL) of HES. Cells were frozen ($-196\text{ }^{\circ}\text{C N}_{2(l)}$, 180 seconds) and thawed rapidly ($45\text{ }^{\circ}\text{C}$ water, 600 seconds). Each data point was measured (mean) in quintuplicate with the (whiskers) error bars representing \pm standard deviation and the upper and lower box limits the upper and lower quartiles.

As aforementioned a rapid thawing strategy was used in order to minimize the damage arising from ice recrystallization. However cryodamage derived from ice recrystallization can be illustrated by cryopreserving ovine RBCs in the presence of 215 mg/mL and 130 mg/mL HES and thawing at various rates including those that encourage ice recrystallization. During this process a rapid (but different) freezing rate ($\text{IPA}_{(l)}/\text{CO}_{2(s)}$ ($-78\text{ }^{\circ}\text{C}$)) was again utilized in order attenuate ice crystal growth during freezing enabling rapid nucleation and the presence of only small but tolerable extracellular ice crystals, thus minimizing damage during

freezing and focusing principally on damage arising during thawing. The relationship of ice crystal size and freezing rate has been previously discussed and illustrated in Figure 2.21. The highest thawing rate (45 °C water) yielded substantially higher levels of cell recovery (77.6 % ± 6.2 % and 42.8 % ± 9.5 % at 215 mg/mL and 130 mg/mL respectively) than either of the significantly slower (23 °C air and 4 °C air) thawing rates that promote ice recrystallization⁶¹ as seen in Figure 3.6. Thawing at a modest 23 °C elicited significant ice recrystallization derived cryodamage, depressing cell recovery nearly 4-fold in a 130 mg/mL HES solution from 42.8 % ± 9.5 % to 11.7 % ± 10.1 %. Thawing cells at an even slower rate (4 °C) did not further alter cell recovery significantly (16.2 % ± 8.6 %) highlighting that extensive ice recrystallization damage can arise from even moderate thawing rates. At the higher concentration tested (215 mg/mL HES) the damaging effect of slow thawing was still significant with comparable losses equating to approximately 30 % of the total cell population due to ice recrystallization. It is worth highlighting (as previously noted) that greater volumes (1 unit = 470 mL) more relevant to clinical scenarios^{62,63} would have a larger extent of heterogeneous thawing and thus may be expected to be even more susceptible to ice recrystallization derived cryodamage. Limiting the impact of ice recrystallisation is especially important when samples are thawed incorrectly or in environments where rapid controlled thawing is not easily available.

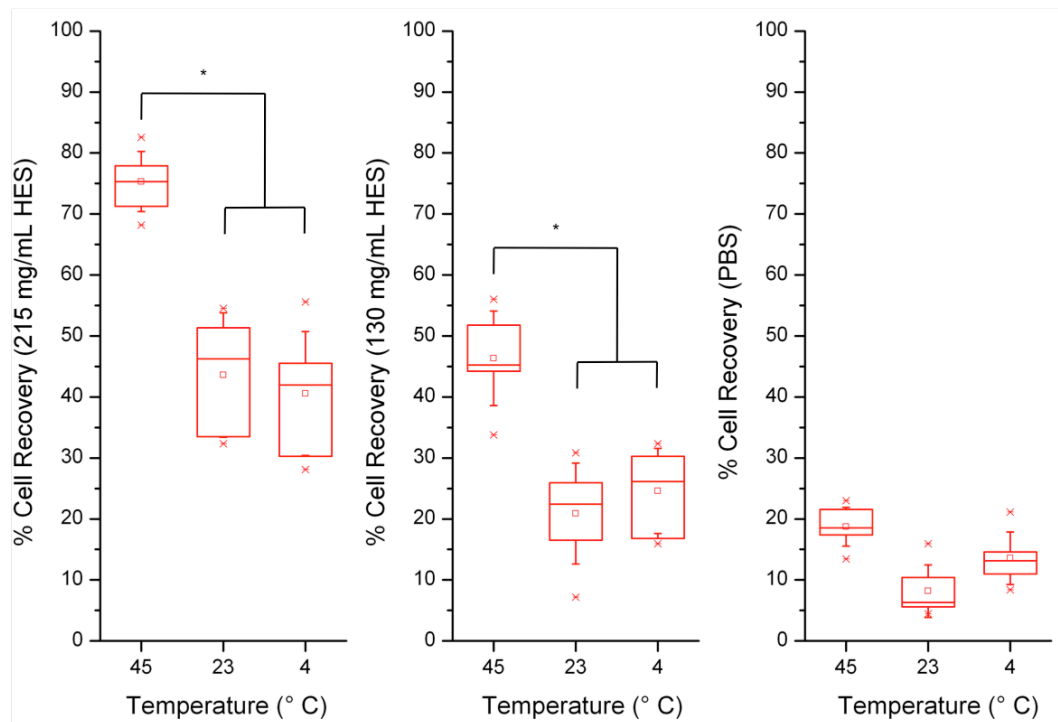


Figure 3.6. Impact of thawing temperature (°C) on ovine RBC cryopreservation. (%) Cell recovery of ovine RBCs (100 μ L) supplemented with either 0, 130 or 215 mg/mL HES in PBS after cryopreservation (-78 °C CO_{2(s)}/IPA_(l), 60 seconds/ -78 °C CO_{2(s)}, 20 minutes) with an either a rapid (45 °C water, 600 seconds), slow (23 °C air, 45 minutes) or very slow (4 °C air, 150 minutes) thawing rate. Each data point was measured (mean) in quintuplicate with the (whiskers) error bars representing \pm standard deviation and the upper and lower box limits the upper and lower quartiles. Statistical difference (*) ($p < 0.05$) as determined by the Students t-test.

3.3.4. Cryopreservation of Ovine RBCs with HES supplemented with PVA.

Cryodamage from ice recrystallization significantly reduces the recovery of ovine RBCs (Figure 3.6). Therefore the addition of IRI active compounds attenuating ice recrystallization *in vitro* may improve cell recovery during cryopreservation by eliminating or dampening this mechanism of cryodamage. However as previously

reported with the use of recombinant AFPs I, II and III and a synthetic AF(G)P mimic in conjunction with HES in the cryopreservation of human RBCs a balance must be sort between IRI and DIS.⁶⁴⁻⁶⁶ DIS can greatly increase mechanical damage outweighing the benefits that IRI provides. Further work using site-directed mutagenesis⁶⁷ to influence the IRI and DIS activity of a recombinant (*Macrozoarces americanus*) AFP III appeared to agree with this hypothesis.⁶⁵

To examine the effect of PVA addition, RBCs were cryopreserved with 130 mg/mL HES. 130 mg/mL HES had the most significant fold reduction in cell recovery due to ice recrystallization and thus was examined with and without a comparatively low concentration (10 mg/mL) of 9 kDa PVA. 10 mg/mL 9 kDa PVA has a very strong IRI activity (Figure 2.14.) suppressing ice recrystallization (Chapter 2). Furthermore 9 kDa PVA is not cytotoxic with ovine RBCs stored with 15 mg/mL 9 kDa PVA at 4 °C for 6 days eliciting a haemolytic value of 2.3 % ± 1.6 % which is not significantly different to ovine RBCs stored under the same conditions for a comparable length of time (7 days and a haemolytic value of 3.4 % ± 0.7 %) in the absence of 9 kDa PVA (Figure 3.7.). No notably elevated levels of haemolysis are detected with the addition of 15 mg/mL 9 kDa PVA to human RBCs either over a comparable time frame but it must be noted that the storage of human RBCs (as with ovine RBCs (Figure 3.1.)) in simple isotonic solutions tends to a greater rate of haemolysis. Furthermore 9 kDa PVA (membrane impermeable) functions purely as an extracellular CPA meaning its removal would be inline with HES if indeed at all necessary⁶⁸ and therefore far more trivial than glycerol and other intracellular CPAs.⁶⁹

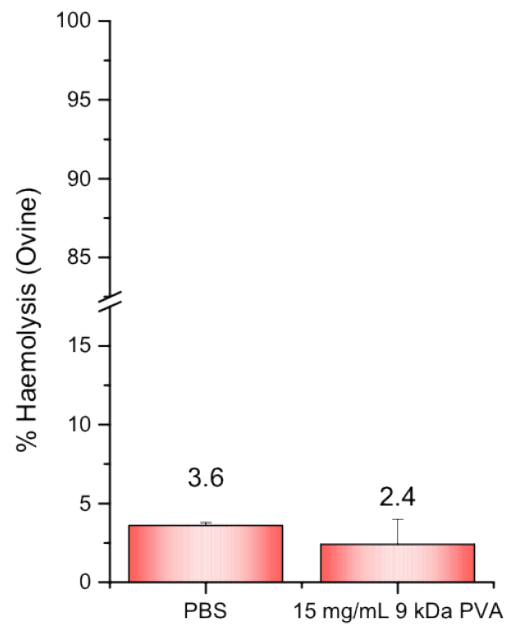


Figure 3.7. Cytotoxicity of 15 mg/mL 9 kDa PVA to ovine RBCs. Cytotoxicity of 15 mg/mL 9 kDa PVA to ovine RBCs after 6 days in a simple isotonic solution stored at 4 °C. Each data point was measured (mean) in triplicate with the error bars representing \pm standard deviation.

The addition of 10 mg/mL 9 kDa PVA did improve cell recovery when ovine RBCs were cryopreserved with 130 mg/mL HES but perhaps even more remarkably is that the presence of 9 kDa PVA alone in the absence of HES elicited a comparable amount of cell recovery as illustrated in Figure 3.8. Nevertheless the overall level of cell recovery is reasonably low (19.9 % \pm 6.1 %) and not to clinical standards the comparatively small amounts of 9 kDa PVA needed to attain this effect compared to traditional CPAs does create much intrigue and promise. Further refinements in terms of PVA concentration, haematocrit and the freezing and thawing strategy in addition to changes in MW and hydrolysis could allow additional improvements. The investigation of branched and star polymer derivatives and PVA (block) copolymers may also yield even more potent IRI compounds. Further development could emphasize

the importance of PVA as a supplement to traditional cryoprotectants and with the possibility of substituting significant amounts of intracellular CPAs for small quantities of PVA. However under these conditions the presence of both 130 mg/mL HES and 10 mg/mL 9 kDa PVA does not lead to a cumulative level of cell recovery (14.7 % \pm 10.5 %) indicative of non-complimentary mechanisms.

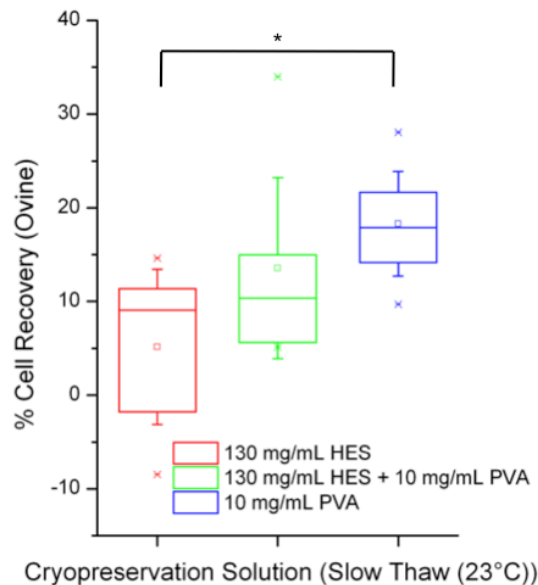


Figure 3.8. Cryopreservation of ovine RBCs supplemented with 130 mg/mL HES and/or 10 mg/mL 9 kDa PVA. Rapid (-78 °C CO_{2(s)}/IPA_(l), 60 seconds/ -78 °C CO_{2(s)}, 20 minutes) freezing with a slow (23 °C air, 45 minutes) thawing rate. Each data point was measured (mean) in quintuplicate with the (whiskers) error bars representing \pm standard deviation and the upper and lower box limits the upper and lower quartiles. Statistical difference (*) ($p < 0.01$) as determined by the Students t-test.

The previous work of Carpenter *et al* that as aforementioned used AFP I in conjunction with HES highlighted that high concentrations of AFP I (1.54 mg/mL) actually decreased cell recovery and that a moderate concentration of AFP I that still retained significant IRI activity had the greatest benefit.⁶⁴ Therefore it was

hypothesized that reducing the concentration of 9 kDa PVA whilst lowering IRI marginally but still retaining significant activity may have a similar effect and thus the optimal concentration of 9 kDa PVA may actually be lower than 10 mg/mL. Reducing 9 kDa PVA concentration has the obvious benefit of requiring even less cryoprotectant. This rationale is further strengthened by previous observations that have suggested that PVA can incite DIS in a concentration dependant manner.^{70,71} DIS has been attributed to the reduction in cryoprotection by promoting an increase in mechanical damage offsetting the benefits attained from IRI.^{64,72} This property has even been exploited by using AFP I (*Pseudopleuronectes americanus*) as a cryoadjuvant (4 mg/mL) in cryosurgery, significantly increasing ablation in subcutaneous tumors but only after a double freeze treatment.⁷³ Therefore ranges of 9 kDa PVA concentrations from 0.5 mg/mL to 10 mg/mL were investigated as illustrated in Figure 3.9. Concentrations greater than 10 mg/mL were not considered as at concentrations higher than this difficulties in solubility without heating beyond 37 °C would be encountered without an appreciable increase in IRI activity, highlighting the importance of other physiochemical properties in developing novel IRI active compounds.⁶¹ A similar rationale was responsible for choosing 9 kDa PVA as opposed to 31 kDa PVA or 85 kDa PVA, which are other commercially available preparations of comparable cost. It must be noted that decreasing the MW of PVA does have a consequential effect on IRI but that this effect is only significant with PVA at a MW lower than 6.5 kDa. The extent of PVA hydrolysis is also important as acetylation greater than 20 % also results in a reduction in IRI activity.⁷⁴ Reducing the concentration of 9 kDa PVA did result in improved cell recoveries as illustrated in Figure 3.9. 1 mg/mL 9 kDa PVA conferred the greatest cell recovery (40.2 % ± 5.1 %) under the same conditions examined with a progressive reduction in cell recovery at concentrations higher than this. At 0.5 mg/mL 9 kDa PVA whereby a significant reduction in IRI activity begins (Figure

2.17.) cell recovery begins to decrease (36.7 % ± 11.6 %). Furthermore RBCs cryopreserved with 8 kDa PEG (non-IRI active (Figure 2.14.)) had minimal cryoprotective effect at comparable concentrations furthering strengthening that the IRI activity of 9 kDa PVA contributes to improved cryoprotection and enhanced cell recovery.

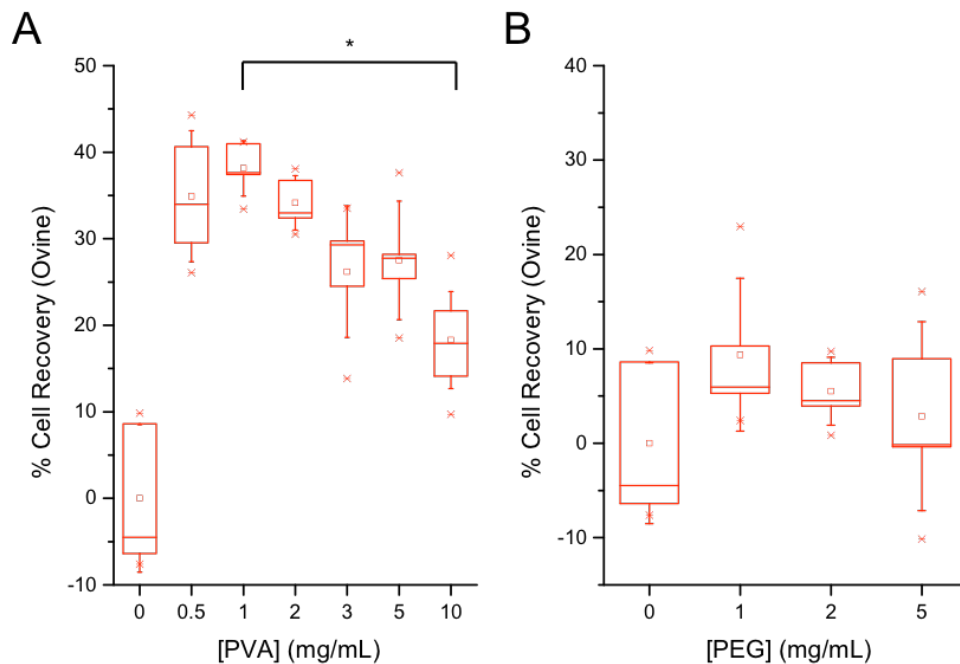


Figure 3.9. Cryopreservation of ovine RBCs with either 9 kDa PVA or 8 kDa PEG. (%) Cell recovery of ovine (1 mL) supplemented with either (A) 9 kDa PVA (0.5 – 10 mg/mL) or 8 kDa PEG (1 – 5 mg/mL) after cryopreservation (-78 °C CO_{2(s)}/IPA, 60 seconds/ -78 °C CO_{2(s)}, 20 minutes) with a slow (23 °C air, 30 minutes) thawing rate. Each data point was measured (mean) in quintuplicate with the (whiskers) error bars representing ± standard deviation and the upper and lower box limits the upper and lower quartiles. Statistical difference (*) (p < 0.01) as determined by the Students t-test.

3.3.5. Cryopreservation of Human RBCs with HES supplemented with PVA.

Though ovine RBCs provide an easily accessible and affordable model for human RBCs, notable differences are present in the RBCs of these two species.³⁵ Differences between species are as aforementioned include membrane permeability and cell size, which for instance affect the toxicity of glycerol and DMSO (Figure 3.2. and Figure 3.3.). Fundamentally though such difference are not apparent with the extracellular CPAs HES or PVA that have no detrimental effect under similar conditions. Therefore it was critical to assess whether or not similar supplementation of 9 kDa PVA could attain improvements in the recovery of human RBCs. It has already been demonstrated that the cryopreservation of human RBCs using HES is dependant upon HES concentration (Figure 3.5.B). The similar susceptibility of human RBCs to ice recrystallization damage during slow thawing is also apparent (Figure 3.10.). The addition of 1 mg/mL 9 kDa PVA to 215 mg/mL HES did result critically, in an elevated level of cell recovery ($60.2 \% \pm 14.9 \%$) compared to 215 mg/mL HES alone ($26.0 \% \pm 12.5 \%$), though the improvement was still below the cell recovery attained when cells were thawed rapidly minimizing IR ($81.8 \% \pm 5.7 \%$) as demonstrated in Figure 3.11. The use of both HES and 9 kDa PVA represents a remarkable level of recovery and closely reflects the results of others with a similar haematocrit and HES concentration but with the substitution of AFPs or a synthetic AF(G)P mimic for 9 kDa PVA.⁶⁴⁻⁶⁶ AFPs as already noted are hard to isolate or produce recombinantly on a large scale and synthetic AF(G)P mimics have only been produced in small quantities where as PVA is routinely synthesised on a tonne scale, with a proven biodegradability and biocompatibility as a foodstuff.^{75,76} PVA therefore has great potential as an extracellular CPA with

possible application to a wide variety of biological materials and is explored in this context in the following chapters (Chapter 4 and 5).

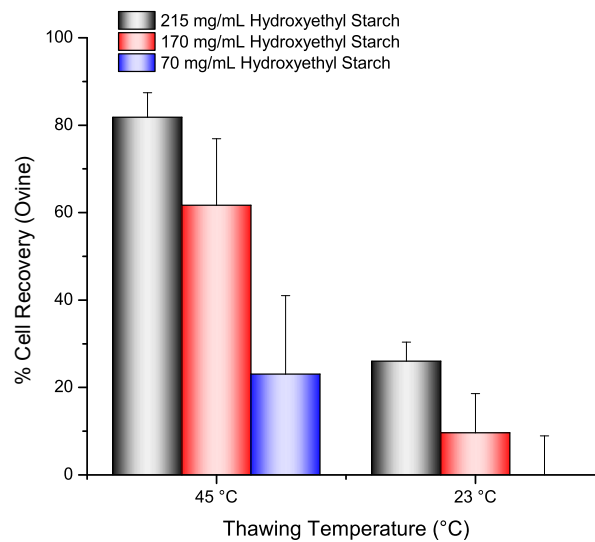


Figure 3.10. Impact of thawing temperature (°C) on human RBC cryopreservation. (%) Cell recovery of human RBCs (200 μ L) supplemented with either 70 mg/mL, 170 mg/mL or 215 mg/mL HES after cryopreservation (-196 °C $N_{2(l)}$, 180 seconds) with an either a rapid (45 °C water, 600 seconds) or slow (23 °C air, 45 minutes) thawing rate. Each data point was measured (mean) in quintuplicate with the error bars representing \pm standard deviation.

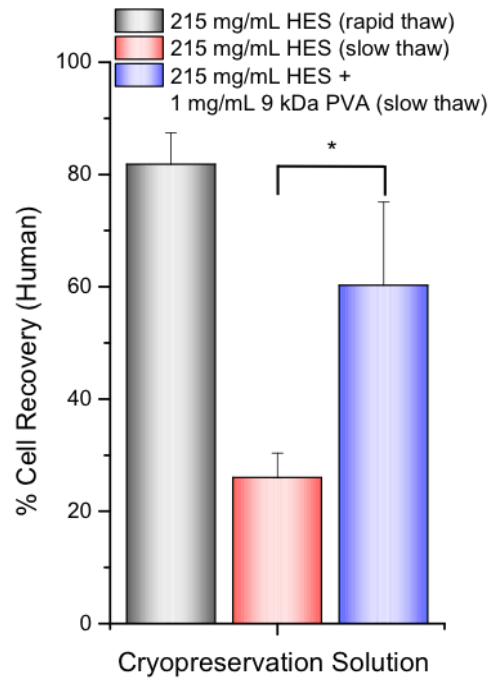


Figure 3.11. Cryopreservation of human RBCs supplemented with 215 mg/mL HES and/or 1 mg/mL 9 kDa PVA. (%) Cell recovery of human RBCs (200 μ L) supplemented with 215 mg/mL HES with or without 1 mg/mL 9 kDa PVA after cryopreservation (freeze (N_{2l}) / 180 seconds)) with either a rapid (45 $^{\circ}$ C, water bath / 600 seconds) or slow (23 $^{\circ}$ C, air / 900 seconds) thawing rate. Each data point was measured (mean) in quintuplicate with the error bars representing \pm standard deviation. Statistical difference (*) ($p < 0.01$) as determined by the Students t-test.

3.4. CONCLUSIONS.

9 kDa PVA has been successfully demonstrated to have no significant cytotoxicity at concentrations that have a proven IRI activity (Chapter 2) to ovine and human RBCs. Conversely both the organic solvents DMSO and glycerol which are popular cryoprotectants (with a range of biological materials) showed substantial cytotoxicity at concentrations far lower than that necessary for reported cryoprotection when added and mixed directly. The polysaccharide HES that has a demonstrable cryoprotective effect showed no cytotoxicity but has been shown to possess substantial clinical side effects *in vivo* in its primary role as a plasma expander, which has resulted in its withdrawal in the EU and USA signifying the need for novel cryoprotectants. The impact of slow thawing was also confirmed to be highly detrimental even at moderate thawing rates to both ovine and human RBCs emphasizing the impact of ice recrystallization derived cryodamage. 9 kDa PVA alone was able to cryopreserve a significant proportion of ovine RBCs subjected to slow thawing with an optimum concentration of 1 mg/mL. Concentrations higher than this resulted in reduced cell recoveries that were attributed to a potential DIS activity of 9 kDa PVA mirroring findings in literature that use AFPs. Furthermore HES (215 mg/mL) supplemented with 9 kDa PVA (1 mg/mL) was able to substantially improve the cell recovery of human RBCs subjected to a harmful slow thawing rate. These results prove the ability of small concentrations of the extracellular polymer 9 kDa PVA to attenuate ice crystal growth promoted by the use of slow thawing *in vitro* and limit this mechanism of cryodamage to enhance overall cell recovery.

3.5. MATERIALS AND METHODS.

3.5.1. Purification of HES, PVA and PEG.

HES, 9 kDa PVA and 8 kDa PEG were prepared using the methodology listed in Section 2.5.2.

3.5.2. Preparation of Ovine RBCs.

A suitably sized aliquot of (haematocrit 32 % - 52 %) ovine (*Ovis aries*) RBCs (defibrinated) as supplied (TCS Biosciences Ltd, Oxfordshire, UK) and shipped overnight was centrifuged (23 °C, 10 minutes, 1950 x g) and the top layer (containing any residual plasma with all its constituents) removed. The top layer was immediately replaced with an equivalent volume of PBS. Ovine RBCs were then used immediately or stored at 4 °C for a maximum of 1 week (haemolysis 3.7 % ± 0.7 %). Immediately prior to use ovine RBCs were mixed by inversion to ensure a homogenous suspension of cells.

3.5.3. Preparation of Human RBCs.

Human RBCs were sourced from healthy male volunteers with informed consent on demand and collected in polypropylene 6mL EDTA vacutainers[®] (BD Ltd, Oxford, UK) to prevent coagulation. Aliquots were then centrifuged (23 °C, 10 minutes, 1950 x g) and the top layer containing plasma and other constituents removed and replaced with an equivalent volume of PBS. Human RBCs were then used immediately or stored at 4 °C for a maximum of 3 days on a SRT2 roller mixer (Bibby Scientific Limited, Stone, UK) to ensure a homogenous suspension of cells.

3.5.4. Haemolysis measurement of Ovine RBCs stored at 4 °C and 23 °C.

Upon delivery 50 mL aliquots of ovine RBCs were prepared as described previously and stored statically at the appropriate temperature. For each data point 50 µL aliquots in triplicate were diluted in 50 µL PBS and vortexed rigorously. A 20 µL aliquot was then diluted in 200 µL PBS and vortexed meticulously before centrifugation (23 °C, 5 minutes, 1950 x g). 50 µL of supernatant was then transferred to 150 µL PBS in duplicate in a clear flat bottom 96-well polystyrene plate and absorbance measured at 450 nm using a Multiskan ascent plate reader (Thermo-scientific Ltd, Hampshire, UK). A background value of 200 µL PBS was recorded and subtracted to give a final absorbance value with the mean and standard deviation reported (Figure 3.1.). This generated data that enabled the calculation of both (%) cell recovery and (%) haemolysis. (Equations 3.1.A and 3.1.B.). The absorbance value attained on day 1 was taken as 0% haemolysis. A mean value for 100% haemolysis was calculated in parallel by preparing samples in triplicate with H₂O(l) instead of PBS to induce osmotic shock and therefore total haemolysis. Samples were taken at regular intervals over either a 35 or 42 day period to monitor the extent of haemolysis when stored unagitated at 4 °C and 23 °C.

$$\text{A } (\%) \text{ Haemolysis} = \frac{\left[\text{Abs}_{(450 \text{ nm})}(\text{Sample}) - \text{Abs}_{(450 \text{ nm})}(0\%) \right]}{\left[\text{Abs}_{(450 \text{ nm})}(100\%) - \text{Abs}_{(450 \text{ nm})}(0\%) \right]}$$

$$\text{B } (\%) \text{ Cell Recovery} = 100 \% - (\%) \text{ Haemolysis}$$

Equation 3.1. Equations used to calculate (A) (%) Haemolysis and (B) (%) Cell Recovery of ovine and human RBCs.

3.5.5. Measurement of Glycerol, DMSO, HES and PVA cytotoxicity in Ovine and Human RBCs.

Freshly prepared aliquots of ovine and human RBCs were diluted in quintuplicate in an equal volume of analyte prepared at an appropriate concentration in PBS to give a total volume ranging between 100 μL and 1000 μL (as indicated in the main text). Samples were then vortexed to ensure homogeneity and gently agitated (200 rpm) for 120 minutes (or longer where specified) at 23 $^{\circ}\text{C}$ with haemolysis measured as described previously. Samples that were deemed cytotoxic (10 % haemolysis or above) were repeated at a lower concentration over a shorter duration such that a range of concentrations and durations are reported to highlight any significant cytotoxicity.

3.5.6. Cryopreservation of Ovine and Human RBCs with HES.

Freshly prepared ovine and human RBCs were diluted in quintuplicate in an equal volume of HES in PBS to a desired final concentration ranging between 46 mg/mL – 215 mg/mL to a volume of 100 μL (ovine) or 200 μL (human) prior to vortexing. Samples were then rapidly cooled as desired either in $\text{N}_{2(l)}$ for 180 seconds prior to thawing or an $\text{IPA}_{(l)}/\text{CO}_{2(s)}$ slurry (-78 $^{\circ}\text{C}$) for 60 seconds and then $\text{CO}_{2(s)}$ for 20 minutes prior to thawing. Samples were either thawed at 45 $^{\circ}\text{C}$ (water), 23 $^{\circ}\text{C}$ (air) or 4 $^{\circ}\text{C}$ (air) as described in the main text before (%) cell recovery was measured as described previously and compared with (unprotected) treated (0 % cell recovery) and untreated (100 % cell recovery) H_2O and PBS controls respectively with the mean and standard deviation reported (Equation 3.1.).

3.5.7. Cryopreservation of Ovine and Human RBCs with HES and/or 9 kDa PVA.

Freshly prepared ovine and human RBCs were diluted in quintuplicate in an equal volume of HES and/or 9 kDa PVA in PBS to a desired final concentration (as indicated in Figure 3.8. and 3.11.) to a volume of 100 μL (ovine) or 200 μL (human) prior to vortexing. Samples were then rapidly cooled in an $\text{IPA}_{(l)}/\text{CO}_{2(s)}$ slurry ($-78\text{ }^{\circ}\text{C}$) for 60 seconds and then $\text{CO}_{2(s)}$ for 20 minutes (ovine and human) or in $\text{N}_{2(l)}$ ($-196\text{ }^{\circ}\text{C}$) for 180 seconds (human) prior to thawing at $45\text{ }^{\circ}\text{C}$ (water, 600 seconds), or $23\text{ }^{\circ}\text{C}$ (air, 45 minutes) to modulate either rapid and slow thawing. (%) Cell recovery was then calculated using aforementioned methodologies (Equation 3.1.).

3.5.8. Cryopreservation of Ovine RBCs with 9 kDa PVA or 8 kDa PEG.

Freshly prepared ovine RBCs were diluted in quintuplicate in an equal volume of 9 kDa PVA (ovine and human) or 8 kDa PEG (ovine) in PBS to a desired final concentration ranging between 0.5 mg/mL – 10 mg/mL (as indicated in Figure 3.9.) to a volume of 1 mL (ovine) or 200 μL (human) prior to vortexing. Samples were then rapidly cooled in an $\text{IPA}_{(l)}/\text{CO}_{2(s)}$ slurry ($-78\text{ }^{\circ}\text{C}$) for 60 seconds and then $\text{CO}_{2(s)}$ for 20 minutes prior to thawing at $23\text{ }^{\circ}\text{C}$ (air / 45 minutes). (%) Cell recovery was then calculated using aforementioned methodologies (Equation 3.1.).

3.6. REFERENCES.

1. Scott, K. L., Lecak, J. & Acker, J. P. Biopreservation of red blood cells: past, present, and future. *Transfus Medicine Rev* **19**, 127–142 (2005).
2. Heaton, A. *et al.* Use of Adsol[®] preservation solution for prolonged storage of low viscosity AS-1 red blood cells. *Brit J Haematol* **57**, 467–478 (1984).
3. Rock, G., Poon, A., Haddad, S., Romans, R. & St Louis, P. Nutricel as an additive solution for neonatal transfusion. *Transfus Sci* **20**, 29–36 (1999).
4. Valeri, C., Pivacek, L., Cassidy, G. & Ragno, G. The survival, function, and hemolysis of human RBCs stored at 4° C in additive solution (AS-1, AS-3, or AS-5) for 42 days and then biochemically modified, frozen, thawed, washed and stored at 4° C in sodium chloride and glucose solution for 24 hours. *Transfusion* **40**, 1341–1345 (2000).
5. Meyer, E. K., Dumont, D. F., Baker, S. & Dumont, L. J. Rejuvenation capacity of red blood cells in additive solutions over long-term storage. *Transfusion* **51**, 1574–1579 (2011).
6. Högman, C. F. & Meryman, H. T. Storage parameters affecting red blood cell survival and function after transfusion. *Transfus Med Rev* **13**, 275–296 (1999).
7. Blood Facts and Statistics | American Red Cross. [redcrossblood.org at <http://www.redcrossblood.org/learn-about-blood/blood-facts-and-statistics>](http://www.redcrossblood.org/learn-about-blood/blood-facts-and-statistics)
8. Perrotta, P. L. & Snyder, E. L. Non-infectious complications of transfusion therapy. *Blood Rev* **15**, 69–83 (2001).
9. Brecher, M. E. & Hay, S. N. Bacterial Contamination of Blood Components. *Clin. Microbiol. Rev.* **18**, 195–204 (2005).
10. Mazur, P. Freezing of living cells: mechanisms and implications. *Am J Physiol* C125–C142 (1984).
11. Fowler, A. & Toner, M. Cryo-Injury and Biopreservation. *Ann NY Acad Sci* **1066**, 119–135 (2005).
12. Meryman, H. T. The Relationship between Dehydration and Freezing Injury in the Human Erythrocyte. *Cellular Injury and Resistance in Freezing Organisms* **2**, 231–244 (1967).
13. Lovelock, J. E. Het mechanism of the protective action of glycerol against haemolysis by freezing and thawing. *Biochimica et Biophysica Acta (BBA)* **11**, 28–36 (1953).
14. Pegg, D. E. & Diaper, M. P. On the mechanism of injury to slowly frozen erythrocytes. *Biophys J* **54**, 471–488 (1988).
15. Pegg, D. E. & Diaper, M. P. The effect of initial tonicity on freeze/thaw injury to human red cells suspended in solutions of sodium chloride. *Cryobiology* **28**, 18–35 (1991).
16. Pegg, D. E. The effect of cell concentration on the recovery of human erythrocytes

- after freezing and thawing in the presence of glycerol. *Cryobiology* **18**, 221–228 (1981).
17. Nei, T. Mechanism of freezing injury to erythrocytes: Effect of initial cell concentration on the post-thaw hemolysis. *Cryobiology* **18**, 229–237 (1981).
 18. Meryman, H. T. Cryopreservation of living cells: principles and practice. *Transfusion* **47**, 935–945 (2007).
 19. Muldrew, K. & McGann, L. E. Mechanisms of intracellular ice formation. *Biophys J* **57**, 525–532 (1990).
 20. Sputtek, A., Kuhn, P. & Rowe, A. W. Cryopreservation of Erythrocytes, Thrombocytes, and Lymphocytes. *Trans Med Hemother* **34**, 262–267 (2007).
 21. Valeri, C. R. & Runck, A. H. Long Term Frozen Storage of Human Red Blood Cells: Studies *in vivo* and *in Vitro* of Autologous Red Blood Cells Preserved up to Six Years with High Concentrations of Glycerol. *Transfusion* **9**, 5–14 (1969).
 22. Sputtek, A. Cryopreservation of red blood cells and platelets. *Methods Mol Biol* **368**, 283–301 (2007).
 23. Spinella, P. C. *et al.* Constant challenges and evolution of US military transfusion medicine and blood operations in combat. *Transfusion* **52**, 1146–1153 (2012).
 24. Lelkens, C. C. M., Koning, J. G., de Kort, B., Floot, I. B. G. & Noorman, F. Experiences with frozen blood products in the Netherlands military. *Transfus Apher Sci* **34**, 289–298 (2006).
 25. Rowe, A., Eyster, E. & Kellner, A. Liquid nitrogen preservation of red blood cells for transfusion. A low glycerol-Rapid freeze procedure. *Cryobiology* **5**, 119–128 (1968).
 26. Meryman, H. T. & Hornblower, M. A method for freezing and washing red blood cells using a high glycerol concentration. *Transfusion* **12**, 145–156 (1972).
 27. Lelkens, C., Noorman, F., Koning, J. & Lange, R. Stability after thawing of RBCs frozen with the high-and low-glycerol method. *Transfusion* **43**, 157–164 (2003).
 28. Meryman, H. T. Cryoprotective agents. *Cryobiology* **8**, 173–183 (1971).
 29. Mohandas, N. & Gallagher, P. G. Red cell membrane: past, present, and future. *Blood* **112**, 3939–3948 (2008).
 30. Gier, J., Deenen, L. L. M. & Senden, K. G. Glycerol permeability of erythrocytes. *Experientia* **22**, 20–21 (1966).
 31. Moore, T. J. Glycerol permeability of human fetal and adult erythrocytes and of a model membrane. *J Lipid Res* **9**, 642–646 (1968).
 32. Waugh, R. & Evans, E. A. Thermoelasticity of red blood cell membrane. *Biophys J* **26**, 115–131 (1979).
 33. Gershfeld, N. L. & Murayama, M. Thermal instability of red blood cell membrane bilayers: Temperature dependence of hemolysis. *J Membrane Biol* **101**, 67–72 (1988).
 34. Zou, C., Agar, N. & L, J. G. Haemolysis of human and sheep red blood cells in glycerol media: the effect of pH and the role of band 3. *Comp Biochem Physiol A*

- 127**, 347–353 (2000).
35. Wessels, J. & Veerkamp, J. H. Some aspects of the osmotic lysis of erythrocytes III. Comparison of glycerol permeability and lipid composition of red blood cell membranes from eight mammalian species. *Biochimica et Biophysica Acta (BBA)* **291**, 190–196 (1973).
 36. Huggins, C. E. Prevention of Hemolysis of Large Volumes of Red Blood Cells Slowly Frozen and Thawed in the Presence of Dimethylsulfoxide. *Transfusion* **3**, 483–493 (1963).
 37. Notman, R., Noro, M., O'Malley, B. & Jamshed, A. Molecular basis for dimethylsulfoxide (DMSO) action on lipid membranes. *J Am Chem Soc* **129**, 13982–13983 (2006).
 38. Lovelock, J. E. & Bishop, M. Prevention of Freezing Damage to Living Cells by Dimethyl Sulphoxide. *Nature* **183**, 1394–1395 (1959).
 39. Da Violante, G. *et al.* Evaluation of the Cytotoxicity Effect of Dimethyl Sulfoxide (DMSO) on Caco2/TC7 Colon Tumor Cell Cultures. *Biol Pharm Bull* **25**, 1600–1603 (2002).
 40. Sperling, S. & Larsen, I. G. Toxicity of Dimethylsulphoxide (DMSO) To Human Corneal Endothelium In Vitro. *Acta Ophthalmol* **57**, 891–898 (2009).
 41. Song, Y. C., Pegg, D. E. & Hunt, C. J. Cryopreservation of the Common Carotid Artery of the Rabbit: Optimization of Dimethyl Sulfoxide Concentration and Cooling Rate. *Cryobiology* **32**, 405–421 (1995).
 42. Penninckx, F., Cheng, N., Kerremans, R. & Van Damme, B. The Effects of Different Concentrations of Glycerol and Dimethylsulfoxide on the Metabolic Activities of Kidney Slices. *Cryobiology* **20**, 51–60 (1983).
 43. Davis, J. M., Rowley, S. D., Braine, H. G., Piantadosi, S. & Santos, G. W. Clinical toxicity of cryopreserved bone marrow graft infusion. *Blood* **75**, 781–786 (1990).
 44. Mancias-Guerra, C. *et al.* Dimethyl Sulfoxide-Induced Toxicity in Cord Blood Stem Cell Transplantation: Report of Three Cases and Review of the Literature. *Acta Haematol* **122**, 1–5 (2009).
 45. Nishihara, G., Sakemi, T., Ikeda, Y., Baba, N. & Shimamoto, Y. Multiple organ failure associated with dimethylsulfoxide and hydroxyethyl starch in autologous blood stem cell transplantation. *Nephron* **72**, 356–357 (1996).
 46. Horn, E. P. *et al.* Transfusion of autologous, hydroxyethyl starch-cryopreserved red blood cells. *Anesth Analg* **85**, 739–745 (1997).
 47. Kim, H. *et al.* A comparative study of the effects of glycerol and hydroxyethyl starch in canine red blood cell cryopreservation. *J Vet Med Sci* **66**, 1543–1547 (2004).
 48. Stolzing, A., Naaldijk, Y., Fedorova, V. & Sethe, S. Hydroxyethyl starch in cryopreservation - mechanisms, benefits and problems. *Transfus Apher Sci* **46**, 137–147 (2012).
 49. Boldt, J., Mayer, J., Brosch, C. & Lehmann, A. Volume replacement with a balanced hydroxyethyl starch (HES) preparation in cardiac surgery patients. *J*

- Cardiothor Vasc An* **24**, 399–407 (2010).
50. Treib, J., Baron, J., Grauer, M. & Strauss, R. G. An international view of hydroxyethyl starches. *Intens Care Med* **25**, 258–268 (1999).
 51. Mosbah, I. B. *et al.* Effects of polyethylene glycol and hydroxyethyl starch in University of Wisconsin preservation solution on human red blood cell aggregation and viscosity. *Transplant P* **38**, 1229–1235 (2006).
 52. Sun, W. Q., Wagner, C. T. & Connor, J. The Glass Transition Behaviors of Hydroxyethyl Starch Solutions. *Cell Preserv Technol* **2**, 55–65 (2004).
 53. Madjdpour, C. *et al.* Molecular weight of hydroxyethyl starch: is there an effect on blood coagulation and pharmacokinetics? *Brit J Anaesth* **94**, 569–576 (2005).
 54. Knorpp, C. T., Merchant, W. R., Gikas, P. W., Spencer, H. H. & Thompson, N. W. Hydroxyethyl starch: extracellular cryoprotective agent for erythrocytes. *Science* **157**, 1312–1313 (1967).
 55. Thomas, M. J. G., Parry, E. S., Nash, S. G. & Bell, S. H. A method for the cryopreservation of red blood cells using hydroxyethyl starch as a cryoprotectant. *Transfus Sci* **17**, 385–396 (1996).
 56. Lionetti, F. J. & Hunt, S. M. Cryopreservation of human red cells in liquid nitrogen with hydroxyethyl starch. *Cryobiology* **12**, 110–118 (1975).
 57. Allen, E. D. & Weatherbee, L. Ultrastructure of red cells frozen with hydroxyethyl starch. *J Microsc* **117**, 381–394 (1979).
 58. Spieles, G. *et al.* The effect of storage temperature on the stability of frozen erythrocytes. *Cryobiology* **32**, 366–378 (1995).
 59. Nolan, J. P. & Mythen, M. G. I. Hydroxyethyl starch: here today, gone tomorrow. *Brit J Anaesth* **111**, 321–324 (2013).
 60. Reinhart, K. & Takala, J. Hydroxyethyl starches: what do we still know? *Anesth Analg* **112**, 507–511 (2011).
 61. Gibson, M. I. Slowing the growth of ice with synthetic macromolecules: beyond antifreeze(glyco) proteins. *Polym Chem* **1**, 1141–1152 (2010).
 62. Brecher, M. E., Monk, T. & Goodnough, L. T. A standardized method for calculating blood loss. *Transfusion* **37**, 1070–1074 (1997).
 63. Karkouti, K. *et al.* The independent association of massive blood loss with mortality in cardiac surgery. *Transfusion* **44**, 1453–1462 (2004).
 64. Carpenter, J. F. & Hansen, T. N. Antifreeze protein modulates cell survival during cryopreservation: mediation through influence on ice crystal growth. *Proc Natl Acad Sci USA* **89**, 8953–8957 (1992).
 65. Chao, H., Davies, P. L. & Carpenter, J. F. Effects of antifreeze proteins on red blood cell survival during cryopreservation. *J Exp Biol* **199**, 2071–2076 (1996).
 66. Matsumoto, S. *et al.* Effects of synthetic antifreeze glycoprotein analogue on islet cell survival and function during cryopreservation. *Cryobiology* **52**, 90–98 (2006).
 67. Chao, H., Davies, P. L., Sykes, B. D. & Sönnichsen, F. D. Use of proline mutants to help solve the NMR solution structure of type III antifreeze protein. *Protein Sci* **2**, 1411–1428 (1993).

68. Sputtek, A., Horn, E. P., Schulte am Esch, J. & Kühnl, P. Cryopreservation of red blood cells using hydroxyethyl starch (HES) - From laboratory investigations to clinical application. *Anasth Intensiv Notf* **36**, S162–164 (2001).
69. Pallotta, V., D'Amici, G. M., D'Alessandro, A., Rossetti, R. & Zolla, L. Red blood cell processing for cryopreservation: from fresh blood to deglycerolization. *Blood Cells Mol Dis* **48**, 226–232 (2012).
70. Budke, C. & Koop, T. Ice recrystallization inhibition and molecular recognition of ice faces by poly(vinyl alcohol). *ChemPhysChem* **7**, 2601–2606 (2006).
71. Inada, T. & Lu, S.-S. Inhibition of recrystallization of ice grains by adsorption of poly (vinyl alcohol) onto ice surfaces. *Cryst Growth Des* **3**, 747–752 (2003).
72. Chaytor, J. L. *et al.* Inhibiting ice recrystallization and optimization of cell viability after cryopreservation. *Glycobiology* **22**, 123–133 (2012).
73. Muldrew, K. *et al.* Flounder antifreeze peptides increase the efficacy of cryosurgery. *Cryobiology* **42**, 182–189 (2001).
74. Congdon, T., Notman, R. & Gibson, M. I. Antifreeze (Glyco)protein Mimetic Behavior of Poly(vinyl alcohol): Detailed Structure Ice Recrystallization Inhibition Activity Study. *Biomacromolecules* **14**, 1578–1586 (2013).
75. DeMerlis, C. & Schoneker, D. Review of the oral toxicity of polyvinyl alcohol (PVA). *Food Chem Toxicol* **41**, 319–326 (2003).
76. Matsumura, S., Kurita, H. & Shimokobe, H. Anaerobic biodegradability of polyvinyl alcohol. *Biotechnol Lett* **15**, 749–754 (1993).

CHAPTER 4.

4. ICE RECRYSTALLIZATION INHIBITORS IMPROVE THE CRYOPRESERVATION OF IMMORTALIZED CELL LINES.

4.1. CHAPTER SUMMARY.

The application of poly(vinyl alcohol) (PVA) that has been previously identified (Chapter 2) as a potent ice recrystallization inhibition (IRI) active compound is explored as a cryoprotectant for immortalized mammalian cell lines namely A549, BeWo and FAO cells. Mammalian cell lines are frequently used as models for a multitude of diseases where primary material is scarcely available, as they can be grown quickly with reproducible and defined phenotypic characteristics and can also undergo extensive genetic manipulation. The supplementation of low concentrations (≤ 2 mg/mL) of 9 kDa PVA to high concentrations of DMSO (≥ 4 % (v/v)) aids the cryopreservation of each cell type. Each cell variety was examined under several experimental conditions and where tested were able to undergo complex modifications that invoke changes in gene expression amongst standard several measures of viability. Higher concentrations (10 mg/mL) of 9 kDa PVA in addition to 1 mg/mL 31 kDa PVA were detrimental to the cryopreservation process and cause a significant reduction in cell recovery compared to cryopreservation in the complete absence of any additives. This is due to their tendency to promote DIS at these concentrations despite not being

cytotoxic at concentrations far greater than this at physiological (37 °C) temperatures.

4.2. INTRODUCTION.

The importance of mammalian cell culture in research and development is highly significant, with attempts to culture mammalian tissue explants dating back one hundred years.^{1,2} However not until the routine availability of complex cell mediums was the establishment of a variety of (immortalized) mammalian cell lines possible.³ In the present day, the European collection of cell cultures (ECACC) for example contains over 40,000 cell lines from 45 species and 50 tissue types representative of 800 genetic disorders.⁴ Many cell lines have been developed as *in vitro* models for a multitude of diseases due to their reproducible genotypes and phenotypes, especially in the fields of oncology and neurobiology.⁵⁻⁷ Furthermore cell lines can be cultured to produce cells in vast quantities quickly and numerous techniques exist that enable extensive genetic manipulation.^{8,9} As a result of their versatility there is a sustained interest to use mammalian cell lines recombinantly to produce therapeutics that cannot be produced in simpler bacterial and yeast species due to their inability to perform complex posttranslational modifications.¹⁰⁻¹³ Additionally an extensive array of high throughput assays have been developed that measure the viability, proliferation and functionality of cultured cells by a range of analytical endpoints that investigate both apoptotic and necrotic cell death pathways.¹⁴⁻²⁰

The importance of cryopreservation can be accentuated by the high cost of continuous propagation, the likelihood of microbial and cross contamination in addition to genetic drift that occurs with ceaseless passaging causing non-representative phenotypic changes.^{21,22} Techniques and protocols to cryopreserve cultured mammalian cells have however remained relatively unchanged with a continued reliance on the organic solvent, DMSO. Compared to advances in their application, the overall yields of cells recovered post

cryopreservation tends to have had relatively little improvement. Though a great clinical need for red blood cells (Chapter 3) is immediately apparent their relative availability from source as well as their comparative robustness to physical stimuli and simplicity due to their non-nucleated nature separates them from mammalian cell cultures. Differences that can be highlighted fundamentally by the preference for DMSO (mammalian cell culture) as opposed to glycerol (RBCs) as the membrane CPAs of choice reflected somewhat by their distinctively different membrane compositions and permeabilities.²³ Mammalian cell lines contain nucleic material and thus undergo mitosis, which is a highly regulated and intricate process. The majority of mammalian cell lines are derived from oncogenic tissues, which by their very nature tend to arise from errors in cell division. As a consequence the majority of immortalized cell lines are aneuploid (containing an abnormal karyotype). For instance the popular HEK 293 cell line has an average of 64 chromosomes per cell including 4 copies of chromosomes 17 and 22 with the equally prevalent Caco-2 and MCF7 cell lines possessing chromosomal counts of 96 and 82 respectively and therefore their complexity is far greater than red blood cells.²⁴⁻²⁷ This complexity may be reflected in their sensitivity to cryopreservation treatments.

A vital principle to clarify is the differences between the two main mechanisms of cell death, necrosis and apoptosis. Necrosis can be defined as the physical destruction or loss of cell integrity due to extremes in the prevailing cell environment such as pH, temperature and osmotic pressure.²⁸ In contrast apoptosis is a controlled system of programmed cell death activated in senescent cells as a consequence of damage spontaneously accumulated from their native surroundings.^{29,30} The initiation of apoptosis is triggered biochemically by a variety of signaling cascades. Apoptosis can also be inadvertently activated by environmental stresses and the presence of other damaged or destroyed cells that perturb cellular homeostasis, which is of particular importance in

cryopreservation.^{31,32} However apoptotic pathways in mammalian cell lines have a propensity to be adversely effected due to their oncogenic nature. As a consequence of this and other previously aforementioned factors immortalized cell lines cannot substitute the use of primary cells entirely but have greater reproducibility and a wealth of literature to draw upon historically. Mammalian cell culture therefore remains a powerful investigative tool.

Few studies have investigated the use of cryopreservatives other than extracellular CPAs such as a DMSO with immortalised mammalian cells, fewer still with properties akin to AF(G)Ps and AFPs. A few exceptions include a study by Liu *et al.* who demonstrated the cytotoxicity of AF(G)P8 to HEK 293 (human) cells but AF(G)P8 was well tolerated by Rtgill-W1 (fish (non-mammalian)) and WRL-68 (human) cells.³³ Chaytor *et al.* later showed the impact of moderate IRI active monosaccharides and disaccharides on the cryopreservation of WRL-68 cells and were able to eliminate DMSO and attain comparable levels of cell recovery. However these protocols still necessitated high concentrations of cryoprotectant, though inherently impermeable these compounds can be readily internalised by a variety of transmembrane transporters.³⁴ Critically though the work of Leclère *et al.* showed the effect of two C-linked AF(G)P analogues, which had a more pronounced IRI activity were able to cryopreserve WRL-68 cells. As seen with the use of PVA with RBCs (Chapter 2) increasing the concentration of each analogue corresponded with a decrease in recovery. These results give promise that the attenuation of ice recrystallization with PVA may allow improvements in cell recovery but in a concentration dependant manner.^{35,36}

4.3. RESULTS AND DISCUSSION.

4.3.1. Cytotoxicity of DMSO to lung adenocarcinoma (A549) cells.

For the cryopreservation of mammalian cells the cryoprotective agent (CPA) of choice is DMSO but it is often required at concentrations as high as 10 % (v/v).³⁷ However it is well documented that high concentrations of DMSO can have adverse effects on cell integrity at physiological temperatures.^{38,39} Therefore it is important to assess the ability of DMSO to cause lysis at physiological (37 °C) temperatures. The reasoning being that when cells have been thawed and plated a notable amount of DMSO will persist especially if the cells cannot be centrifuged and washed prior. Only when sufficient time has allowed cells to adhere can the medium containing DMSO be removed and exchanged. As a consequence cells will be exposed to significant amounts of DMSO at physiological (37 °C) temperatures. A549 cells (Figure 4.1.A) are a frequently utilized cell line derived from a lung adenocarcinoma patient 40 years ago and often used as a model for type II alveolar epithelial cells and is a typical and representative cell line to investigate initially.^{40,41} Figure 4.1.B highlights the relative amounts of (confluent) A549 cells recovered after a 4 hour incubation with 0 % (v/v) – 20 % (v/v) DMSO quantified by the MTT (metabolism) and neutral red (NR) (compartmentalization) assays (Section 4.5.7 and Section 4.5.8). A strong correlation between DMSO (% (v/v)) concentration and recovery was attained. For example cell recoveries of 74.9 % ± 9.5 % (MTT) and 80.3 % ± 1.8 % (NR) were obtained with 5 % (v/v) DMSO which is a significant reduction in cell number over a relatively short time period. To further emphasize the impact of DMSO a low density of A549 cells were incubated over a 3 day period to assess the relative population of cells as a consequence of the supplementation

of DMSO between 0 % (v/v) – 6 % (v/v) DMSO (Figure 4.1.C). A low density of cells was used in order to ensure that within this time frame A549 cells did not attain a confluent state and were still undergoing exponential growth where possible. A substantial reduction in cell number was attained even at the low concentration of 2 % (v/v) DMSO with recoveries of 59.3 % \pm 2.1 % (MTT) and 77.2 % \pm 5.5 % (NR). The supplementation of PVA (IRI active) may aid cryopreservation and thus reduce the amount of DMSO necessary to attain significant cell recovery and could be highly beneficial with respect to cell recoveries and have additional benefits with sensitive downstream applications.^{42,43}

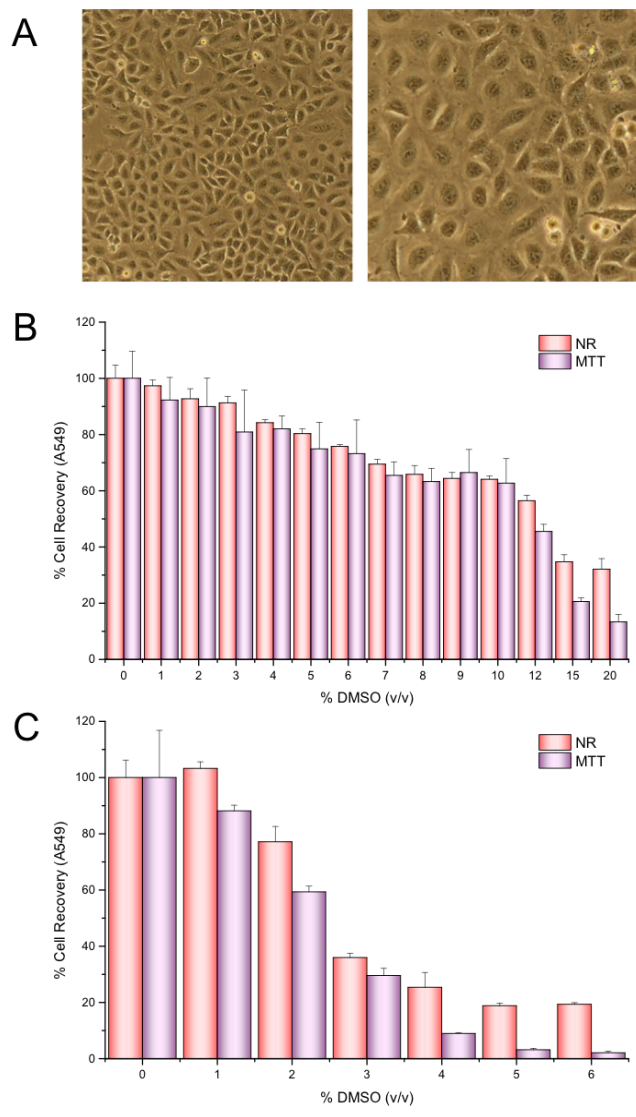


Figure 4.1. (%) Cell recovery of A549 cells exposed to various levels of DMSO at 37 °C. (A) Phase contrast micrographs demonstrating confluent A549 cells (40x magnification (left) and 100x magnification (right)). (B) Confluent cells incubated for 4 hours with various concentrations of DMSO in triplicate and (C) Seeded (low density) cells incubated in triplicate for 3 days (to allow proliferation) in the presence of various concentrations of DMSO. Each concentration was assessed by both the MTT and NR assays and referenced against untreated controls. Values represent the mean of 3 wells each measured in duplicate with the error bars representing \pm standard deviation.

4.3.2. Cryopreservation of lung adenocarcinoma (A549) cells.

Current protocols typically recommend 10 % (v/v) DMSO for mammalian cell culture cryopreservation.³⁷ A549 cells are however sold commercially as frozen aliquots containing 5 % (v/v) DMSO.⁴⁴ As a consequence defining the optimum concentration (% (v/v)) of DMSO for cryopreservation provides a starting point for optimization prior to the addition of IRI active additives. Testing the cryoprotective effects of DMSO also serves to define the upper and lower limits at which point DMSO ceases to give feasible cell recoveries and provide target areas whereby the addition of IRI active compounds may be of benefit.⁴⁵ Figure 4.2 shows the effect of A549 cells cryopreserved in an absence of medium as several studies have indicated a desire to remove or limit the presence of FBS^{46,47} with concentrations of DMSO up to 20 % (v/v) using a rapid freezing and slow thawing strategy (Section 4.5.5). A concentration of 4 % (v/v) DMSO was defined as the optimum concentration of DMSO for the (%) cell recovery of A549 cells (referred to as 100 %). The commonly cited concentration of 10 % (v/v) DMSO by contrast elicited lower cell recoveries of 65.1 % \pm 24.8 % (MTT) and 34.3 % \pm 21.8 % (NR) by comparison using these freezing and thawing parameters. DMSO is known to alter membrane plasticity and thus as a result perturb membrane integrity and therefore can cause cells to be more susceptible to lysis. This effect is especially apparent at physiologically relevant temperatures (Figure 4.1.).

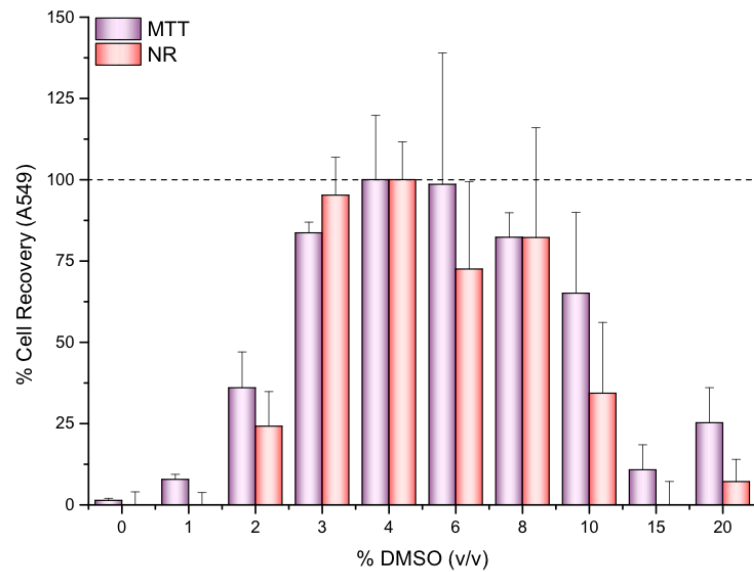


Figure 4.2. Cryopreservation of A549 cells with various concentrations of DMSO. (%) Cell recovery of A549 cells cryopreserved with various concentrations of DMSO in PBS measured by both MTT and NR assays and referenced against the most effective concentration (4 % (v/v) DMSO). Values represent the mean of 2 cryovials each plated in 2 wells and measured in duplicate with the error bars representing \pm standard deviation.

Concentrations of 2 % (v/v) DMSO and lower and 15 % (v/v) DMSO and higher gave unacceptably low levels of recovered cells thus necessitating the presence of at least 3 % (v/v) DMSO. In addition to the low levels of cells recovered the presence of non-viable cells or lysed but adherent cell debris may negatively affect proliferation and have detrimental effects on the remaining cell population in terms of the presence of apoptotic inducers and necrotic factors.⁴⁸ As a result of the findings presented (Figure 4.2) all ongoing cryopreservation studies with A549 cells were conducted with 4 % (v/v) DMSO supplemented with or without various concentrations of IRI active additives in PBS. The cryopreservation of A549 cells supplemented with between 0 mg/mL and 10 mg/mL 9 kDa PVA was

examined (Figure 4.3.A). Thawing cells rapidly (37 °C, water) and thus limiting ice recrystallization gave the highest recoveries whereas identical components and conditions with the exception of a slow thawing rate (23 °C, air) caused a reduction in cell number. A rapid thawing temperature of 37 °C is the temperature used in typical protocols and thus used here as opposed to 45 °C utilized in parts of chapter 2. A slow thawing rate emphasizes the impact of ice recrystallization in a similar manner to that illustrated with both ovine and human RBCs (Figure 3.6 and Figure 3.10). The addition of 1 mg/mL 9 kDa PVA however did appear to promote a greater level of cell recovery if only marginal in this scenario (113.8 % ± 16.0 % (MTT) and 106.7 % ± 21.0 % (NR)). Though even a marginal increase could be beneficial. Interestingly the addition of higher amounts of 9 kDa PVA that promotes a stronger IRI effect (Figure 2.17.) but at concentrations that are not cytotoxic (Figure 4.3.B) at physiologically relevant temperatures, results in a reduction in cell recovery. The extent of this reduction is concentration dependant with the addition of 10 mg/mL 9 kDa PVA proving to be exceptionally detrimental with cell recoveries of 44.1 % ± 3.3 % (MTT) and 22.2 % ± 0.8 % (NR). This effect was observed in a similar fashion with ovine RBCs (Figure 3.9.A) and in several publications with AFPs^{49,50} and a synthetic AF(G)P mimic.⁵¹ A reduction in cell recovery has been attributed to an increase in mechanical damage due to the onset of dynamic ice shaping (DIS), with PVA shown to induce DIS activity at high concentrations but concentrations that are far higher than those required for an IRI effect.⁵²

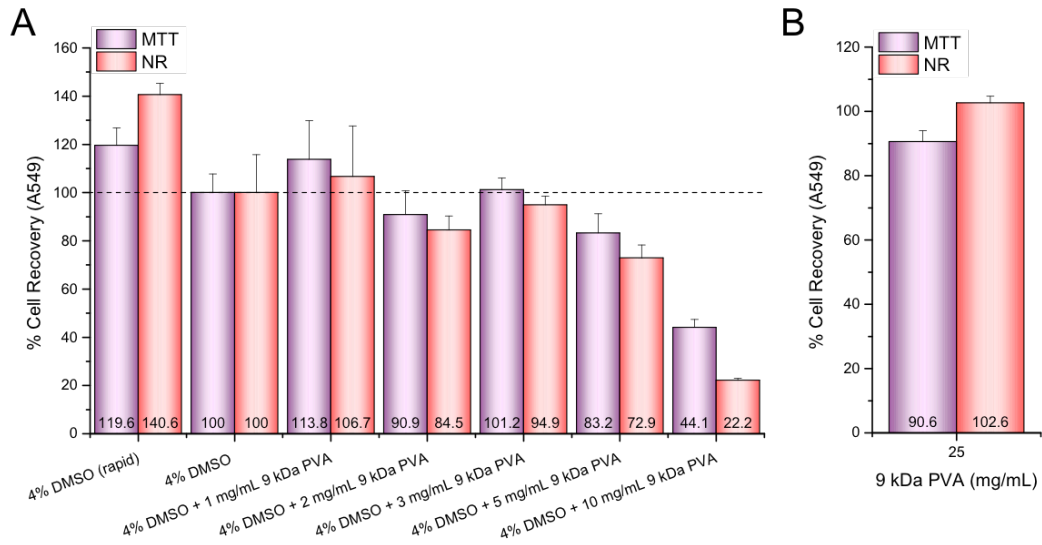


Figure 4.3. Cytotoxicity and cryopreservation impact of 9 kDa PVA on A549 cells. (A) (%) Cell recovery of A549 cells cryopreserved with 4 % (v/v) DMSO supplemented with various concentrations of 9 kDa PVA in PBS measured by both MTT and NR assays. (B) Cytotoxicity of 25 mg/mL 9 kDa PVA on confluent cells incubated for 4 hours. Values represent the mean of 3 wells each measured in duplicate with the error bars representing \pm standard deviation. Values represent the mean of 2 cryovials each plated in 2 wells and measured in duplicate with the error bars representing \pm standard deviation.

Having shown the effect of increasing 9 kDa PVA concentration on reducing cell recovery, it was important to assess if the addition of a PVA with a greater IRI (and DIS) activity at a similar concentration still provoked a reduction in cell recovery. Examining the effect of a more potent PVA at an equivalent mass concentrations is to ensure that the reduction in activity is not a direct consequence of simply introducing more PVA that could be limiting cell recovery by an otherwise unidentified effect, though at physiologically relevant temperatures 9 kDa PVA has been shown to be well tolerated (Figure 4.3.A). For that reason a cryopreservation experiment was undertaken with the more IRI

potent (Figure 2.17.) compound 31 kDa PVA at 1 mg/mL, which with 9 kDa PVA was beneficial. In addition to assessing the effect of the similar sized non-IRI isomer 8 kDa PEG. Figure 4.4.A shows crucially that the presence of 1 mg/mL 31 kDa PVA is detrimental (27.7 % \pm 2.2 %) whereas the presence of 1 mg/mL 9 kDa PVA still retained a beneficial effect (124.6 % \pm 3.3 %) in an independently conducted experiment separate from the data presented in Figure 4.3. In contrast 1 mg/mL 8 kDa PEG had neither a beneficial nor detrimental effect (92.1 % \pm 20.6 %).

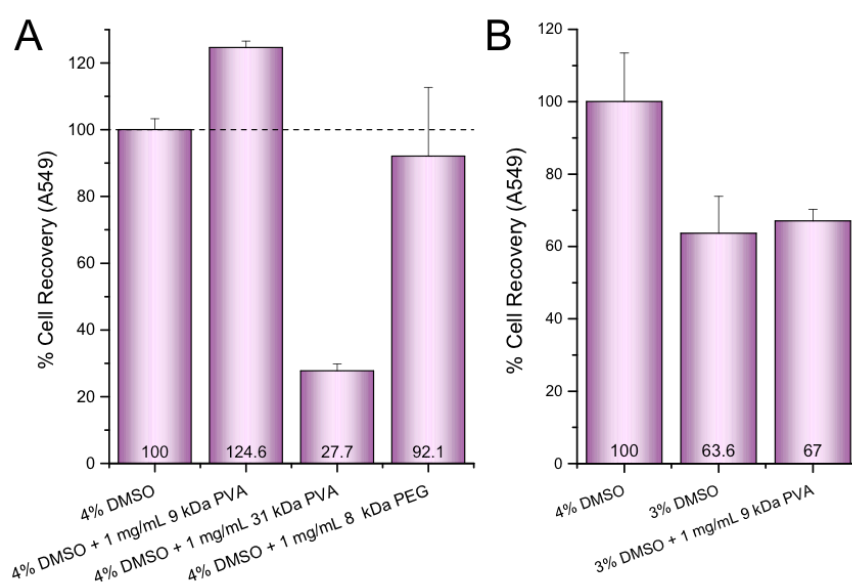


Figure 4.4. Cryopreservation of A549 cells with 9 kDa PVA, 31 kDa PVA, 8 kDa PEG and lower DMSO (% (v/v)) concentrations. (A) 4 % (v/v) DMSO supplemented with or without 1 mg/mL of either 9 kDa PVA, 31 kDa PVA or 8 kDa PEG in PBS or (B) A549 cells cryopreserved with one of 4 % (v/v) DMSO, 3 % (v/v) DMSO or 3 % (v/v) DMSO with 1 mg/mL 9 kDa PVA in PBS. Each experiment was measured by the MTT assay. Values represent the mean of 2 cryovials each plated in 2 wells and measured in duplicate with the error bars representing \pm standard deviation.

Figure 4.4. rationalises the need to further investigate the use of PVA as an IRI active cryoprotectant, especially as IRI activity has been shown to be heavily

influenced by both MW and hydrolysis.⁵³ As the presence of DMSO was shown to promote lysis and slow proliferation rates an experiment was undertaken to assess whether reducing the concentration of DMSO which lowers cell recovery could be offset by the beneficial effects of adding 1 mg/mL 9 kDa PVA (Figure 4.4.B). The effect of lowering DMSO content from 4 % (v/v) to 3 % (v/v) did yield a reduction in cell recovery ($63.6 \% \pm 10.3 \%$), which was not significantly improved by the addition of 1 mg/mL 9 kDa PVA ($67.0 \% \pm 3.2 \%$). Figure 4.4B shows the importance of DMSO in maintaining membrane plasticity (Chapter 1).^{54,55} A 25 % reduction in DMSO concentration is likely to significantly alter membrane plasticity and cause cell loss during freezing there by lowering the number of (viable) cells that can be protected by IRI activity during thawing. The effect of PVA is independent of plasticity (and freezing) and thus it is unsurprising that IRI activity is unable to rescue cell recovery to the level observed when using 4 % (v/v) DMSO. The localisation of PVA during the cryopreservation process in terms of whether or not PVA is membrane penetrative is of critical importance, as this will determine the ability of PVA to influence intracellular ice crystal growth.^{56,57} PVA localisation will influence the ease with which PVA can be removed post thaw. The presence of intracellular ice is highly destructive so to limit its growth would be highly desirable but this is offset by the ease and speed with which thawed cells need to be processed. This requires the removal of cryoprotectants which is intrinsically harder with membrane permeable CPAs⁵⁸, but if PVA is membrane permeable its low concentration, biocompatibility and biodegradability may negate this issue.^{59,60}

4.3.3. Uptake of FITC conjugated 9 kDa PVA in lung adenocarcinoma (A549) cells.

It is important to assess whether or not PVA is able to penetrate (either actively or passively) immortalized cells and thus act as an intracellular CPA and impact the growth of intracellular ice, the presence of which is highly dependant on the cryopreservation protocol utilized.⁶¹ Fluorescein isothiocyanate (FITC) is a highly fluorescent non-toxic compound with an excitation maximum of 494 nm and emission maximum of 521 nm. FITC can be easily conjugated to many molecules including proteins such as streptavidin and more complex structures, in particular antibodies and therefore has widespread biotechnological applications including enzyme linked immunosorbent assays (ELISA).⁶² As a result 9 kDa PVA was conjugated with FITC with the extent of conjugation quantified to ensure a sufficient proportion of molecules were conjugated to enable detection (Section 4.5.10.). Approximately 6 % of the 9 kDa PVA population was conjugated (Section 4.5.11.) and though a relatively low proportion the high molar extinction co-efficient (68,000 M⁻¹cm⁻¹) of FITC ensures that the fluorescent intensity of a 5 mg/mL 9 kDa PVA (non-toxic) solution was far above detection limits. A549 cells were incubated over a 3-day period with 5 mg/mL FITC conjugated 9 kDa PVA (Figure 4.5.) in complete medium (Section 4.5.12.). FITC is known to not alter the membrane permeability dramatically of conjugated products and the uptake of large FITC-conjugated molecules such as chitosan and bovine serum albumin (BSA) with A549 cells has been previously demonstrated.^{63,64} Furthermore FITC has been successfully conjugated to numerous polymeric assemblies and nanoparticles that aim to improve drug delivery.^{65,66} It has also found versatility coupled to polypeptides helping to identify peptide sequences that enhance membrane permeability.⁶⁷ After incubation the effluent containing FITC - 9 kDa PVA was removed and the cells twice washed with PBS in order to remove any

residual fluorescence that may generate a false positive before the cells were lysed to liberate any internalized FITC - 9 kDa PVA, with each solution analyzed for FITC - 9 kDa PVA content. Figure 4.5. highlights that no significant amounts of 9 kDa PVA is internalized, especially not an amount that would have a significant IRI effect. The absence of PVA internalization is critical as it simplifies the removal of 9 kDa PVA post cryopreservation. The extracellular localization of PVA also shows that PVA acts as an IRI active compound exclusively in an extracellular context, which highlights further the necessity to avoid the formation of intracellular ice by using a slow cooling rate allowing the controlled efflux of water from cells.⁶⁸ The removal of cryoprotectants from cryopreserved cells and tissues is highly desirable in order to limit the potential impact on downstream research efforts and clinical applications.^{42,43}

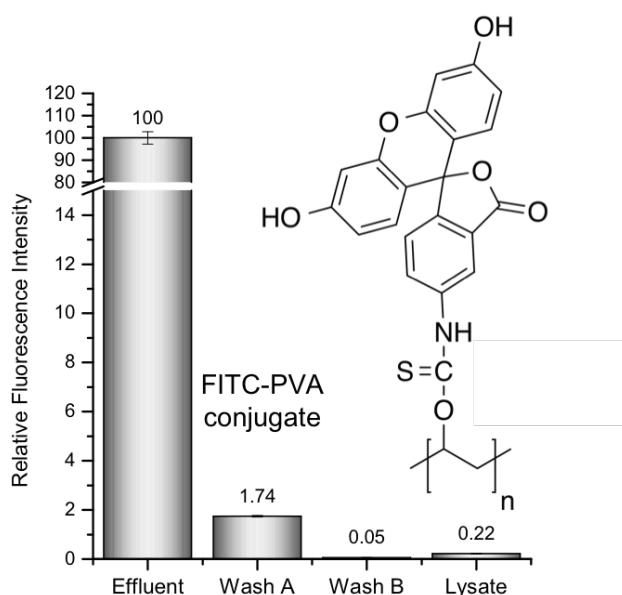


Figure 4.5. Relative uptake of 5 mg/mL 9 kDa PVA conjugated with FITC in A549 cells. Uptake of 5 mg/mL PVA-FITC (average conjugation rate 6.3 % \pm 0.4 %) incubated with A549 cells for 3 days prior to analysis. Values represent the mean relative fluorescence intensity of 3 wells each measured in triplicate with the error bars representing \pm standard deviation.

4.3.4. Cryopreservation of human choriocarcinoma (BeWo) cells.

A549 cells are an excellent and popular cell line that can be easily propagated and are widely used as a model for type II alveolar epithelial cells.⁴¹ The MTT and NR assays used to quantify their viability are standardized high throughput assays used extensively in industry and academia for toxicological studies.⁶⁹ However these assays are only indicative of a single property being either the reduction of MTT due to mitochondrial activity (by the actions of several dehydrogenases) or the pH driven lysosomal (pH 4-5) specific uptake and retention of neutral red dye.^{14,15,70,71} Ideally an ability to measure the functionality of cells on a more complex scale (i.e. modifications that invoke changes in gene expression) would be of further benefit and a more robust assessment of normality. BeWo cells which were derived from a human choriocarcinoma are a cell line of interest to those who study placental development.⁷² BeWo cells possess an ability to undergo a gross and inducible change, syncytialization.⁷³ Syncytialization *in vivo* is the generation of a villous epithelium tissue on the placenta as a result of cell fusion and is as a consequence the only villous tissue to have direct contact with maternal blood.⁷⁴ Syncytialization can be induced *in vitro* in BeWo cells by the addition of forskolin⁷⁵ giving a characteristic morphological change. A direct consequence of syncytialization is the production of the hormone β -human chorionic gonadotropin (β -hCG).⁷⁶⁻⁷⁸ However JEG-3 cells have also been shown to produce β -hCG in response to forskolin but not undergo the characteristic morphological changes, dissociating biochemical and morphological differentiation from one another.⁷⁹ β -hCG has a similar structure to many other reproductive hormones including follicle stimulating hormone (FSH) and luteinizing hormone (LH). However β -hCG has a different expression profile in that it is exclusively produced in significant quantities by syncytiotrophoblasts

during the formation of placental tissue in pregnancy.^{80,81} For that reason the presence of β -hCG is commonly used as an indicator of pregnancy with a range of immunochromatographic assays commercially available.⁸²

Figures 4.6.A shows the lack of 9 kDa PVA cytotoxicity even at 50 mg/mL with figure 4.6.B showing the cryopreservation of BeWo cells using an identical methodology to that adopted with the previously tested A549 cells (Section 4.3.1.). Figure 4.6. highlights the benefits of using 4 % (v/v) DMSO over 10 % (v/v) DMSO (74.7 % \pm 7.2 %) the beneficial effects of adding 1 mg/mL or 2 mg/mL 9 kDa PVA (157.9 % \pm 4.1 % and 177.5 % \pm 0.7 % respectively). Furthermore the harm that strong IRI (and DIS) activities can induce with 10 mg/mL 9 kDa PVA and 1 mg/mL 31 kDa PVA reducing cell recovery to values of 52.6 % \pm 2.8 % and 4.7 % \pm 4.5 % respectively. These observations are highly significant given the relatively low concentration of 9 kDa PVA added to attain such increases in cell recovery. Therefore the response of BeWo cells is similar to that of A549 cells with the addition 9 kDa PVA again proving advantageous at low concentrations using a rapid freezing strategy in the absence of complete medium.

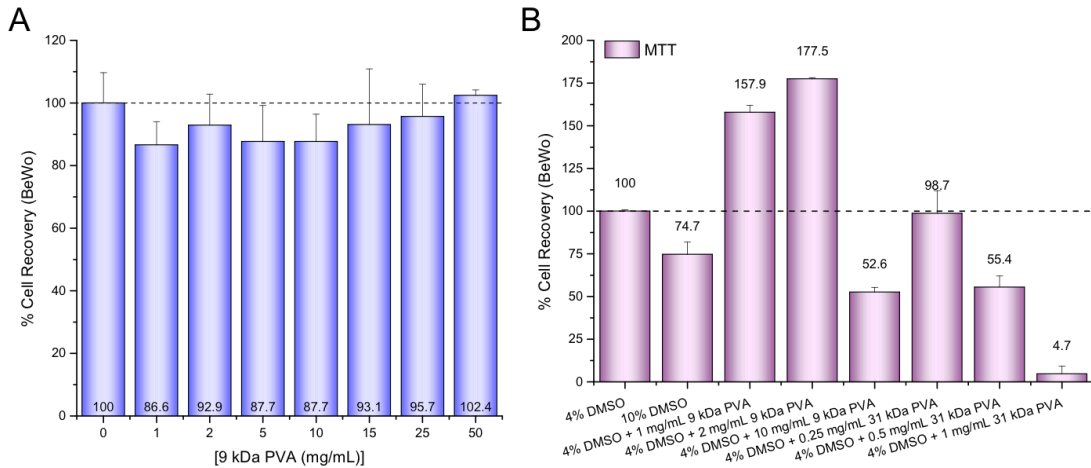


Figure 4.6. Cytotoxicity and cryopreservation impact of 9 kDa PVA on BeWo cells. (A) Confluent BeWo cells incubated for 4 hours with 9 kDa PVA between 0 – 50 mg/mL and measured by the non-destructive resazurin reduction assay. Values represent the mean of 3 wells each measured in duplicate with the error bars representing \pm standard deviation. (B) (%) Cell recovery of BeWo cells using 4 % (v/v) DMSO supplemented with either 9 kDa or 31 kDa PVA in PBS measured by the MTT assay. Values represent the mean of 2 cryovials each plated in 3 wells and measured in duplicate with the error bars representing \pm standard deviation.

However as shown in Section 4.3.2., 9 kDa PVA is non-penetrative and therefore has minimal impact on intracellular ice. As a consequence of this and in order to reduce the probability of intracellular ice formation that rises with increasing freezing rate a slow freezing rate was applied (Section 4.5.6.); with a slightly higher DMSO concentration (6 % (v/v)) and in complete medium that aids to accelerate water exchange by generating a larger osmotic gradient.⁸³ A slow freezing rate was achieved using a Nalgene “Mr Frosty™” freezing container that incites a freezing rate of approximately 1 °C/min. BeWo cells were frozen to -80 °C overnight and then transferred to N_{2(l)} (-196 °C) for 35 days. Previous

experiments focussed on short term freezing whereas this extended time frame is more akin to a research environment. After thawing, cells were then analysed using a non-destructive viability test that monitors the conversion (postulated to be due to mitochondrial enzymes⁸⁴) of resazurin into the fluorophore resorufin (Section 4.5.9.) over 3 consecutive days with separate experiments to show that the cells are able to proliferate and remain viable even 72 hours later. The results of which are shown in Figure 4.7.

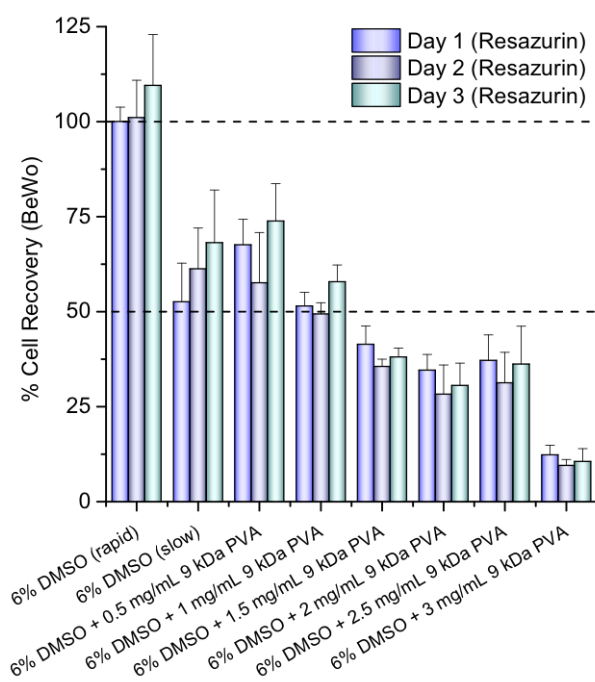


Figure 4.7. Cryopreservation of BeWo cells with 6 % (v/v) DMSO and 9 kDa PVA. Prolonged cryopreservation (slow freezing) of BeWo cells with 6 % (v/v) DMSO with or without various concentrations of 9 kDa PVA in complete medium as measured by the resazurin reduction assay on consecutive days. Values represent the mean of 2 cryovials each plated overnight in 3 wells and measured in duplicate with the error bars representing \pm standard deviation.

Under these conditions the addition of 0.5 mg/mL 9 kDa PVA proved the most beneficial in terms of immediate (Day 1) cell recovery with recoveries of 67.5 % \pm 6.8 % (6 % (v/v) DMSO + 0.5 mg/mL 9 kDa PVA) compared to 52.5 % \pm 10.5 % (6 % (v/v) DMSO (slow thaw)). Values that were referenced against a 6 % (v/v)

DMSO with a fast thawing rate (minimal ice recrystallization) with gradual escalations in 9 kDa PVA proving detrimental following trends seen previously and in literature (Section 4.3.1.). However as elaborated prior BeWo cells are able to undergo syncytialization upon the addition of forskolin and produce β -hCG. It was reasoned therefore that the extent of β -hCG production would be proportional to cell number. Complete medium containing 50 μ M forskolin was for that reason added for 48 hours to induce syncytialization with a medium change after 24 hours, aliquots were then taken to enable β -hCG detection. To qualitatively assess β -hCG production standard immunochromatographic assays (Section 4.5.14.) predominantly used to determine pregnancy were utilized (Figure 4.8.). In each instance β -hCG was successfully detected (sensitivity 25 mIU/mL) indicating syncytialization.

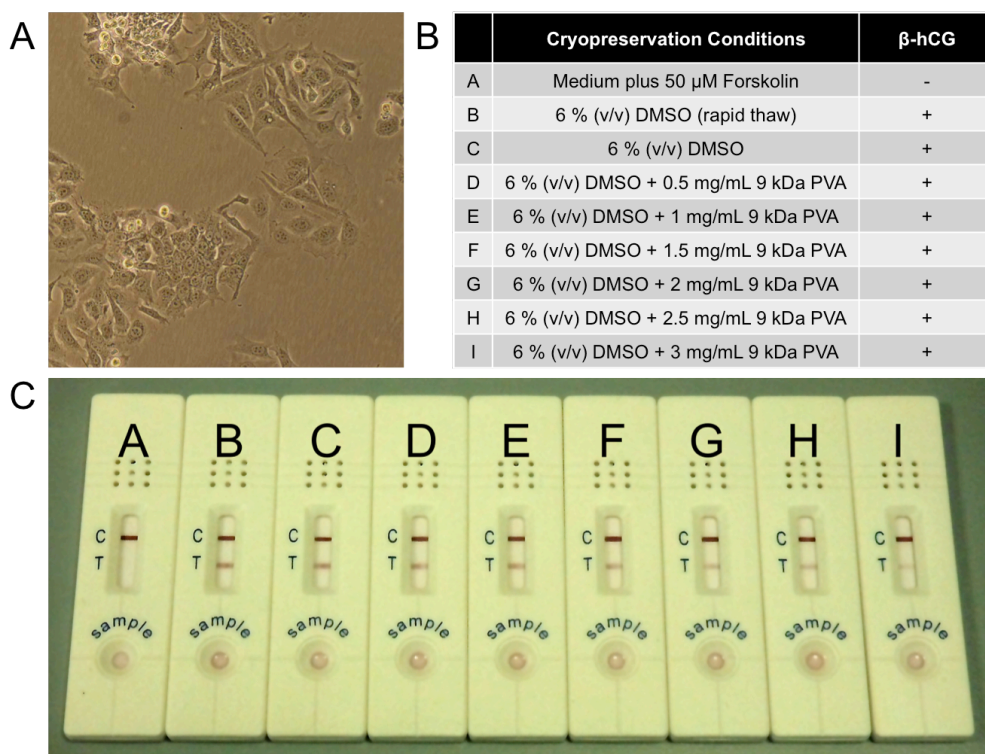


Figure 4.8. Qualitative assessment of BeWo cell syncytialization subsequent to forskolin treatment (50 μ M). (A) Phase contrasted micrograph (40x magnification) of BeWo cells pre-forskolin treatment. (B) Table highlighting the detection of β -hCG (48 hours after forskolin addition) using immunochromatographic assays principally used to detect pregnancy. (C) Image highlighting immunochromatographic assay outcomes outlined in the above table.

From Figure 4.8.C it is immediately apparent that all cells recovered after cryopreservation produced a detectable level of β -hCG indicative of syncytialization with Figure 4.8.A showing BeWo cells prior to syncytialization using an inverted phase contrast microscope. However in an attempt to further quantify the amount of β -hCG produced a quantitative measure was used, namely an ELISA specific for β -hCG which allows the a range of samples to be quantified in parallel without further downstream processing as cell culture medium does not adversely effect the performance of the assay (Section 4.5.14). Figure 4.9 shows the outcome of this analysis with a standard curve (Figure

4.9.A) allowing the conversion of the raw absorbance data into concentration values (pg/mL). An appreciable amount of β -hCG was detected in each sample again indicative of β -hCG production however the values did not correlate with the recoveries determined by the resazurin assays prior (Figure 4.7.). The lack of correlation between cell number and β -hCG production may be due to the effect of cell density on the rate and onset of syncytialization meaning that β -hCG production does not necessarily scale linearly with cell density.⁸⁵ A possible consequence being that the health of the cells recovered at higher 9 kDa PVA concentrations maybe superior and thus more responsive to forskolin treatment.

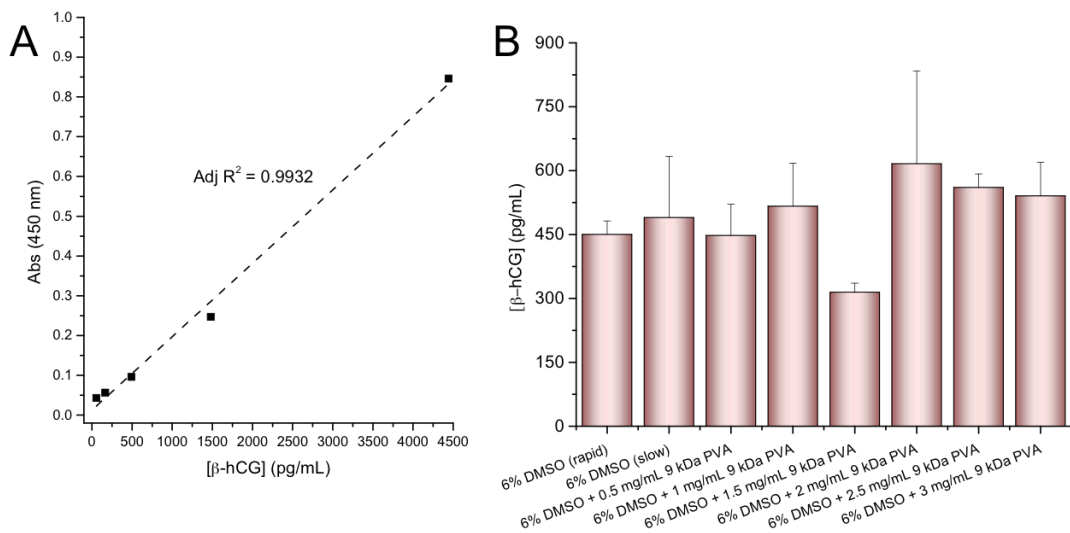


Figure 4.9. Quantitative assessment of BeWo cell syncytialization subsequent to forskolin treatment (50 μ M). (A) Standard curve quantifying β -hCG concentration (pg/mL) fitted with a linear model with a strong positive correlation between concentration (pg/mL) and absorbance at 450 nm ($\text{Adj } R^2 = 0.9932$). (B) β -hCG concentration (pg/mL) detected by ELISA from syncytialized BeWo cells cryopreserved under each of the tested conditions. Values represent the mean of 2 cryovials each plated for 3 days and measured in duplicate with the error bars representing \pm standard deviation.

This data therefore suggests that BeWo cells can be cryopreserved under conditions that mimic current freezing protocols for a prolonged period of time (35

days) and thawed under harsh conditions that promote ice recrystallization, which has a harmful effect on cell recovery. The addition of low concentrations (0.5 mg/mL) of 9 kDa PVA with an established IRI activity and biocompatibility at concentrations up to the highest concentration tested of 50 mg/mL (which nears the limit of solubility) is able to have a positive impact on cell recovery. An additional 25 % of cells are successfully recovered which is attributed to the presence of 0.5 mg/mL 9 kDa PVA compared to identical conditions that lack 9 kDa PVA. However the addition of 9 kDa PVA is unable to fully eliminate the damage arising from slow thawing that no doubt has an effect of the rate of cell rehydration also. Furthermore the inducible process of syncytialization is unaffected with the presence of β -hCG indicative of syncytialization detected by two independent methods. Figures 4.8 and 4.9 emphasize that the use of 9 kDa PVA in cryopreservation does not adversely affect this biologically complex transformation.

The attenuation of ice recrystallization and resulting impact on cell recovery is even more pronounced in a low DMSO (4 % (v/v)) serum free mixture supplemented with (1 mg/ml and 2 mg/mL) 9 kDa PVA. This methodology also uses a non-ideal rapid freezing technique but still elicits significant cell recovery. The addition of 1 mg/mL and 2 mg/mL 9 kDa PVA allows an additional 58 % and 78 % of cells to be recovered successfully (4.6.B). In line with the findings attained with A549 cells (Figure 4.4.A) the addition of small amounts of 9 kDa PVA is beneficial but increasing the concentration of 9 kDa PVA to elicit a stronger IRI activity is detrimental which as aforementioned is postulated by an increased DIS effect caused by increasing concentrations of PVA.⁵² However the onset of DIS could not be ascertained by microscopy. Improving the cryopreservation of primary and clinically relevant cells, tissues and even organs that have scarce availability and short storage times is the ultimate goal.

Understanding how close mimics of primary cells⁸⁶ behave and how PVA influences their recovery is vital. This leads to studies investigating the cryopreservation of FAO cells in the following section that are an excellent model for rat hepatocytes.^{87,88}

4.3.5. Cryopreservation of rat hepatoma (FAO) cells.

FAO cells are epithelial cells derived from the chemical carcinogenesis of a rat (*Rattus norvegicus*) inciting a H-35 reuben hepatoma approximately 50 years ago.^{89,90} FAO cells also commonly referred to as H4IIE cells are a popular mimic for rat (liver) hepatocytes that are a frequently used primary tissue in pharmacokinetic and pharmacodynamic studies^{91,92} in particular they are used in monitoring the impact of xenobiotics on cytochrome p450s that metabolize the vast majority of pharmaceutical drugs.⁹³ Though the expression of cytochrome p450s is reduced in hepatic cell lines including the often used human hepatoma cell line HepG2^{94,95} they still retain importance in drug metabolism studies and in *in vitro* toxicity screening.⁹⁶⁻⁹⁸ FAO cells are also of particular interest due to a behaviour that they share with primary rat hepatocytes, the steroid driven induction of tyrosine aminotransferase (TAT) expression.⁹⁹⁻¹⁰² TAT catalyses the conversion of L-tyrosine to *p*-hydroxyphenylpyruvate (pHPP) that is then further catalyzed by pHPP oxidase. Studies by Diamondstone allowed development of an assay that allows pHPP oxidase inhibition by Sodium diethyldithiocarbamide (DDC) and the base catalysis of pHPP to *p*-hydroxybenzaldehyde (pHBA) that has a strong absorbance at 331 nm allowing relative assessments of TAT expression.¹⁰³ Therefore FAO cells are a suitable model for primary rat hepatocytes with a shared enzymatic endpoint. To begin with the cytotoxicity of 9 kDa PVA, 31 kDa PVA and DMSO was assessed (Figure 4.10.) with neither 10 mg/mL 9 kDa PVA or 4 mg/mL 31 kDa PVA proving detrimental. However as with

A549 cells increasing amounts of DMSO instigated a significant loss in cell recovery even at concentrations as low as 2 % (v/v) DMSO (85.2 % \pm 4.6 % (resazurin) and 67.8 % \pm 13.3 % (MTT)).

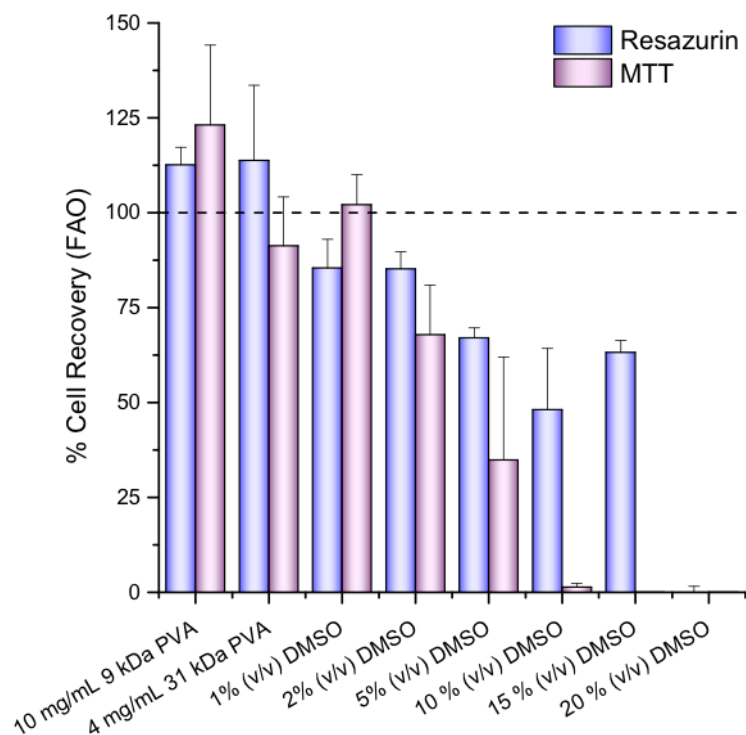


Figure 4.10. Cytotoxicity of 9 kDa PVA, 31 kDa PVA and DMSO on Confluent FAO cells. FAO cells incubated for 4 hours with either 9 kDa PVA, 31 kDa PVA or DMSO and measured by the MTT and Resazurin assays. Values represent the mean of 3 wells each measured in duplicate with the error bars representing \pm standard deviation.

As with BeWo cells and using the same rationale the forthcoming experiments used a slow freezing rate in complete medium with the supplementation of different IRI additives. To begin with the FAO cells were cryopreserved with various concentrations of DMSO and thawed slowly to identify a concentration for optimal cell recovery. The recovery of cells was assessed over 3 consecutive days post thaw using the resazurin assay with 6 % (v/v) DMSO proving to be the best concentration giving values relative to 10 % (v/v) DMSO of 134.3 % \pm 10.4 % (Figure 4.11.). Going forward all cryopreservation studies using FAO cells

used 6 % (v/v) DMSO. The addition of 9 kDa PVA again proved beneficial at low concentrations with 0.5 mg/mL 9 kDa PVA, 1 mg/mL 9 kDa PVA and 2 mg/mL 9 kDa PVA with values of 111.0 % \pm 10.6 %, 114.1 % \pm 4.7 % and 96.5 % \pm 13.7 % respectively (Figure 4.12.). These values are referenced against 6 % (v/v) DMSO (rapid thaw) (100 %). Figure 4.12 implies that in this instance the supplementation of 9 kDa PVA is able to attenuate all ice recrystallization damage (6 % (v/v) DMSO (slow thaw), 68.5 % \pm 4.6 % cell recovery) with comparable recoveries to that when a rapid thawing rate is used. Critically the addition of large amounts of 9 kDa PVA (10 mg/mL) as with every other model system tested proved detrimental to cell recovery (51.8 % \pm 19.1 %).

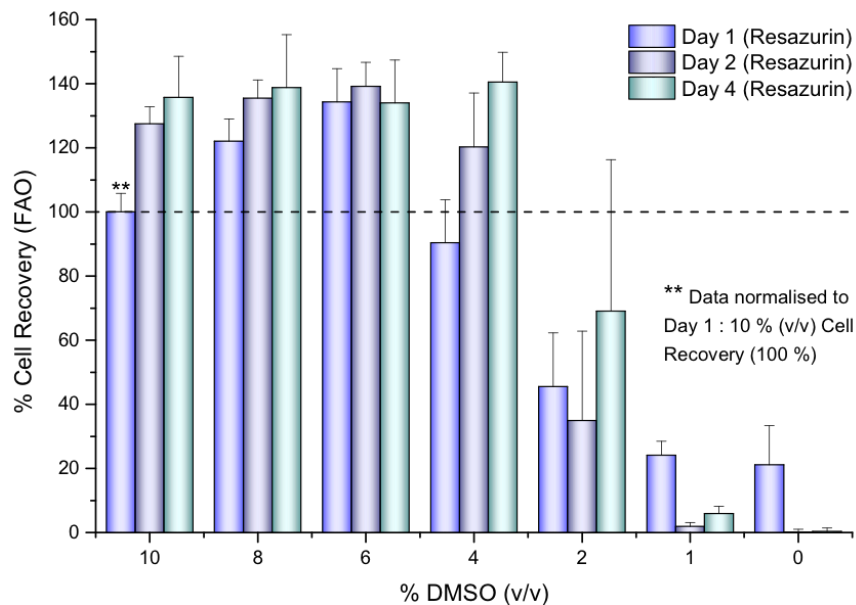


Figure 4.11. Cryopreservation of FAO cells with various concentrations of DMSO. Cryopreservation (slow freezing) of FAO cells with various concentrations of DMSO (% (v/v)) in complete medium (slow thaw). Values represent the mean of 2 cryovials each plated in 3 wells and measured in duplicate with the error bars representing \pm standard deviation and referenced against 10 % (v/v) DMSO on day 1.

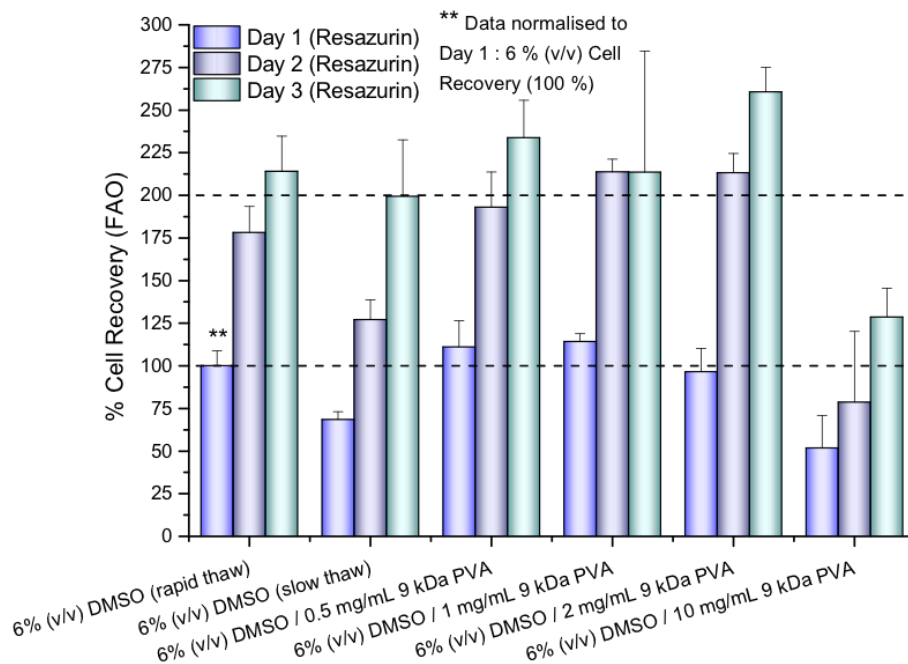


Figure 4.12. Cryopreservation of FAO cells with 6 % (v/v) DMSO and 9 kDa PVA. Cryopreservation (slow freezing) of FAO cells with 6 % (v/v) DMSO with or without various concentrations of 9 kDa PVA in complete medium as measured by the resazurin assay after 1, 2 and 3 days post plating. Values represent the mean of 2 cryovials each plated in 3 wells and measured in duplicate with the error bars representing \pm standard deviation and referenced against 6 % (v/v) DMSO (rapid thaw) on day 1.

Figure 4.12. suggests a significant increase in cell recovery occurs upon the addition of 9 kDa PVA. As a result of the increase in cell recovery the aforementioned TAT assay was performed in order to quantify the production of pHBA without the steroid driven induction that elevates TAT expression (Section 4.6.17.). Figure 4.13.A shows the absorbance spectrum of pHBA highlighting the absorbance maximum at 331 nm with Figure 4.13.B showing the kinetics of the base catalysis of pHPP to pHBA with near completion after a period of 1800 seconds. Figure 4.13.C shows the linear relationship between pHBA concentration and absorbance at 331 nm with a strong positive correlation ($\text{Adj-R}^2 = 0.9996$) allowing the accurate quantification of pHBA concentration (μM).

Figure 4.13.D shows the concentration of pHBA attained from FAO cells cryopreserved with 6 % (v/v) DMSO supplemented with and without 9 kDa PVA. Samples supplemented with 0.5 mg/mL 9 kDa PVA and 1 mg/mL 9 kDa PVA elicited higher concentrations of pHBA compared to 6 % (v/v) DMSO alone with these values correlating with the improvements detected using the resazurin assay (Figure 4.12.). However the concentration of pHBA in samples supplemented with 2 mg/mL 9 kDa PVA was not significantly greater as shown by the division of (%) cell recovery by the concentration of pHBA (μM) (Figure 4.13.E).

To further probe the cryoprotective effect of 9 kDa PVA on FAO cells one final experiment was performed that utilized 9 kDa PVA at 0.5 mg/mL intervals between 0 mg/mL and 2.5 mg/mL (Figure 4.14.A) and is thus different to figure. 4.12. In this experiment the presence of 0.5 mg/mL 9 kDa PVA proved the most beneficial ($93.7 \% \pm 10.2 \%$) with gradual decreases in cell recovery with increasing concentration. The addition of 2.5 mg/mL 9 kDa PVA had no beneficial effect over the presence of 6 % (v/v) DMSO alone at $77.3 \% \pm 7.4 \%$ and $79.1 \% \pm 6.1 \%$ respectively. Furthermore the addition of 9 kDa PVA had no significant impact on the proliferation rates as the relative improvements in cell recovery translated over a period of 72 hours (Figure 14.4.B).

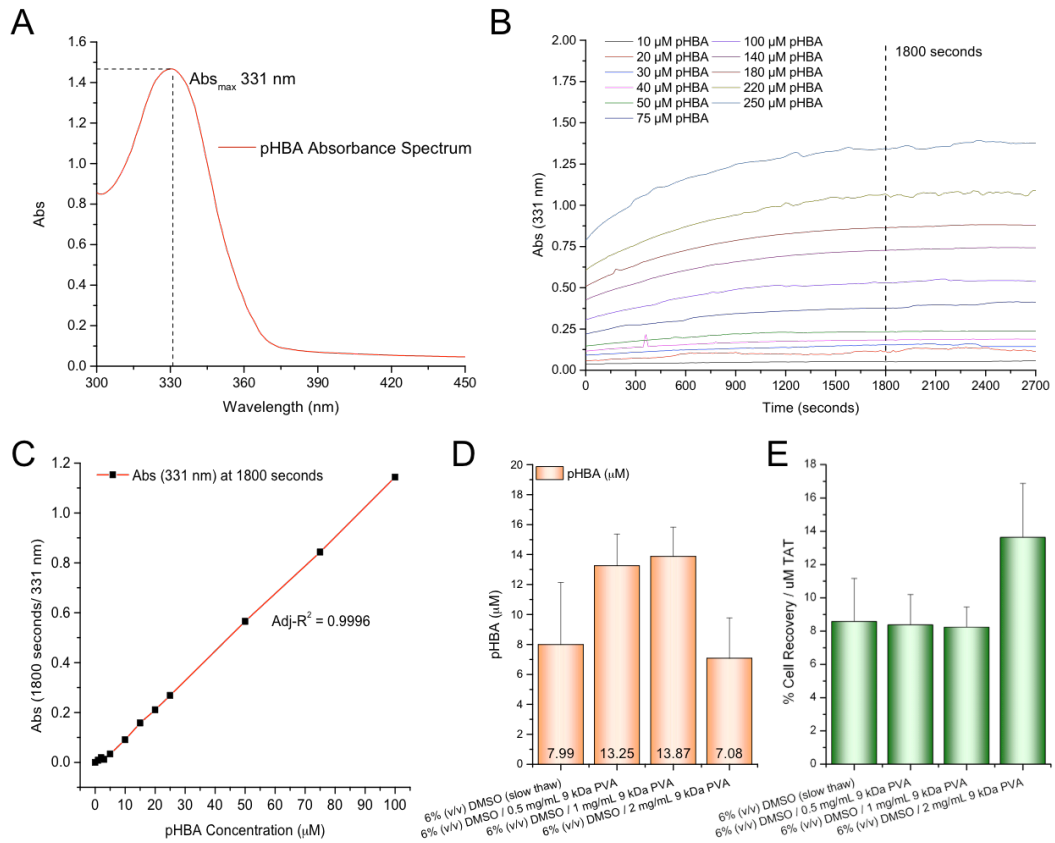


Figure 4.13. TAT assay standards and measurements with FAO cells. (A) Absorbance spectrum of pHBA highlighting an absorbance maximum at 331 nm. (B) Kinetic plots of the base catalysis of pHPA into pHBA over a period of 45 minutes. (C) Graph showing pHBA concentration (μ M) vs. Abs (331 nm) highlighting the proportional increase in absorbance with increasing concentration ($Adj R^2 = 0.9996$). (D) Levels of pHBA (μ M) indicative of the relative levels of TAT expression and by virtue FAO population. Values represent mean values of 2 cryovials each plated overnight in triplicate prior to TAT liberation and enzymatic catalysis of L-tyrosine to pHPA and the base catalysis of pHPA to the chromophore pHBA. (E) % Cell recovery per μ M of pHBA indicative of the quantity of cells required per μ M of pHBA with lower values suggestive of greater vitality.

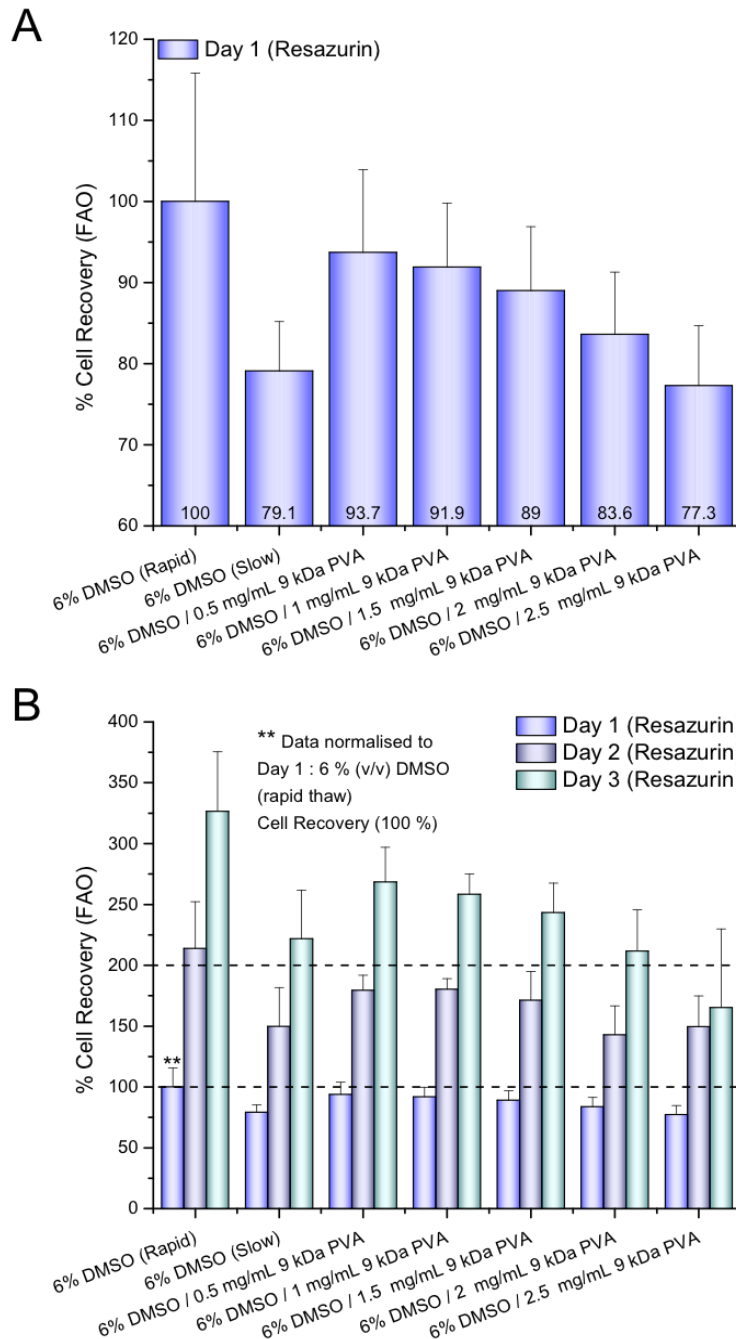


Figure 4.14. Cryopreservation of FAO cells with 6 % (v/v) DMSO and 9 kDa PVA at smaller concentration intervals. Cryopreservation (slow freezing) of FAO cells with (A) 6 % (v/v) DMSO with or without various concentrations of 9 kDa PVA in complete medium as measured by the resazurin assay. (B) Cryopreservation of FAO cells with recovery assessed over 72 hours. Values represent the mean of 2 cryovials each plated overnight in 3 wells and measured in duplicate with the error bars representing \pm standard deviation.

4.4. CONCLUSIONS.

9 kDa PVA has been successfully used as an IRI active macromolecule to improve the cryopreservation of 3 distinctly different cell lines (A549, BeWo and FAO) significantly despite the addition of only a proportionately low concentration of PVA. The susceptibility of A549 cells to DMSO at concentrations used in current cryopreservation protocols at physiologically relevant temperatures was shown highlighting the need to limit its application. Using the optimal DMSO concentration of 4 % (v/v) DMSO and a rapid freezing protocol in the absence of medium the supplementation of a low (1 mg/mL) concentration of 9 kDa PVA enhanced cell recovery. At concentrations higher than this cell recovery was reduced and speculated to be due to increased DIS activity as a similar reduction was identified with a more potent IRI compound (31 kDa PVA) at an equivalent concentration. However 9 kDa PVA was not an effective substitute for DMSO and shown to be membrane impermeable and thus only influences extracellular ice growth.

A similar relationship was shown with BeWo cells using a rapid freezing strategy. A slow freezing rate with a slightly higher DMSO concentration of 6 % (v/v) in complete medium to aid water exchange was used that has the effect of lowering the probability of intracellular ice formation which 9 kDa PVA is unable to influence. Under these conditions that are more akin to traditional methodologies the addition of 0.5 mg/mL 9 kDa PVA proved the most beneficial with higher concentrations having an analogous detrimental effect with cells stored in N_{2(l)} for 35 days. However all recovered cells were able to undergo some form of syncytialization a complex morphological and biochemical change evidenced by

the production of β -hCG quantified by two separate methods and thus the use of 9 kDa PVA does not inhibit this complex biochemical process.

Finally the addition of 0.5 mg/mL 9 kDa PVA provided a cryoprotective effect in the cryopreservation of FAO cells that are an excellent model system for primary rat hepatocytes using a slow freezing rate. The benefit of PVA addition was evidenced by two independent methodologies with beneficial effects shown even after a period of 72 hours. The consequence of 0.5 mg/mL stepwise increments in 9 kDa PVA highlighted further that simply increasing IRI activity does not lead to greater cell recoveries. Although the beneficial effects seen in each cell variety justify the investigation of primary tissues that have the greatest clinical fragility and demand.

4.5. MATERIALS AND METHODS

4.5.1. Cell culture reagents and conditions.

All cell cultures reagents were sourced from either Life Technologies Ltd, Paisley, UK or Sigma-Aldrich Company Ltd, Dorset, UK and of the highest attainable quality and stored at 4 °C or -20 °C as instructed when not in use. Complete medium consisted of RPMI (with phenol red) containing 10 % (v/v) FBS plus 100 U/mL Penicillin and 100 µg/mL Streptomycin (unless otherwise specified) and all cells were incubated at 37 °C in a 5 % CO_{2(g)} humidified atmosphere. PBS was prepared in house and autoclaved prior to use. All cell culture plasticware was obtained from Greiner Bio-One Ltd, Gloucestershire, UK and all cell culture experiments were performed in a class II biosafety cabinet to ensure sterility with cells regularly assessed for bacterial, fungal and yeast contamination.

4.5.2. Rejuvenation of cells from cryopreserved stocks.

A single 1 mL cryopreserved aliquot (10 % (v/v) DMSO in complete medium) in a 1.8 mL cryovials of cells was removed from cryostorage (N_{2(l)}) and immediately thawed rapidly in a 37 °C water bath. Thawed cells were then immediately placed in a 75 cm² flask containing 20 mL of pre-warmed medium and incubated overnight. Phase-contrast light microscopy (Nikon UK Limited, Surrey, UK) was used to confirm the presence of adherent cells and the medium aspirated and cells washed with 10 mL of PBS to remove any non-adherent cells, debris and residual DMSO. 20 mL of pre-warmed medium was added and cells incubated until confluency.

4.5.3. Passaging of cultured cells.

The following details how to passage cells from one 175 cm² flask into another 175 cm² flask. All quantities were scaled linearly according to any changes in the surface area(s) or number of flasks/plates required. Confluence was defined as 70-80 % of the total surface area consisting of cultured cells as assessed by phase-contrasted light microscopy and all cells were incubated at 37 °C in a 5 % CO_{2(g)} humidified atmosphere.

Medium from confluent cells was removed and the cells washed with 25 mL pre-warmed (37 °C) PBS and replaced with 3.5 mL (pre-warmed) 0.25 % (w/v) trypsin solution. The flask was incubated for a minimum of 2 minutes (5 minute maximum) to ensure all cells were detached but not allowed to aggregate. The trypsin solution was immediately neutralized by the addition of 3.5 mL of complete medium. A 1 mL aliquot was removed and transferred into a 175 cm² flask containing 25 mL of pre-warmed (37 °C) media. The flask was then replaced in the incubator and cells allowed to adhere and proliferate to (70 % - 80 %) confluency.

4.5.4. Cytotoxicity of DMSO, 9 kDa PVA and 31 kDa PVA.

Cells (A549⁴¹, BeWo⁷² and FAO⁸⁹) were grown to confluence in either 48-well or 24-well plates as required and washed with an appropriate amount of pre-warmed PBS before the addition of 400 µL complete medium supplemented with the desired concentration of the analyte under scrutiny. Cells were then incubated for 4 hours prior to analysis using one or more of the MTT, NR or resazurin assays. Additionally in the case of assessing the impact of DMSO on the proliferation of A549 cells a low density of A549 cells were plated in a 48-well

plate and incubated with 400 μL of complete medium supplemented with the desired concentration of DMSO and analyzed by the MTT, NR and resazurin assays.

4.5.5. Cryopreservation of cells using a rapid freezing rate in the absence of complete medium.

A549 cells and BeWo cells (where indicated prior) were subjected to a rapid freezing protocol as follows with the same procedure undertaken for each cell line. Cells were grown to confluency and trypsinised according to Section 4.5.3. prior to centrifugation at 23 $^{\circ}\text{C}$ and 1000 rpm and resuspended in pre-warmed PBS to amount equivalent to 750 μL per sample. 700 μL of the cell suspension was placed in 1.8 mL cryovials for each analyte mixture in duplicate and the desired amount of DMSO, PVA and PBS added to give a final volume of 1 mL. Cryovials were then mixed gently by inversion to ensure a homogenous cell suspension. Cells were then frozen as individual aliquots in a pre-cooled $\text{IPA}_{(l)}/\text{CO}_{2(s)}$ slurry (-78 $^{\circ}\text{C}$) for 60 seconds and then buried in $\text{CO}_{2(s)}$ for 20 minutes prior to thawing by either a rapid or slow thawing technique as required. Rapid thawing was defined as the immersion of the cryovial in a 37 $^{\circ}\text{C}$ water bath until no ice visibly remained. Slow thawing was achieved by thawing cells in air at room temperature (approximately 23 $^{\circ}\text{C}$) until no ice visibly remained. Subsequent to thawing, cells were plated as desired in a 48 well or 24 well plate with 30 μL and 60 μL aliquots of each thawed aliquot added to 600 μL pre warmed complete medium and incubated overnight. Plates were then assessed by phase contrast microscopy and samples with the most suitable cell density (i.e. 30 μL or 60 μL supplements) assessed by the MTT and NR assays.

4.5.6. Cryopreservation of cells using a slow freezing rate in the presence of complete medium.

FAO and BeWo cells (where indicated prior) were subjected to a slow freezing protocol as follows with the same procedure for each cell line. 1 mL aliquots of cells in 1.8 mL cryovials were prepared in an identical manner to Section 4.5.5. but substituting PBS for complete medium. Cells were then chilled at 4 °C for 120 minutes and then mixed gently by inversion and positioned in a Nalgene “Mr Frosty™” placed at -80 °C to achieve a cooling rate of 1 °C/min and kept at -80 °C for between 24 and 72 hours and then either transferred to N_{2(l)} as required or thawed (Section. 4.5.5.) and analyzed using the MTT and resazurin assays

4.5.7. MTT reduction assay.

The following details a MTT reduction assay¹⁴ for cells seeded in a 24-well (1.92 cm² surface area per well) plate format. All quantities were scaled linearly according to any changes in surface area(s) and the same protocol applied to each cell variety that have approximately equal sensitivity and responsiveness. Complete medium was removed and cells washed with 600 µL of pre-warmed (37 °C) PBS and replaced with 300 µL of pre-warmed (37 °C) complete medium and 50 µL of 5 mg/mL MTT in PBS and incubated for 4 hours. The cells were examined briefly using phase contrast light microscopy for the presence of the insoluble formazan product (Figure 4.15.). The medium and MTT mixture was aspirated and replaced with 300 µL of 90 % (v/v) IPA / 10 % (v/v) DMSO, 0.1 % HCl_(aq) and incubated for 20 minutes at 23 °C and 200 rpm to enable lysis and solubilisation giving a uniform purple colouration. 100 µL aliquots were then in duplicate transferred to a 96-well plate and absorbance measured at 595 nm

(Multiskan Ascent, Fisher Scientific UK Ltd, Leicestershire, UK). The values attained were then contrasted against untreated controls. A percentage estimation of cell recovery could then be calculated (Equation 4.1.).

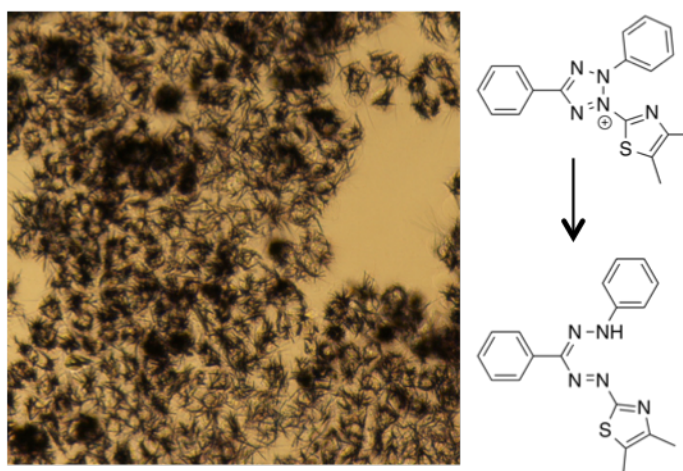


Figure 4.15. Phase contrasted micrograph of A549 cells after MTT assay. Exemplifying the presence of the insoluble and crystalline formazan product after a 4 hour incubation period (100x magnification) .

Equation 4.1. Calculation of (%) relative metabolic activity using the MTT assay.

$$(\%) \text{ Relative metabolic activity} = \frac{\left[\text{Abs}(595\text{nm}) (\text{Sample}) - \text{Abs}(595\text{nm}) (0\%) \right]}{\left[\text{Abs}(595\text{nm}) (100\%) - \text{Abs}(595\text{nm}) (0\%) \right]}$$

4.5.8. Neutral red uptake assay.

The following details a neutral red (NR) uptake assay¹⁵ for A549 cells seeded in a 24-well (1.92 cm² surface area per well) plate format. All quantities were scaled linearly according to any changes in the surface area(s) cultured and the same protocol applied to each cell variety that have approximately equal sensitivity and responsiveness. Complete medium was removed and cells washed with 600 μ L

of pre-warmed (37 °C) PBS and replaced with complete medium with 120 µL pre-warmed neutral red solution that was diluted 10-fold in PBS from the originally provided 0.33' %(w/v) stock solution. The cells were then incubated for 2 hours. The neutral red solution was then discarded and the cells examined briefly using phase contrast light microscopy for the presence of stained cells (Figure 4.16.) prior to two washes with 600 µL PBS. 600 µL of 1 % (v/v) acetic acid, 50 % (v/v) ethanol solution was added and the cells left for 10 minutes at 23 °C and 200 rpm to enable lysis and solubilisation giving a uniform pink colouration. 150 µL aliquots were then in duplicate transferred to a 96-well plate and absorbance measured at 540 nm (Multiskan Ascent, Fisher Scientific UK Ltd, Leicestershire, UK). The values attained were then contrasted against untreated controls. A percentage estimation of cell recovery could then be calculated (Equation 4.2.).

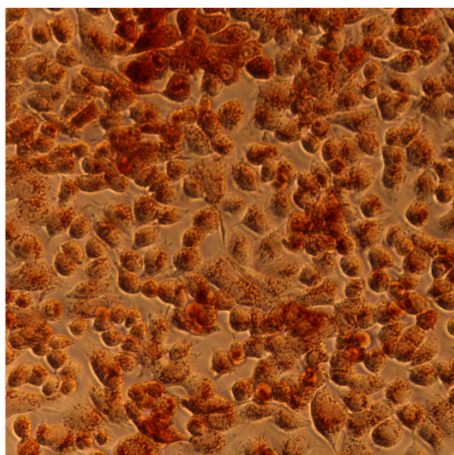


Figure 4.16. Phase contrasted micrograph of A549 cells after NR assay. Exemplifying the presence of the neutral red stained cells after a 2-hour incubation period (100x magnification).

Equation 4.2. Calculation of (%) relative dye uptake using the NR assay.

$$(\%) \text{ Relative dye uptake} = \frac{\left[\text{Abs}_{(540 \text{ nm})}(\text{Sample}) - \text{Abs}_{(540 \text{ nm})}(0\%) \right]}{\left[\text{Abs}_{(540 \text{ nm})}(100\%) - \text{Abs}_{(540 \text{ nm})}(0\%) \right]}$$

4.5.9. Resazurin reduction assay.

The following details a resazurin reduction assay^{104,105} for cells seeded in a 48-well (0.95 cm² surface area per well) plate format. Complete medium was removed and cells washed with 400 μ L of pre-warmed PBS and replaced with 200 μ L of pre-warmed complete medium and supplemented with 10 μ L 0.33' mg/mL resazurin in triplicate. The cells were then incubated for 3 hours (unless stated otherwise) allowing the conversion of resazurin to the highly fluorescent chromophore resorufin prior to subsequent conversion to the non-fluorescent compound hydroresorufin (Figure 4.17.). 50 μ L aliquots were taken in duplicate and added to 50 μ L PBS in a 96 well plate and fluorescence measured using excitation and emission wavelengths of 530/25 nm and 590/30 nm respectively using a BioTek Synergy HT plate reader (BioTek UK, Bedfordshire, UK).

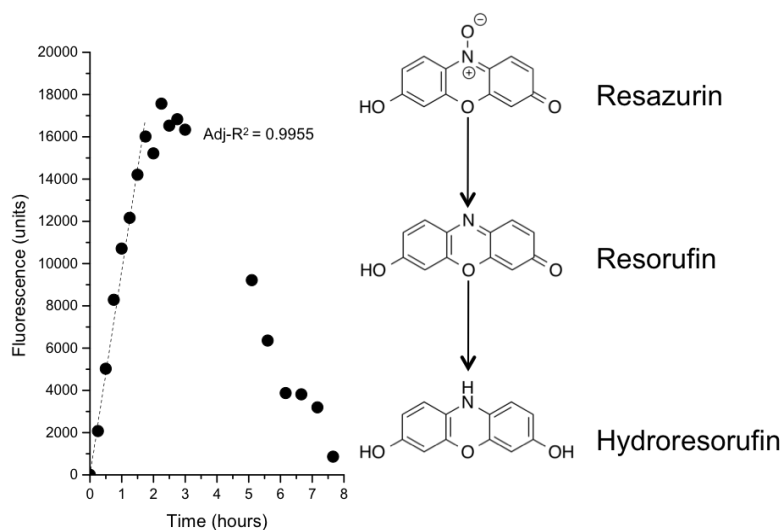


Figure 4.17. Assessment of resorufin and hydroresorufin production in FAO cells. Confluent FAO cells incubated with 0.0833' mg/mL resazurin to assess the reduction of non-fluorescent resazurin to the highly fluorescent resorufin at frequent intervals (increase in fluorescence) prior to further reduction to non-fluorescent hydroresorufin (decrease in fluorescence).

The values attained were then contrasted against untreated controls. A percentage estimation of cell recovery could then be calculated (Equation 4.3.). If required for subsequent time points, cells were washed with 400 μ L of pre-warmed PBS and 400 μ L of complete medium added and incubated for experimentation the following day.

Equation 4.3. Calculation of (%) relative fluorescence using the resazurin assay.

$$(\%) \text{ Relative fluorescence} = \frac{\left[\text{Fluorescence}(590/30\text{ nm}) (\text{Sample}) - \text{Fluorescence}(590/30\text{ nm}) (0\%) \right]}{\left[\text{Fluorescence}(590/30\text{ nm}) (100\%) - \text{Fluorescence}(590/30\text{ nm}) (0\%) \right]}$$

4.5.10. Conjugation and purification of FITC-labeled PVA.

100 mg of purified PVA was dissolved with 1 mg/mL FITC in DMSO to a final concentration of 10 mg/mL PVA and 0.1 mg/mL FITC and kept at 23 °C whilst gently agitated for 48 hours in an absence of light. This solution was then dialysed (MWCO:1000, Spectrum Laboratories Inc, CA, USA)) repeatedly with 4 L of ultrahigh purity (18.2 m Ω cm (resistivity) at 23 °C) H₂O_(l) with a minimum of 5 H₂O_(l) changes at regular intervals to remove any unbound dye. The sample was then freeze-dried overnight giving a compound with a characteristically pale lime green colouration. Conjugated PVA could then be store at 23 °C in an absence of light indefinitely until required.

4.5.11. Determination of FITC conjugation.

The extent of FITC conjugation could be calculated spectrophotometrically using a BioTek Synergy HT plate reader (BioTek UK, Bedfordshire, UK). The

absorbance at 494 nm (adsorption maximum) of 200 μL aliquots of 1, 0.5, 0.25 and 0.125 mg/mL conjugated polymer in $\text{H}_2\text{O}_{(l)}$ was measured in a clear flat bottomed 96-well plate. The background absorbance of unconjugated polymer at equivalent concentrations was also measured and these values subtracted. The concentration of FITC could then be approximated using the Beer-Lambert law (Equation 4.4.) given that the molar extinction coefficient (ϵ) of FITC ($68,000 \text{ M}^{-1} \text{cm}^{-1}$) and path length (l) (0.48 cm). The ratio of FITC:Compound could then be calculated and an estimation of the percentage of molecules labeled with FITC (assuming only 1 conjugation event per molecule).

Equation 4.4. Beer-Lambert law

$$\text{Concentration (M)} = \frac{\text{Abs}_{(494 \text{ nm})}}{\epsilon(\text{M}^{-1} \cdot \text{cm}^{-1}) \cdot l(\text{cm})}$$

4.5.12. Assessment of conjugated FITC-9 kDa PVA uptake in A549 cells.

A549 cells were plated at a low density in a 48-well plate with 400 μL of medium supplemented with 5 mg/mL of FITC-conjugated polymer and incubated. After 3 days the FITC containing effluent was removed and cells washed twice with 400 μL PBS prior to lysis with 400 μL 100 mg/mL SDS. The FITC content of each solution was then measured in triplicate (100 μL) by fluorescence in a 96 well plate using a BioTek Synergy HT plate reader (BioTek UK, Bedfordshire, UK) with excitation and emission wavelengths of 485/20 nm and 520/20 nm respectively at sensitivity 35. The FITC content of each solution was then referenced against the FITC supplemented medium of each compound allowing FITC uptake to be calculated (Equation 4.5.).

Equation 4.5. Calculation of 9 kDa PVA – FITC uptake.

$$(\%) \text{ 9 kDa PVA uptake} = \frac{\left[\text{Fluorescence}_{(520/20nm)}(\text{Sample}) \right]}{\left[\text{Fluorescence}_{(520/20nm)}(\text{Effluent}) \right]}$$

4.5.13. Forskolin treatment of BeWo cells to incite syncytialization and β -HCG expression.

The following details the syncytialization of BeWo cells incited by the addition of Forskolin. Forskolin was prepared in DMSO at a final concentration of 10 mM and stored at 4 °C until required. A 30 μ L aliquot of BeWo cells post-cryopreservation with 600 μ L of complete medium were seeded in triplicate in 48-well plates and incubated for 3 days. The medium was then replaced with 400 μ L of complete medium supplemented with Forskolin at a final concentration of 50 μ M and incubated for 72 hours. After 72 hours the cells were assessed using an inverted phase contrast light microscope to assess the morphology and integrity of the cells. A 300 μ L aliquot of media was removed prior to β -HCG quantification.

4.5.14. β -HCG detection via immunochromatographic and (ELISA) enzyme-linked immunosorbent assays.

Detection of β -HCG was by two separate methods. A qualitative assessment for β -HCG used immunochromatographic assays supplied from SureScreen Diagnostics Ltd, Derbyshire, UK. Each assay had a sensitivity of 25 mIU/mL. In each instance 200 μ L of cell culture medium (Section 4.5.13.) was applied as two separate 100 μ L aliquots and kept at 23 °C for a minimum of 2 minutes prior to inspection with two solid bars indicative of β -HCG (Figure 4.8.). A quantitative

measure of β -HCG production was achieved using a β -HCG specific ELISA kit specific for detecting β -HCG present within cell culture medium purchased from Sigma-Aldrich Company Ltd, Dorset, UK and following the as supplied protocol.

4.5.15. Tyrosine amino transferase (TAT) enzymatic assay.

Cryopreserved FAO cells were washed twice with 300 μ L PBS prior to the addition of 50 μ L of 0.25 % (v/v) trypsin for 2 minutes before the addition of 150 μ L of complete medium. A 180 μ L aliquot was then transferred into 500 μ L eppendorf tubes and centrifuged for 5 minutes at 1000 rpm and 4 $^{\circ}$ C. The supernatant was removed and the cells resuspended in 180 μ L of PBS prior to cell lysis. Cell lysis was achieved using a freeze-thaw method. FAO cells were frozen quickly in an $\text{IPA}_{(l)} / \text{CO}_{2(s)}$ slurry (-78 $^{\circ}$ C) for 2 minutes and then thawed at room temperature for 10 minutes. This process was repeated 3 times in order to maximize lysis and therefore the amount of freely available TAT. The conversion of L-tyrosine into *p*-hydroxyphenylpyruvic acid (pHPP) and then the chromophore *p*-hydroxybenzaldehyde (pHBA) was attained as follows^{103,106}. A 120 μ L aliquot of 32 μ M (5.82×10^{-3} mg/mL) L-tyrosine (substrate), 0.5 mM (0.124 mg/mL) pyridoxal-5'-phosphate (co-factor) and 8 mM (1.802 mg/mL) sodium diethyldithiocarbamide (inhibits the action of pHPP oxidase) was added to a 40 μ L aliquot of cell lysate in duplicate in 500 μ L eppendorf tubes and pre-warmed at 37 $^{\circ}$ C for 20 minutes. To initiate the reaction 40 μ L 50 mM (7.306 mg/mL) α -ketoglutaric acid (co-factor) was added and the samples incubated at 37 $^{\circ}$ C for 20 minutes to enable the conversion of L-tyrosine to pHPP. To stop the reaction a 30 μ L aliquot of 10 M $\text{NaOH}_{(aq)}$ was added and the sample vortexed immediately and a 100 μ L aliquot transferred to a 96 well plate. $\text{NaOH}_{(aq)}$ addition also served to catalyze the conversion of pHPP into pHBA. Measurement of pHBA was achieved by measuring the absorbance after 1800 seconds at which

point pHPP to pHBA conversion is near total (Figure 4.13.B). The absorbance maximum of pHBA is 331 nm (Figure 4.13.A). The derived data can then be used to comparatively estimate the amount of TAT in each sample and the amount of pHBA can be quantified against a pHBA standard curve (Figure 4.13.C).

4.6. REFERENCES.

1. Carrel, A. On the permanent life of tissues outside of the organism. *J Exp Med* **15**, 516–528 (1912).
2. Rous, P. & Jones, F. S. A method for obtaining suspensions of living cells from the fixed tissues and for the plating out of individual cells. *J Exp Med* **23**, 549–555 (1916).
3. Morgan, J. F., Morton, H. J. & Parker, R. C. Nutrition of Animal Cells in Tissue Culture. I. Initial Studies on a Synthetic Medium. *Exp Bio Med* **73**, 1–8 (1950).
4. *About ECACC*. at <<http://www.phe-culturecollections.org.uk/aboutus/ecacc.aspx>>
5. Carney, D. N. *et al.* Establishment and Identification of Small Cell Lung Cancer Cell Lines Having Classic and Variant Features. *Cancer Res* **45**, 2913–2923 (1985).
6. Masters, J. R. W. Human cancer cell lines: fact and fantasy. *Nat Rev Mol Cell Biol* **1**, 233–236 (2000).
7. Lendahl, U. & McKay, R. D. G. The Use of Cell Lines in Neurobiology. *Trends Neurosci* **13**, 132–137 (1990).
8. Grimm, S. The art and design of genetic screens: mammalian culture cells. *Nat Rev Genet* **5**, 179–189 (2004).
9. Sedivy, J. M. New Genetic Methods for Mammalian Cells. *Nat Biotechnol* **6**, 1192–1196 (1988).
10. Andersen, D. & Krummen, L. Recombinant protein expression for therapeutic applications. *Curr Opin Biotech* **13**, 117–123 (2002).
11. Lee, T. H. Y. *et al.* Glycosylation in a mammalian expression system is critical for the production of functionally active leukocyte immunoglobulin-like receptor A3 protein. *J Biol Chem* **288**, 32873–32873 (2013).
12. Zhu, J. Mammalian cell protein expression for biopharmaceutical production. *Biotechnol Adv* **30**, 1158–1170 (2012).
13. Wurm, F. M. Production of recombinant protein therapeutics in cultivated mammalian cells. *Nat Biotechnol* **22**, 1393–1398 (2004).
14. Mosmann, T. Rapid colorimetric assay for cellular growth and survival: application to proliferation and cytotoxicity assays. *J Immunol Methods* **65**, 55–63 (1983).
15. Repetto, G. & Del Peso, A. Neutral red uptake assay for the estimation of cell viability/cytotoxicity. *Nat Protoc* **3**, 1125–1131 (2008).
16. Boyce, S. T., Anderson, B. A. & Rodriguez-Rilo, H. L. Quantitative assay for quality assurance of human cells for clinical transplantation. *Cell Transplantation* **15**, 169–174 (2006).
17. Mickuviene, I., Kirvelienu, V. & Juodka, B. Experimental survey of non-clonogenic viability assays for adherent cells in vitro. *Toxicol In Vitro* **18**, 639–648 (2004).
18. Korzeniewski, C. & Callewaert, D. M. An enzyme-release assay for natural cytotoxicity. *J Immunol Methods* **64**, 313–320 (1983).

19. Cook, J. A. & Mitchell, J. B. Viability measurements in mammalian cell systems. *Anal Biochem* **179**, 1–7 (1989).
20. Krishan, A. Rapid flow cytofluorometric analysis of mammalian cell cycle by propidium iodide staining. *J Cell Biol* **66**, 188–193 (1975).
21. Capes-Davis, A. *et al.* Check your cultures! A list of cross-contaminated or misidentified cell lines. *Int J Cancer* **127**, 1–8 (2010).
22. Buehring, G. C., Eby, E. A. & Eby, M. J. Cell line cross-contamination: how aware are Mammalian cell culturists of the problem and how to monitor it? *In Vitro Cell Dev Biol* **40**, 211–215 (2004).
23. Scott, K. L., Lecak, J. & Acker, J. P. Biopreservation of red blood cells: past, present, and future. *Transfus Medicine Rev* **19**, 127–142 (2005).
24. Kitano, H. Opinion: Cancer as a robust system: implications for anticancer therapy. *Nat Rev Cancer* **4**, 227–235 (2004).
25. HEK-293 (ATCC® CRL-1573™)
. at <<http://www.lgcstandards-atcc.org/Products/All/CRL-1573.aspx>>
26. Caco-2 (ATCC® HTB-37™). at <<http://www.lgcstandards-atcc.org/products/all/HTB-37.aspx>>
27. MCF7 (ATCC® HTB-22™). at <<http://www.lgcstandards-atcc.org/Products/All/HTB-22.aspx>>
28. Raffray, M. & Gerald M, C. Apoptosis and necrosis in toxicology: A continuum or distinct modes of cell death? *Pharmacol Therapeut* **75**, 153–177 (1997).
29. Golstein, P. & Kroemer, G. Cell death by necrosis: towards a molecular definition. *Trends Biochem Sci* **32**, 37–43 (2007).
30. Edinger, A. L. & Thompson, C. B. Death by design: apoptosis, necrosis and autophagy. *Curr Opin Cell Biol* **16**, 663–669 (2004).
31. Baust, J. & Van Buskirk, R. Cell viability improves following inhibition of cryopreservation-induced apoptosis. *In Vitro Cell Dev Biol* **36**, 262–270 (2000).
32. DeLong, M. J. Apoptosis: A Modulator of Cellular Homeostasis and Disease States. *Ann NY Acad Sci* **842**, 82–90 (1998).
33. Liu, S. *et al.* *In vitro* studies of antifreeze glycoprotein (AFGP) and a C-linked AFGP analogue. *Biomacromolecules* **8**, 1456–1462 (2007).
34. Chaytor, J. L. *et al.* Inhibiting ice recrystallization and optimization of cell viability after cryopreservation. *Glycobiology* **22**, 123–133 (2012).
35. Liu, S. & Ben, R. N. C-linked galactosyl serine AFGP analogues as potent recrystallization inhibitors. *Org Lett* **7**, 2385–2388 (2005).
36. Leclere, M., Kwok, B. K., Wu, L. K., Allan, D. S. & Ben, R. N. C-linked antifreeze glycoprotein (C-AFGP) analogues as novel cryoprotectants. *Bioconjugate Chem* **22**, 1804–1810 (2011).
37. Day, J. G. & Stacey, G. *Cryopreservation and Freeze-Drying Protocols*. (Humana Press, 2007).
38. Notman, R., Noro, M., O'Malley, B. & Jamshed, A. Molecular basis for dimethylsulfoxide (DMSO) action on lipid membranes. *J Am Chem Soc* **129**,

- 13982–13983 (2006).
39. Gordeliy, V. I., Kiselev, M. A., Lesieur, P., Pole, A. V. & Teixeira, J. Lipid membrane structure and interactions in dimethyl sulfoxide/water mixtures. *Biophys J* **75**, 2343–2351 (1998).
 40. Giard, D. J. *et al.* In vitro cultivation of human tumors: establishment of cell lines derived from a series of solid tumors. *J Natl Cancer Inst* **51**, 1417–1423 (1973).
 41. Lieber, M., Smith, B., Szakal, A., Nelson-Rees, W. & Todaro, G. A continuous tumor-cell line from a human lung carcinoma with properties of type II alveolar epithelial cells. *Int J Cancer* **17**, 62–70 (1976).
 42. Craig, A. M., Blythe, L. L., Appell, L. H. & Slizeski, M. L. Evaluation of the potential for interference by dimethyl sulfoxide (DMSO) in drug detection in racing animals. *J Vet Pharmacol Ther* **10**, 298–304 (1987).
 43. Tjernberg, A., Markova, N., Griffiths, W. J. & Hallén, D. DMSO-related effects in protein characterization. *J Biomole Screen* **11**, 131–137 (2006).
 44. A549 (ATCC® CCL-185™)
. at <<http://www.lgcstandards-atcc.org/products/all/CCL-185.aspx>>
 45. Gibson, M. I. Slowing the growth of ice with synthetic macromolecules: beyond antifreeze(glyco) proteins. *Polym Chem* **1**, 1141–1152 (2010).
 46. Froud, S. J. The development, benefits and disadvantages of serum-free media. *Dev Biol Stand* **99**, 157–166 (1999).
 47. Sinacore, M. S., Drapeau, D. & Adamson, S. R. Adaptation of Mammalian Cells to Growth in Serum-Free Media. *Mol Biotechnol* **15**, 249–258 (2000).
 48. Baust, J. M. Molecular Mechanisms of Cellular Demise Associated with Cryopreservation Failure. *Cell Preserv Technol* **1**, 17–31 (2002).
 49. Carpenter, J. F. & Hansen, T. N. Antifreeze protein modulates cell survival during cryopreservation: mediation through influence on ice crystal growth. *Proc Natl Acad Sci USA* **89**, 8953–8957 (1992).
 50. Chao, H., Davies, P. L. & Carpenter, J. F. Effects of antifreeze proteins on red blood cell survival during cryopreservation. *J Exp Biol* **199**, 2071–2076 (1996).
 51. Matsumoto, S. *et al.* Effects of synthetic antifreeze glycoprotein analogue on islet cell survival and function during cryopreservation. *Cryobiology* **52**, 90–98 (2006).
 52. Budke, C. & Koop, T. Ice recrystallization inhibition and molecular recognition of ice faces by poly(vinyl alcohol). *ChemPhysChem* **7**, 2601–2606 (2006).
 53. Congdon, T., Notman, R. & Gibson, M. I. Antifreeze (Glyco)protein Mimetic Behavior of Poly(vinyl alcohol): Detailed Structure Ice Recrystallization Inhibition Activity Study. *Biomacromolecules* **14**, 1578–1586 (2013).
 54. Singer, S. J. & Nicolson, G. L. The fluid mosaic model of the structure of cell membranes. *Science* **175**, 720–731 (1972).
 55. Redwood, W. R. & Haydon, D. A. Influence of temperature and membrane composition on the water permeability of lipid bilayers. *J Theor Biol* **22**, 1–8 (1969).
 56. Muldrew, K. & McGann, L. E. Mechanisms of intracellular ice formation. *Biophys J*

- 57**, 525–532 (1990).
57. Acker, J. P. & McGann, L. E. Membrane damage occurs during the formation of intracellular ice. *Cryo Lett* **22**, 241–254 (2001).
 58. Meryman, H. T. Cryoprotective agents. *Cryobiology* **8**, 173–183 (1971).
 59. Griffith, M. & Ewart, K. V. Antifreeze proteins and their potential use in frozen foods. *Biotechnol Adv* **13**, 375–402 (1995).
 60. Matsumura, S., Kurita, H. & Shimokobe, H. Anaerobic biodegradability of polyvinyl alcohol. *Biotechnol Lett* **15**, 749–754 (1993).
 61. Leibo, S. P. & Mazur, P. The role of cooling rates in low-temperature preservation. *Cryobiology* **8**, 447–452 (1971).
 62. Butler, J. E. Enzyme-Linked Immunosorbent Assay. *J Immunoassay* **21**, 165–209 (2000).
 63. Yumoto, R., Suzuka, S., Oda, K., Nagai, J. & Takano, M. Endocytic uptake of FITC-albumin by human alveolar epithelial cell line A549. *DMPK* **27**, 336–343 (2012).
 64. Huang, M., Ma, Z., Khor, E. & Lim, L.-Y. Uptake of FITC-chitosan nanoparticles by A549 cells. *Pharm Res* **19**, 1488–1494 (2002).
 65. Li, C. & Liu, S. Polymeric assemblies and nanoparticles with stimuli-responsive fluorescence emission characteristics. *Chem Comm* **48**, 3262 (2012).
 66. Soppimath, K. S., Aminabhavi, T. M., Kulkarni, A. R. & Rudzinski, W. E. Biodegradable polymeric nanoparticles as drug delivery devices. *J Control Release* **70**, 1–20 (2001).
 67. Morris, M. C., Depollier, J., Mery, J., Heitz, F. & Divita, G. A peptide carrier for the delivery of biologically active proteins into mammalian cells. *Nat Biotechnol* **19**, 1173–1176 (2001).
 68. Levin, R. L. & Miller, T. W. An optimum method for the introduction or removal of permeable cryoprotectants: isolated cells. *Cryobiology* **18**, 32–48 (1981).
 69. Foster, K., Oster, C., Mayer, M., Avery, M. & Audus, K. Characterization of the A549 cell line as a type II pulmonary epithelial cell model for drug metabolism. *Exp Cell Res* **243**, 359–366 (1998).
 70. Fehrenbacher, N. & Jäättelä, M. Lysosomes as Targets for Cancer Therapy. *Cancer Res* **65**, 2993–2995 (2005).
 71. Berridge, M. V. & Tan, A. S. Characterization of the Cellular Reduction of 3-(4,5-dimethylthiazol-2-yl)-2,5-diphenyltetrazolium bromide (MTT): Subcellular Localization, Substrate Dependence, and Involvement of Mitochondrial Electron Transport in MTT Reduction. *Arch Biochem Biophys* **303**, 474–482 (1993).
 72. Pattillo, R. & Gey, G. The establishment of a cell line of human hormone-synthesizing trophoblastic cells in vitro. *Cancer Res* **28**, 1231–1236 (1968).
 73. Orendi, K., Gauster, M., Moser, G., Meiri, H. & Huppertz, B. The choriocarcinoma cell line BeWo: syncytial fusion and expression of syncytium-specific proteins. *Reproduction* **140**, 759–766 (2010).
 74. Huppertz, B. IFPA Award in Placentology Lecture: Biology of the placental

- syncytiotrophoblast – Myths and facts. *Placenta* **31**, S75–S81 (2010).
75. Delidakis, M., Gu, M., Hein, A., Vatish, M. & Grammatopoulos, D. Interplay of cAMP and MAPK pathways in hCG secretion and fusogenic gene expression in a trophoblast cell line. *Mol Cell Endocrinol* **332**, 213–220 (2010).
 76. Pattillo, R. A. *et al.* Control mechanisms for gonadotrophic hormone production in vitro. *In Vitro* **6**, 205–214 (1970).
 77. Pattillo, R. A., Gey, G. O., Delfs, E. & Mattingly, R. F. Human Hormone Production in vitro. *Science* **159**, 1467–1469 (1968).
 78. Morrish, D. W., Bhardwaj, D., Dabbagh, L. K., Marusyk, H. & Siy, O. Epidermal growth factor induces differentiation and secretion of human chorionic gonadotropin and placental lactogen in normal human placenta. *J Clin Endocrinol Metab* **65**, 1282–1290 (1987).
 79. Al-Nasiry, S., Spitz, B., Hanssens, M., Luyten, C. & Pijnenborg, R. Differential effects of inducers of syncytialization and apoptosis on BeWo and JEG-3 choriocarcinoma cells. *Hum Reprod* **21**, 193–201 (2006).
 80. Braunstein, G. D., Rasor, J., Danzer, H., Adler, D. & Wade, M. E. Serum human chorionic gonadotropin levels throughout normal pregnancy. *Am J Obstet Gynecol* **126**, 678–681 (1976).
 81. Kliman, H. J., Nestler, J. E., Sermasi, E., Sanger, J. M. & Strauss, J. F. Purification, Characterization, and *in vitro* Differentiation of Cytotrophoblasts from Human Term Placentae. *Endocrinology* **118**, 1567–1582 (1986).
 82. Cervinski, M. A. *et al.* Qualitative point-of-care and over-the-counter urine hCG devices differentially detect the hCG variants of early pregnancy. *Clin Chim Acta* **406**, 81–85 (2009).
 83. Meryman, H. T. Cryopreservation of living cells: principles and practice. *Transfusion* **47**, 935–945 (2007).
 84. De Fries, R. & Mitsuhashi, M. Quantification of mitogen induced human lymphocyte proliferation: Comparison of alamarbluetm assay to ³h-thymidine incorporation assay. *J Clin Lab Anal* **9**, 89–95 (1995).
 85. Prouillac, C. & Lecoecur, S. The role of the placenta in fetal exposure to xenobiotics: importance of membrane transporters and human models for transfer studies. *Drug Metab Dispos* **38**, 1623–1635 (2010).
 86. Pan, C., Kumar, C., Bohl, S., Klingmueller, U. & Mann, M. Comparative Proteomic Phenotyping of Cell Lines and Primary Cells to Assess Preservation of Cell Type-specific Functions. *Mol Cell Proteomics* **8**, 443–450 (2009).
 87. Scarino, M. L. & Howell, K. E. The Fao cell. A tissue culture model for lipoprotein synthesis and secretion. I. Characterization of the system. *Exp Cell Res* **170**, 1–14 (1987).
 88. Decaens, C., Durand, M., Grosse, B. & Cassio, D. Which in vitro models could be best used to study hepatocyte polarity? *Biol Cell* **100**, 387–398 (2008).
 89. Pitot, H. C., Peraino, C., Morse, P. A. & Potter, V. R. Hepatomas in tissue culture compared with adapting liver *in vivo*. *Natl Cancer Inst Monogr* **13**, 229–245

- (1964).
90. Reuber, M. D. A transplantable bile-secreting hepatocellular carcinoma in the rat. *J Natl Cancer Inst* **26**, 891–899 (1961).
 91. Donato, M. T., Gomezlechon, M. J. & Castell, J. V. A Microassay for Measuring Cytochrome p450IA1 and Cytochrome p450IIB1 Activities in Intact Human and Rat Hepatocytes Cultured on 96-Well Plates. *Anal Biochem* **213**, 29–33 (1993).
 92. Gomez-Lechon, M., Donato, M., Castell, J. & Jover, R. Human Hepatocytes in Primary Culture: The Choice to Investigate Drug Metabolism in Man. *CDM* **5**, 443–462 (2004).
 93. Lin, J. H. & Lu, A. Y. H. Inhibition and Induction of Cytochrome p450 and the Clinical Implications. *Clin Pharmacokinet* **35**, 361–390 (1998).
 94. Knowles, B., Howe, C. & Aden, D. P. Human hepatocellular carcinoma cell lines secrete the major plasma proteins and hepatitis B surface antigen. *Science* **209**, 497–499 (1980).
 95. Aden, D. P., Fogel, A., Plotkin, S., Damjanov, I. & Knowles, B. B. Controlled synthesis of HBsAg in a differentiated human liver carcinoma-derived cell line. *Nature* **282**, 615–616 (1979).
 96. Rodríguez-Antona, C. *et al.* Cytochrome p450 expression in human hepatocytes and hepatoma cell lines: molecular mechanisms that determine lower expression in cultured cells. *Xenobiotica* **32**, 505–520 (2002).
 97. Fujimura, H., Murakami, N., Miwa, S., Aruga, C. & Toriumi, W. The suitability of rat hepatoma cell line H4IIE for evaluating the potentials of compounds to induce CYP3A23 expression. *Exp Toxicol Pathol* **64**, 527–533 (2012).
 98. Schoonen, W. G. E. J., Stevenson, J. C. R., Westerink, W. M. A. & Horbach, G. J. Cytotoxic effects of 109 reference compounds on rat H4IIE and human HepG2 hepatocytes. III: Mechanistic assays on oxygen consumption with MitoXpress and NAD(P)H production with Alamar Blue™. *Toxicol In Vitro* **26**, 511–525 (2012).
 99. Auricchio, F., MARTIN, D. & TOMKINS, G. Control of Degradation and Synthesis of Induced Tyrosine Aminotransferase studied in Hepatoma Cells in Culture. *Nature* **224**, 806–808 (1969).
 100. Baxter, J. D. & Tomkins, G. M. The relationship between glucocorticoid binding and tyrosine aminotransferase induction in hepatoma tissue culture cells. in *Proc Natl Acad Sci USA* **65**, 709–715 (1970).
 101. Valeriote, F. A., Auricchio, F., Tomkins, G. M. & Riley, D. Purification and Properties of Rat Liver Tyrosine Aminotransferase. *J Biol Chem* **244**, 3618–3624 (1969).
 102. Gurr, J. A. & Potter, V. R. Independent induction of tyrosine aminotransferase activity by dexamethasone and glucagon in isolated rat liver parenchymal cells in suspension and in monolayer culture in serum-free media. *Exp Cell Res* **126**, 237–248 (1980).
 103. Diamondstone, T. I. Assay of tyrosine transaminase activity by conversion of p-hydroxyphenylpyruvate to p-hydroxybenzaldehyde. *Anal Biochem* **16**, 395–401

- (1966).
104. McMillian, M. K. *et al.* An improved resazurin-based cytotoxicity assay for hepatic cells. *Cell Biol Toxicol* **18**, 157–173 (2002).
 105. O'Brien, J., Wilson, I., Orton, T. & Pognan, F. Investigation of the Alamar Blue (resazurin) fluorescent dye for the assessment of mammalian cell cytotoxicity. *Eur J Biochem* **267**, 5421–5426 (2000).
 106. Gagne, D., Labhili, M. & Pons, M. Description and analysis of differential sensitivity to glucocorticoids in Fao cells. *J Steroid Biochem* **31**, 917–925 (1988).

CHAPTER 5.

5. ICE RECRYSTALLIZATION INHIBITORS IMPROVE THE CRYOPRESERVATION OF PRIMARY CELLS.

5.1. CHAPTER SUMMARY.

The application of poly(vinyl alcohol) (PVA) that has been previously identified (Chapter 2) as a potent ice recrystallization inhibition (IRI) compound is explored as a cryoprotectant for improving the cryopreservation of primary cells, namely rat hepatocytes and mouse mesenchymal stem cells (MSCs). There is a great clinical and pharmacological demand for primary cells, tissues and organs in the fields of transplantation, pharmacology and regenerative medicine. Low concentrations of 9 kDa PVA are shown to improve the recovery of cryopreserved rat hepatocytes when a slow thawing strategy was used, though higher concentrations proved detrimental in agreement with observations noted prior with RBCs and immortalized cell lines (Chapter 3 and Chapter 4). In addition to improving the cryopreservation of rat hepatocytes, low concentrations of 9 kDa PVA may also be of benefit in the cryopreservation of mouse MSCs though further work is required to accurately confirm any beneficial effect. The presence of 9 kDa PVA during the cryopreservation process critically however did not affect the potential of mouse MSCs to undergo differentiation (adipogenesis) into adipocytes. This suggests the 9 kDa PVA may be a powerful

tool for modulating IR activity and limit cryodamage that arises as a consequence.

5.2. INTRODUCTION.

Primary (nucleated) cells are biological materials with the greatest clinical value. Whether these are cells such as hepatocytes or islets sourced from living or deceased donors for use in transplantation¹⁻⁴ or the isolation of pluripotent stem cells. Pluripotent stem cells of which are of increasing importance due to the growth of tissue engineering and regenerative medicine.^{5,6} Greater availability of primary cells undoubtedly has the potential to dramatically advance healthcare in the 21st century with their direct therapeutic application and in accelerating pharmaceutical development as more relevant pharmacological models.⁷⁻⁹ However the cryopreservation of primary cells is poorly implemented except in the field of reproductive medicine in which samples tend to be successfully and routinely managed albeit on a small scale.¹⁰ This accomplishment has had a fundamental impact on embryology and in the selective breeding of livestock in agriculture.^{11,12} In contrast to the successful cryostorage of primary reproductive material few strategies for the long term cryostorage of large tissues and organs exist whereby the utilization of short term hypothermic perfusion techniques predominate.¹³ However such solutions may be more susceptible to bacterial contamination. This contamination has resulted in scenarios whereby such solutions have had to be withdrawn from clinical use¹⁴⁻¹⁶ and thus an alternative to prolong the storage of primary biological materials safely and effectively is a highly desired attribute. The need for improved cryopreservation strategies is critical more than ever with the emergence of stem cell therapies that may become more frequently utilized in the coming decades especially with an aging population and increasing drives towards personalized medicine.¹⁷⁻²⁰

Current strategies to cryopreserve primary cells, tissues and organs have focused on the use of organic solvents that have had effectiveness with less

sensitive and less valuable biological materials and with vitrification strategies that aim to eliminate ice formation.²¹⁻²³ However the use of organic solvents and the high concentrations required in order for them to be effective cryoprotectants is undesirable as such solvents possess cytotoxic properties that cannot be neutralized easily.²⁴ Plus the removal of these (membrane permeable) cryoprotectants is non-trivial. The vitrification of biological samples is also currently limited to small volumes. Additionally devitrification and then consequently ice formation during thawing would also need to be averted as rapidly thawing large volumes homogeneously to overcome ice recrystallisation is not practically achievable.²⁵⁻²⁷

A few studies have investigated the use of AFPs, AF(G)Ps and closely related derivatives but with varied success.²⁸ In particular these proteins and compounds have failed to successfully cryopreserve cardiac tissues due to the tendencies of these molecules to actually heighten cryodamage as a consequence of DIS and intracellular ice formation.^{29,30} Success has been demonstrated though with both islets³¹ and hepatocytes³² whereby improvements in cell recovery were attained by the supplementation of comparatively low concentrations of IRI active molecules. In addition to studies that use AFPs and AF(G)Ps the supplementation of oligosaccharides including trehalose, raffinose and maltoheptose at (high) concentrations that have moderate IRI activity (Figure 2.27 and Figure 2.28) to rat hepatocytes had a demonstrable cryoprotective effect, though their protective effect is more akin to their ability to incite vitrification as oppose to their actions as mildly active IRI compounds.³³ To date though no known studies have been reported that investigates the use of naturally occurring antifreezes or closely related mimics thereof with haematopoietic, embryonic or mesenchymal stem cells (MSCs). The addition of PVA has been reported to be beneficial with MSCs using a DMSO free method in both a vitrifying and non-vitrifying context however.³⁴ Cell recovery under these

conditions was greatest when using a vitrifying method with the addition of PVA allowing an additional 25% of cells to be recovered. PVA has been shown elsewhere to assist in the preventing nucleation under vitrifying conditions and also limit ice crystal growth in these solutions.³⁵ Observations identified with RBCs (Chapter 3) and with immortalized mammalian cell lines (Chapter 4) in conjunction with literatures findings warranted the preliminary investigation of PVA with primary cells in order assess its cryoprotective potential as an IRI active compound and compatibility with downstream applications.

5.3. RESULTS AND DISCUSSION.

5.3.1. Cryopreservation of Primary Rat Hepatocytes.

The demand for hepatic tissue can be emphasized by the number of liver transplants undertaken per annum in addition to the length of current waiting lists that further stresses the desire to maintain the highest possible viabilities *ex vivo* in order to ensure that no material is wasted given the scarcity of clinically eligible donors. For example the number of liver transplant procedures undertaken in the US in 2011 and in 2012 was approximately 6,000 in each year yet the number of recipients awaiting transplantation exceeded 15,000.^{3,36} The shortage of human hepatic tissue means that rat hepatocytes are routinely used in *in vitro* studies especially with regards to assessing the toxicity and metabolism of xenobiotics.³⁷⁻⁴⁰ Rat hepatocytes are therefore still of importance with many similarities to human hepatocytes and so a representative model. However rat hepatocytes were still only available in limited quantities (Figure 5.1.).

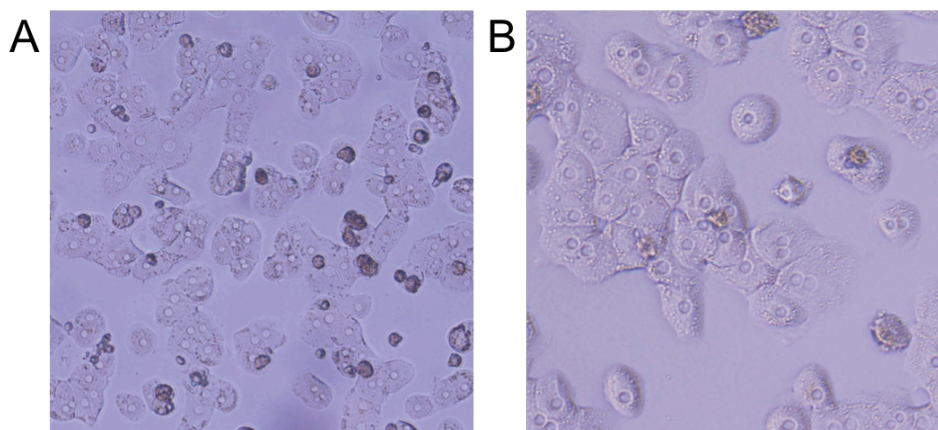


Figure 5.1. Phase contrast light micrographs of primary rat hepatocytes. 24 hours after isolation plated on collagen coated plates at (A) 100x magnification and (B) 200x magnification.

Due to the lack of available material a full investigation into the cytotoxic effects of DMSO on rat hepatocytes was not undertaken as with immortalized mammalian cells (Section 4.3.1.). DMSO is known to be cytotoxic to rat hepatocytes and have a minor effect on hepatocyte gene expression, though these changes in expression were considered to have minimal toxicological impact. At high concentrations of DMSO however such alterations may become significant.⁴¹ Differences in the cell culture conditions can also influence gene expression profiles.⁴² Furthermore some studies have however actively investigated how the supplementation of low concentrations of DMSO (up to 2 % (v/v)) which can be reasonably well tolerated with beneficial effects *in vitro* that enable prolonged maintenance.⁴³⁻⁴⁷

However it is important to investigate the potential influence that 9 kDa PVA may have, though the biocompatibility of 9 kDa PVA has proven exemplary with previously tested cells (Figures 3.2., 4.1. and 4.10.). The impact of 20 mg/mL 9 kDa PVA incubated with freshly isolated hepatocytes over a 4-hour period was assessed by the resazurin reduction assay.⁴⁸ Figure 5.2. shows the relative fluorescence both before and after the addition of 20 mg/mL 9 kDa PVA, which as established prior is far greater than the amount required to have a IRI effect (Figure 2.17.) with a cell viability equivalent to 85.0 % \pm 11.2 % attained. Therefore a slight cytotoxic effect at this concentration and at physiological temperatures for a prolonged period may be apparent. However several studies have shown that the concentration of numerous (liver specific) cytochrome p450 isoforms declines rapidly after isolation.⁴⁹ Cytochrome p450s are known to metabolize (phase I) a vast majority of commercially available pharmaceutical xenobiotics by catalyzing their oxidation. This decline is significant in terms of the desire to minimize any post-thaw processing to maintain their usefulness as a valid drug metabolism model,⁵⁰ with rat hepatocytes (relative catalytic activity after 24 hours of 53 % \pm 5 %) having a greater susceptibility than human

hepatocytes (relative catalytic activity after 24 hours of $81 \% \pm 10 \%$).⁵¹ Though the exact catalytic mechanism for the reduction of resazurin to resorufin is unknown at present⁵² they may be a similar effect that results in a decline in the rate of resazurin conversion that accounts at least partially for the perceived lower cell viability. The presence of adherent but non-viable material (Figure 5.1.) in which the isolated rat hepatocytes contained a notable proportion of non-viable cells ($21.7 \% \pm 5.7 \%$) deemed by a trypan blue exclusion assay might also affect the longevity of maintaining rat hepatocytes *ex vivo*.

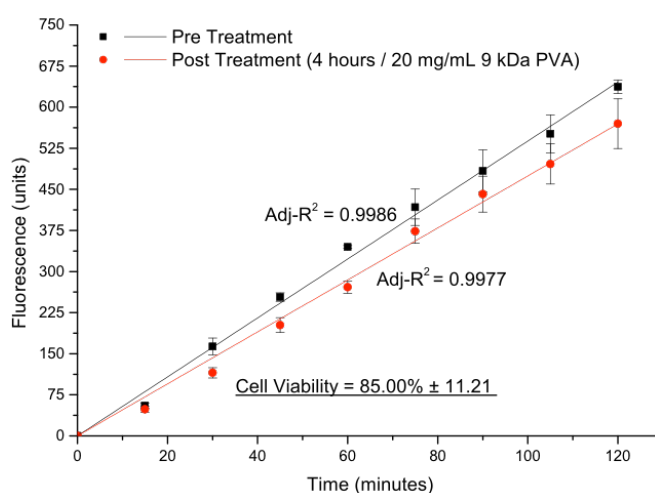


Figure 5.2. Cytotoxicity of 9 kDa PVA to rat hepatocytes. Resorufin fluorescence over a 2-hour incubation period showing the rate of resazurin to resorufin conversion prior to and after addition of 20 mg/mL 9 kDa PVA incubated for 4 hours.

Cryopreservation of rat hepatocytes⁵³ (1×10^6 cells) was undertaken using slow-freezing (Section 5.5.3.) with 10 % (v/v) DMSO supplemented with or without various concentrations of 9 kDa PVA (Figure 5.3.) inline with current protocols. The addition of low concentrations of 9 kDa PVA (1 mg/mL) improved recovery levels ($49.1 \% \pm 5.4 \%$) compared to DMSO alone ($35.4 \% \pm 3.0 \%$) when using a slow thawing strategy that promotes ice recrystallization but these values were still far lower than when using a rapid thawing strategy (100 %). High concentrations of 9 kDa PVA (10 mg/mL) however proved dramatically

detrimental with cell recovery equal to just 11.6 % \pm 7.4 % following trends observed with all other cell types tested and thus should not be surprising (Figures 3.9., 4.3., 4.4., 4.6., 4.7., 4.12. and 4.14.). Going forward therefore with an ample supply of cells, investigating whether or not larger (or smaller) PVA molecules that have varied IRI (and DIS) activities also display a concentration dependant benefit as cryoprotectants in order to identify the optimum concentration of PVA for a variety of MWs and whether or not this correlates with a single IRI value.

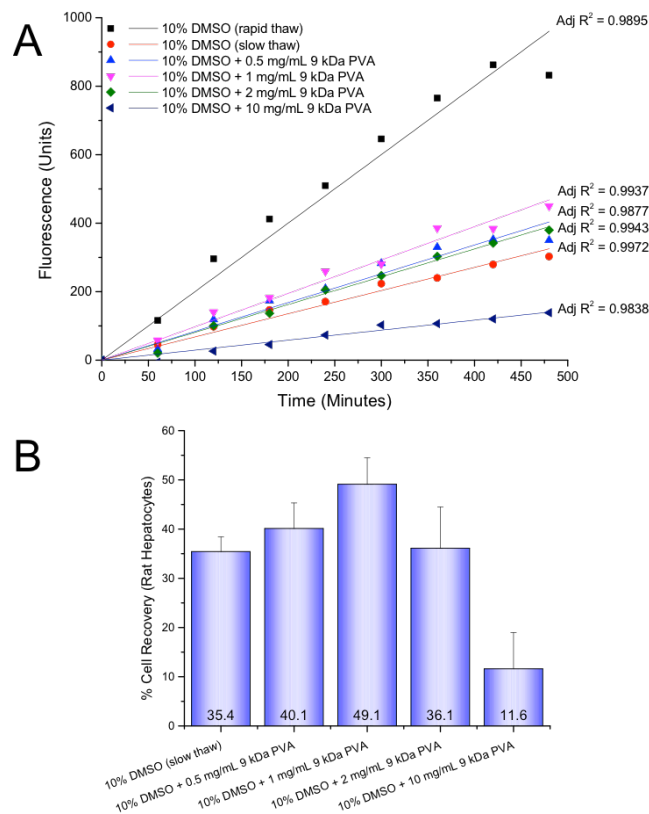


Figure 5.3. Impact of 9 kDa PVA on the cryopreservation of rat hepatocytes.

Cryopreservation of rat hepatocytes with 10 % (v/v) DMSO supplemented with and without various concentrations of 9 kDa PVA. (A) Resazurin assay undertaken on cryopreserved rat hepatocytes with fluorescence values measured at 60-minute intervals. (B) (%) Cell recovery of rat hepatocytes cryopreserved with and without 9 kDa PVA referenced against rapidly thawed 10 % (v/v) DMSO samples (minimal ice recrystallization damage). Values represent the mean of 2 cryovials measured individually with the error bars representing \pm standard deviation.

5.3.2. Cryopreservation of Mouse Mesenchymal Stem Cells.

Mesenchymal stem cells (MSCs) (Figure 5.4.) can be derived from either umbilical cord blood (UCB)⁵⁴ or from bone marrow tissue.⁵⁵ MSCs are of interest in that they are able to proliferate significantly *in vitro* yet still retain a multipotent capacity. MSCs are typically able to differentiate into adipocytes, chondrocytes or osteocytes each with specific phenotypes.⁵⁶ MSCs have also been forcibly differentiated into non-typical MSC derived endpoints such as neuronal⁵⁷ and myogenic cells.⁵⁸ Therefore there is abundant interest in the cryopreservation of MSCs due to their therapeutic potential.⁵⁹ However there must be caution concurrently as for example undifferentiated MSCs applied to damaged cardiac tissues resulted in a subset of the population differentiating into fibroblastic scar tissue which could prove problematic in the recovery process after a myocardial infarction.^{60,61} However MSCs are largely considered to be safe for therapeutic use according to a review of recently conducted clinical trials.⁶²

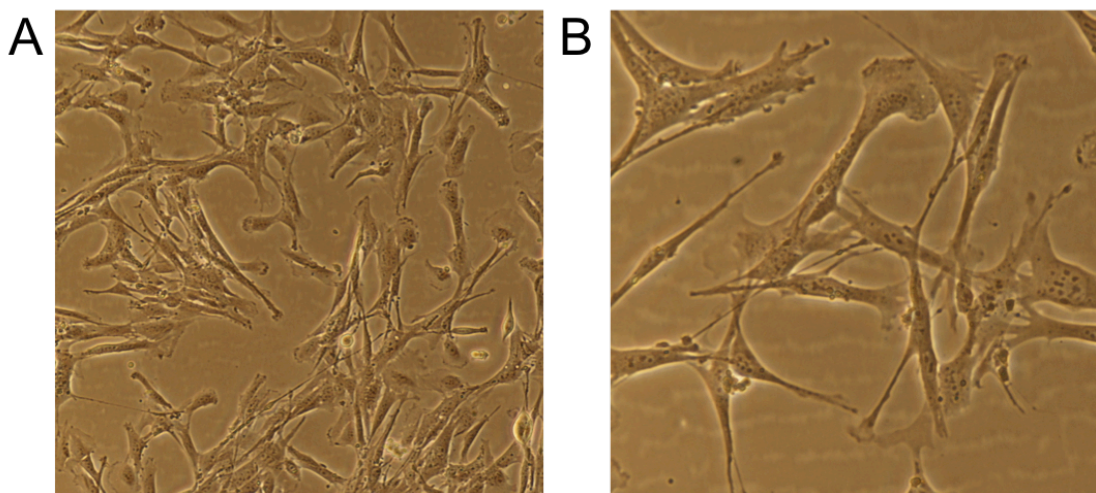


Figure 5.4. Phase contrast light micrographs of mouse mesenchymal stem cells. Mouse MSCs prior to cryopreservation and adipogenesis. (A) 100x magnification and (B) 200x magnification.

The cryopreservation of MSCs is therefore complicated in that any cryopreservation process needs to not interfere with their proliferative capacity and differentiation potential. This means neither reducing the number of inducible fates nor triggering spontaneous differentiation. The cryopreservation of MSCs is of particular importance therefore as continuously propagated MSCs will begin to lose their multipotency even after a few passages.^{63,64} The cost of reagents (due to their purity and complex composition) is also another factor that supports the long term cryostorage of MSCs. Therefore any potential improvements to the cryopreservation of MSCs that also lessens the concentration of DMSO required for cryopreservation would be advantageous. Figure 5.5. shows how the supplementation of 9 kDa PVA to 10 % (v/v) DMSO which is the concentration used in the majority of cryopreservation (slow freezing) protocols at present affects cell recovery (100 % cell recovery refers to the number of cells recovered after cryopreservation using a rapid thawing strategy) of mouse MSCs (Section 5.5.4.). A clear difference between thawing MSCs slowly (66.5 % \pm 2.2 %) and rapidly (100 % \pm 3.2 %) is apparent indicative of IR damage with the addition of small concentrations of (1 mg/mL) 9 kDa PVA having a possible cryoprotective effect (72.3 % \pm 19.8 %) but more data would be necessary to corroborate this, though as with all other cell types the presence of greater amounts of 9 kDa PVA proved injurious with 3 mg/mL 9 kDa PVA eliciting cell recovery equivalent to 43.2 % \pm 3.7 %.

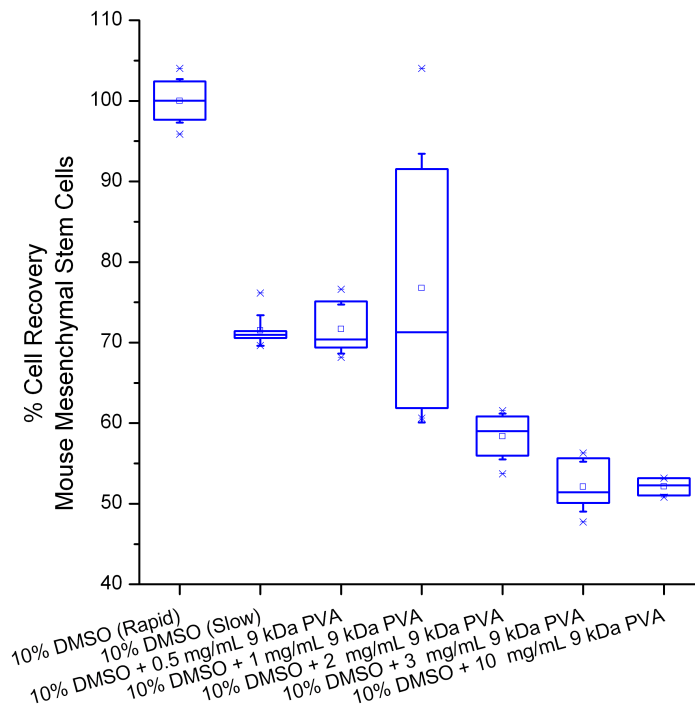


Figure 5.5. Impact of 9 kDa PVA on the cryopreservation of Mouse MSCs.

Resazurin assay of mouse MSCs cryopreserved with 10 % (v/v) DMSO supplemented with and without 9 kDa PVA. Values represent the mean of 2 cryovials plated in triplicate measured in duplicate with the error bars representing \pm standard deviation.

Though the resazurin reduction assay is a good indicator of overall cell viability the ability of recovered MSCs to undergo differentiation that is a complex transformation reliant on the correct signalling of numerous biochemical pathways is a more stringent examination of the effects of 9 kDa PVA supplementation in the cryopreservation process. Three fates (adipocytes, chondrocytes, osteocytes) are inducible using commercially available cocktails allowing detectable phenotypic changes over a 7-14 day period. Therefore MSCs assessed using the resazurin assay prior were evaluated for their potential to differentiate (adipogenesis) into adipocytes (Section 5.5.5.).⁶⁵ Figure 5.6. shows a representative phase contrast micrograph 9 days after the application of adipocyte differentiation medium (critically differentiation inhibits any sizable

proliferation) that successfully shows the presence of visible lipid droplets (black arrows) that are a phenotypic characteristic of adipocytes.⁶⁶

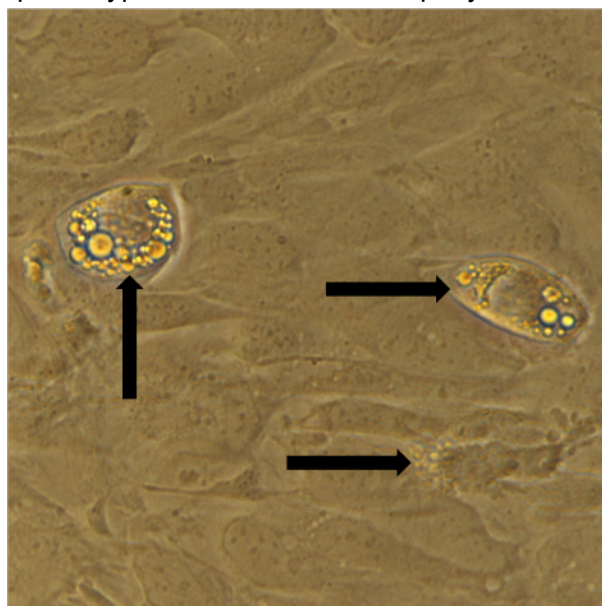


Figure 5.6. Visual assessment of mouse MSC adipogenesis. Phase contrast light micrograph of mouse MSCs subsequent to cryopreservation and 9 days post adipogenesis induced differentiation (200x magnification). Arrows highlight the presence of lipid droplets indicative of adipocytes.

To further clarify the existence of adipocytes, the cells were fixed 11 days after the application of adipocyte differentiation medium using a 2 % (v/v) glutaldehyde solution and stained using two non-competitive fluorescent dyes. The first dye utilised was Hoechst 33258 that is a fluorescent dye with a high affinity for DNA (chromatin) with excitation and emission maximums of 352 nm and 461 nm respectively.^{67,68} Hoechst 33258 will therefore bind any cells present regardless of whether or not they have undergone differentiation. As a result of the non-cell specificity of Hoechst 33258 a second dye specific for adipocytes was used. LipidTOX™ Red is a fluorophore that binds specifically to neutral lipids and thus an excellent indicator of adipogenesis and has excitation and emission maximums of 577 nm and 609 nm respectively. The ratio of each dye (Figure 5.7.) therefore shows the effect that 9 kDa PVA has had on the ability of the cell population to undergo adipogenesis.

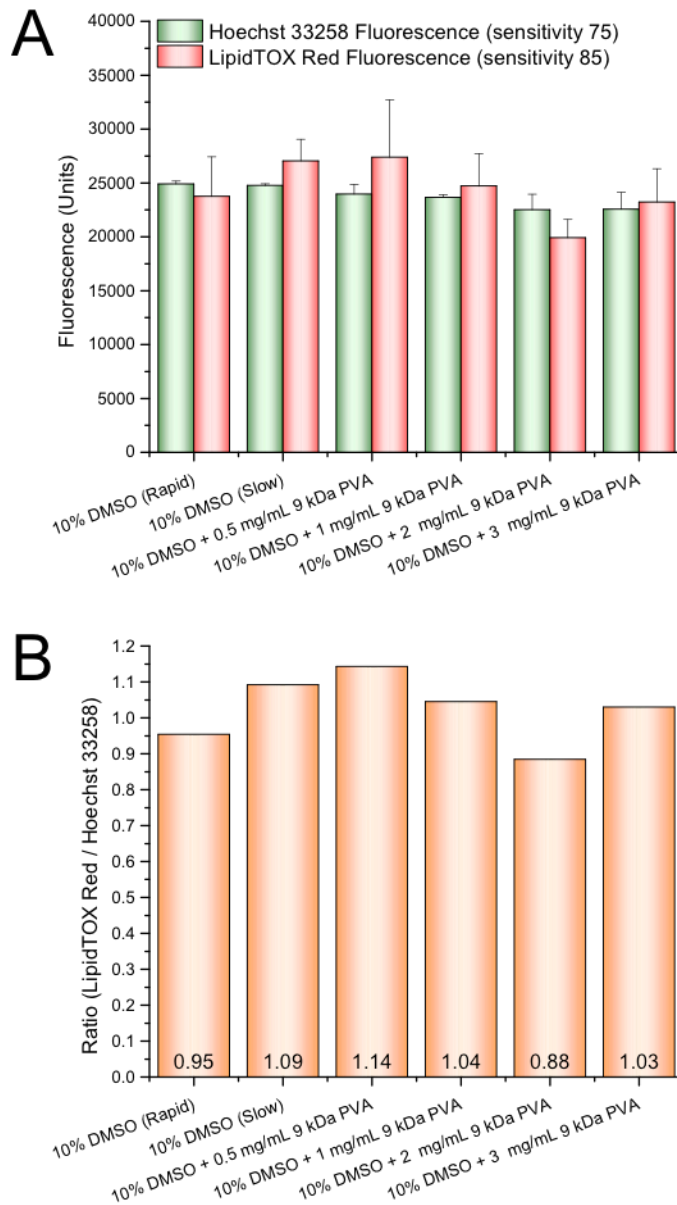


Figure 5.7. Fluorescence intensities of Hoechst 33258 and LipidTOX™ Red as indicators of adipogenesis. (A) Relative fluorescence intensities of Hoechst 33258 (460/40 nm) and LipidTOX™ Red (640/40 nm) consequent to fluorophore staining of cells cryopreserved using a variety of solutions. (B) Ratio of LipidTOX™ Red:Hoechst 33258 highlighting relatively consistent levels of adipogenesis.

Figure 5.7.A. shows that the relative fluorescence intensities of both dyes are roughly equal across each of the cryopreservation solutions (but not to each

other given the different sensitivities employed) emphasizing that adipogenesis is approximately uniform (Figure 5.7.B.). 9 kDa PVA is perceived to act only in an extracellular context due to its membrane impermeability with A549 cells (Section 4.3.3.) and there is no reason to assume otherwise here and thus 9 kDa PVA is removed prior to the initiation of adipogenesis. This shows that the presence of 9 kDa PVA during cryopreservation does not affect the ability of cells to differentiate into adipocytes with the presence of lipid droplets (Figure 5.6.) and resulting LipidTOX™ Red staining. Further work would ideally investigate the ability of (9 kDa PVA) cryopreserved MSCs to differentiate into both chondrocytes and osteocytes that both have well defined endpoints and further refine the concentrations of both DMSO and 9 kDa PVA to identify the optimum composition for cryopreservation. Plus the rate at which differentiation occurs to ensure no significant changes in behavior are observed due to the presence of 9 kDa PVA in the cryopreservation process would be a valid measure of normality. In addition, application to human MSCs to assess whether these behave in a similar fashion would be an attractive avenue of interest from a clinical point of view. Plus the ability to improve the cryopreservation of other stem cell types (embryonic and haematopoietic) that would potentially yield the greatest clinical benefit.⁶⁹⁻⁷¹

The application of 9 kDa PVA has from these early observations arguably not had as profound a benefit with primary cells as noted elsewhere in Chapter 3 and Chapter 4 with other cell types. A possible rationale for a reduction in the benefit of 9 kDa PVA is that the use of a higher concentration of DMSO (10 % (v/v)) will alter the thawing process meaning the onset of thawing will differ, beginning at a lower temperature (Figure 2.24.).⁷² Furthermore the presence of greater amounts of DMSO will affect extracellular ice crystal growth in part due to the alteration in the melting point. Suppression of the melting point in these system will reduce IR partially and henceforth decrease the amount of IR damage that can be

subsequently attenuated. However this reduction in IR damage does not justify the concentration of DMSO because as noted elsewhere DMSO is significantly cytotoxic. Therefore lowering the concentration of DMSO (that may prove beneficial to recovery regardless) applied is likely to give an advantageous effect superior to those observed here (Figure 5.3. and Figure 5.5). For the reason that extracellular ice formation drives the efflux of H₂O and hence aids to avoid intracellular ice formation that is highly damaging. There is no doubt that a higher concentration of DMSO will also cause an increase in H₂O efflux but as the system approaches equilibrium (by the passive diffusion of DMSO) the greater amount of DMSO will only account for a small difference proportionately in osmotic pressure. Extracellular ice formation lowers the extracellular liquid H₂O content increasing solute concentration concurrently as solutes are not incorporated into ice (solute rejection).⁷³ Solute rejection also serves to change the viscosity that further influences ice formation, differences in temperature will also cause changes in thermodynamics that will influence the rate of H₂O exchange and ice crystal growth.^{23,74} Extracellular ice formation is therefore an important part of the cryopreservation process in promoting cellular dehydration, though subsequent growth is not desirable as iterated previously. A lower concentration (i.e. lower than 10 % (v/v)) of DMSO may therefore in this instance prove beneficial and thus improve the overall rates of cell recovery upon the addition of 9 kDa PVA (Chapter 3 and Chapter 4) and thus remains a tantalizing area of future investigation.

5.4. CONCLUSIONS.

The application of IRI active 9 kDa PVA to two distinctive primary cell varieties has been investigated in order to improve their cryopreservation with an eventual aim of reducing the currently high concentrations of cytotoxic organic solvents such as DMSO required in existing cryopreservation strategies. Freshly isolated primary hepatocytes were shown to be tolerant of 20 mg/mL 9 kDa PVA that is a concentration far than necessary for IRI activity. The addition of low concentrations (1 mg/mL) of 9 kDa PVA proved beneficial when utilizing a slow thawing strategy at improving the number of cells recovered post thaw. However the addition of higher concentrations of 9 kDa PVA (10 mg/mL) that have a superior activity and thus greater potential at attenuating IR cryodamage were detrimental and this is speculated to be due to a secondary DIS effect that enhances mechanical damage offsetting to the benefits attained from IRI, similar to findings observed and reported elsewhere. Secondly the potential of 9 kDa PVA to improve the cryopreservation of mouse MSCs was undertaken showing a mild beneficial effect at low concentrations though further work is needed to clarify this. Nevertheless higher concentrations of 9 kDa PVA appeared to again be detrimental to total cell recovery as with rat hepatocytes no doubt due to a similar increase in the level of DIS induced mechanical damage. However the presence of 9 kDa PVA during cryopreservation at all concentrations tested appeared to have minimal influence on the downstream ability of mouse MSCs to undergo adipogenesis with an approximately proportional number of adipocytes detected in each instance. Therefore the presence of 9 kDa PVA at low concentrations (1 mg/mL) that influences extracellular ice crystal growth during thawing can be a powerful tool for attenuating IR without intolerable levels of DIS that elevate mechanical damage and thus improve the recovery of primary cells as a supplement to traditional cryopreservation strategies.

5.5. MATERIALS AND METHODS

5.5.1. Isolation and preparation of Rat Hepatocytes.

Approximately 1.5×10^7 of freshly isolated rat (sprague dawley) hepatocytes were provided by the Marrion Bessin Liver Centre at The Albert Einstein College of Medicine, Bronx, NY, USA prepared according standard (percoll) protocols.⁷⁵ A small aliquot was taken and diluted 6.66'-fold in complete medium (DMEM, High Glucose + 10 % (v/v) FCS and supplemented with Penicillin (100 U/mL) and Streptomycin (100 μ g/mL) all of which were sourced from Sigma Aldrich Corp., MO, USA) to estimate viability using a standard trypan blue exclusion assay with the proportion of viable cells equal to 78.3 % \pm 5.7 % of the observable population. Cells were then processed immediately according to the following procedures for use in cytotoxicity or cryopreservation assays.

5.5.2. Cytotoxicity assessment of 9 kDa PVA with Rat Hepatocytes.

Fresh rat hepatocytes were isolated as above with 8×10^5 cells plated in triplicate with 5 mL of pre-warmed (37 °C) complete medium on to 60 mm \varnothing collagen (type I) coated plates (BD Biosciences, CA, USA) and incubated (37 °C / CO_{2(g)}) for 3 hours. After 3 hours cells were washed twice with 5 mL of pre-warmed PBS to remove any non-adherent extracellular debris and replaced with 5 mL of pre-warmed complete medium and incubated overnight. Approximately 36 hours later cells were imaged by phase contrast microscopy (Figure 5.1.) to visualize and clarify the presence of adherent cells. The inherent metabolic activity of untreated cells was then assessed using the resazurin assay. Measuring the inherent metabolic activity involved the addition of 5 mL of complete medium plus 250 μ L

of 0.33' mg/mL resazurin in PBS. Cells were then incubated for a period of 2 hours with 50 μ L aliquots taken at 15-minute intervals and the relative fluorescence measured (excitation and emission wavelengths of 530 nm / 25 nm and 590 nm / 30 nm) using a BioTek Synergy HT plate reader (BioTek UK, Bedfordshire, UK). After the 2-hour incubation period the cells were washed twice with 5 mL of pre-warmed PBS and replaced with 5 mL complete medium containing 20 mg/mL 9 kDa PVA and incubated for 4 hours. Finally cells were washed twice with 5 mL of pre-warmed PBS and an identical resazurin assay performed. (%) Cell viability was quantified according to Equation 5.1. with values for each time point used to define the mean (%) cell viability \pm standard deviation.

Equation 5.1. Calculation of (%) Cell viability at specific time points using the resazurin assay.

$$(\%) \text{ Cell Viability} = \frac{\left[\text{Fluorescence}_{(590/30\text{nm})}(\text{Pre-treatment}_{(x-\text{min})}) - \text{Fluorescence}_{(590/30\text{nm})}(0\text{min}) \right]}{\left[\text{Fluorescence}_{(590/30\text{nm})}(\text{Post-treatment}_{(x-\text{min})}) - \text{Fluorescence}_{(590/30\text{nm})}(0\text{min}) \right]}$$

5.5.3. Cryopreservation assessment of 9 kDa PVA with Rat Hepatocytes.

Approximately 3 mL of 4.2×10^6 cells/mL of freshly isolated rat hepatocytes were diluted in 10 mL of pre-warmed complete medium and centrifuged at 500 rpm at 23 °C for 5 minutes. The supernatant containing any small extracellular material was discarded and the cells resuspended in 5.5 mL of complete medium to a final concentration approximating 2.29×10^6 cells/mL. 440 μ L aliquots were then transferred into 1.8 mL cryovials (as used previously with immortalized mammalian cell lines) and 560 μ L of the desired cryopreservation solution that comprised a final concentration of DMSO equal to 10 % (v/v) and various amount of 9 kDa PVA as indicated in Figure 5.3. Samples were prepared in duplicate and

gently mixed by inversion to ensure a homogenous suspension of cells. Cells were then frozen using standard protocols. This involved transferring each vial into a Nalgene “Mr. Frosty™” freezing container that has a fixed cooling rate approximating 1 °C/min and were kept at 4 °C for 60 minutes. Cells were then mixed by inversion and then transferred to a -80 °C freezer for 90 minutes and then finally transferred to N_{2(l)} (-196 °C) overnight. The following day cells were either thawed rapidly (37 °C, water) or slowly (23 °C, air) as required (Figure 5.3.) and plated with 5 mL of pre-warmed complete medium on a 60 mm Ø collagen (type I) coated plate. Cells were then incubated for 3 hours. After 3 hours cells were washed twice with 5 mL of pre-warmed PBS to remove any non-adherent cells and debris and replaced with 5 mL of pre-warmed complete medium and incubated overnight prior to assessing viability using the aforementioned resazurin assay described in Section 5.5.2. except that the assay was performed for an 8-hour duration with samples taken at 60-minute intervals for analysis with (%) cell recovery calculated using Equation 4.3. with 10 % (v/v) DMSO (rapid thaw) referenced as 100 % cell recovery.

5.5.4. Preparation and cryopreservation of Mouse Mesenchymal Stem Cells.

A frozen 1 mL aliquot (60 % (v/v) DMEM/F12 medium with GlutaMAX™-I plus 30 % (v/v) FBS (MSC-qualified) and 10 % (v/v) DMSO) of mouse (C57BL/6) mesenchymal stem cells (approximately 1×10^6 cells) and all reagents required for their subsequent propagation and differentiation were purchased from Life Technologies Ltd, Renfrewshire, UK. Complete MSC medium is defined as DMEM/F12 medium with GlutaMAX™-I plus 10 % (v/v) FBS (MSC-qualified) supplemented with gentamicin, penicillin and streptomycin at final concentrations of 5 µg/mL, 100 U/mL and 100 µg/mL. To revive the as supplied mouse MSCs

stored in $N_{2(l)}$ MSCs were thawed rapidly for 2 minutes in a 37 °C water bath. Cells were then transferred into a 50 mL Falcon tube and 10 mL of pre-warmed (37 °C) complete MSC medium added slowly. Cells were then centrifuged at 300 x g and 23 °C for 5 minutes and the resultant supernatant discarded with cells resuspended in 5 mL of complete MSC medium. Cells were divided evenly between 2 separate 75 cm² flasks containing 15 mL of complete MSC medium and incubated (5 % $CO_{2(g)}$ / 37 °C) overnight. The presence of adherent cells were assessed by phase contrast microscopy (Figure 5.4.) and allowed to reach 70 % - 80 % confluence. The passaging of mouse MSCs was undertaken by washing cells with 15 mL of pre-warmed PBS before the addition of 2 mL of TrypLE™ express dissociation reagent and incubated for two minutes to promote cell detachment prior to neutralization with 5 mL of complete MSC medium. Cells were then centrifuged as previous and transferred evenly between 3 separate 175 cm² flasks containing 25 mL of complete MSC medium and incubated until confluent to attain a suitable quantity of cells relevant for cryopreservation, with medium changes every 2-3 days. The doubling time under these conditions was just under 24 hours. Prior to cryopreservation MSC cells were subjected to a trypan blue exclusion assay with cell viability in excess of 99 %. Cryopreservation was achieved by trypsinising cells as described prior and prepared as 1 mL aliquots in duplicate in 1.8 mL cryovials supplemented with 10 % (v/v) DMSO and the relevant concentration of 9 kDa PVA as shown in Figure 5.5. Cells were frozen slowly in a “Mr. Frosty™” freezing container by being transferred to 4 °C for 60 minutes prior to gentle mixing by inversion and placed in a -80 °C freezer overnight and then $N_{2(l)}$ for 2 days. Cells were then thawed either rapidly (37 °C (water bath)) or slowly (23 °C (air)) as required and 30 µL and 60 µL aliquots each added in triplicate to separate 48 well plates containing 600 µL of pre-warmed complete MSC medium overnight. The following day cells were washed with pre-warmed PBS and 600 µL of fresh medium added. After a further 24 hours the confluency of each 48 well plated was estimated by phase contrast

microscopy and a resazurin assay as described in Section 4.5.9. performed on the most relevant plate (i.e. less than 70 % confluent) with cell recovery calculated according to Equation 4.3.

5.5.5. Adipogenesis of Mouse Mesenchymal Stem Cells.

Cryopreserved mouse MSCs that were subjected to a resazurin assay as described in Section 5.5.4. were washed twice with 600 μL of pre-warmed PBS and 400 μL of StemPro[®] adipocyte differentiation medium added and cells incubated for 10 days with (400 μL) differentiation medium changed every 3 days. Cells were visualized every 2/3 days by phase contrast microscopy to identify changes in morphology and the presence of lipid droplets indicative of adipocytes (Figure 5.6.). To further clarify differentiation cells were fixed using a 2 % (v/v) glutaldehyde solution and stained with an adipocyte specific fluorophore (LipidTOX[™] red) that has a high affinity for neutral lipid droplets and a non-competing nuclear specific fluorophore (Hoechst 33258). Subsequent to staining cells were washed twice with PBS and solubilized with 150 μL DMSO and incubated at 23 °C and shaken at 200 rpm for 60 minutes in the absence of light to ensure solubilization. Samples were then pooled and 200 μL aliquots measured using a BioTek Synergy HT plate reader (BioTek UK, Bedfordshire, UK) to detect the presence of LipidTOX[™] red (excitation 590 nm / 20 nm, emission 640 nm / 40 nm) and Hoechst 33258 (excitation 360 nm / 40 nm, emission 460 nm / 40 nm) as shown in Figure 5.7.

5.6. REFERENCES.

1. Merani, S. & Shapiro, A. M. J. Current status of pancreatic islet transplantation. *Clin Sci* **110**, 611–625 (2006).
2. Opar, A. As demand for organs expands, so does transplant technology. *Nat Med* **14**, 225 (2008).
3. Wolfe, R. A., Roys, E. C. & Merion, R. M. Trends in organ donation and transplantation in the United States, 1999–2008. *Am J Transplant* **10**, 961–972 (2010).
4. Shapiro, A. M. *et al.* Islet transplantation in seven patients with type 1 diabetes mellitus using a glucocorticoid-free immunosuppressive regimen. *N Engl J Med* **343**, 230–238 (2000).
5. Orlando, G. *et al.* Regenerative medicine and organ transplantation: past, present, and future. *Transplantation* **91**, 1310–1317 (2011).
6. Atala, A. Engineering tissues, organs and cells. *J Tissue Eng Regen Med* **1**, 83–96 (2007).
7. Groszmann, R. J., Iwakiri, Y. & Taddei, T. H. Engineering liver tissue from induced pluripotent stem cells: A first step in generating new organs for transplantation? *Hepatology* 1–4 (2013).
8. Wong, V. W., Sorkin, M. & Gurtner, G. C. Enabling stem cell therapies for tissue repair: current and future challenges. *Biotechnol Adv* **31**, 744–751 (2013).
9. McGinnity, D. F., Soars, M. G., Urbanowicz, R. A. & Riley, R. J. Evaluation of fresh and cryopreserved hepatocytes as *in vitro* drug metabolism tools for the prediction of metabolic clearance. *Drug Metab Dispos* **32**, 1247–1253 (2004).
10. Song, Y., Sharp, R., Lu, F. & Hassan, M. The future potential of cryopreservation for assisted reproduction. *Cryobiology* **60**, S60–S65 (2010).
11. Newton, H., Aubard, Y., Rutherford, A. & Sharma, V. Ovary and ovulation: Low temperature storage and grafting of human ovarian tissue. *Hum Reprod* **11**, 1487–1491 (1996).
12. Mazur, P. Freezing of living cells: mechanisms and implications. *Am J Physiol* C125–C142 (1984).
13. Fuller, B. J. & Lee, C. Y. Hypothermic perfusion preservation: The future of organ preservation revisited? *Cryobiology* **54**, 129–145 (2007).
14. Viaspan product recall. *nhsbt.nhs.uk* at <http://www.nhsbt.nhs.uk/news/2012/newsrelease300312.html>
15. Bristol-Myers Squibb: Company Statement on VIASPAN®. *bms.com* at <http://www.bms.com/news/features/2012/Pages/viaspan-03302012.aspx>
16. Wakelin, S. J. *et al.* The incidence and importance of bacterial contaminants of cadaveric renal perfusion fluid. *Transplant Int* **17**, 680–686 (2005).
17. Sinha, G. Coalition aims to accelerate translation of cell therapies. *Nat Biotechnol* **30**, 573–574 (2012).

18. Quevedo, H. C. *et al.* Allogeneic mesenchymal stem cells restore cardiac function in chronic ischemic cardiomyopathy via trilineage differentiating capacity. *Proc Natl Acad Sci USA* **106**, 14022–14027 (2009).
19. Trounson, A. O., Thakar, R. G., Lomax, G. & Gibbons, D. Clinical trials for stem cell therapies. *BMC Med* **9**, 52 (2011).
20. Scott, C., Caulfield, T., Borgelt, E. & Illes, J. Personal medicine - the new banking crisis. *Nat Biotechnol* **30**, 141–147 (2012).
21. Fahy, G. M. *et al.* Cryopreservation of organs by vitrification: perspectives and recent advances. *Cryobiology* **48**, 157–178 (2004).
22. Kuleshova, L., Gouk, S. & Huttmacher, D. W. Vitrification as a prospect for cryopreservation of tissue-engineered constructs. *Biomaterials* **28**, 1585–1596 (2007).
23. Fowler, A. & Toner, M. Cryo-Injury and Biopreservation. *Ann NY Acad Sci* **1066**, 119–135 (2005).
24. Fahy, G. M. Cryoprotectant toxicity neutralization. *Cryobiology* **60**, 545–553 (2010).
25. Fahy, G. M., Saur, J. & Williams, R. J. Physical problems with the vitrification of large biological systems. *Cryobiology* **27**, 492–510 (1990).
26. Macfarlane, D. R. Devitrification in glass-forming aqueous solutions. *Cryobiology* **23**, 230–244 (1986).
27. Karlsson, J. O. M. A Theoretical Model of Intracellular Devitrification. *Cryobiology* **42**, 154–169 (2001).
28. Brockbank, K. G. M., Campbell, L. H., Greene, E. D., Brockbank, M. C. G. & Duman, J. G. Lessons from nature for preservation of mammalian cells, tissues, and organs. *In Vitro Cell Dev Biol* **47**, 210–217 (2010).
29. Wang, T., Zhu, Q., Yang, X., Layne, J. R., Jr & Devries, A. L. Antifreeze glycoproteins from antarctic notothenioid fishes fail to protect the rat cardiac explant during hypothermic and freezing preservation. *Cryobiology* **31**, 185–192 (1994).
30. Mugnano, J. A., Wang, T., Layne, J. R., Jr, Devries, A. L. & Lee, R. E. Antifreeze glycoproteins promote intracellular freezing of rat cardiomyocytes at high subzero temperatures. *Am J Physiol* **269**, R474–R479 (1995).
31. Matsumoto, S. *et al.* Effects of synthetic antifreeze glycoprotein analogue on islet cell survival and function during cryopreservation. *Cryobiology* **52**, 90–98 (2006).
32. Rubinsky, B., Arav, A., Hong, J. S. & Lee, C. Y. Freezing of Mammalian Livers with Glycerol and Antifreeze Proteins. *Biochem Biophys Res Commun* **200**, 732–741 (1994).
33. Miyamoto, Y., Suzuki, S., Nomura, K. & Enosawa, S. Improvement of hepatocyte viability after cryopreservation by supplementation of long-chain oligosaccharide in the freezing medium in rats and humans. *Cell Transplantation* **15**, 911–919 (2006).

34. Wang, H.-Y., Lun, Z.-R. & Lu, S.-S. Cryopreservation of umbilical cord blood-derived mesenchymal stem cells without dimethyl sulfoxide. *Cryo Lett* **32**, 81–88 (2011).
35. Wang, H.-Y., Inada, T., Funakoshi, K. & Lu, S.-S. Inhibition of nucleation and growth of ice by poly(vinyl alcohol) in vitrification solution. *Cryobiology* **59**, 83–89 (2009).
36. OPTN: Organ Procurement and Transplantation Network. *optn.transplant.hrsa.gov* (2013). at <<http://optn.transplant.hrsa.gov/data/>>
37. Jacobsen, J. K., Jensen, B., Skonberg, C., Hansen, S. H. & Badolo, L. Time-course activities of Oct1, Mrp3, and cytochrome p450s in cultures of cryopreserved rat hepatocytes. *Eur J Pharm Sci* **44**, 427–436 (2011).
38. Griffin, S. J. & Houston, J. B. Prediction of in vitro intrinsic clearance from hepatocytes comparison of suspensions and monolayer cultures. *Drug Metab Dispos* **33**, 115–120 (2005).
39. Miyauchi, S., Sawada, Y., Iga, T., Hanano, M. & Sugiyama, Y. Comparison of the Hepatic Uptake Clearances of Fifteen Drugs with a Wide Range of Membrane Permeabilities in Isolated Rat Hepatocytes and Perfused Rat Livers. *Pharm Res* **10**, 434–440 (1993).
40. Bachmann, K., Byers, J. & Ghosh, R. Prediction of in vivo hepatic clearance from in vitro data using cryopreserved human hepatocytes. *Xenobiotica* **33**, 475–483 (2003).
41. Sumida, K. *et al.* Effects of DMSO on gene expression in human and rat hepatocytes. *Hum Exp Toxicol* **30**, 1701–1709 (2011).
42. Tuschl, G. & Mueller, S. O. Effects of cell culture conditions on primary rat hepatocytes-cell morphology and differential gene expression. *Toxicology* **218**, 205–215 (2006).
43. Jacob, S. W. & Herschler, R. Pharmacology of DMSO. *Cryobiology* **23**, 14–27 (1986).
44. Cable, E. E. & Isom, H. C. Exposure of primary rat hepatocytes in long-term DMSO culture to selected transition metals induces hepatocyte proliferation and formation of duct-like structures. *Hepatology* **26**, 1444–1457 (1997).
45. Serra, R. & Isom, H. C. Stimulation of DNA synthesis and protooncogene expression in primary rat hepatocytes in long-term DMSO culture. *J Cell Physiol* **154**, 543–553 (1993).
46. Villa, P., Arioli, P. & Guitani, A. Mechanism of maintenance of liver-specific functions by DMSO in cultured rat hepatocytes. *Exp Cell Res* **194**, 157–160 (1991).
47. Isom, H. C., Secott, T., Georgoff, I., Woodworth, C. & Mummaw, J. Maintenance of differentiated rat hepatocytes in primary culture. *Proc Natl Acad Sci USA* **82**, 3252–3256 (1985).
48. McMillian, M. K. *et al.* An improved resazurin-based cytotoxicity assay for hepatic cells. *Cell Biol Toxicol* **18**, 157–173 (2002).

49. Binda, D., Lasserre-Bigot, D., Bonet, A. & Thomassin, M. Time course of cytochromes p450 decline during rat hepatocyte isolation and culture: effect of I-NAME. *Toxicol In Vitro* **17**, 59–67 (2003).
50. Paine, S. W., Parker, A. J., Gardiner, P., Webborn, P. J. H. & Riley, R. J. Prediction of the Pharmacokinetics of Atorvastatin, Cerivastatin, and Indomethacin Using Kinetic Models Applied to Isolated Rat Hepatocytes. *Drug Metab Dispos* **36**, 1365–1374 (2008).
51. Ubeaud, G., Schiller, C. D., Hurbin, F., Jaeck, D. & Coassolo, P. Comparison of the stability of some major cytochrome p450 and conjugation reactions in rat, dog and human hepatocyte monolayers. *Eur J Drug Metab Ph* **26**, 37–45 (2001).
52. Quent, V. M. C., Loessner, D., Friis, T., Reichert, J. C. & Hutmacher, D. W. Discrepancies between metabolic activity and DNA content as tool to assess cell proliferation in cancer research. *J Cell Mol Med* **14**, 1003–1013 (2010).
53. Son, J. H., Kim, K.-H., Nam, Y.-K., Park, J.-K. & Kim, S.-K. Optimization of cryoprotectants for cryopreservation of rat hepatocyte. *Biotechnol Lett* **26**, 829–833 (2004).
54. Lee, O., Kuo, T., Chen, W. & Lee, K. Isolation of multipotent mesenchymal stem cells from umbilical cord blood. *Blood* **103**, 1669–1675 (2004).
55. Tropel, P. *et al.* Isolation and characterisation of mesenchymal stem cells from adult mouse bone marrow. *Exp Cell Res* **295**, 395–406 (2004).
56. Pittenger, M. F. *et al.* Multilineage Potential of Adult Human Mesenchymal Stem Cells. *Science* **284**, 143–147 (1999).
57. Yu, Q. *et al.* Wnt/ β -catenin signaling regulates neuronal differentiation of mesenchymal stem cells. *Biochem Biophys Res Commun* **439**, 297–302 (2013).
58. Gang, E. J. *et al.* Skeletal Myogenic Differentiation of Mesenchymal Stem Cells Isolated from Human Umbilical Cord Blood. *Stem Cells* **22**, 617–624 (2004).
59. Picinich, S. C., Mishra, P. J., Mishra, P. J., Glod, J. & Banerjee, D. The therapeutic potential of mesenchymal stem cells. *Expert Opin Biol Th* **7**, 965–973 (2007).
60. Cao, T. *et al.* An overview and synopsis of techniques for directing stem cell differentiation in vitro. *Cell Tissue Res* **315**, 291–303 (2004).
61. Wang, J.-S., Shum-Tim, D., Chedrawy, E. & Chiu, R. C. J. The coronary delivery of marrow stromal cells for myocardial regeneration: Pathophysiologic and therapeutic implications. *J Thoracic Cardiovasc Sur* **122**, 699–705 (2001).
62. Lalu, M. M. *et al.* Safety of cell therapy with mesenchymal stromal cells (SafeCell): a systematic review and meta-analysis of clinical trials. *PLoS one* **7**, e47559 (2012).
63. Meirelles, L. D. S. & Nardi, N. B. Murine marrow-derived mesenchymal stem cell: isolation, in vitro expansion, and characterization. *Brit J Haematol* **123**, 702–711 (2003).
64. Siddappa, R., Licht, R., van Blitterswijk, C. & de Boer, J. Donor variation and loss of multipotency during in vitro expansion of human mesenchymal stem cells for

- bone tissue engineering. *J Orthop Res* **25**, 1029–1041 (2007).
65. Ross, S. E. *et al.* Inhibition of Adipogenesis by Wnt Signaling. *Science* **289**, 950–953 (2000).
 66. Beller, M., Thiel, K., Thul, P. J. & Jäckle, H. Lipid droplets: A dynamic organelle moves into focus. *FEBS Lett* **584**, 2176–2182 (2010).
 67. Cesarone, C. F., Bolognesi, C. & Santi, L. Improved microfluorometric DNA determination in biological material using 33258 Hoechst. *Anal Biochem* **100**, 188–197 (1979).
 68. Sterzel, W., Bedford, P. & Eisenbrand, G. Automated determination of DNA using the fluorochrome Hoechst 33258. *Anal Biochem* **147**, 462–467 (1985).
 69. Sensebe, L., Krampera, M., Schrezenmeier, H., Bourin, P. & Giordano, R. Mesenchymal stem cells for clinical application. *Vox Sang* **98**, 93–107 (2010).
 70. Koutsoumbelis, S. & Grande, D. A. Regenerative medicine: the clinical benefit of stem cells in cartilage regeneration. *Nat Rev Rheumatol* **9**, 265–266 (2013).
 71. Lindvall, O. & Kokaia, Z. Stem cells in human neurodegenerative disorders — time for clinical translation? *J Clin Inv* **120**, 29–40 (2010).
 72. Hopkins, J. B., Badeau, R., Warkentin, M. & Thorne, R. E. Effect of common cryoprotectants on critical warming rates and ice formation in aqueous solutions. *Cryobiology* **65**, 169–178 (2012).
 73. Morris, G. & Acton, E. Controlled Ice nucleation in cryopreservation – a review. *Cryobiology* **66**, 85–92 (2012).
 74. Meryman, H. T. Cryopreservation of living cells: principles and practice. *Transfusion* **47**, 935–945 (2007).
 75. Neufeld, D. S. *Isolation of Rat Liver Hepatocytes*. (Basic Cell Culture Protocols, 1997).

CONCLUSIONS

Poly(vinyl alcohol) (PVA) has been investigated as an ice recrystallization inhibitor (IRI) in order to improve the cryopreservation of biological materials. Despite investigating a wide range of saccharides (mono-, di- and oligo-), low molecule weight polyols and synthetic and natural polymers only PVA retains a high IRI activity. This activity is comparable to naturally occurring antifreeze proteins (AFPs) and antifreeze (glyco)proteins (AF(G)Ps) yet retains greater availability, affordability and a proven biocompatibility (Chapter 2). PVA is applied as a cryopreservative improving the cryopreservation of a variety of biological materials by attenuating ice recrystallisation during thawing in conjunction with traditional cryoprotective agents. It has been demonstrated that PVA can be successfully applied to red blood cells (Chapter 3), immortalized mammalian cell lines (Chapter 4) and primary cells (Chapter 5). In each instance PVA has no detrimental effects on each cell type in terms of functionality post thaw. Furthermore as PVA acts exclusively in an extracellular context PVA can be removed easily unlike traditional membrane permeable additives that are also required at significantly higher concentrations. However increasing PVA concentration that heightens IRI activity is disadvantageous due to the secondary property of dynamic ice shaping that intensifies mechanical damage outweighing its advantageous effect. Future work would continue to explore PVA as a cryoprotectant with an even wider range of cell varieties in order to perfect its application in cryopreservation protocols. In addition to this investigating a wide variety of PVA molecules with different configurations, extent of hydrolysis and molecule weights could elucidate a more detailed understanding of the IRI process leading to even more potent IRI cryopreservatives with widespread clinical applications that unobtainable at present.

AWARDS AND CONFERENCE PROCEEDINGS

AWARDS.

Fellowships

- Warwick Transatlantic Fellowship. Competitively awarded fellowship enabling a 3-month international secondment to The Albert Einstein College of Medicine, Bronx, NY, USA.
- Warwickshire Private Hospital Charitable Trust Grant. Selectively awarded fellowship enabling a 3-month international secondment to The Albert Einstein College of Medicine, Bronx, NY, USA.

Poster Prizes

- 1st place. *SCRA workshop: Novel Technologies for Live Cell Imaging*, University of Warwick, Coventry, UK (21/09/12)
- 1st place. *RSC Young Members Symposium 2012*, University of Nottingham, Nottingham, UK (13/06/12)

Bursaries

- Student bursary awarded by Biochemical Society to attend a three day conference entitled "Biochemical Determinants of Tissue Regeneration", Shrigley Hall, Macclesfield, UK (11/12/13 – 13/12/13).
- Travel bursary awarded by The Royal Society of Chemistry to attend a one day symposium entitled "Chemical Tools and Challenges in Systems Biology". Burlington House, London, UK (27/09/11).

CONFERENCE PROCEEDINGS.

Oral Contributions

- *RSC Carbohydrate Group Young Members Meeting 2013*, Burlington House, London, UK (11/03/13)
- *Nanopeptide 2012*, University of Manchester, Manchester, UK (12/11/12-14/11/12)
- *RSC Carbohydrate Group Autumn Meeting*, University of Birmingham, Birmingham, UK (27/09/12-28/09/12)

Poster Contributions

- *Biochemical Determinants of Tissue Regeneration*, Shrigley Hall, Macclesfield, UK (11/12/13-13/12/13)
- *RSC Carbohydrate Group Young Members Meeting 2013*, Burlington House, London, UK (11/03/13)
- *Spinks Symposium 2013: Regenerative Medicine*, Burlington House, London, UK (28/01/13)
- *RSC Biomaterials Chemistry Group 7th Annual Meeting*, Sheffield Hallam University, Sheffield, UK (08/01/13 - 09/01/13)
- *RSC Postgraduate Symposium on Nanotechnology*, University of Birmingham, Birmingham, UK (14/12/12)
- *Nanopeptide 2012*, University of Manchester, Manchester, UK (12/11/12-14/12/12)
- *RSC Carbohydrate Group Autumn Meeting*, University of Birmingham, Birmingham, UK (27/09/12 - 28/09/12)
- *SCRA workshop: Novel Technologies for Live Cell Imaging*, University of Warwick, Coventry, UK (21/09/12)
- *Warwick Polymer 2012*, University of Warwick, Coventry, UK (09/07/12 - 12/07/12)
- *RSC Young Members Symposium 2012*, University of Nottingham, Nottingham, UK (13/06/12)
- *RSC Bio-organic Group Postgraduate Symposium 2012*, Cardiff University, Cardiff, UK (19/04/12)
- *RSC Protein and Peptide Science Group (PPSG) Early Stage Researcher Meeting 2011*, Royal Society of Chemistry, London, UK (08/11/11)

CURRICULUM VITAE

PERSONAL DETAILS

- Name - Robert Deller
- Date of Birth - 20th of January 1987
- Email - r.c.deller@googlemail.com
- Telephone - +447969450423
- Address - Department of Chemistry, University of Warwick, Library Bridge Road, Coventry, CV4 7AL, UK
- Website - http://www.warwick.ac.uk/go/gibsongroup/members/robert_deller

EDUCATION

University of Warwick

- Interdisciplinary Ph.D (Pass), 2010 – 2014, Molecular Organisation & Assembly of Cells (MOAC) Doctoral Training Centre.
- Mathematical Biology and Biophysical Chemistry MSc (Distinction), 2009 - 2010.
- Biochemistry with Intercalated Year BSc (2nd class honours, upper division), 2005 - 2009.

RESEARCH EXPERIENCE

- Warwick transatlantic fellowship, Department of Endocrinology, Albert Einstein College of Medicine, New York. (Jun 2013 – Aug 2013).
- Intercalated year placement, Discovery Drug Metabolism and Pharmacokinetics, AstraZeneca PLC, Charnwood. (Sep 2007 – Sep 2008).
- Undergraduate research scholarship scheme. Eastmond Group, Department of Life Sciences, University of Warwick. (Jul 2007 – Aug 2007).

AWARDS

- Best Academic Poster - SCRA workshop: Novel technologies for live cell imaging. (Sep 2012)
- Best Academic Poster - RSC Young Members Symposium 2012. (Jun 2012)

PUBLICATION RECORD

- Saaka, Y., Deller, R.C., Rodger, A. & Gibson, M.I. *Macromolecular Rapid Communications*, **2012**, **33**, 779 - 784.
- Deller, R.C., Congdon, T.C., Sahid, M.A., Morgan, M., Vatish, M., Mitchell, D.A., Notman, R. & Gibson, M.I. *Biomaterials Science*, **2013**, **1**, 478 – 485.
- Freese, C., Unger, R.E., Deller, R.C., Gibson, M.I., Brochhausen, C., Klok, H-A. & Kirkpatrick C.J., **2013**, *Biomaterials Science*, **2013**, **1**, 824 – 833.
- Deller, R.C., Vatish, M., Mitchell, D.A. & Gibson, M.I. doi:10.1038/ncomms4244 (*Nature Communications*).
- Deller, R.C. & Gibson M.I., UK Patent Application, **2012**.

SCIENTIFIC COMMUNITY ACTIVITIES

- Warwick Postgraduate Research Ambassador (Oct 2012 – Jan 2014).
- Chemistry Postgraduate Student Staff Liaison Committee, Doctoral training centre representative (Jun 2012 – Jul 2013).
- Co-organisation of Warwick-China Polymer Chemistry Symposium. (Jul 2012).

CONFERENCE ATTENDANCE

Attendance at 16 UK conferences covering diverse topics from organic synthesis to regenerative medicine. I have delivered 11 poster presentations and 3 oral presentations. This includes,

- RSC Carbohydrate Group Young Members Meeting, *Burlington House, London, March 2013. Oral Presentation*
- RSC Biomaterials Chemistry Group 7th Annual Meeting, *Sheffield Hallam University, Jan 2013.*
- Nanopeptide 2012, *University of Manchester, Nov 2012. Oral Presentation*
- RSC Carbohydrate Group Autumn Meeting, *University of Birmingham, Sep 2012. Oral Presentation*

REFEREES

Prof. Alison Rodger (MOAC Director)
Professor of Chemistry
Department of Chemistry
University of Warwick
Coventry
CV4 7AL
A.Rodger@warwick.ac.uk

Dr. Matthew I. Gibson (Ph.D Supervisor)
Assistant Professor of Chemistry
Department of Chemistry
University of Warwick
Coventry
CV4 7AL
M.I.Gibson@warwick.ac.uk

Dr. Manu Vatish (Ph.D Supervisor)
Senior Fellow in Obstetrics
Nuffield Department of Obstetrics and
Gynaecology
John Radcliffe Hospital
University of Oxford
Oxford
OX3 9DU
manu.vatish@obs-gyn.ox.ac.uk

Dr. Dan Mitchell (Ph.D Supervisor)
RCUK Academic Fellow
Clinical Sciences Research Institute
University of Warwick
Coventry
CV2 2DX
D.Mitchell@warwick.ac.uk

CONTRIBUTIONS TO PUBLISHED WORK.

The following details personal contributions to published work subjected to peer review.

- Deller, R. C., Vatish, M., Mitchell, D.A. & Gibson, M.I. Synthetic polymers enable non-vitreous cellular cryopreservation by reducing ice crystal growth during thawing. *Nat. Commun.* doi:10.1038/ncomms4244

Contributed to experimental design and assisted in obtaining all experimental data including IRI measurements and all cryopreservation data, performing a significant amount of the data analysis prior to assisting in the writing and reviewing of the article during the publication process.

- Deller, R. C. *et al.* Ice recrystallization inhibition by polyols: comparison of molecular and macromolecular inhibitors and role of hydrophobic units. *Biomater. Sci.* **1**, 478–485 (2013).

Contributed to experimental design and assisted in obtaining all experimental data including a substantial proportion of IRI measurements and dye inclusion assay data, performing a significant amount of the data analysis prior to assisting in the writing and reviewing of the article during the publication process.

- Freese, C. *et al.* Uptake of poly(2-hydroxypropylmethacrylamide)-coated gold nanoparticles in microvascular endothelial cells and transport across the blood–brain barrier. *Biomater Sci* **1**, 824–833 (2013).

Contributed to experimental work that involved the quantification of AuNPs by ICP-AES and assisting in the reviewing of the article during the publication process.

- Saaka, Y., Deller, R.C., Rodger, A. & Gibson, M. I. Exploiting thermoresponsive polymers to modulate lipophilicity: interactions with model membranes. *Macromol Rapid Commun* **33**, 779–784 (2012).

Contributed to experimental work that involved the preparation, handling and imaging of ovine erythrocyte material and assisting in the reviewing of the article during the publication process.